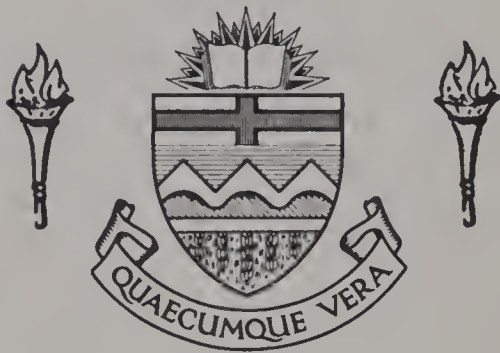


# For Reference

NOT TO BE TAKEN FROM THIS ROOM

Ex LIBRIS  
UNIVERSITATIS  
ALBERTAENSIS



86-59











THE UNIVERSITY OF ALBERTA

RELEASE FORM

NAME OF AUTHOR: Daniel J. Kontak

TITLE OF THESIS: Geology, Geochronology and Uranium  
Mineralization in the Central Mineral  
Belt of Labrador, Canada

DEGREE FOR WHICH THESIS WAS PRESENTED: Master of Science

YEAR THIS DEGREE GRANTED: 1980

Permission is hereby granted to THE UNIVERSITY  
OF ALBERTA LIBRARY to reproduce single copies of this  
thesis and to lend or sell such copies for private,  
scholarly or scientific research purposes only.

The author reserves other publication rights,  
and neither the thesis nor extensive extracts from it may  
be printed or otherwise reproduced without the author's  
written permission.





THE UNIVERSITY OF ALBERTA

GEOLOGY, GEOCHRONOLOGY, AND URANIUM  
MINERALIZATION IN THE CENTRAL MINERAL BELT  
OF LABRADOR, CANADA

by



DANIEL J. KONTAK

A THESIS

SUBMITTED TO THE FACULTY OF GRADUATE STUDIES AND RESEARCH  
IN PARTIAL FULFILMENT OF THE REQUIREMENTS FOR THE DEGREE  
OF MASTER OF SCIENCE

DEPARTMENT OF GEOLOGY

EDMONTON, ALBERTA

SPRING, 1980



THE UNIVERSITY OF ALBERTA  
FACULTY OF GRADUATE STUDIES AND RESEARCH .

The undersigned certify that they have read, and recommend to the Faculty of Graduate Studies and Research, for acceptance, a thesis entitled Geology, Geochronology, and Uranium Mineralization in the Central Mineral Belt of Labrador, Canada submitted by Daniel J. Kontak, B.Sc., in partial fulfilment of the requirements for the degree of Master of Science.





## Abstract

An extensive study of geological, geochronological (Rb/Sr, U/Pb), and geochemical nature in the Central Mineral Belt of Labrador, Canada, was initiated to solve several age-relationship problems and to study the nature and genesis of certain uranium deposits within the aforementioned area. Rb/Sr dating, combined with petrographic - and geochemical - studies, support the following conclusions concerning age relationships and igneous activity/evolution within the Central Mineral Belt:

- (i) That the Bruce River (1520 Ma) and Minisinakwa ( $1538 \pm 25$  Ma) volcanics are time stratigraphic equivalents and together with the Petscapiskau volcanics ( $1525 \pm 62$  Ma) once formed a much more extensive volcanic province ( $\sim 5,000 \text{ km}^2$ ) during the Helikian period.
- (ii) That the Walker Lake ( $1550 \pm 50$  Ma) and Otter Lake ( $1496 \pm 37$  Ma) granites are not time stratigraphic equivalents, but may however be related to the same evolving igneous magmatic system at depth (see iv).
- (iii) That the Aillik Group acid volcanic rocks ( $1767 \pm 4$  Ma) of the McLean Lake - Walker Lake area are related either diachronously or unconformably to the northerly member of the Aillik Group found along Kaipokok Bay. It is suggested that this Group be subdivided and redefined as two new groups.



(iv) That the Aillik Group acid volcanics, the Bruce River Group and the Minisinakwa volcanics, and the Otter Lake and Walker Lake granites were derived by crustal fusion of older continental crust during Aphebian to Helikian times. A model is proposed whereby igneous activity progressed from east to west as a result of the eastward migration of the continental crust over a "hot spot" from Aphebian to Helikian times (i.e. analogous to the evolution of the Hawaiian chain).

Geological mapping, combined with U/Pb dating, oxygen isotope, fluid inclusion, geochemical, and mineralogical studies, have lead to the recognition of four uraniferous sub-provinces within the Central Mineral Belt. These are represented by the following: (i) the Stormy Lake deposit, (ii) the Michelin - Burnt Lake deposits, (iii) the Moran Lake 'C' Zone deposit, and (iv) the Kitts Pond - Moran Lake 'B' Zone deposits.

The first sub-province is represented by the Stormy Lake Uranium deposit, an unconformity-controlled vein-type deposit. Remobilization of uranium, possibly out of the Paleohelikian Bruce River felsic volcanics, occurred during the waning stages of the Grenville Orogeny (~900 Ma ago ?) and was selectively deposited at the unconformity interface between the volcanics and overlying Neohelikian Seal Lake Group sediments (i.e., polymictic conglomerates in this case). Fluid inclusion and oxygen isotope studies suggest a temperature





of formation of  $\sim 150^{\circ}\text{C}$  at a depth of  $\leq 300$  metres.

The Michelin-Burnt Lake deposits, hosted by altered felsic volcanics, represent the second uraniferous sub-province.

It is suggested that uranium was originally deposited by mobilization and reconcentration during metasomatic (alkali) alteration of the felsic volcanics  $\sim 1800$  Ma ago (type deposit: Burnt Lake) and later upgraded during Grenvillian tectonism  $\sim 1100$  Ma ago (type deposit: Michelin).

The third sub-province is characterized by a miogeoclinal association of mafic volcanics, chemical sediments, and argillites of Aphebian Aillik - and Moran Lake - Groups.

Uranium was originally concentrated during deposition of the shelf-facies pelites but reconcentrated and upgraded by subsequent geologic processes. At the Kitts deposit the nature and age of mineralization ( $\sim 1750$  Ma) suggests that the Hudsonian orogeny was responsible for the epigenetic, vein-like character of the pitchblende mineralization. At the Moran Lake 'B' Zone deposits, anorthositic dykes cutting Helikian sediments of the Heggart Lake Formation are believed to have remobilized uranium  $\sim 1740$  Ma ago which was originally concentrated in the Aphebian Moran Lake Group known to underlie the area.

A fourth uraniferous sub-province is represented by the Moran Lake 'C' Zone deposit where hydrothermal fluids carry uranium ascended along faults and the uranium was precipitated



out along favorable horizons (i.e. carbonate rich horizons in this case). U/Pb dating indicates an age of  $\sim 1540$  Ma. for the mineralization, thus suggesting (i) a genetic relationship between this event and late stage volcanism in the Bruce River Group known to contain numerous uraniferous showings, and (ii) a possible magmatic origin for the uranium bearing fluid.





## Acknowledgements

The author acknowledges with a debt of gratitude the supervision provided from the commencement to completion of this study by Drs. R. D. Morton and H. Baadsgaard of the University of Alberta, and Drs. R. Smyth and D. Bailey and Mr. B. Ryan of the Newfoundland Department of Mines and Energy.

Dr. R. D. Morton is thanked for introducing the author to the field of uranium geology, for excellent supervision during the course of the study, and for his constant wit, enthusiasm, and encouragement offered forever freely. Dr. Baadsgaard is acknowledged for the copious hours volunteered assisting with the isotopic analyses and also for nurturing along the author in the field of Rb/Sr and U/Pb geochronology and for the many long discussions from which the author profited immensely.

The staff of the Newfoundland Department of Mines and Energy introduced the author to the field area and provided financial and logistical support during the course of the 1977 field season. Also acknowledged is M. Flanagan for providing excellent field assistance and good companionship during the field work.

Shell Canada Ltd. is thanked for housing the author while working at Moran Lake, and Brinex Exploration Ltd. is likewise acknowledged for providing accommodation at Kitts



Pond and also for permitting core sampling at Kitts and Burnt Lake deposits which turned out to be invaluable to the success of the study.

Several people are acknowledged for their assistance with certain aspects of the thesis; Dr. K. Hattori for carrying out the oxygen isotope analyses; Dr. D. Smith and staff for assisting with the microprobe analyses; Mr. W. Day for helping with the Rb isotopic analyses; Mr. S. Brame for introducing the author to the fluid inclusion apparatus and for providing suggestions concerning the interpretation of the data; Mr. B. Blaxley, and Mr. C. Sullivan for assisting with the preparation of petrographic specimens; and Dr. G. Holland who performed the trace element analyses.

The author is very grateful to Mrs. Bev MacIsaac for typing the manuscript.

Finally, the author acknowledges financial support provided by a University of Alberta teaching assistantship and a National Research Council of Canada scholarship for 1977-1978.



## TABLE OF CONTENTS

	Page
Library release form . . . . .	i
Title page . . . . .	ii
Signed approval page . . . . .	iii
Abstract . . . . .	iv
Acknowledgement . . . . .	viii
 Chapter 1:	
1.1 Introduction (location of area, purpose) . . . . .	1
1.2 Previous work . . . . .	9
1.3 Regional Geology	
1.3.1 Introduction . . . . .	12
1.3.2 Geology - Superior Province .	14
- Churchill Province . .	14
- Nain Province . . . . .	15
- Grenville Province . .	16
- Central Mineral Belt .	18
1.3.3 Economic Geology . . . . .	30
 Chapter 2:	
2.1 Introduction to Rb/Sr Geochronology .	34
2.2 Specimen collection . . . . .	34
2.3 Sample preparation and analytical procedure . . . . .	36
2.4 Treatment of data . . . . .	44
2.5 Geology of the study areas	
2.5.1 Walker Lake Area . . . . .	53
2.5.2 Otter Lake- Nipishish Lake Area . . . . .	64
2.5.3 Bruce River Area . . . . .	72
2.6 Geochemistry of Rock Suites	
2.6.1 Preparation of samples and analytical procedure . . . .	75
2.6.2 Treatment of data . . . . .	77
2.6.3 Discussion of results . . . .	80
2.7 Rb/Sr Geochronology	
2.7.1 The Aillik Volcanics . . . . .	96
2.7.2 The Otter Lake Granite . . . .	98
2.7.3 The Bruce River Volcanics . .	99
2.7.4 The Minisinakwa Volcanics . .	100
2.7.5 The Walker Lake Granite . . .	101
2.8 Discussion and Interpretation . . . .	102



	Page
Chapter 3:	
3.1 Introduction and previous work of the Stormy Lake area .	110
3.2 Regional geology	111
3.3 Local geology	
3.3.1 Stratigraphy . . . . .	116
3.3.2 Structure . . . . .	122
3.3.3 Metamorphism . . . . .	126
3.4 Mineralization . . . . .	129
3.5 Fluid inclusion study	
3.5.1 Introduction	134
3.5.2 Previous work as applied to U-deposits . . . . .	134
3.5.3 Procedure . . . . .	135
3.5.4 Analyses and results . . .	136
3.5.5 Discussion and inter- pretation . . . . .	142
3.5.6 Conclusions . . . . .	146
3.6 Oxygen isotope study . . . . .	147
3.7 Uranium-lead dating . . . . .	153
3.8 Discussion and interpretation . .	157
Chapter 4:	
4.1 Introduction and previous work of Burnt Lake Area . . . .	164
4.2 Regional geology . . . . .	165
4.3 Local geology	
4.3.1 Stratigraphy . . . . .	167
4.3.2 Structure . . . . .	177
4.4 Amphibole and pyroxene analyses	
4.4.1 Introduction and procedure . . . . .	181
4.4.2 Amphibole analyses . . . .	182
4.4.3 Pyroxene analyses . . . . .	188
4.5 Major and trace element geochemistry	194
4.5.1 Introduction . . . . .	194
4.5.2 Major elements . . . . .	195
4.5.3 Trace elements . . . . .	197
4.6 Mineralization . . . . .	203
4.7 Uranium-lead dating . . . . .	207
4.8 Discussion and interpretation . .	214





	Page
Chapter 5:	
5.1 Introduction to the Moran Lake Area . . . . .	219
5.2 Regional Geology of Moran Lake Area . . . . .	219
5.3 Moran Lake 'B' Zone - Introduction and previous work . . . . .	223
5.4 Local Geology of the 'B' Zone	223
5.4.1 Sediments (Heggart Lake) . .	228
5.4.2 Dykes (i), (ii), (iii), (iv), (v) . . . . .	231
5.4.3 Gabbro Stock . . . . .	236
5.5 Mineralization . . . . .	238
5.6 Uranium-lead dating . . . . .	244
5.7 Discussion and interpretation . . .	247
5.8 The Moran Lake 'C' Zone, Introduction and previous work . . .	251
5.9 Local geology of the 'C' Zone . . .	254
5.10 Origin of the volcanic breccia . . .	262
5.11 Mineralization . . . . .	265
5.12 Uranium-lead dating . . . . .	268
5.13 Discussion and interpretation . . .	270
Chapter 6:	
6.1 Introduction and previous work of the Kitts Pond Area . . . . .	275
6.2 Regional geology of Kaipokok Bay Area . . . . .	277
6.3 Local geology of the Kitts Pond Area . . . . .	279
6.4 Mineralization . . . . .	282
6.5 Uranium-lead dating . . . . .	286
6.6 Discussion and Interpretation . . .	291
Chapter 7: Synthesis and conclusions	294
Appendix I U-Pb procedure	306
I.1 Sampling procedure . . . . .	306
I.2 Analytical procedure . . . . .	307
I.3 Treatment of data . . . . .	308
References	357
Vita	



## List of Tables

Table	Description	Page
1	Stratigraphic relationships between the east, central and western parts of the Central Mineral Belt	19
2	Stratigraphic compilation of the Bruce River Group	26
3	List of previous geochronological studies completed in the Central Mineral Belt	35
4	Replicate $^{87}\text{Sr}/^{86}\text{Sr}$ determinations	45
5	Summary of Rb/Sr data	46
6	Modal analyses of Walker Lake Granite	58
7	Modal analyses of Otter Lake Granite	67
8	Standards used for microprobe analysis of glasses	78
9	Chemical analyses and norms for the Otter Lake Granite, Walker Lake Granite, Bruce River volcanics and Minisinakwa volcanics	79
10	List of molecular proportions of $(\text{CaO} + \text{Na}_2\text{O} + \text{K}_2\text{O})$ and $\text{Al}_2\text{O}_3$	92
11	Isotopic composition of pitchblende from Stormy Lake	131
12	$\delta^{18}\text{O}$ of hydrothermal fluids for Stormy Lake	152
13	Standards used for microprobe analyses of pyroxene and amphibole	183
14	Chemical analyses and structural formulae of amphiboles	184
15	Chemical analyses and structural formulae of pyroxenes	189
16	Whole rock chemical analyses	196



Table	Description	Page
17	Trace element analyses	198
18	Isotopic composition of pitchblende from Burnt Lake	206
19	Isotopic composition of uranium mineralization from Moran Lake	242
20	Uranium assays of mineralized unit, Moran Lake 'C' Zone	267
21	Isotopic composition of pitchblende from Kitts	287



## List of Figures

Figure		Page
1	Regional geology of Labrador	3
2	Geology of the Central Mineral Belt, Labrador	5
3	Geology of the Walker Lake-MacLean Lake Area	38
4	Geology of the Otter Lake-Nipishish Lake Area	40
5	Geology of the Bruce Lake Area	41
6	Isochron plot of the Aillik Group volcanics	47
7	Isochron plot of the Otter Lake Granite	48
8	Isochron plot of the Bruce River Group volcanics	49
9	Isochron plot of the Minisinakwa volcanics	50
10	Combined isochron plot of the Bruce River and Minisinakwa Volcanics	51
11	Isochron plot of the Walker Lake Granite	52
12	Ternary diagram (quartz-feldspar-plagioclase) for Walker Lake and Otter Lake Granites	59
13	$Al_2O_3$ and $Fe_2O_3$ versus $SiO_2$ diagram	81
14	$TiO_2$ and $MgO$ versus $SiO_2$ diagram	82
15	$K_2O$ , $CaO$ , and $Na_2O$ versus $SiO_2$ diagram	83
16	AFM diagram	84
17	$(Na_2O + K_2O)$ versus $SiO_2$ diagram	85
18	$Al_2O_3$ versus normative plagioclase diagram	86
19	Rb versus Sr diagram	87
20	Color index versus normative plagioclase diagram	88
21	$K_2O$ versus $SiO_2$ diagram	89





Figure		Page
22	An:Or:Ab <sup>1</sup> (normative) diagram	90
23	Combined isochron plot of the Aillik Group volcanics, Bruce River Group volcanics, Minisnakwa volcanics, Otter Lake Granite and Walker Lake Granite	108
24	Regional geology of the Stormy Lake area	112
25	Local geology of the Stormy Lake uranium showing	118
26	$\beta$ plot (38 points)	124
27	$\pi$ plot (43 points)	124
28	1% equal area projection contoured for $S_0$	125
29	1% equal area projection contoured for $S_2$	125
30	Rosette diagram of joints and fractures	127
31	EDA scan of pitchblende	132
32	Histogram of heating and freezing temperatures, S-1 (quartz)	138
33	Histogram of heating and freezing temperatures, 2nd blast (quartz)	138
34	Histogram of heating and freezing temperatures, 3rd blast (quartz)	138
35	Histogram of heating and freezing temperatures, S-17 (quartz)	138
36	Histogram of heating and freezing temperatures, S-40 (quartz)	138
37	Histogram of heating and freezing temperatures, fluorite	138
38	Combined histogram of filling (homogenization) temperatures of quartz specimens	140
39	Phase diagram for the system $H_2O$ -NaCl	141



Figure		Page
40	Temperature correction curves for 15% NaCl solution at various pressures	144
41	Boiling point curves for H <sub>2</sub> O liquid and for brines of constant composition	145
42	Oxygen isotope data for quartz, calcite, Hematite, muscovite, and feldspar from Stormy Lake uranium showing	149
43	1000 In $\alpha$ 1-2 versus T <sup>o</sup> C diagram	150
44	Concordia diagram for uranium mineralization, Stormy Lake	154
45	<sup>207</sup> Pb/ <sup>204</sup> Pb versus <sup>206</sup> Pb/ <sup>204</sup> Pb diagram for uranium mineralization, Stormy Lake	156
46	Local geology of the Burnt Lake uranium showing	169
47	B plot (101 points)	178
48	$\pi$ plot (143 points)	178
49	1% equal area projection contoured for S <sub>0</sub>	178
50	1% equal area projection contoured for S <sub>1</sub>	178
51	Compositional range and classification of the glaucophane-riebeckite amphiboles	186
52	Pyroxene analyses plotted in the alkali pyroxene diagram	191
53	Phase diagram for system Na <sub>2</sub> O:SiO <sub>2</sub> :Fe <sub>2</sub> O <sub>3</sub>	192
54	Th, Rb, Sr versus U diagram	199
55	Zr, Pb, Zn versus U diagram	200
56	Rb versus Sr diagram	201
57	Scintillometer survey of Burnt Lake uranium showing	204
58	Concordia diagram for uranium mineralization from Burnt Lake	208



Figure		Page
59	Concordia diagram for uranium mineralization from the Burnt Lake showing, Michelin deposit, Emben showing, and John Michelin showing	210
60	$^{207}\text{Pb}/^{204}\text{Pb}$ versus $^{206}\text{Pb}/^{204}\text{Pb}$ plot of uranium mineralization, Burnt Lake	212
61	Regional geology of the Moran Lake area	221
62	Local geology of the Moran Lake 'B' Zone uranium showing	225
63	Local geology of the Moran Lake 'B' Zone after Ellingwood (1958)	227
64	Scintillometer survey of the Moran Lake 'B' Zone	240
65	EDA scan of brannerite	241
66	Concordia diagram for uranium mineralization, Moran Lake 'B' Zone	245
67	$^{207}\text{Pb}/^{204}\text{Pb}$ versus $^{206}\text{Pb}/^{204}\text{Pb}$ plot of uranium mineralization, Moran Lake 'B' Zone	246
68	Local geology of the Moran Lake 'C' Zone uranium showing	253
69	Concordia diagram for uranium mineralization, Moran Lake 'C' Zone	269
70	$^{207}\text{Pb}/^{204}\text{Pb}$ versus $^{206}\text{Pb}/^{204}\text{Pb}$ plot for uranium mineralization, Moran Lake 'C' Zone	271
71	Regional geology of the Kaipokok Bay area	276
72	Local geology of the Kitts uranium deposit	281
73	EDA scan of pitchblende and coffinite	284
74	Concordia diagram for uranium mineralization, Kitts	288



Figure		Page
75	$^{207}\text{Pb}/^{204}\text{Pb}$ versus $^{206}\text{Pb}/^{204}\text{Pb}$ plot for uranium mineralization, Kitts	290
76	Sketch map of the geologic environment for Moran Lake 'B' Zone	300
77	Schematic diagram of Burnt Lake-Michelin type uranium mineralization	302
78	Schematic diagram of Stormy Lake vein-type uranium mineralization	303
79	Sketch map of the geologic environment for Moran Lake 'C' Zone	304





# LIST OF PLATES

Plate	Description	Page
1	$F_1$ fold in Seal Lake sediments	311
2	$F_2$ folds in Seal Lake sediments	311
3	$F_2$ fold in outlier of Seal Lake Group rocks	313
4	Aerial view of Stormy Lake uranium showing	313
5	Unconformity between Bruce River Group and Seal Lake Group	315
6	Cross-bedding in quartzites	315
7	Sphene in meta-argillite	317
8	Quartz cobble conglomerate	317
9	Infolding ( $F_2$ ) along Seal Lake-Bruce River unconformity	319
10	Crenulated schist in late stage quartz vein	319
11	Vein-type uranium mineralization at Stormy Lake	321
12	Uranium mineralization at Stormy Lake	321
13	Hematite crystal in quartz vein	323
14	Pitchblende mineralization incorporating hematite blades	325
15	Fluorite bands in metarhyolite	325
16	Primary fluid inclusions in quartz	325
17	Fluid inclusion in fluorite	325
18	Lithic tuff	323
19	Mafic banding (pyroxene and amphibole) in metatuff	327



Plate	Descriptions	Page
20	Mafic banding in metatuff (closeup)	327
21	Tuffaceous fragments in metatuff	329
22	Contact between mafic rich and leuco- cratic portions of metatuff in thin section	329
23	Magnesioriebeckite in thin section	331
24	Aegerine-augite and pitchblende in thin section	331
25	Radioluxograph of mineralized tuff	333
26	Radioluxograph of mineralized tuff	333
27	Hematitic alteration of metatuff	335
28	Pitchblende mineralization	333
29	Polymictic boulder conglomerate of the Heggart Lake Formation	335
30	Anorthosite dyke	337
31	Thin section of anorthosite dyke	341
32	Thin section of medium-grained anor- thosite dyke	337
33	Feldspar porphyry dyke cutting sediments	339
34	Thin section of altered feldspar porphyry dyke	339
35	Thin section of altered feldspar- pyroxene porphyry dyke	342
36,37	Radioluxograph of mineralized rocks	341
38	Sphene crystal in anorthosite dyke with associated uranium minerali- zation(in thin section)	342
39	Brannerite mineralization	344
40	Pillowed basalts of the Moran Group	346



Plate	Description	Page
41	Oligomictic conglomerate of Heggart Lake Formation	346
42	Volcanic breccia of Heggart Lake Formation	348
43	Lithic tuff exhibiting bedding (?) in thin section	344
44	Thin section of lithic fragments in volcanic breccia	348
45	Thin section of Moran Group volcanic fragments in volcanic breccia	350
46	Thin section of volcanic rock of Heggart Lake Formation	344
47	Veinlets of plagioclase cutting volcanic breccia	344
48	Conglomerate overlying volcanic breccia unit	350
49	Mafic dyke cutting Heggart Lake Formation sediments	352
50	Radioluxograph of mineralized volcanic breccia	354
51	Radioluxograph of mineralized volcanic breccia	354
52	Radioluxograph of mineralized metapelite	356
53	Pitchblende mineralization	356
54	Pitchblende altered to coffinite	356
55	Pitchblende mineralization containing galena	356



## CHAPTER I

### 1.1 Location:

The study area is located in Labrador, more specifically that part of the southern Nain Province referred to as the Central Mineral Belt (Smyth et al., 1975). The area extends from Makkovik on the east coast of Labrador inland for 260 km to the Smallwood Reservoir. The area is uninhabited except for a few coastal ports such as Postville on the north shore of Kaipokok Bay and Makkovik on the east coast (Figure 1 and 2).

Access to the field area is restricted to fixed wing aircraft and helicopter which fly out of Goose Bay, although some waterways such as the Kanairiktok and Naskaupi Rivers permit limited penetration into the field area.

The physiography consists of flat lying to undulating glacial terrain blanketed with till and outwash with limited positive relief except in the eastern part of the area where granitic terrain predominates forming distinct topographic highs (i.e. Monkey Hill, Benedict Mountains).

Vegetation is restricted to low-lying valleys where fairly dense coniferous growth occurs; again this is mainly in the central and western parts of the area with the eastern area essentially barren of tree growth. However, the entire belt is blanketed by a prolific growth of green moss thus necessitating one to carry a grub hoe on all







Figure 1

Sedimentary and metamorphic rocks:    Intrusive rocks:

Grenville Province

Hadrynian



Arkosic sedimentary rocks of the Double Mer Formation

Helikian and earlier



Metamorphic rocks, mainly quartzofeldspathic gneisses

Helikian



Anorthosites; gabbros, and associated acidic intrusives

Helikian and earlier



Massive to poorly foliated acidic intrusives

Churchill Province

Helikian



Sedimentary rocks and mafic volcanics of the Seal Lake Group

Aphebian



Sedimentary and volcanic rocks of the Labrador Trough (black are gabbroic sills)

Aphebian and earlier



Metamorphic rocks, mainly quartzofeldspathic gneisses and granulites

Aphebian



Acidic intrusives and associated metamorphic rocks

- - - Grenville Front

Nain Province

Helikian



Sedimentary and volcanic rocks of the Bruce River Group

Aphebian



Sedimentary and volcanic rocks of the Ramah, Mugford, Moran, and Aillik Groups

Archean



Basement gneisses

Superior Province

Archean



Granulite gneisses and acidic intrusives

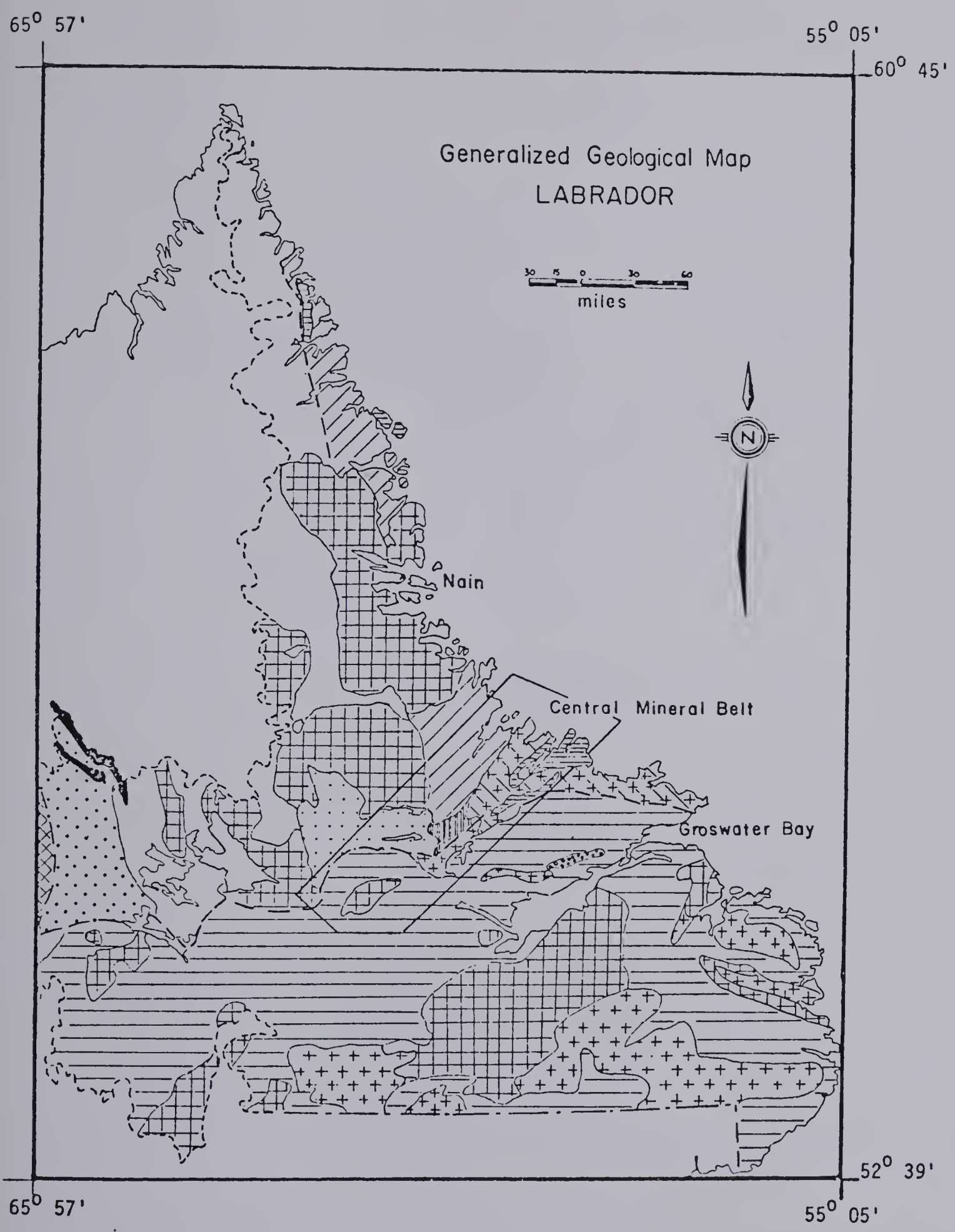






Figure 2

**Intrusive Rocks:**

**Hudsonian to Helikian**



Adanellite



Anorthosites, gabbros, and associated rocks



Undifferentiated granite; a - Otter Lake Granite (1496 Ma);  
b - Walker Lake Granite (1550 Ma).

**Sedimentary and Intrusive Rocks:**

**Neohelikian**



Seal Lake Group (undifferentiated mafic volcanics and sedimentary rocks)

~~~~~ U/C ~~~~~

**Paleohelikian**



Letitia Lake Porphyry (quartz feldspar porphyries intruded by agpatitic alkaline complexes)



Petscapiskau Group (acid to intermediate volcanic flows and pyroclastics)



Bruce River Group (acid and mafic volcanics, tuffaceous sediments, sandstone and conglomerate)

~~~~~ U/C ~~~~~

**Aphebian**



Moran Group (dolostone, argillite, mafic volcanics)



Aillik Group { upper-felsic volcanics, sandstone, conglomerate  
lower-mafic volcanics, metasediments

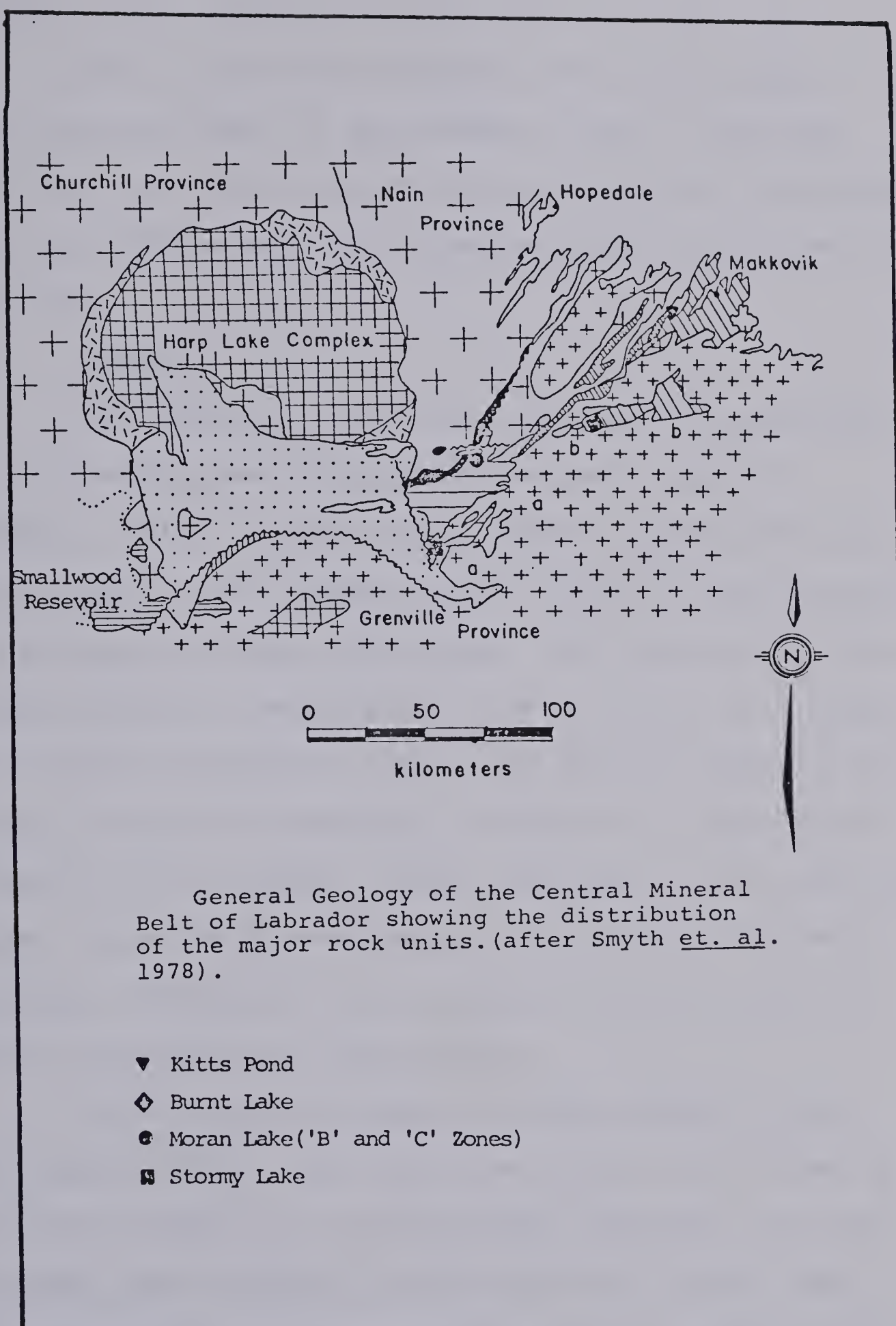
~~~~~ U/C ~~~~~

**Archean**



Granite, gneiss, reconstituted equivalents







traverses if one wishes to observe any outcrop.

Due to the severe climatic conditions field seasons are restricted to the months of June, July and August, and even then Mother Nature only permits geologists to scar her surface with grub hoes and geological picks 70% of the time.

Purpose:

This project, which was predominantly geochronological in nature, was initiated to augment regional (1:100,000 scale) mapping of the Central Mineral Belt of Labrador begun in 1974 (Smyth et al., 1975) by the Newfoundland Department of Mines and Energy. The study consisted of two parts, first to investigate in detail the age and genesis of several previously identified uranium showings and, secondly, to generate five Rb-Sr isochrons on lithologies specified by Dr. Ron Smyth (chief geologist for the Labrador Division) where age determinations were required to unravel ambiguities inherent in the geological record already documented at the outset of this project.

Previous work by Beaven (1958), Gandhi et al. (1969), Gandhi (1976), and Minatidis (1976) had defined the Central Mineral Belt as a "uraniferous province" but these studies were only cursory in nature and did little other than to document the type of mineralization present. With the onset of the uranium boom in the early 1970's, a



proliferation of new ideas on the genesis of uranium ores occurred as a result of the discovery of a diversity of new type-deposits. It was hoped that this recent work would benefit a study of this nature and permit one to recognize uraniferous subprovinces and also to outline areas of high potential. Five areas were selected ( Stormy Lake, Burnt Lake, Moran Lake 'B' and 'C' Zones, and Kitts Pond ) after reading the available literature and consulting with government geologists. The areas spanned the length of the Central Mineral Belt and included all the major lithologies considered to be suitable host rocks for uranium mineralization.

Regional mapping of the Central Mineral Belt by Government geologists during 1974 (Smyth et al., 1975) and 1976 (Smyth, 1977; Ryan, 1977) had outlined several problem areas where dating was required in order to permit correlation of lithologies and time scale classification (cf. Stockwell, 1964). More specifically, lack of outcrop and a large area underlain by granitic terrain in the central portion of the Central Mineral Belt prevented one from determining several important geological relationships, namely the following:

- i) The stratigraphy of the Aphebian Allik Group. Previous work had defined two distinct geological provinces in the eastern part of the Central Mineral Belt characterized by basic volcanics and metapelitic schists found in





the Kitts-Posthill Belt and another dominated by acid volcanics found in the Walker Lake-MacLean Lake area. The two provinces were thought to be time stratigraphic equivalents, diachronously related, or possibly separated by an unconformity, thus implying a major time break in the geologic record and requiring reclassification,

ii) Whether the acid volcanics and volcaniclastics of the Aillik Group were equivalent to acid volcanics of the Bruce River Group found further to the west. The presence of an unconformity between the Aphebian Moran Group basic volcanics and shales and the Paleohelikian Bruce River Group suggested to Smyth et al. (1975) and Smyth (1977, pers. comm.) that a similar situation might exist in the Aillik, thus permitting correlation between the two areas and a division of the latter into lower and upper units of Aphebian and Helikian age, respectively.

iii) Whether a unit of acid to intermediate volcanics and volcaniclastics, referred to informally as the Minisinkwa Volcanics, found north of Nipishish Lake were equivalent to similar rocks of the Bruce River Group or the Aillik Group. Although located on strike with the acid volcanics of the Aillik Group the rocks exhibited features more characteristic of Bruce River Group volcanics (i.e. feldspar phenocrysts, rather than quartz and feldspar phenocrysts as found in the Aillik Group volcanics). However, the presence





of the Gravelly River shear zone immediately north of the sequence prevented positive correlation of the volcanics with the Bruce River Group and a granitic batholith (the Walker Lake Granite) prevented their correlation with the Aillik Group found further to the east.

iv) Whether the Otter Lake Granite found in the central portion of the Central Mineral Belt was equivalent to the Walker Lake Granite which underlies the map area further to the east and their ages. Mapping by Smyth (1977), Smyth et al. (1975), Ryan (1978), and Bailey (1978) outlined two large granitic bodies which shared similar characteristics (i.e. leucocratic granites with mafic rich portions, both of which had syenitic to monzonitic phases and contained dioritic inclusions). A large area covered by glacial drift north of Nipishish Lake prevented one from tracing the units into each other and thus dating appeared to be the only alternative approach.

In order to solve these problems, five rock suites were selected for Rb-Sr dating: i) the Walker Lake Granite; ii) the Otter Lake Granite; iii) the Bruce River Group; iv) the Minisinakwa Volcanics; and v) the Aillik Group acid volcanics.

## 1.2 Previous Work

Steinhauer (1814), Lieber (1860), Packard (1891)



and Daly (1902) provide the earliest interpretations of the geology of Labrador focusing on the coastal sections, as did Kranck (1939, 1953) and Douglas (1953) during their coastal excursions from Domino Run to Hopedale. Reconnaissance mapping by the Geological Survey of Canada produced the first regional maps of the central Mineral Belt (Fahrig, 1959; Christie et al., 1953; Stevenson, 1970; Williams, 1970), along with numerous additional publications of geochemical (Baragar, 1969), geochronological (Leech et al., 1963; Grasty et al., 1969), and geophysical (Fahrig and Larochelle, 1972; Roy and Fahrig, 1973) nature. Green (1972, 1974) published the first geological reports showing the broad regional relationship of the Central Mineral Belt in Labrador and its geological affinities to southwestern Greenland has been discussed by Sutton et al. (1971), Bridgewater (1970), and Currie et al. (1975).

Recently more detailed studies of the various rock groups have been completed. Gandhi et al. (1969) gave a comprehensive report on the Aillik Group outcropping over the eastern portion of the Central Mineral Belt which expanded on the previous work of King (1963) and Gill (1966). However, remapping of this area by Bailey (1978, 1979), White (1976) and Clark (1970, 1974) produced notable revisions, most significantly the reclassification of Gandhi et al.'s (1969) feldspathic quartzites as acid volcanics. Smyth



et al. (1975, 1978) remapped the central part of the Central Mineral Belt and recognized an unconformity between William's (1970) Lower and Middle divisions of the Croteau Group (Fahrig, 1957) and their subsequent reclassification as the Aphebian Moran Group and Peleohelikian Bruce River Group respectively. Brummer and Mann's (1961) lengthy description of the Neohelikian Seal Lake Group, which forms the youngest of the three main rock divisions in the Central Mineral Belt, remains essentially unchanged. Additional geological references describing the geology are found in the files of the Newfoundland Department of Mines and Energy (e.g. Ryan, 1977; Ryan and Harris, 1978; Smyth, 1977; Smyth and Marten, 1975; Marten, 1975) and Brinex.

The area has been explored intensively for base metals and uranium. Evans (1952) and Brummer and Mann (1961) describe the native copper occurrences of the Seal Lake district which they compare to the Keweenawan district of Michigan in terms of lithology, age, and mineralization. Brummer and Mann (1961), Evans and Dujardin (1961), and Curtis et al. (1974) describe complex REE mineralization in alkaline complexes in the Seal Lake area which are correlated to the Gardar Province of Southern Greenland, host of the Ilimaussag uranium deposit (Boshe et al., 1974). Uranium mineralization, however, is presently the focus of exploration throughout the Central Mineral Belt. Beaven





(1958) first described uraniferous occurrences recognizing the area as a uranium province. Subsequent studies include Smyth and Marten's (1975) report on the basal unconformity of the Seal Lake Group; Smyth and Ryan's (1977) study of the Moran Lake district where uranium is associated with mafic dykes and breccias; Minatidis' (1976) comparative study of several uranium deposits; Gandhi's (1976) geochronological study of several deposits in the Aillik Group, and Kontak's (1978) preliminary report on the uranium occurrences discussed within this text.

The present study is too broad to discuss all the previous work concerning the various topics covered within this study (i.e. Rb-Sr dating; U-Pb dating; fluid inclusions; oxygen isotopes; geochemistry; etc.) and will thus be reviewed separately when discussed.

### 1.3 Regional Geology

#### 1.3.1 Introduction

The regional geology of Labrador is shown in figure 1. The first compilation map of the area was produced by Greene (1972) and the accompanying report (Greene, 1974) represented the first attempt to outline the geology of Labrador.

Labrador contains four of the six geologic provinces as designated by Stockwell (1964), the





Nain-, Superior-, Churchill-, and Grenville-Provinces, of which the Nain Province is confined wholly to Labrador. The age of the rocks found within Labrador range from Archean (i.e. the Saglek area) to Mesozoic (i.e. the Mestastin Formation and the Redmond Formation). Although the geology of Labrador has been mapped, it has been completed in only a cursory fashion and as a result numerous discrepancies, contradictions, and errors abound in the literature. Similarly, this study suffers the same failings in places.

The study area is restricted to the southern part of Labrador within an area (260 km x 40 km) referred to as the "Central Mineral Belt" extending from the coast at Makkovik southwestwards to the Smallwood Reservoir. It consists of supracrustal rocks of Archean to Neohelikian age which rest upon older basement gneisses and are intruded by numerous granitoid bodies and diabase dykes. Due to the dominantly northwest-southwest structural trend and its distinct supracrustal assemblage Taylor (1971) referred to it as the Makkovik Subprovince, part of the larger Nain Province. The oblique trend of the structural style of the subprovince is apparently due to rotation of the area approximately  $55^{\circ}$  during a period 1500 - 1200 my ago (Roy and Fahrig, 1973).

### 1.3.2 Geology

As mentioned previously, Labrador has been divided



geologically into four structural provinces by Stockwell (1964), whose proposals were modified by Taylor (1971) and Greene (1974). These shall be discussed separately in a cursory fashion and then the Central Mineral Belt will be described in more detail.

### Superior Province

The Superior Province underlies the westernmost portion of Labrador and occupies the smallest area of the structural provinces. It is characterized by east-west structural trends and by Archean ages (Stockwell, 1964; Goodwin et al., 1972). It is underlain by granulite gneisses and by acidic intrusives, and is unconformably bounded by the Churchill Province to the east.

### The Churchill Province

The Churchill Province has recently been extended by Taylor (1971) to include the western Nain Subprovince of Stockwell (1963, 1964) as a result of mapping by Taylor (1969, 1970) who failed to detect any tectonic break between the Nain and Churchill Provinces. Although the structural styles in the areas are similar, there still remains conflict between age determinations in this annexed portion of the Nain and the rest of the Churchill Province. The northern boundary of the Churchill with the Nain is marked by a mylonite zone (Taylor, 1969, 1970) and its southern boundary,



although covered by supracrustals, is assumed to be represented by the Pocket Knife Fault (Greene, 1974).

The Churchill Province is divisible into two north trending belts; the Labrador Trough, composed of Aphebian sediments and mafic volcanics with large deposits of iron formation, and an eastern zone of high grade metamorphic rocks.

It is important to note that Greene (1974) extends the Churchill Province to include the Seal Lake Group (Brummer and Mann, 1961), formerly assigned to the Grenville by Stockwell et al., (1970) and to the Grenville Foreland Zone by Wynne-Edwards (1972). This supracrustal sequence forms the western portion of the Central Mineral Belt.

### The Nain Province

The Nain Structural Province, as defined by Taylor (1971), is the only structural province wholly contained within Labrador and is characterized by north trending structures and Archean ages, except in the south. In the latter case the Archean rocks and overlying supracrustals of Aphebian age have been affected by the Hudsonian Orogeny, thus resetting the K-Ar isotopic clocks. The southern portion, where northeast-southwest trends and Aphebian ages predominate, has been set aside by Taylor (1971) as a subprovince of the Nain, the Makkovik Subprovince.





In the north the Nain province is underlain by a high-grade metamorphic terrain of Archean age and is locally overlain by Aphebian supracrustals. These include the Ramah Group (Knight, 1973; Knight and Morgan, 1976) recently dated at 1892 Ma (Wanless and Loveridge, 1978), the Mugford Group (Smyth, 1975; Barton, 1975) and the Snyder Group. The groups are believed to be of equivalent age and their correlation has recently been discussed by Smyth and Knight (1978). Supracrustals also outcrop in the south in the Makkovik Subprovince and will be discussed separately later on.

### Grenville Province

The Grenville Province extends into the southern portion of Labrador, striking in an east-west direction. Its northern contact, the Grenville Front, lies south of the Central Mineral Belt where extensive faulting and mylonisation occurred (Fahrig, 1957; Stevenson, 1970; Williams, 1970), however, the eastward extension of this front to the Labrador coast has been a point of contention for some time. Stockwell (1963, 1964) originally extended the front too far north, although Wanless et al., (1967) agreed with this. Mapping by Stevenson (1970) and dating by Grasty et al., (1969) showed that the front was located further south, passing out to sea along Pottles Bay. Taylor (1971) moved the front further south to the north shore of Groswater Bay





and Greene(1974) relocated it along the northern shore of Pottles Bay pending further age dating.

Wynne-Edwards (1972) includes the rocks of the Central Mineral Belt in the Grenville Foreland Belt, more specifically the Nain Foreland Zone. Further to the south the area is underlain by high-grade metamorphic rocks (paragneiss) and is overlain by undisturbed arkosic sediments of the Double Mer Formation (Kranck, 1953; Stevenson, 1970).

Large parts of Labrador are underlain by anorthosite and adamellite, part of a broad northeast belt of intrusions which extend from the Adirondack Massif in New York State to the Nain Province in Labrador. The Labrador anorthosites include the Nain anorthosite (Wheeler, 1942, 1960), Michikamau anorthosite (Emslie, 1965, 1970) and the Harp Lake anorthosite. These represent part of an extensive thermal event, the Elsonian Orogeny (Stockwell, 1964), and are characterized by K-Ar ages in the range 1300 - 1400 Ma with younger ages found in bodies further to the south.

Southern Labrador is cut by numerous diabase dykes, trending east-west. They are predominantly of Grenville age and K-Ar ages cluster around 950 Ma (Gandhi et al., 1969; Grasty et al., 1969), however, premetamorphic dykes of older age do occur (Stevenson, 1970). Younger lamprophyric dykes dated at 575 Ma (Leech et al., 1963) are also known to occur on the coast at Makkovik.



Comparisons have been made between the geology of Greenland and Labrador, particularly with reference to the Saglek area (Collerson et al., 1976) and southern Labrador, where agpaitic intrusions, part of Red Wine Alkaline Province, occur (Currie et al., 1975). These comparisons arise from studies involving continental drift and plate tectonics, and a full treatment of the problem is discussed by Windley (1976).

#### Geology of the Central Mineral Belt

The Central Mineral Belt (seen in figure 2), is a lenticular belt (approximately 260 x 40 km) of Proterozoic supracrustal rocks which stretches from the Labrador coast at Makkovik southwestwards to the Smallwood Reservoir. It has been divided into four distinct geological groups -- the Seal Lake Group to the west, the Moran and Bruce River Groups in the central portion, and the Aillik Group to the east. Three of these groups lie within the Makkovik Subprovince, and the fourth, the Seal Lake Group, lies within the Churchill Province as redefined by Greene (1974). The stratigraphy of the Central Mineral Belt is presented in Table 1, this includes modifications made as a result of this study.

The Aphebian Aillik Group, originally referred to as the "Aillik Series" (Kranck, 1953; Douglas, 1953; Gandhi



TABLE 1

| Age & Events      | West                           | Major Intrusions             | Central                                           | Major Intrusions               | East                            | Intrusions                                                   |
|-------------------|--------------------------------|------------------------------|---------------------------------------------------|--------------------------------|---------------------------------|--------------------------------------------------------------|
| Grenville Orogeny | Seal Lake Group<br>+1323 Ma    | Red Wine Complex<br>+1345 Ma | Seal Lake Group<br>(outliers)                     |                                |                                 |                                                              |
| Neohelikian       | U/C                            | Adamellite<br>*1450 Ma       | U/C                                               |                                |                                 |                                                              |
| Elsonian Event    | Letitia Lake Porphyry          | Anorthosite                  | +1520 Ma                                          | Otter Lake Granite<br>+1496 Ma |                                 |                                                              |
| Paleohelikian     | Petscapiskau Group<br>+1525 Ma |                              | Bruce River Group<br>Uranium Mineral,<br>*1770 Ma |                                |                                 | Walker Lake Granite<br>o 1645 Ma (hbl)                       |
| Hudsonian Orogeny | U/C                            |                              | U/C                                               |                                |                                 | Dominantly Granite<br>(i.e. Long Island Gneiss<br>o 1832 Ma) |
| Aphebian          |                                |                              | Moran Group                                       |                                | Upper Aillik Group<br>+1770 Ma  |                                                              |
|                   |                                |                              |                                                   |                                | U/C(?)                          |                                                              |
|                   |                                |                              |                                                   |                                | Lower Aillik Group<br>o 1832 Ma |                                                              |
| Kenoran Archean   | Archean Basement               |                              | U/C                                               |                                | U/C                             |                                                              |
|                   |                                |                              | Archean Basement                                  |                                | Archean Basement                |                                                              |

+ Rb-Sr (age calculated using  $\lambda = 1.42 \times 10^{-11}$  yrs<sup>-1</sup>; \*U-Pb; o K-Ar.





et al., 1969), until redefined by Stevenson (1970), consists of a bimodal volcanic sedimentary assemblage, ~7620 metres in thickness (25,000 ft) (King, 1963; Gandhi et al., 1969; Stevenson, 1970), unconformably overlying the Archean Hopedale Complex (Kranck, 1953; Sutton, 1972). The Hopedale Gneiss consists of highly contorted, banded gneisses in which the leuco- and melano-cratic layers vary in width from a few inches to several feet, frequently grading into small intrusive bodies of granite (Gandhi et al., 1969; Sutton, 1972). Results of K-Ar dating indicate Archean ages (Wanless et al., 1965; Leech et al., 1963) except along the southern shore of Kaipokok Bay (Gandhi et al., 1969) where Hudsonian ages occur as a result of metamorphism during the Hudsonian Orogenic event. During this latter event the basement-cover contact was modified and nearly completely obliterated and local pegmatitic material can be seen cutting the overlying Aphebian sequence, as for example in the Kitts Pond area (Marten, 1971).

The Aillik Group in the northern part of the Central Mineral Belt (i.e. in the Kitts Pond-Post Hill Belt) consists predominantly of metasediments, including shales, quartzites, conglomerates, limestone, iron formation, and mafic volcanics (both massive and pillowed) (Gandhi et al., 1969). The metamorphic grade of these rocks is of green-schist to amphibolite grade. Further to the south, the





sequence is dominated by acid volcanics with lesser amounts of tuffaceous sediments, quartzites, mafic volcanics and variable sandstones (Watson-White, 1976; Bailey, 1978). Although the rocks have undergone regional metamorphism the grade does not appear to be as high as in the north except locally along shear zones (Bailey, 1978).

Dating of the metasediments and metavolcanics in the north by K-Ar method reflect the Hudsonian metamorphism, giving ages of 1497 - 1545 Ma (Gandhi et al., 1969), however, uranium mineralization at Kitts Pond has been dated at ~1750 Ma (see Chapter 6) and the Long Island Gneiss, intrusive into the Aillik Group, gives a K-Ar age of  $1832 \pm 58$  Ma. Dating of the acid volcanics east of Walker Lake further to the south gave a Rb-Sr isochron age of  $1767 \pm 4$  Ma. These ages would thus imply that the two sequences were not deposited contemporaneously and therefore are not time stratigraphic equivalents.

Several large granitoid bodies of Hudsonian-, and possibly Grenville-age cut the Aillik Group. A large granitic batholith terminates the westward extension of the Aillik Group west of Stipek Lake (Smyth, 1977). The Walker Lake Granite, one of the phases of this granitic mass, gave K-Ar dates of  $1437 \pm 36$  Ma on biotite and  $1645 \pm 46$  Ma for hornblende (Wanless et al., 1974); Rb-Sr dating of the granite was unsuccessful (see Chapter 3). In the eastern



part of the Aillik Group the Strawberry Granite is the most prominent intrusive body and is a massive, fresh, medium- to coarse-grained, pink granite (Stevenson, 1970 ; Kranck, 1953) dated by K-Ar at  $1600 \pm 34$  Ma. A grey, medium- to coarse-grained, massive granite occurs widely throughout the homogeneous pink granite and may represent a different generation of igneous activity. Also cutting the Aillik Group is a prekinematic intrusion, the Long Island Gneiss which was dated using the K-Ar method at  $1832 \pm 58$  Ma (Gandhi et al., 1969). Kranck (1953) and Stevenson (1970) also describe syenitic rocks which cut all the above-mentioned units occurring either as stocks or dykes. The youngest intrusive rocks are mafic dykes of pre- and postmetamorphic age (i.e. Grenville). These occur as long sinuous dykes in the southern part of the area and form prominent topographic highs easily distinguishable on airphotos. Towards the Grenville Front they commonly give K-Ar ages in the 900-1000 Ma range (Gandhi et al., 1969; Grasty et al., 1969).

The rocks of the Aillik Group have undergone a single cycle of orogenic deformation (Gandhi et al., 1969), although several phases are recognized as part of this event in the Kaipokok Bay area (Clark, 1971; Sutton et al., 1971). However, Bailey (1978) recognizes effects of a second orogenic event of Grenville age further to the south in the Walker Lake-McLean Lake area. In the north the structure is



characterized by north-south trending zones 2 - 5 km wide refolded into tight, northeast and southwest plunging folds. In the south of the dominant structural style is tight isoclinal folding trending northeast-southwest with parallel shears usually replacing anticlinal limbs (Bailey, 1978).

The central part of the Central Mineral Belt, extending from Stipeck Lake in the east to Pocket Knife Lake in the West, is underlain by rocks of Aphebian to Paleohelikian age forming the Moran- and Bruce River-Groups respectively (Smyth et al., 1975). These two groups were originally referred to as the Croteau Series by Halet (1946) in a private company report to Dome Exploration. Fahrig (1959) published the first geological map of the western part of the area and redefined the Croteau Series as the Croteau Group, and Williams (1970) mapped the eastern part of the area. Although previous workers recognized the stratigraphic divisions in the area they did not realize the unconformable relationship between the lower and upper units. The recognition of this unconformity by Smyth et al., (1975) subsequently led to the redefining of the Croteau Group into two divisions, the Aphebian Moran Group and Paleohelikian Bruce River Group.

The Moran Group forms a northeast trending belt extending from Pocket Knife Lake in the west to Island Pond in the northeast. It consists of a (1500 - 1600 m thick)





succession of quartzite, iron formation, slate, dolostone, mudstone, and mafic volcanics. Ryan (1978) reported quench texture in thin sections of the mafic units which also exhibit pillowed structures, however, east of Croteau Lake hexagonal cooling joints are developed in the volcanics indicating subaerial deposition (Smyth et al., 1975). To the north the basal unit of the Moran Lake Group overlies the Archean basement which includes granodiorite, migmatite and gneiss.

The Moran Group suffered polyphase deformation prior to the deposition of the overlying Bruce River Group. The first phase produced a slaty cleavage and the second an axial cleavage northeast to northwest with open to closed steeply plunging folds frequently overturned to the north (Smyth et al., 1975). Ryan (1978) reports slivers of the Moran Group infolded in the Archean gneiss in the northeast part of the area.

The Paleohelikian Bruce River Group outcrops over most of the middle area of the Central Mineral Belt, occupying a large open synclinal structure which trends northeast-southwest and plunges to the southwest. The group corresponds to Fahrig's (1957) upper division of the Croteau Group and Williams (1970) Middle and Upper Croteau Group. Three divisions are recognized within the group (Stockwell et al., 1970; Smyth et al., 1975) with a total thickness approximately





10,000 metres (Table 2). The lower division, the Heggart Lake Formation, unconformably overlies the Moran Group and occupies a graben-like structure east of Moran Lake. It consists predominantly of polymictic conglomerate with minor red sediments, and felsic and mafic volcanics. The middle division consists of a basal conglomerate horizon with the majority of the section composed of tuffaceous sandstone and tuff. The uppermost division comprises mafic to acid flows and sills, thick ignimbritic sheets and minor agglomerate, tuff and sandstone. This division has been dated at  $\sim 1520$  Ma (see Chapter 2) using the Rb-Sr method.

The Bruce River Group has been deformed into large, open upright folds that plunge gently to the southwest, an associated fabric is poorly to well developed and is generally axial planar. This fabric is better developed towards the south where the metamorphic grade generally increases (Ryan, 1978). Extensive faulting, trending north-south to northeast-southwest and east-west, has modified the regional geology with the latter set displacing the north-south structures. Ryan (1978) reports an earlier event of reverse faulting which juxtaposed older basement rocks against the younger Bruce River Group rocks. Several shear zones (i.e. Gravelly River, Bruce River, and Minisinakwa) cut the region in a northeast-southwest direction.

The area has been intruded extensively by granitic to mafic bodies. The Junior Lake Granite, east of Moran



TABLE 2

| WEST                                                                                        |                       | EAST                                                              |                       | MINERALIZATION |
|---------------------------------------------------------------------------------------------|-----------------------|-------------------------------------------------------------------|-----------------------|----------------|
| UNIT                                                                                        | Thickness<br>(meters) | UNIT                                                              | Thickness<br>(meters) |                |
| Ignimbrite                                                                                  | 3,000                 | Ignimbrite, rare<br>beds of tuff and<br>tuffaceous sand-<br>stone | 3,000                 | U              |
| Mafic volcanic<br>flows, minor tuff                                                         | 16                    | Mafic volcanic<br>flows, minor tuff<br>and sandstone              | 800                   | Cp, Bn, Gn     |
| Ignimbrite                                                                                  | 170                   | Ignimbrite                                                        | 170                   |                |
| Mafic volcanic<br>flows, minor<br>agglomerate, tuff<br>and sandstone                        | 900                   | Mafic volcanic<br>flows, minor tuff-<br>aceous sandstone          | 1,100                 | Cp, Cc, Bn     |
| Ignimbrite (only<br>north of East<br>Lake)                                                  | 300                   | Ignimbrite                                                        | 700                   |                |
| Mafic volcanic<br>flows, agglomerate<br>and minor thin<br>ignimbrite units<br>at Sosia Lake | 320                   | Mafic volcanic<br>flows                                           | 35                    |                |
| Flow laminated<br>rhyolite or<br>ignimbrite                                                 | 400                   | Ignimbrite<br>Crystal feldspar<br>tuff                            | 700<br>100            | Cp, Gn         |
| Mafic volcanic<br>flows,<br>plagioclase porphyry,<br>minor tuffaceous<br>Sandstone.         | 830                   |                                                                   |                       |                |

DIVISION 3



TABLE 2 - continued

|            | WEST                                           |                       | EAST                                                                         |                       |                |
|------------|------------------------------------------------|-----------------------|------------------------------------------------------------------------------|-----------------------|----------------|
|            | UNIT                                           | Thickness<br>(meters) | UNIT                                                                         | Thickness<br>(meters) | MINERALIZATION |
| DIVISION 2 | Purple porphyritic<br>'dacite'                 | 1,100                 | Grey porphyritic<br>'dacite'                                                 | 800                   | Cp, Cc, Bn     |
|            | Mafic volcanics                                | 100                   | Mafic volcanics                                                              | 170                   |                |
|            | Tuffaceous sand-<br>stones minor acid<br>tuff. | 1,000                 | Tuffaceous sand-<br>stone, minor acid<br>tuff                                | 1,000                 |                |
| DIVISION 1 | Conglomerate                                   | 30                    | Conglomerate                                                                 | 30-60                 | U, Cp          |
|            |                                                |                       | Heggart Lake<br>Conglomerate,<br>minor sandstone,<br>mafic volcanic<br>flows | 1,000                 |                |

Stratigraphic compilation of the Bruce River Group

(U=uranium; Cp=chalcopyrite; Bn=bornite; Gn=galena; Cc=chalcoocite)





Lake, was emplaced prior to the deposition of the Heggart Lake Formation which overlies it unconformably (Smyth et al., 1975). Most of the region from Otter Lake to Stipec Lake south of the Gravelly River shear zone is underlain by the Otter Lake Granite, a medium- to coarse-grained biotite monzonite and granodiorite dated by the Rb-Sr method at  $1497 \pm 37$  Ma (see Chapter 2). This is cut by a sheet-like body of fine-grained, foliated, pink muscovite-biotite granite in the Nipishish Lake area (Ryan, 1978). Minor gabbro, diorite, porphyry and leucogranite also crop out. A coarse-grained gabbroic dyke, the Michael Gabbro, extends in an east-west direction along the southern area.

The western part of the Central Mineral Belt is underlain by the Neohelikian Seal Lake Group, a continental succession of mafic volcanics and sediments intruded by numerous diabase and gabbroic sills approximating 10,000m thick (Fahrig, 1957, 1959; Brummer and Mann, 1961; Christie et al., 1953). It forms an arcuate east-west trending synclinorium (125km x 47km) overturned to the north and truncated to the south by thrust faults. It overlies unconformably both the Bruce River Group in the Stormy Lake Area (Smyth and Marten, 1975) and the Letitia Lake Porphyry south of Seal Lake (Marten, 1975). The presumed unconformity along its northern contact with the Harp Lake anorthosite is obscured by drift, however, Roy and Fahrig (1973) have pointed out



that its aeromagnetic pattern can be traced southwards under the Seal Lake Group for approximately 19 km thus suggesting that the Seal Group is relatively thin along this margin.

The lower part of the Seal Lake Group consists of basal conglomerate intercalated with massive quartzites and mafic volcanics of tholeiitic composition (Baragar, 1974). The central and upper parts of the succession consist of red and white quartzite and slate with minor conglomerate and carbonate. Some volcanics occur in the upper formations associated with native copper which Evans (1952) thought analagous to the Keweenawan area of Ontario. Most of the succession represents continental deposition except for a thin black shale-dolomite unit near its centre and Baragar (1969) and Fahrig (1957, 1959) report some poorly developed pillow textures indicating subaqueous deposition. The metamorphic grade is predominantly prehnite-pumpellyite facies (Baragar, 1974) except in the south where it increases to greenschist facies due to the proximity of the Grenville Front. Wanless et al., (1978) recently dated the volcanic units at  $1323 \pm 92$  Ma using the Rb-Sr method.

The area has been folded into a large synclinorium, the axial trace of which is continuous into the hinge zone of the folded Bruce River Group further to the east. The folds are typically overturned to the north and dip steeply towards the south. Along the southern margin east-west



trending thrust zones are quite common with slices of granite and lower formations of the Seal Group thrust over the younger members.

Most of the intrusive rocks in the area, except for sills and dykes, are pre-Seal Lake Group in age. The Harp Lake Anorthosite in the north acted as a buttress during the folding of the area. The Letitia Porphyry (Marten, 1975) represents the epizonal phase of a larger pluton to the south which has been cut by agpaitic intrusions of the Red Wine Alkaline Complex (Currie et al., 1975).

### 1.3.3 Economic Geology

The Central Mineral Belt contains numerous mineral occurrences with base metals and uranium being the most significant. Evans (1952) compared the Seal Lake Area with its native-copper showings to the Keeweenawan rocks of the Michigan native-copper district and Beavan (1958) recognized the belt as a "uraniferous province." At present most exploration being conducted is directed towards uranium, with Stormy Lake, Moran Lake, Kitts Pond-Post Hill Belt, Makkovik, and Michelin-Burnt Lake areas receiving the majority of attention.

Uranium occurs within all the Proterozoic groups discussed under regional geology. The Aillik Group is host to the Kitts, Nash and Michelin deposits with known reserves





of 11,000,000 lbs. of  $U_3O_8$  (McMillan, 1977), in addition to numerous other occurrences such as Inda, Nash, Gear and Rainbow (Gandhi, 1974). Uranium mineralization occurs in either meta-argillites (i.e. Kitts Pond) or in metarhyolites which are apparently metasomatized (i.e. Michelin, Burnt Lake) with mineralization intimately associated with alkali pyroxene and amphibole. Robinson (1956) refers to nineteen discoveries made by Brinex during the 1955 field season in the Makkovik area within granitized sediments and reported assays of up to 4%  $U_3O_8$  and 800 oz. Ag/ton. Barua (1969) studied the association  $U \pm Mo$  in pegmatitic dykes cutting metarhyolites on the Makkovik coast. Uranium is also known to occur along fractures and shear zones within granites in the vicinity of Walker Lake (Smyth, 1977); for example, the Active Pond and Elbow Pond showings (Gandhi and Guiton, 1975) and the Walker Lake East showing (Krajewski, 1975). These occurrences are commonly related to shears at granite-rhyolite contacts, especially in the Walker Lake-Mustang Lake areas (White, 1977).

Although no significant unaniferous zones have been discovered in the Moran Group, Bernazeaud(1965) reports the discovery of radioactive dolomite pebbles in the conglomerates of the Heggart Lake Formation. The author feels that this group merits further attention in the continued search for uranium and this will be discussed in this





thesis (see Chapters 5 and 7).

Uraniferous horizons occur in the basal member and uppermost member of the Bruce River Group. In the Heggart Lake conglomerate uranium is found in the basal section in the Moran Lake area (Smyth and Ryan, 1977; Ryan, 1977). At Moran Lake uranium is found in sheared conglomerates, volcanic breccias and anorthositic dykes, and in the Brown and Ferguson Lakes area in sheared conglomerates and tuffaceous sandstones, commonly associated with mafic dykes. Numerous uraniferous showings also occur in acid volcanics and ignimbrites in the uppermost division of the Bruce River Group, notably in shear zones as at Madsen Lake (Piche, 1955), Boundary Lake (Robinson, 1956; Ryan, 1978), and Sylvia Lake. Grab samples from these localities ranged from 0.1% to 0.4%  $U_3O_8$  over various distances but indicate that ore potential is there.

The Seal Lake Group also contains uraniferous horizons, notably in its basal member, the Bessie Lake Formation. The most promising locality to date is located at Stormy Lake where arkosic conglomerates unconformably overlie Bruce River volcanics and vein-type mineralization occurs associated with quartz, carbonate, fluorite, chalcopryrite, hematite, pyrite, chalcocite, and native silver (Robinson, 1956; Smyth and Marten, 1975).

Although uranium has received the most attention



from exploration companies other metals have been the focus of attention in the past. The Seal Lake area, with over 250 known copper showings (Brummer and Mann, 1961), was the first to be examined in detail with a number of companies undertaking projects during the 1950's. The Red Wine Alkaline Province, located south of Seal Lake and forming part of the Letitia Porphyry (Marten, 1975), is a unique beryllium deposit explored by Kennco Exploration Ltd., Frobisher and Rio Tinto Canada. Reserves in the area include 11,000 tons per vertical foot of material averaging 0.35 - 0.40% BeO continuing to a depth of 200 feet (Evans and Dijardin, 1962) and another zone of gneiss, 2,400 feet long and 1 $\frac{1}{4}$  feet wide reported to average 0.24% Nb (Smyth et al., 1975). Smyth (1977) and Ryan (1977) mentioned abundant pyrite-pyrrhotite bearing gossan zones within the Moran Group, and Ellingwood (1958) describes a lead-zinc carbonate showing in the Moran Group volcanics located on the north shore of Moran Lake.



## CHAPTER 2

### RUBIDIUM-STRONTIUM DATING

#### 2.1 Introduction

A whole rock Rb/Sr dating program to study five rock suites (two intrusive and three extrusive) was undertaken to supplement the regional mapping of the Central Mineral Belt completed by Smyth et al., (1975), Ryan (1976,1978), Smyth (1977) and Bailey (1978), where ambiguity still remained concerning the ages of particular rock suites. The suites selected for dating included the Otter Lake Granite (Smyth et al., 1975; Ryan, 1978), the Bruce River volcanics and its equivalent the Minisinakwa volcanics (Smyth et al., 1975; Ryan, 1978), the Aillik volcanics (Watson-White, 1976; Bailey, 1978) and the Walker Lake Granite (Smyth, 1977; Bailey, 1978; Watson-White, 1976).

Previous relevant radiometric dating completed in the Central Mineral Belt is summarized in table 3. All the Rb-Sr ages have been recalculated using a decay constant of  $\lambda = 1.42 \times 10^{-11} \text{ yrs}^{-1}$  which was the value employed during this project (Steiger and Jager, 1977).

#### 2.2 Specimen Collection

Sample collection was proceeded with only after regional mapping of the particular unit of interest had been completed. In each case an attempt was made to collect a





TABLE 3

| <u>Method</u> | <u>Rock</u>            | <u>†† Age (initial ratio)</u>                       | <u>Source</u>                  |
|---------------|------------------------|-----------------------------------------------------|--------------------------------|
| Rb-Sr         | Seal Lake Group        | 1323 $\pm$ 92<br>.7035 $\pm$ .0008                  | Wanless & Loveridge<br>(1978)  |
| + Rb-Sr       | Red Wine Complex       | 1345 $\pm$ 75<br>.7021 $\pm$ .0103                  | Blaxland & Curtis<br>(1978)    |
| Rb-Sr         | Petscapiskau Volcanics | 1525 $\pm$ 62<br>.7048 $\pm$ .0006                  | Wanless & Loveridge<br>(1978)  |
| Rb-Sr         | Bruce River Volcanics  | 1526 $\pm$ 44<br>.7038 $\pm$ .0015                  | Wanless & Loveridge<br>(1972)  |
| K-Ar          | Walker Lake Granite    | 1645 $\pm$ 46(hornblende)<br>1437 $\pm$ 36(biotite) | Wanless & Loveridge<br>(1974)  |
| Rb-Sr         | Aillik Volcanics       | 1676 $\pm$ 8<br>.7041 $\pm$ .0003                   | Watson-White<br>(1976)         |
| K-Ar          | Hopedale Gneiss        | 1728 $\pm$ 32(biotite)                              | Gandhi <u>et al.</u><br>(1969) |
| K-Ar          | Long Island Gneiss     | 1832 $\pm$ 58(hornblende & biotite)                 | Gandhi <u>et al.</u><br>(1969) |

---

+ no  $\lambda$  value reported.

†† all Rb-Sr ages calculated using  $\lambda = 1.42 \times 10^{-11} \text{ yrs}^{-1}$



suite consisting of between sixteen and twenty sample locations which covered the widest compositional range available. From each location two 8 - 6 kg samples were collected of the freshest rock available, free of any veining (i.e. epidote, carbonate, quartz), alteration, fractures, and distant from any shear zone.

Sample locations for each of the five suites are given in Figures 3 to 5. In the case of the Walker Lake and Otter Lake Granites, and the Aillik and Bruce River volcanics, the suites collected represent a small percentage of the total outcropping area of the respective units. In contrast to this the samples of the Minisinakwa volcanics represent regional collecting. Each of these methods has its own merits although in theory both should provide good isochrons assuming the Rb/Sr system has remained closed and undisturbed since the time the rock was formed.

### 2.3 Sample Preparation and Analytical Procedure

All samples collected were first reduced in size to approximately 1 kg specimens and run through a jaw crusher several times, being sure to wash the machine between samples to prevent contamination. The pulverized samples were then quartered and enough material selected to give ~10 oz of <200 mesh size rock powder after crushing in a "Tema Swing Mill."





Figure 3

Geology of the Walker Lake-MacLean Lake Area (after Bailey, 1978)

Neohelikian:



Massive to foliated gabbro

Aphebian-Helikian:



Coarse-grained porphyritic and massive (hornblende) granite



Medium- to coarse-grained biotite granite



Fine- to medium-grained leucogranite

Aphebian:

Upper Aillik Group



Massive feldspar rhyolite and quartz rhyolite; tuffaceous sediment



Maroon, grey, green tuffaceous sediment

Archean:



Coarse- to fine-grained foliated granite

Amphibolite, migmatite

|                                    |           |       |
|------------------------------------|-----------|-------|
| Fault or shear                     | . . . . . | _____ |
| Bedding (tops known; tops unknown) | . . . .   | / /   |
| Igneous banding                    | . . . . . | A     |
| Gneissic foliation                 | . . . . . | ↗     |
| Schistosity                        | . . . . . | ↗     |
| Anticline, anticline overturned    | . . . . . | ↗ ↘   |
| Syncline, syncline overturned      | . . . . . | ↘ ↗   |

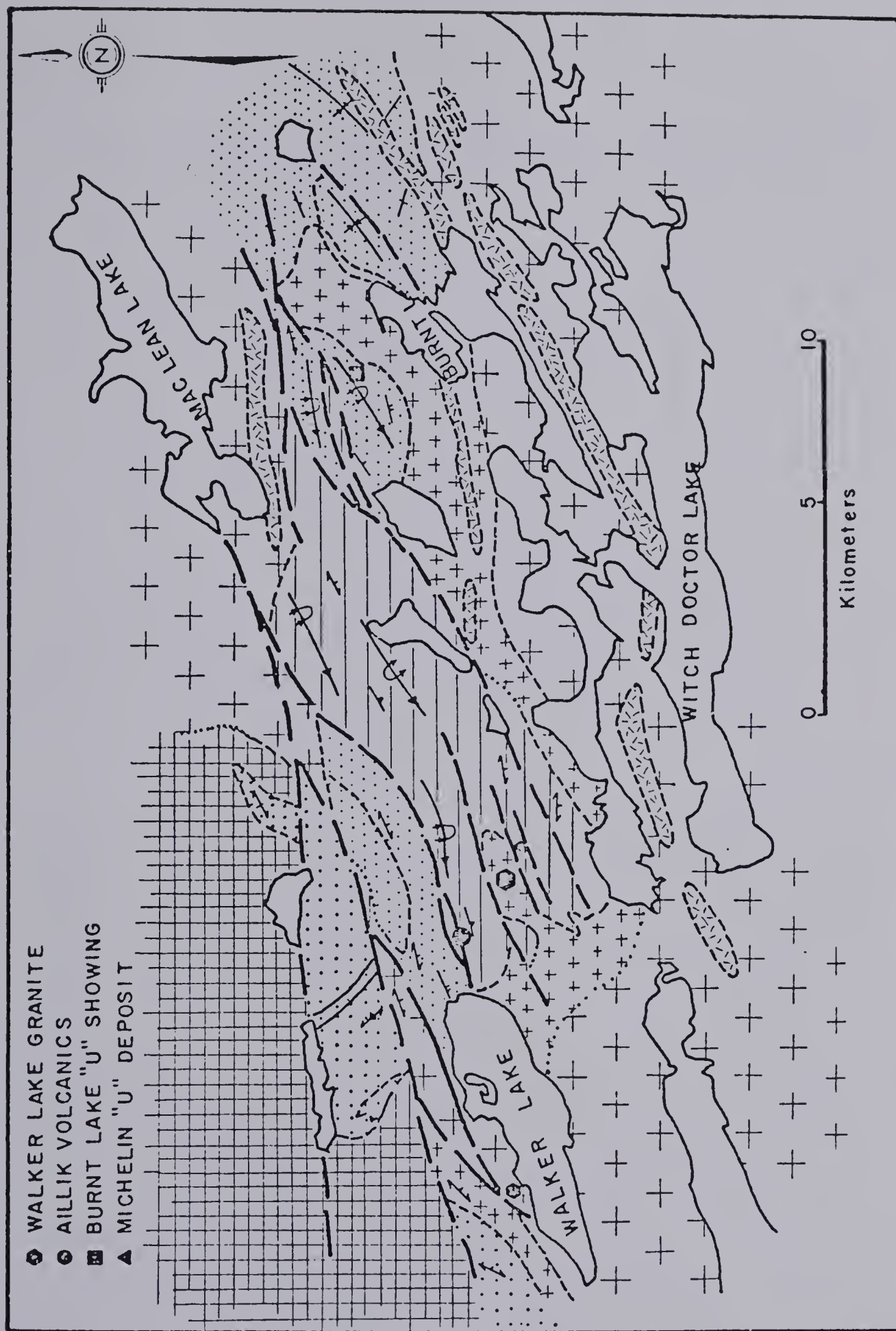








Figure 4

Geology of the Otter Lake-Nipishish Lake Area (after Ryan and Harris, 1978)




Neohelikian

Seal Lake Group

-  Bessie Lake Formation conglomerate, quartzite, mafic volcanics




~~~~~ U/C ~~~~~

Elsonian (?)

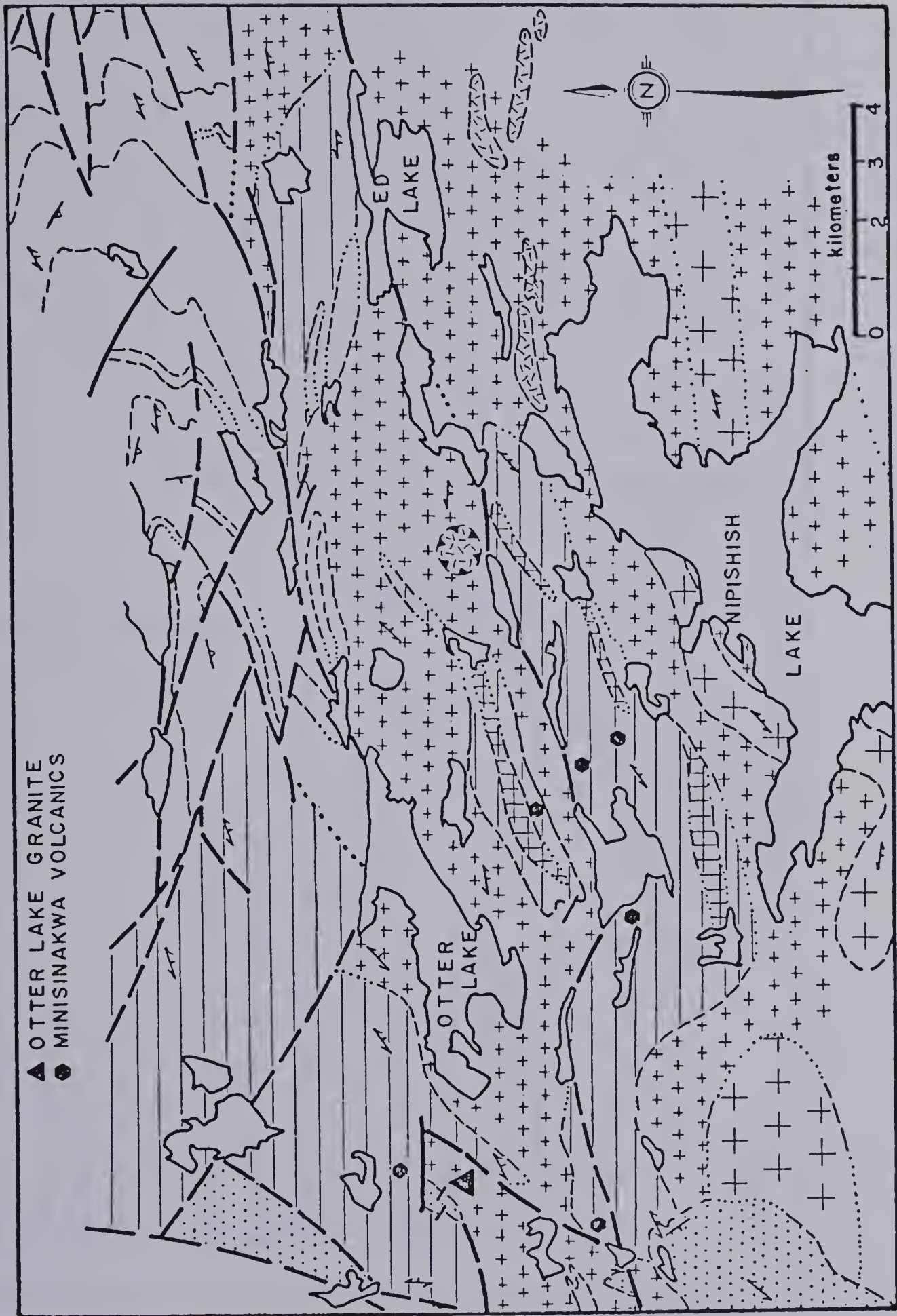
-  Coarse-grained gabbro
-  Fine-grained, biotite-muscovite granite and aplite
-  Otter Lake Granite; medium- to coarse-grained biotite hornblende granite

Paleohelikian

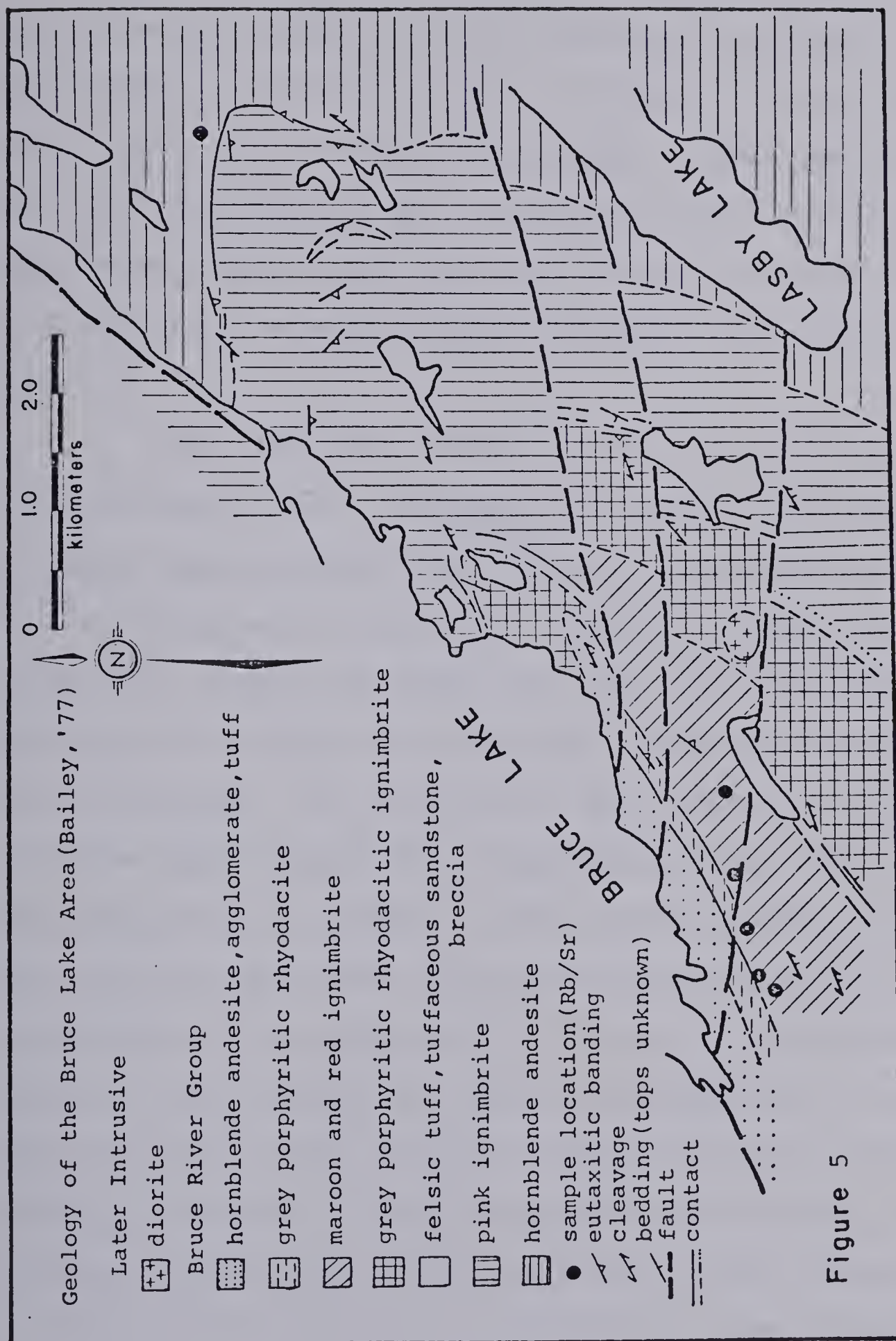
Bruce River Group

-  Andesite flows; tuffaceous sediment
-  Ignimbrite and flows of acidic composition
-  Undifferentiated volcanics and sediments of Bruce Lake map area (see Figure 5)

|                           |       |
|---------------------------|-------|
| Fault or shear . . . . .  | _____ |
| Bedding . . . . .         | /     |
| Igneous banding . . . . . | /     |
| Schistosity . . . . .     | /     |











The rock powders were run on a Phillips XRF unit and semi-quantitative Rb and Sr abundance obtained. The six samples in each suite which provided the most favorable Rb/Sr ratios were selected for dating. These rock powders were then recrushed in the "Tema Swing Mill" to ensure a homogeneous mixture and quartered to give approximately 90 grams of material to be used in Rb-Sr analysis and whole rock chemistry.

The strontium isotopic composition was obtained in the following manner: A sample was weighed out such that it contained approximately 20ug  $^{86}\text{Sr-N}$ , equivalent to the amount of  $^{84}\text{Sr}$  contained in the spike. Into the teflon beaker containing the sample was added the spike and approximately 20 - 25 cc of distilled water wash and the mixture then evaporated to dryness. The residue was then dissolved in a mixture of HF and concentrated  $\text{HNO}_3$  (approximately  $5 \times \text{HNO}_3 = \text{HF}$ ) and then evaporated to dryness. The residue was dissolved three more times in distilled water and concentrated  $\text{HNO}_3$ , saving the solution on the third time rather than evaporating it to dryness. The solution was then transferred into a silica centrifuge tube which contained three drops of concentrated  $\text{Ba}(\text{NO}_3)_2$  solution. A white precipitate of  $\text{Ba}(\text{NO}_3)_2$  formed which also coprecipitates Sr and other alkali elements with it, thus removing Sr from the solution. After centrifuging and pouring off the supernate the crystalline white precipi-



tate was dissolved in a minimum of distilled water, and concentrated  $\text{HNO}_3$  added to promote the precipitation of  $\text{Ba}(\text{NO}_3)_2$ . The precipitation was repeated two times. After completion of this step the precipitate was dissolved in 0.5 ml of 2.5 N  $\text{HCl}$  and run through an anion exchange column to separate the Sr from the other alkalis. The strontium was loaded on a double rhenium filament as a chloride and run on a Micromass 30 mass spectrometer by Dr. H. Baadsgaard, University of Alberta.

The rubidium isotopic composition was obtained in the following manner. Based on preliminary Rb contents obtained from XRF results, an aliquot of sample containing approximately 20  $\mu\text{g}$  of Rb was weighed into a platinum crucible. To this was added the Rb spike, 5 drops of concentrated  $\text{H}_2\text{SO}_4$ , 5 ml demineralized water, and 5 ml vapor distilled  $\text{HF}$ . The dish was heated until the sample was completely decomposed. After evaporating the spiked sample solution to dryness, the  $\text{H}_2\text{SO}_4$  was fumed off on a hot plate and the residue ignited at ca.  $900^\circ\text{C}$  for 20 - 30 minutes. Approximately 0.3 ml of demineralized water was added to the residue and the leach poured into a glass centrifuge tube to which was added a few drops of concentrated  $\text{HClO}_4$  which promoted the precipitation of  $(\text{K},\text{Rb})\text{ClO}_4$ . The white precipitate was washed with demineralized water and then dissolved with a few drops of the same water. The perchlorate solution was



loaded directly onto a rhenium filament and run by W. Day on a Nier type, 6-inch,  $60^\circ$ - sector mass spectrometer equipped with facilities for peak switching between pre-set magnet positions and a digital print out.

#### 2.4 Treatment of Data

The constants employed in calculating Rb-Sr dates were  $^{86}\text{Sr}/^{88}\text{Sr}$  (atomic) = 0.1194 and  $\lambda(^{87}\text{Rb}) = 1.42 \times 10^{-11} \text{ yrs}^{-1}$  (Steiger and Jager, 1977). The maximum analytical errors for individual analyses were:  $^{87}\text{Rb}/^{86}\text{Sr} \pm 0.5\%$  and  $^{87}\text{Sr}/^{86}\text{Sr} \pm 0.004$ . Duplicate determinations performed on six samples for  $^{87}\text{Sr}/^{86}\text{Sr}$ , table 4, indicate a standard deviation of  $\pm .002$  for five of the samples and  $\pm .0169$  for the sixth sample ( $1\sigma$  for single repeat). Whole rock Rb-Sr isochrons were computed using an APL Program "RBSRISOCHRON" written by Dr. Baadsgaard and based upon the method of least squares regression for a straight line of York (1966) and McIntyre et al., (1966). The data are given in Table 5 and the resultant isochrons are presented in Figures 6 to 11. All plots have a Mean Square Weighted Deviant (MSWD) value greater than 2.5, implying that the deviation of the points from linearity is greater than can be attributed to analytical error (McIntyre et al., 1966).





TABLE 4

## Replicate Strontium Determinations

| Sample | $^{87}\text{Sr}/^{86}\text{Sr}$ (atomic) |        | $\Delta$ |
|--------|--|--------|----------|
|        | Original                                 | Rerun  |          |
| BR-8   | 1.6778                                   | 1.6947 | 0.0169   |
| BR-5   | 1.0238                                   | 1.0240 | 0.0002   |
| W-8    | 0.7738                                   | 0.7744 | 0.0006   |
| MZ-4   | 0.7516                                   | 0.7516 | 0.00007  |
| M-12   | 0.8840                                   | 0.8866 | 0.0026   |
| MV-5   | 1.2269                                   | 1.2266 | 0.0003   |





TABLE 5

| <u>Sample</u> | <u>Rb ppm</u> | <u>Sr ppm</u> | <u><math>^{87}\text{Sr}/^{86}\text{Sr}</math> (atomic)</u> | <u><math>^{87}\text{Rb}/^{86}\text{Sr}</math> (atomic)</u> |
|---------------|---------------|---------------|--|--|
| W-13          | 185           | 76            | .8496  | 7.0369   |
| W-16          | 244           | 57            | .9862  | 12.3500  |
| W-11          | 219           | 67            | .9281  | 9.4411   |
| W-8           | 210           | 225           | .7757  | 2.6959   |
| W-7           | 120           | 541           | .7166  | 0.5908   |
| W-9           | 256           | 59            | .9808  | 12.5753  |
| MV-1          | 189           | 44            | .9826  | 12.3169  |
| MV-3          | 172           | 32            | 1.0535   | 15.6733  |
| MV-4          | 180           | 55            | .9113  | 9.5624   |
| MV-5          | 161           | 18            | 1.2298   | 26.0034  |
| MV-6          | 278           | 174           | .8125  | 4.6158   |
| MV-9          | 189           | 256           | .7528  | 2.1381   |
| MZ-10         | 173           | 277           | .7444  | 1.0047   |
| MZ-4          | 185           | 245           | .7534  | 2.1870   |
| MZ-7          | 190           | 194           | .7647  | 2.8367   |
| MZ-9          | 188           | 210           | .7608  | 2.5844   |
| MZ-1          | 161           | 327           | .7349  | 1.4245   |
| MZ-14         | 162           | 133           | .7807  | 3.5031   |
| M-1           | 159           | 42            | .9773  | 10.8233  |
| M-2           | 198           | 35            | 1.1464   | 17.4695  |
| M-4           | 217           | 43            | 1.0749   | 14.6496  |
| M-7           | 154           | 78            | .8463  | 5.7150   |
| M-9           | 13            | 34            | .7305  | 1.0858   |
| M-12          | 178           | 67            | .8853  | 7.6553   |
| BR-1          | 194           | 23            | 1.2406   | 24.7364  |
| BR-5          | 250           | 46            | 1.0269   | 15.7797  |
| BR-7          | 207           | 31            | 1.1387   | 19.3936  |
| BR-8          | 184           | 13            | 1.6822   | 42.3760  |
| BR-9          | 204           | 66            | .8920  | 8.9604   |
| BR-14         | 71            | 516           | .7117  | .3945  |



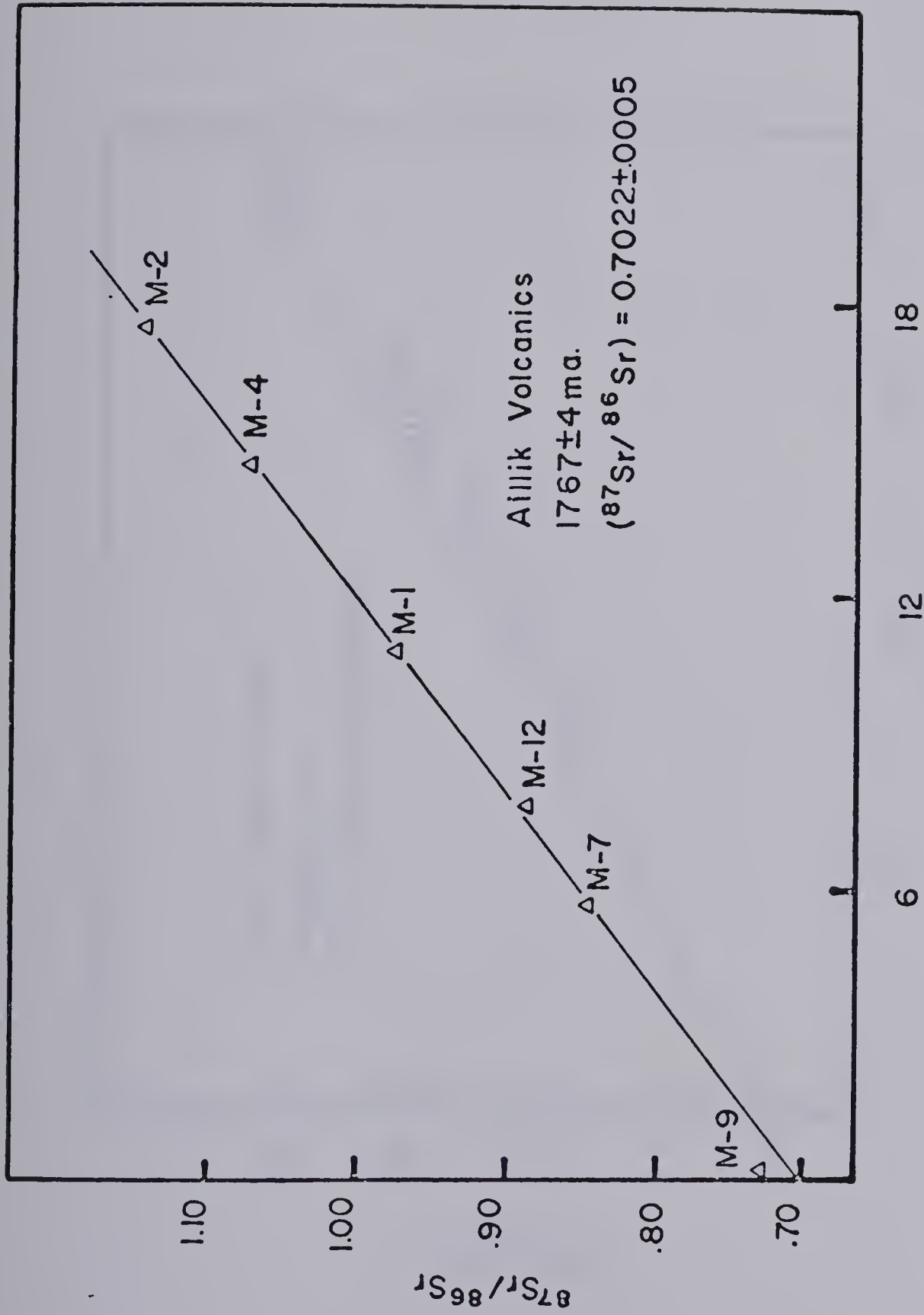


Figure 6

Rb-Sr isochron plot of the Aillik Group volcanics



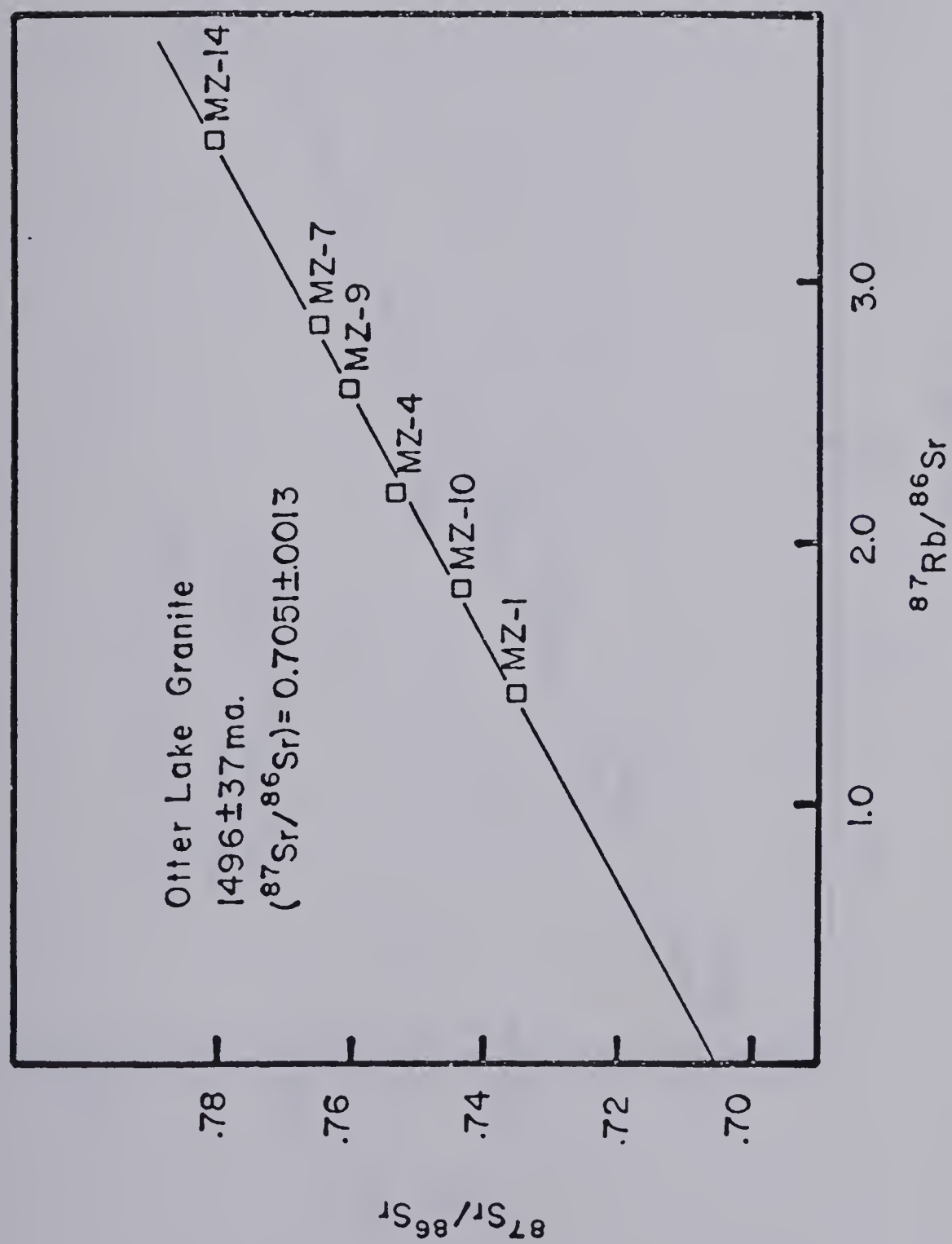


Figure 7

Rb-Sr isochron plot of the Otter Lake Granite





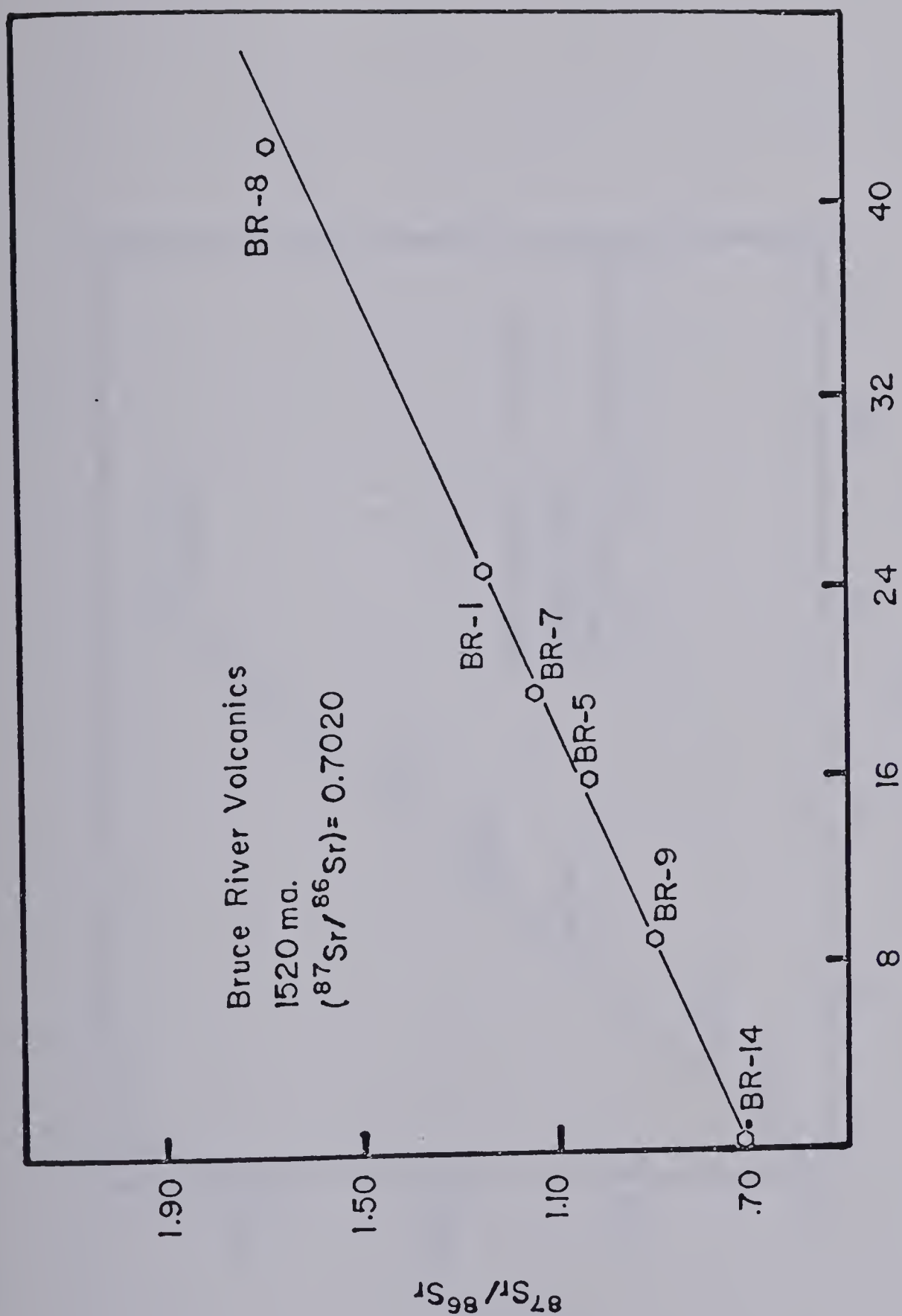

 $^{87}\text{Rb}/^{86}\text{Sr}$ 

Figure 8

Rb-Sr isochron plot of the Bruce River Group volcanics



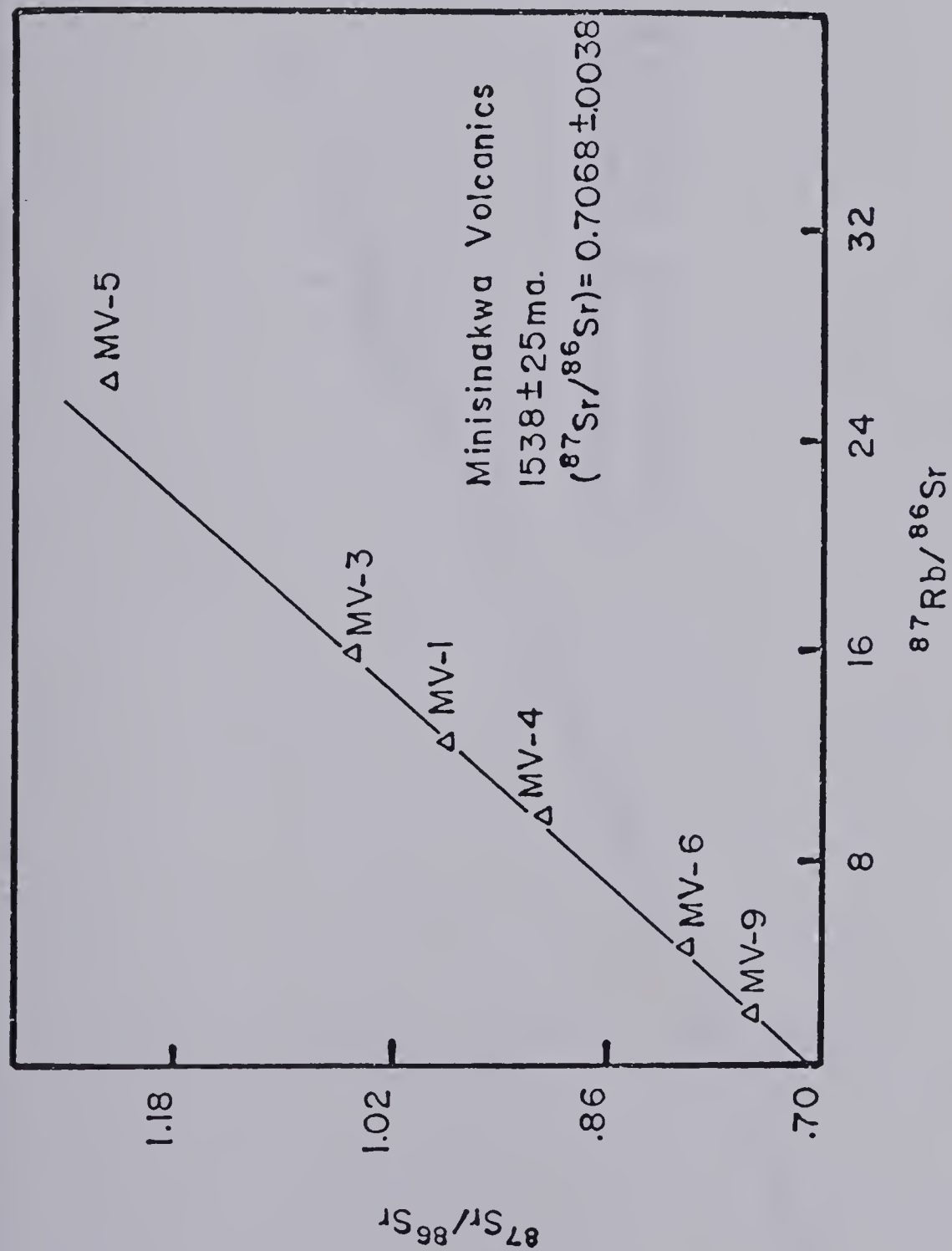


Figure 9

Rb-Sr isochron plot of the Minisinakwa volcanics



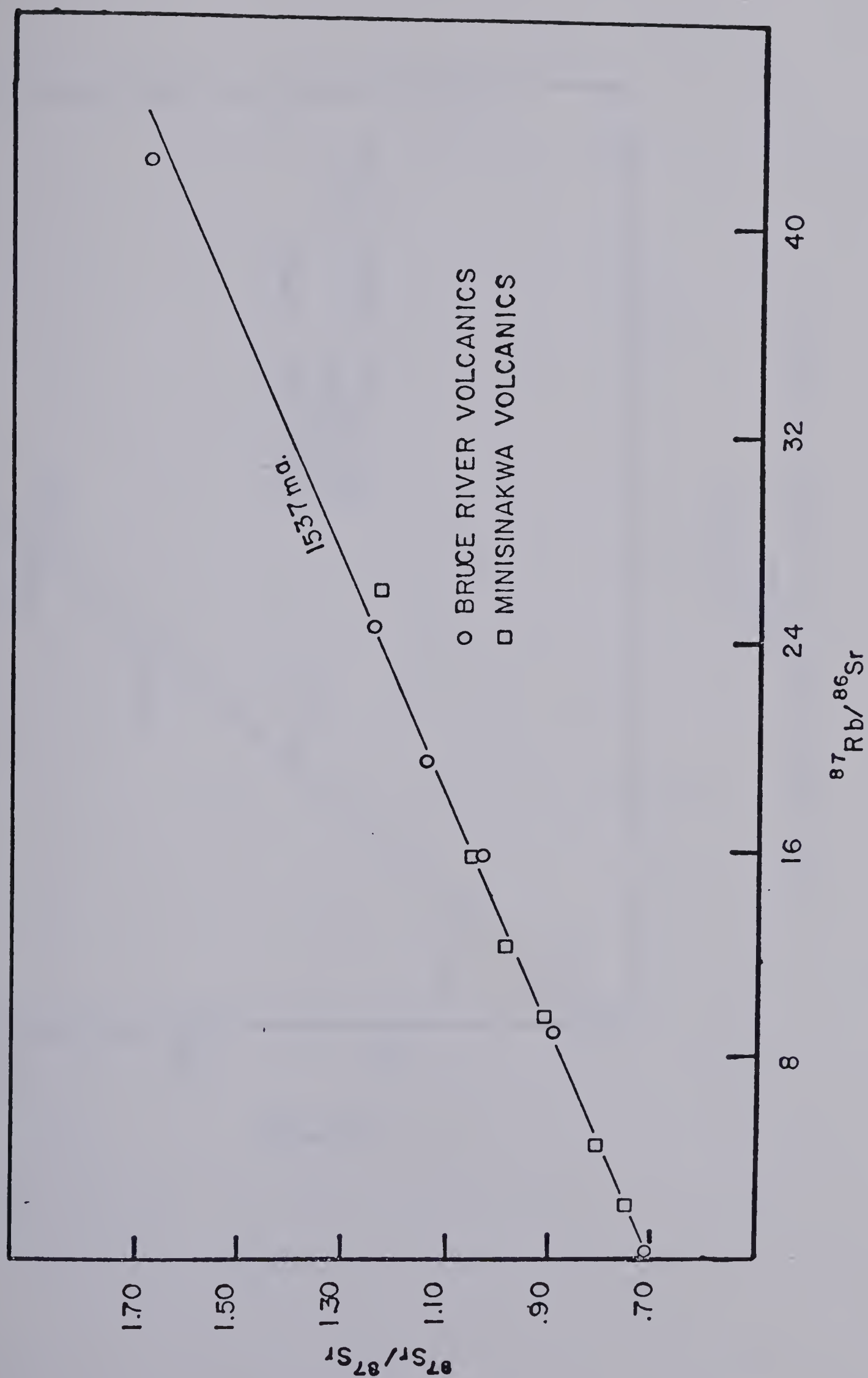


Figure 10

Combined Rb-Sr isochron plot for the Bruce River Group and Minisinkwa volcanics



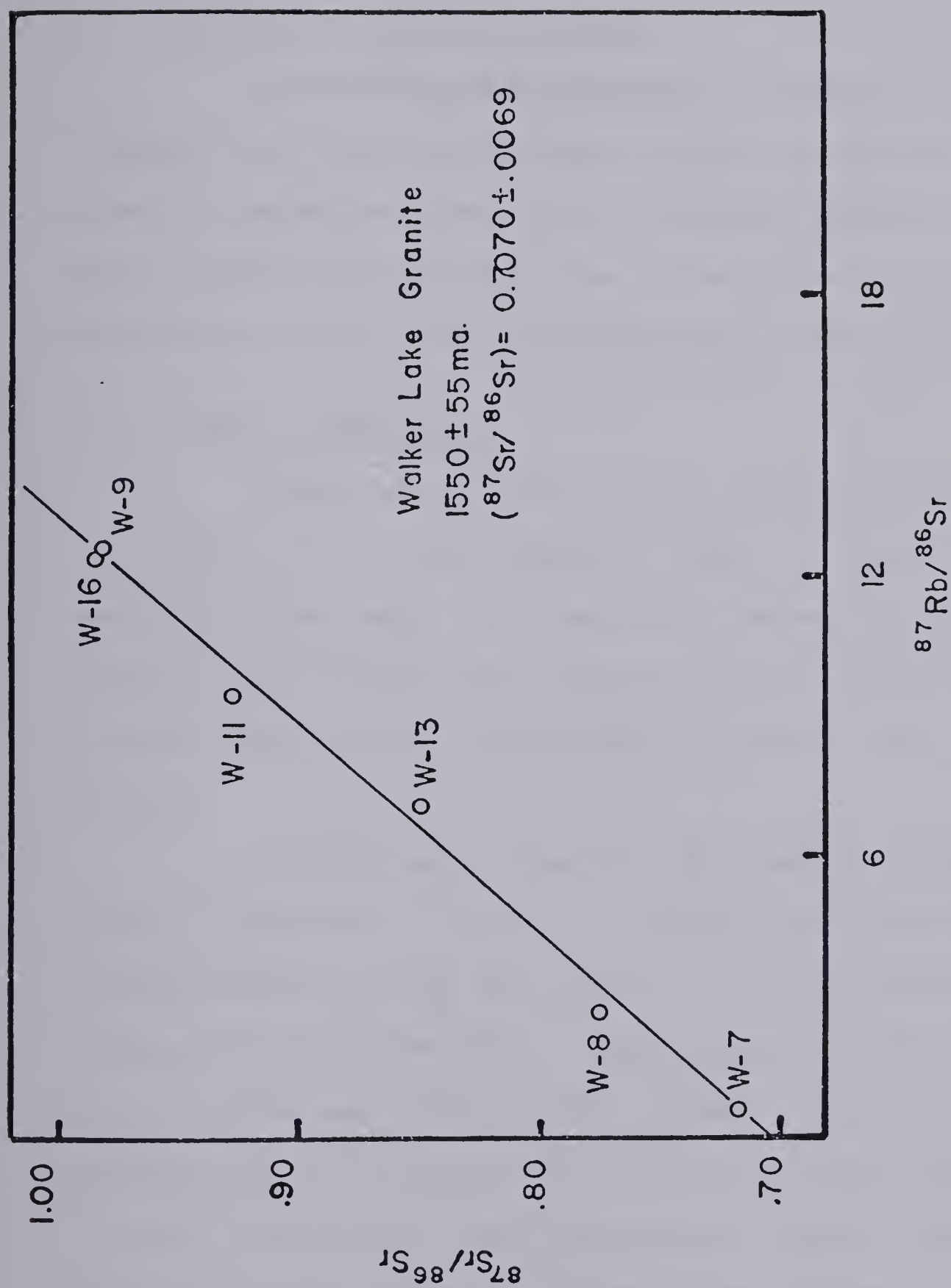


Figure 11

Rb-Sr isochron plot of the Walker Lake Granite





## 2.5 Geology of the Study Areas

The rock suites included in the Rb-Sr geochronological study fall into three regional geographic areas, namely; the Walker Lake Area, the Otter Lake-Nipishish Lake Area, and the Bruce Lake area. The respective geology of these three areas will be described separately below.

### 2.5.1 Walker Lake Area

Sample collection of the Aillik Group Volcanics and the Walker Lake Granite, Figure 3, were carried out east of Walker Lake. The regional geology of the area, Figure 3, has been mapped by Stevenson (1970), Williams (1970), Smyth (1977), Watson-White (1976), and Bailey (1978).

A large area underlain by granite extending from south of Yvon Lake to east of Walker Lake separates the Aphebian Aillik Group to the east from the Aphebian Moran Group, Paleohelikian Bruce River Group and Archean basement rocks to the west. The Aillik Group within the study area consists of felsic rocks of volcanic, volcanoclastic or pyroclastic, tuffaceous, and ignimbritic origin. Bailey (1978) describes these different lithologies within the Walker Lake-McLean Lake Area and also Archean rocks crop out northeast of Walker Lake which may represent the basement



upon which the Aillik Group was deposited. Both Bailey (1978) and Smyth (1977) have observed the Walker Lake Granite cutting Aillik Group volcanics and sediments at the east end of Walker Lake.

In the northwestern part of the map area greenstones, migmatites and gneissic rocks of Archean age crop out (Ryan, 1977). The Aphebian Moran Group, consisting of slates, dolostones, and mafic volcanics, unconformably overlies the older basement rocks (Ryan, 1977) and outcrops in a 15 - 20 km long, sinuous belt stretching from Stipec Lake eastwards to Del Rizzo Lake. The Paleohelikian Bruce River Group (Smyth et al., 1975) outcrops to the north and west of Stipec Lake and consists of a basal conglomerate and sandstone unit, a middle tuffaceous unit, and an upper felsic volcanic-ignimbritic unit. Both Ryan (1977) and Smyth (1977) have observed hornfelsing of tuffaceous sediments of the Bruce River Group and Smyth (1977) has also reported granitic dykes cutting the sediments.

The granitic terrain in the map area has been divided into numerous phases mappable on a regional scale. The oldest is an undifferentiated granite (unit 5, Smyth, 1977) which displays a strong foliation and is overlain unconformably by tuffaceous sediments of the Bruce River Group north of Stipec Lake. A leucogranite outcropping northwest of Stipec Lake is considered to be of Aphebian



age by Smyth (1977; unit 6) on the basis of structural data, however, Ryan (1978; unit 13) considers the same granite to be an extension of the Otter Lake Granite further to the west. The Walker Lake Granite, underlying most of the southern area from Walker Lake westwards to Yvon Lake, consists of two or three (?) recognizable phases (Smyth, 1977; Bailey, 1978). These are a (i) fine- to medium-grained leucogranite and quartz monzonite, (ii) a medium- to coarse-grained, grey and pink biotite granite, biotite-hornblende granite and granodiorite, and (iii) possibly an undefined potassic granite. Generally the Walker Lake Granite is a pink to grey rock containing 10 - 15% biotite and hornblende, often altered to chlorite, and varying proportions of K-feldspar and plagioclase. It varies from undeformed to strongly foliated where shear zones are present. The age relations of the different phases relative to each other is not known although Bailey (1978) suspects that they may be gradational. Other intrusives in the area include a megacrystic granite outcropping northwest of Walker Lake and intrusive into the Walker Lake Granite, and in the south a few plugs of gabbroic material outcrop forming part of the Michael Gabbro (Fahrig and Larochelle, 1972).

#### Petrography of the Walker Lake Granite

Six specimens of the Walker Lake Granite were





examined in thin section, these were from the same rock samples used for radiometric dating.

In hand specimen (total of fourteen different samples) the Walker Lake Granite is a medium-grained, leucogranite consisting of essentially two different phases. Immediately north of Walker Lake it contains approximately 5 - 10% biotite, 10% quartz, 40 - 45% K-feldspar, and 40% plagioclase. The amount of biotite may increase locally, especially where a fabric is developed. The plagioclase, usually a greenish color due to alteration to epidote, and K-feldspar are noticeably coarser than the rest of the rock. In particular, the K-feldspar may appear as phenocrysts up to 15 mm in size compared to the average grain size of 4 - 6 mm; it also displays a well developed zoning easily distinguished in hand specimen. The quartz varies from a smokey grey to a blue color and even in hand specimen can be seen to form aggregates rather than single, large crystals thus suggesting recrystallization. In one locality 3 - 6 cm size inclusions of diorite were contained within a monzonite phase of the granite.

The second phase which was collected, a medium-grained leucogranite, outcrops southeast of Walker Lake and consists of quartz 30%, K-feldspar 50 - 60%, plagioclase 10%, and biotite 5%. The color may vary towards pinkish depending on the presence of either white or pink feldspar.



The texture is medium-grained, equigranular with no phenocrysts of either plagioclase or K-feldspar noted. The plagioclase may again be a greenish color due to alteration to epidote and the quartz was noted to form aggregates rather than large, single crystals. Locally a fabric may be developed due to shearing, a common feature in the area (Bailey, 1978).

Modal analyses of six specimens examined in thin section, Table 6, reflect the compositional difference between the two phases, Figure 12; a potassi rich phase and a quartz monzonite. Specimen W-8 has been invaded by veined (?) quartz biasing its position in the quartz-rich portion of the granite field rather than placing it in the quartz monzonite field.

In thin section the rocks show a hypidiomorphic granular texture, sometimes bordering on allotriomorphic granular or porphyritic. No fabric was observed in thin section, however, other evidence suggesting a past history of deformation was observed. Major mineral phases present in decreasing order of abundance are orthoclase, perthitic orthoclase, microcline, microperthite, quartz and plagioclase with minor biotite, muscovite, hornblende, opaques, and accessory minerals of sphene, apatite, zircon, fluorite, epidote and garnet.

Quartz occurs either as a coarse anhedral phase intergrown with the feldspar and/or as part of a quartzo-



TABLE 6

|             | <u>Walker Lake Granitoids</u> |            |             |             |            |             |
|-------------|-------------------------------|------------|-------------|-------------|------------|-------------|
|             | <u>W-7</u>                    | <u>W-9</u> | <u>W-11</u> | <u>W-16</u> | <u>W-8</u> | <u>W-15</u> |
| plagioclase | 33                            | 16         | 13          | 8           | 10         | 8           |
| quartz      | 16                            | 25         | 35          | 33          | 50-65      | 20-25       |
| feldspar    | 47                            | 58         | 50          | 58          | 35-40      | 65-70       |
| biotite     | 3                             | -          | <0.5        | 1           | 0.5        | <0.5        |
| Muscovite   | -                             | <0.5       | <0.5        | -           | -          | -           |
| opaques     | .5                            | -          | 0.5         | -           | -          | -           |
| chlorite    | .5                            | 1          | tr.         | -           | -          | 0.5         |
| accessory   | tr.                           | tr.        | <0.5        | tr.         | -          | -           |



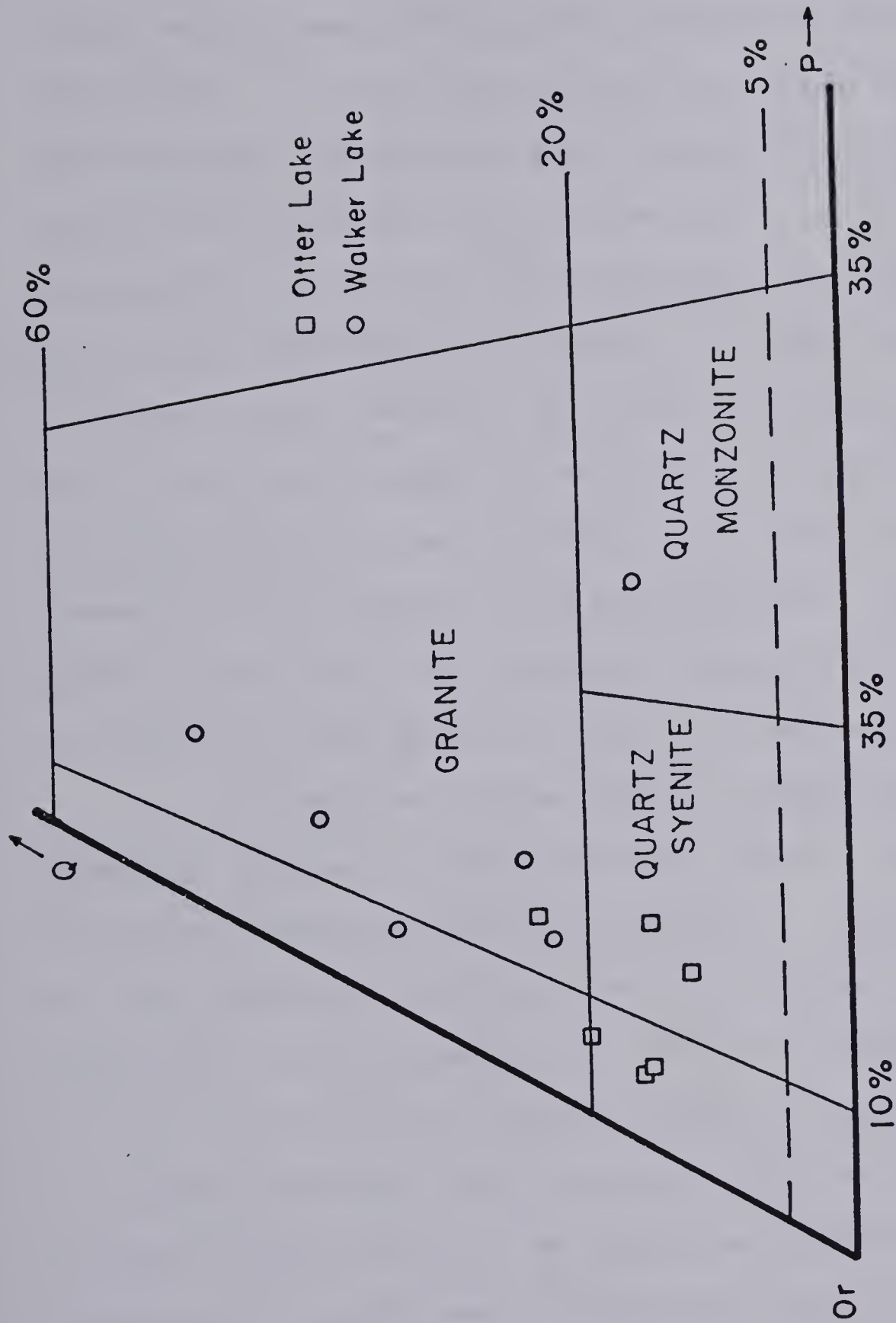


Figure 12

Ternary diagram plot (quartz-K-feldspar-plagioclase) for the Walker Lake and Otter Lake Granites





feldspathic, fine-grained crystalline aggregate which appears to have formed as a result of recrystallization of larger orthoclase crystals, with muscovite also developed in the process. In the former case the larger grains show both straight and embayed grain boundaries with adjoining orthoclase and plagioclase grains and in a few instances granophyric intergrowth with orthoclase was observed (myrmekite). In the latter quartz is either body embayed or shows a well developed granoblastic polygonal texture and in both cases undulose extinction is present. Specimen W-8 shows best the development of the granulated texture believed to have resulted from metamorphism. The coarser quartz grains have inclusions of sericite and rutile whereas the finer grained phases are free of inclusions.

Orthoclase occurs either as equidimensional, coarse, subhedral grains or finer-grained, anhedral grains in a quartzo-feldspathic granular aggregate. Grain boundaries are well preserved but in numerous instances grains are rimmed by a fine aggregate of quartz and K-feldspar  $\pm$  muscovite. In some sections (i.e. perpendicular to the X-axis) two well developed cleavages could be seen, their development perhaps related to deformation. No zoning was observed and carlsbad twinning was rarely seen. Perthitic growth is common with the varieties observed being string and vein perthite. Undulose extinction is common in most grains.



Microcline microperthite is the most abundant constituent of some sections and occurs as large, equidimensional subhedral to anhedral grains. The exsolution texture is commonly string perthite with lesser amounts of vein and broad perthites. Poikilolitic inclusions of sericite are common but not ubiquitous.

Plagioclase, a calcium-rich oligoclase variety ( $An_{26}$ ) occurs as large euhedral to subhedral tabular crystals twinned by the albite, carlsbad and pericline laws. In some cases borders have been badly corroded by later stage formation of orthoclase and myrmekite development was observed a few times. Alteration to green epidote is ubiquitous and in some instances up to 30% of the grain may be affected. Bent twin lamellae, fractured grains, and undulose extinction are all common and finely scaled oscillatory zoning was observed in a few instances.

Biotite(sagenitic) is the main mafic mineral present and is a greenish brown variety owing its color to  $Fe^{2+}$  and low  $Ti + Fe^{3+}$  (Heinrich, 1965). It is anhedral to subhedral in shape and is usually badly corroded and variably altered to chlorite. Euhedral muscovite can be seen to cut across earlier-formed biotite. Inclusions of zircon and sphene are quite common, forming along the cleavage direction. Associated with biotite clusters are accessory euhedral to subhedral sphene and almandine garnet.

Hornblende, where it was observed, occurs as



remnant cores in chlorite and biotite and never as separate, solitary grains. It shows a strong green pleochroism and exhibits its  $120^{\circ}$  cleavage pattern. Hornblende was generally minor although it may have originally accounted for a higher modal content of the granite before subsequent alteration.

Aillik Volcanics - Petrography of Samples Collected from  
Michelin Ridge

Six thin sections of the Aillik volcanics were examined petrographically, these were from the same rock samples used for radiometric dating.

In hand specimen (total of 15 different locations) the Aillik volcanics are quartz-feldspar porphyries of maroon color exhibiting textures indicative of an ignimbritic or nuée ardente origin (Ross, 1960). They lack any well developed fabric but show evidence of having undergone deformation. Veinlets of epidote can be seen randomly cutting through outcrops. The phenocrysts of quartz (2 - 3 mm) and feldspar (3 - 5 mm) commonly compose 15 - 20% of the rock with quartz usually two to three times more abundant and characterized by its blue color and elliptical shape. The feldspar is typically tabular in shape and shows no signs of alteration.

In thin section, the rock consists of variable





proportions of quartz, feldspar, microcline and plagioclase phenocrysts in a recrystallized, microcrystalline quartz and feldspar matrix with accessory epidote, sphene, chlorite, and sericite with coarser lenses of quartz and feldspar which show eutaxitic-like texture, probably recrystallized shards of pumice.

The quartz phenocrysts occur in a variety of forms from euhedral, six-sided cross-sections to elliptical shaped aggregates of finer-grained quartz with well developed triple points. Undulose extinction is common to all the grains as are inclusions of rutile, sericite, and some apatite.

K-feldspars vary from euhedral, unaltered phenocrysts of orthoclase, perthitic orthoclase, microcline and chessboard albite to subhedral and badly fractured and corroded grains. Alteration of feldspar to sodium plagioclase (metasomatism ?), sericite and occasionally carbonate occurs although it is sometimes patchy and not pervasive.

Plagioclase,  $An_{27-34}$ , is subhedral to euhedral, very fresh, and is twinned by the albite and pericline laws. Bent lamellae and undulose extinction are present but not ubiquitous. In one case a large plagioclase grain (6-7 mm) was badly fractured and invaded by the matrix.

The matrix consists of a microcrystalline aggregate of quartz and feldspar with coarser lenses of the same



material where pumiceous fragments have recrystallized. The texture of the matrix could be described as fine-grained granular with good development of triple points indicating recrystallization. In one slide (M-7) up to 2% epidote was present in thin bands parallel to the rock fabric and recrystallized pumice shards. Magnetite may compose up to 2% of the groundmass either as irregular-anhedral grains or cubes.

All thin sections indicated relatively fresh, unaltered felsic volcanics except for M-12 which shows noticeable alteration of both the phenocrysts phase and the matrix. Alteration is primarily sericite, kaolinite, epidote and carbonate although in hand specimen this cannot be discerned.

#### 2.5.2 The Otter Lake - Nipishish Lake Area

Sample collection of the Otter Lake Granite was carried out west of Otter Lake, Figure 4, and for the Minisinkwa volcanics between Otter Lake and Nipishish Lake, figure 4. The regional geology of the area is included in the maps of Fahrig (1959), Smyth et al., (1975), and Ryan (1978).

The map area consists of two major units; the Otter Lake Granite and the Minisinkwa volcanics. The latter is an informal name applied to volcanic rocks of the Paleohelikian Bruce River Group found south of the Gravelly River Shear Zone around Lake Minisinkwa.



The Minisinakwa volcanics correspond to the uppermost division of the Bruce River Group and consist of dacite and rhyodactites, which are generally porphyritic in texture with feldspar dominating, although small quartz eyes, blue in color, are sometimes present. Intercalated with them are thin units of lapilli tuff and crystal tuff, volcanic breccia and tuffaceous sandstone. Porphyritic andesite and poorly- to well-banded, mafic to intermediate tuffs also form local mappable horizons (Ryan, 1978).

The Otter Lake Granite underlies most of the map area east of Otter Lake and forms an extensive batholith stretching eastwards to Stipeck Lake suggesting its equivalence to the Walker Lake Granite. It is typically a medium- to coarse-grained biotite-hornblende granite or monzonite with minor phases of leucogranite and diorite. It is variably altered with completely fresh specimens rarely seen, and displays a local fabric commonly associated with shear zones. It shows intrusive relations into the Minisinakwa volcanics.

West of Nipishish Lake a fine-grained, foliated muscovite-biotite granite and aplite outcrop. West of Katy Lake the aplitic phase was seen cutting the Otter Lake Granite. In the south of the map area coarser grained gabbroic dykes outcrop as part of a northeast-southwest extending sinuous body. A klippen of this rock is found northwest of Nipishish Lake (Ryan, 1978).





### Petrography of the Otter Lake Granite

Six thin sections of the Otter Lake Granite were examined petrographically, these were from the same rock samples used for radiometric dating.

In hand specimen (total of 15 different locations) the Otter Lake Granite is a medium- to coarse-grained, leucocratic to pink monzonite or quartz syenite consisting of 5 - 10% quartz, 10% biotite, 40 - 60% pink or white K-feldspar and 25 - 40% plagioclase. The plagioclase, sometimes a greenish color due to alteration to epidote, and K-feldspar which also shows alteration, are either equigranular with respect to the rest of the rock or form distinctly larger crystals up to 6 - 8 cm in size. In the latter case zoning of these larger crystals can be seen in hand specimens. The quartz is usually a smokey grey variety and occurs as aggregates of finer grains rather than single, coarser grains. Minor amounts of pyrite occur associated with locally developed clusters of biotite. No fabric is present although on a regional traverse the granite may grade into an augen gneiss variety where shear zones are developed (i.e. south of Otter Lake). Fine-grained, aplitic dykes can be seen cutting the host granite, the best example of this phenomenon occurring west of Katy Lake.

Modal analysis of the six specimens examined in thin section, Table 7, are plotted on a ternary diagram,





TABLE 7

Otter Lake Granitoids

|             | <u>MZ-1</u> | <u>MZ-4</u> | <u>MZ-9</u> | <u>MZ-7</u> | <u>MZ-10</u> | <u>MZ-14</u> |
|-------------|-------------|-------------|-------------|-------------|--------------|--------------|
| plagioclase | 9           | 10          | 3           | 15          | 5            | 12           |
| quartz      | 13          | 15          | 16          | 15          | 20           | 23.          |
| feldspar    | 75          | 70          | 80          | 70          | 75           | 65           |
| biotite     | <1          | <1          | 0.5         | -           | -            | -            |
| Muscovite   | -           | -           | -           | -           | -            | -            |
| opaques     | -           | 1           | <1          | 0.5         | -            | -            |
| chlorite    | 2.3         | <1          | 1           | 1           | 0.5          | 1            |
| accessory   | 0.5         | 0.5         | 0.5         | 0.1         | 1            | 0.5          |
| amphibole   | 0.5         | -           | -           | -           | -            | -            |



figure 12, and show the alkalic nature of the granite. In thin section the rock shows a hypidiomorphic to idiomorphic, granular texture with porphyritic varieties due to granulation of the matrix leaving remnant crystals of feldspar and plagioclase. A granular texture of fine-grained K-feldspar quartz <sup>+</sup> muscovite or sericite occurs between orthoclase and quartz or other orthoclase grains. In some instances this texture (i.e. MZ-14) may comprise 20 - 30% of the thin section. The major mineral phases present in decreasing order of abundance are orthoclase, perthitic orthoclase, plagioclase, quartz, microcline, and microcline microperthite, minor amounts of biotite, chlorite, and hornblende and accessory sphene, epidote, magnetite, apatite, zircon and fluorite.

Orthoclase is the main mineral phase present, occurring as coarse, equidimensional subhedral grains sometimes showing euhedral outlines especially in zoned crystals. It also occurs as a fine-grained recrystallized phase intergrown with quartz. Alteration to sericite and a fine, dirty brown material (kaolinite ?) is common; this process is somewhat selective and only the core of the grain or particular zones are altered. Granophyric intergrowths with quartz was observed a few times. Perthitic orthoclase also occurs with the perthite developed as a string or vein type.

Plagioclase, An 26-29, occurs as subhedral to



euohedral grains and in varying degrees of alteration to epidote and sericite. Twinning follows the albite and carlsbad laws and infrequently pericline twinning occurs. Bent twin lamellae and undulose extinction are fairly common.

Quartz occurs mainly as aggregates of anhedral fine- to medium-grains formed from the recrystallization of coarser quartz grains. Undulose extinction is ubiquitous and inclusions of rutile in the coarser grains were frequently observed.

Biotite, a brown green sagenitic variety, occurs as subhedral, rarely euohedral, flakes in clusters replacing hornblende and itself being altered to chlorite. Inclusions of apatite, zircon, and sphene are common forming along cleavage partings. Where chlorite is replacing biotite, rutile occurs as inclusions in the former.

Euohedral to anhedral sphene, up to 4 mm in size, occurs mainly as wedge shaped crystals with a distinct reddish brown pleochroism. Where it occurs as inclusions in associated brown-green biotite, radioactive haloes are common.

#### Petrography of the Minisinakwa Volcanics

Five thin sections of the Minisinakwa volcanics were examined petrographically, from the same rock samples used for radiometric dating.





In hand specimen (total of 15 different locations) the Minisinakwa volcanics vary from massive, buff and purple colored rhyolites frequently containing quartz eyes (1-3%) and euhedral K-feldspar (5-20%), to hornblende andesites. The rhyolites may be of a massive variety or sometimes are quartz sercite schists with or without chlorite. In some instances textures indicative of an ignimbritic origin could be discerned. The andesites are typically dark green in color and may contain phenocrysts (2-4 mm) of plagioclase and/or hornblende. The only visible signs of alteration of the volcanics is a greenish (epidote ?) tinge on the feldspars.

In thin section the rocks consist of variable amounts of quartz, K-feldspar, and plagioclase phenocrysts (section of hornblende andesite was not available) in a microcrystalline, quartz-feldspathic matrix. The matrix is occasionally recrystallized and contains additional minor amounts of muscovite and biotite, and accessory garnet, epidote, carbonate, fluorite and zircon.

Quartz phenocrysts are usually void of inclusions, anhedral in shape, exhibit undulose extinction, are partially recrystallized to a finer-grained aggregate of quartz and are cut by fractures. In some cases they are enveloped by flow banding consisting of recrystallized pumiceous shards composed of quartz and feldspar and exhibiting a granoblastic,



polygonal texture.

Plagioclase (An 26-28) crystals are subhedral to euhedral in habit and of tabular shape. Their cores are frequently in various stages of replacement by epidote and are rimmed by a finer grained aggregate of quartz, feldspar, muscovite and biotite. They are invariably orientated so that their long axis is parallel to both the fabric (if present) and igneous banding.

K-feldspar crystals vary from euhedral to anhedral and may be clear to intensely altered to fine-grained white mica or kaolinite. Their habit varies from rectangular to cubic with the former more predominant. As with the plagioclase they may be bordered by a finer-grained aggregate of quartz and feldspar with lesser biotite and muscovite. Sometimes portions of individual K-feldspar grains are partially replaced by albitic plagioclase, possibly an alteration syncontemporaneous with deposition of the volcanics (Scott, 1971).

The matrix consists predominantly of quartz and feldspar and is usually granoblastic polygonal in texture. A slight lepidoblastic fabric is defined by biotite and muscovite which also parallels remnant igneous banding. In one section (M-3) some grains of euhedral almandine garnet were observed, but whether these are of metamorphic or primary igneous origin was not resolved.



### 2.5.3 The Bruce River Area

Samples of the Bruce River volcanics were collected just south of Bruce Lake, Figure 5. The geology of the area has been mapped on a regional scale by Fahrig (1959) and Smyth et al., (1975), and Figure 5 shows more detailed geology of the area as mapped by Bailey (1977).

The area lies in the nose of a large synclinal structure which has been modified by subsequent faulting. The volcanic sequence is composed of interbedded, fine-grained hornblende andesite flows (units 1 and 7) and ignimbrites of rhyodacitic composition and minor felsic tuffs. Original textures have been preserved and the degree of deformation is negligible compared to the area further to the south. The volcanic pile is cut by an intrusive plug of fine-grained, equigranular diorite of unknown age.

### Petrography of the Bruce River Volcanics

Five thin sections, taken from the specimens used for radiometric dating, were studied petrographically.

In hand specimen (total of 15 different localities) the Bruce River Volcanics are grey, red and maroon colored massive felsites to feldspar porphyries which exhibit characteristics particular to ignimbrites. At the base of the section, east of Bruce Lake, hornblende andesites occur. Phenocrysts in the felsites are predominantly feldspar,





varying between 5% and 15% (although 20 - 25% may occur) and between 4 - 8 mm in size with tabular outlines and slight alteration. Blue quartz phenocrysts, 1 - 3 mm in size and of elliptical shape, do occur but never account for more than 1 - 2% of the mode. A well developed cleavage is locally present but not pervasive throughout the section. Eutaxitic textures, enclosing feldspar crystals when present, are ubiquitous and parallel the metamorphic fabric where developed.

In thin section, orientated phenocrysts of orthoclase, microcline, sanidine, plagioclase and quartz sit in a microlitic matrix which shows well developed flow banding defined by magnetite layering and recrystallized and flattened pumice fragments. Orthoclase is the dominant phenocrystic phase occurring as euhedral to anhedral, equidimensional crystals which may be rimmed by a border of quartz and feldspar or be in various stages of breaking down to an aggregate of finer-grained feldspar which typically exhibits wandering extinction. Alteration to sericite is usually restricted to the central portions of the grain and is never very extensive; alteration to chessboard albite also occurs as patches within some orthoclase grains as does development of carbonate, noticed in BR-8 and especially BR-9. The carbonate alteration is restricted to the phenocrystic phase and was not observed to be developed in the matrix. Where





the eldspar has broken down to a finer-grained aggregate of K-feldspar the boundaries are frequently embayed. Carlsbad twinning was seldomly observed, and in one case hourglass structure was developed.

Plagioclase, An 26-34, occurs as large (4 - 6 mm) tabular, subhedral phenocrysts which are usually badly fractured. It is only slightly altered to sericite and epidote and in a few cases carbonate was developed. Twinning was by the albite, pericline, and carlsbad laws and zoning was absent. Wandering extinction commonly occurred in badly fractured grains.

Sanidine occurs rarely as subhedral equidimensional grains in the phenocrystic phase. Conversion and alteration to other feldspars (Smyth, 1960) may have diminished the original amount of sanidine present to the few grains seen which were fresh and lacked visible signs of alteration.

Quartz occurs in several forms, as euhedral, rhombohedral-hexagonal sections, anhedral to subhedral rhombohedrons, and corroded anhedral, body-embayed grains in various stages of breaking down to finer grained aggregates. Wandering extinction is very common as are accicular inclusions of rutile. Presence of the rhombohedral quartz suggests crystallization of the phase below the quartz inversion temperature of 572°C (Heinrich, 1965).



The matrix consists of a microcrystalline intergrowth of quartz and feldspar, in places bordering on hypocrySTALLINE, with 1 - 3% euhedral to anhedral magnetite. Flow banding and eutaxitic textures are well developed and secondary development of sericite parallels these primary structures. Minor amounts of sphene and epidote are contained within the groundmass.

## 2.6 Geochemistry of the Rock Suites

Whole rock geochemical analysis of the rock samples employed for Rb/Sr dating were performed utilizing the electron microprobe. Whole rock chemistry can be used to define the orogenic setting of igneous rocks (Jakes and White, 1972; MacKenzie and Chappell, 1972) and also to determine if alterations of volcanic rocks have occurred, particularly during devitrification and hydration of glass components (Scott, 1966, 1971; Lipman, 1965). In this study it was also hoped that any alteration which may have affected the Rb-Sr system post rock formation might be detected and thus explain some of the scattering apparent in the isochrons.

### 2.6.1 Preparation of Samples and Analytical Procedure

The samples used for whole-rock major element chemistry were the same specimens employed for Rb/Sr dating. Approximately 1.0 to 1.5 grams of rock powder was weighed into a small porcelain crucible and then heated at 110<sup>0</sup>C for six hours



and weighed immediately to obtain a weight % value for  $\text{H}_2\text{O}^-$ . Next the sample was heated in a furnace at  $1000^\circ\text{C}$  for 2-2½ hours to obtain a weight % value for loss on ignition (i.e. combined value of  $\text{H}_2\text{O}^+$ , F, U,  $\text{PO}_4$ , etc.), again the sample was weighed before and after ignition.

Rock powders were converted to glass by heating in an image furnace at temperatures in the range of  $1300$ - $1500^\circ\text{C}$  under a controlled vacuum. The design and function of this particular piece of equipment and the procedure is described by Schimann and Smith (1979). The glass samples were then crushed and handpicked using a binocular microscope to ensure that only pure glass was to be analyzed. The specimens were then mounted in epoxy and polished on a lead lap in preparation for microprobe analysis. Microprobe analyses on the glasses for nine elements (Na, Mg, Al, Si, K, Ca, Ti, Mn, Fe) were performed using an ARL E.M.X. electron microprobe equipped with a Si(Li) crystal detector and an on-line computer to store data. The energy dispersive analysis system (Smith, 1976) was used in the study. Operating conditions consisted of 15 Kv voltage, emission current of  $200\ \mu\text{A}$ , and beam current of  $0.30\ \mu\text{A}$  and remained constant during the analysis. Willemite was used as a standard to calibrate the EDA spectra being run both before, during and after analysis.

Each glass sample was probed for a total of 400 seconds (live time) under a scanning beam of  $32\ \mu^2$ . The





beam was moved constantly to minimize possible volatilization of the alkali elements and to ensure a representative analysis if the sample was not entirely homogeneous. Elemental concentrations were obtained by comparing the number of counts from a standard to the number of counts collected from the sample over the same period of time, after the appropriate corrections (i.e., ZAF) had been made; the standards employed and their compositions are given in Table 8. The data were processed by a program "EDATA" (Smith and Gold, 1976) which makes the customary corrections along with more complicated adjustments such as peak shift and probe current drift.

#### 2.6.2 Treatment of Data

Elemental concentrations obtained from the program "EDATA" were in the form "weight fraction element" and were then converted to weight % oxide, the results of which are given in Table 9. The concentration of iron is calculated by the probe without distinguishing between the oxidation state, however, an upper limit on  $\text{Fe}_2\text{O}_3$  was set according to the following equation (Irvine and Baragar, 1971):

$$\% \text{Fe}_2\text{O}_3 = \% \text{TiO}_2 + 1.5$$

Additional iron present in excess of this arbitrary upper limit was assumed to be in the ferrous state. Most of the analyses give totals around 102.0. The reason for the high



TABLE 8

Standards used for microprobe analysis of  
whole rock specimens (glasses)

|                                | <u>Willemite</u> | <u>Kaersutite</u><br>639-3A | <u>Grossularite</u><br>639-1 | <u>Augite</u><br>639-4 | <u>Obsidian</u><br>639-10 | <u>Biotite</u><br>639-22A |
|--------------------------------|------------------|-----------------------------|------------------------------|------------------------|---------------------------|---------------------------|
| SiO <sub>2</sub>               | 28.07            | 40.37                       | 39.04                        | 50.72                  | 73.95                     | 32.79                     |
| TiO <sub>2</sub>               | -                | 4.82                        | 0.38                         | 0.73                   | 0.10                      | 3.05                      |
| Al <sub>2</sub> O <sub>3</sub> | 0.04             | 14.91                       | 21.65                        | 7.86                   | 13.30                     | 13.30                     |
| FeO                            | 0.03             | 10.92                       | 1.53                         | 6.77                   | 1.75                      | 30.14                     |
| MnO                            | 4.82             | 0.09                        | 0.61                         | 0.13                   | 0.06                      | 0.38                      |
| MgO                            | 0.12             | 12.80                       | 0.02                         | 16.65                  | 0.06                      | 4.59                      |
| CaO                            | -                | 10.30                       | 36.58                        | 15.82                  | 0.76                      | -                         |
| Na <sub>2</sub> O              | -                | 2.60                        | -                            | 1.27                   | 4.05                      | 0.16                      |
| K <sub>2</sub> O               | -                | 2.05                        | -                            | -                      | 6.00                      | 9.20                      |
| H <sub>2</sub> O               | -                | 0.98                        | -                            | -                      | 0.72                      | 3.58                      |
|                                | -                | -                           | -                            | -                      | -                         | -                         |
| ZnO                            | 66.87            | -                           | -                            | -                      | -                         | -                         |
| Cl                             | -                | -                           | -                            | -                      | 0.36                      | -                         |
| Cr <sub>2</sub> O <sub>3</sub> | -                | -                           | -                            | 0.14                   | -                         | -                         |
| P <sub>2</sub> O <sub>5</sub>  | -                | -                           | -                            | -                      | 0.04                      | 0.05                      |
| Rb <sub>2</sub> O              | -                | -                           | -                            | -                      | -                         | 0.05                      |
| BaO                            | -                | -                           | -                            | -                      | 0.01                      | 0.18                      |



Table 9 Major element geochemistry and normative values for rocks of the Central Mineral Belt

|                                | <u>MZ-1</u> | <u>MZ-4</u> | <u>MZ-7</u> | <u>MZ-9</u> | <u>MZ-10</u> | <u>MZ-14</u> | <u>BR-1</u> | <u>BR-5</u> | <u>BR-7</u> | <u>BR-8</u> | <u>BR-9</u> | <u>BR-14</u> | <u>MV-1</u> | <u>MV-3</u> | <u>MV-4</u> | <u>MV-6</u> | <u>MV-9</u> | <u>M-11</u> | <u>W-7</u> | <u>W-13</u> | <u>W-16</u> | <u>W-8</u> |
|--------------------------------|-------------|-------------|-------------|-------------|--------------|--------------|-------------|-------------|-------------|-------------|-------------|--------------|-------------|-------------|-------------|-------------|-------------|-------------|------------|-------------|-------------|------------|
| Na <sub>2</sub> O              | 4.34        | 4.24        | 4.32        | 4.23        | 4.37         | 4.34         | 4.52        | 3.41        | 4.29        | 4.83        | 4.39        | 4.01         | 3.43        | 3.98        | 4.96        | 3.06        | 3.96        | 4.31        | 3.87       | 4.43        | 4.30        | 4.12       |
| MgO                            | 1.08        | 0.89        | 0.76        | 0.65        | 0.90         | 0.48         | -           | 0.09        | -           | -           | 0.07        | -            | 0.04        | 0.09        | 0.20        | 0.62        | 0.42        | 1.91        | 0.20       | 0.06        | 0.12        | -          |
| Al <sub>2</sub> O <sub>3</sub> | 18.64       | 16.90       | 17.01       | 16.53       | 17.65        | 15.46        | 16.20       | 14.01       | 15.38       | 16.14       | 15.19       | 18.96        | 13.86       | 13.44       | 17.07       | 16.82       | 16.57       | 17.49       | 16.86      | 15.85       | 14.56       | 14.80      |
| SiO <sub>2</sub>               | 64.93       | 67.59       | 69.42       | 69.38       | 67.73        | 72.30        | 71.82       | 76.13       | 72.91       | 72.02       | 73.36       | 64.77        | 77.32       | 77.49       | 70.68       | 69.02       | 69.78       | 63.55       | 69.94      | 73.79       | 75.03       | 74.76      |
| K <sub>2</sub> O               | 6.02        | 5.88        | 6.39        | 6.26        | 6.05         | 5.58         | 6.37        | 6.10        | 6.01        | 5.81        | 5.85        | 10.05        | 5.64        | 5.17        | 5.71        | 7.51        | 6.32        | 3.16        | 5.28       | 5.71        | 5.24        | 5.46       |
| CaO                            | 2.34        | 1.94        | 1.17        | 1.36        | 1.87         | 0.88         | 0.49        | 0.14        | 0.36        | 0.41        | 0.58        | 0.50         | 0.46        | 0.26        | 0.80        | 1.15        | 1.58        | 3.92        | 2.66       | 0.85        | 0.54        | 0.78       |
| TiO <sub>2</sub>               | 0.49        | 0.55        | 0.46        | 0.40        | 0.38         | 0.39         | 0.32        | 0.11        | 0.20        | 0.22        | 0.19        | 0.55         | 0.15        | 0.21        | 0.14        | 0.45        | 0.51        | 0.73        | 0.24       | 0.10        | 0.06        | 0.05       |
| MnO                            | 0.07        | 0.05        | -           | -           | 0.06         | -            | -           | -           | -           | -           | -           | -            | 0.07        | 0.04        | 0.10        | -           | 0.05        | 0.07        | -          | -           | -           | -          |
| Fe <sub>2</sub> O <sub>3</sub> | 1.99        | 2.05        | 1.82        | 1.90        | 1.88         | 1.52         | 1.27        | 0.99        | 1.43        | 1.41        | 1.21        | 1.59         | 0.94        | 0.68        | 1.18        | 1.95        | 1.82        | 2.23        | 1.74       | 1.02        | 0.70        | 0.92       |
| FeO                            | 1.18        | 0.46        | -           | 0.20        | 0.60         | -            | -           | -           | -           | -           | -           | -            | -           | -           | -           | 0.07        | -           | 2.81        | 0.16       | -           | -           | -          |
| H <sub>2</sub> O <sup>-</sup>  | 0.21        | 0.23        | 0.23        | 0.28        | 0.31         | 0.16         | 0.21        | 0.27        | 0.19        | 0.21        | 0.18        | 0.30         | 0.28        | 0.16        | 0.20        | 0.29        | 0.23        | 0.13        | 0.21       | 0.20        | 0.25        | 0.19       |
| H <sub>2</sub> O <sup>+</sup>  | 0.90        | 0.96        | 0.58        | 0.63        | 0.89         | 0.92         | 0.58        | 0.57        | 0.66        | 0.74        | 0.96        | 3.18         | 0.61        | 0.50        | 1.06        | 1.09        | 0.62        | 0.89        | 0.45       | 0.36        | 0.37        | 0.32       |
| other                          |             |             |             |             |              |              |             |             |             |             |             |              |             |             |             |             |             |             |            |             |             |            |
|                                | 102.24      | 101.74      | 102.16      | 101.82      | 102.69       | 102.03       | 101.78      | 101.82      | 101.43      | 101.79      | 101.98      | 103.91       | 102.80      | 102.02      | 102.10      | 102.03      | 101.86      | 101.20      | 101.61     | 102.37      | 101.14      | 101.97     |
|                                |             |             |             |             |              |              |             |             |             |             |             |              |             |             |             |             |             |             |            |             |             | 101.35     |

|    | <u>MZ-1</u> | <u>MZ-4</u> | <u>MZ-7</u> | <u>MZ-9</u> | <u>MZ-10</u> | <u>MZ-14</u> | <u>BR-1</u> | <u>BR-5</u> | <u>BR-7</u> | <u>BR-8</u> | <u>BR-9</u> | <u>BR-14</u> | <u>MV-1</u> | <u>MV-3</u> | <u>MV-4</u> | <u>MV-6</u> | <u>MV-9</u> | <u>M-11</u> | <u>W-7</u> | <u>W-13</u> | <u>W-16</u> | <u>W-8</u> |
|----|-------------|-------------|-------------|-------------|--------------|--------------|-------------|-------------|-------------|-------------|-------------|--------------|-------------|-------------|-------------|-------------|-------------|-------------|------------|-------------|-------------|------------|
| Q  | 9.94        | 14.84       | 15.96       | 16.76       | 13.58        | 22.86        | 19.88       | 32.18       | 24.02       | 20.62       | 23.87       | 1.86         | 34.07       | 33.39       | 17.79       | 18.94       | 18.34       | 14.17       | 21.08      | 23.81       | 28.63       | 26.97      |
| Or | 35.21       | 34.59       | 37.29       | 36.69       | 35.26        | 32.70        | 37.31       | 35.73       | 35.34       | 34.08       | 34.31       | 59.19        | 32.74       | 30.17       | 33.49       | 44.13       | 37.01       | 18.66       | 30.54      | 33.17       | 30.83       | 31.83      |
| Ab | 36.31       | 36.53       | 36.06       | 35.47       | 36.43        | 36.37        | 37.87       | 28.57       | 36.09       | 40.53       | 36.83       | 33.78        | 28.48       | 33.22       | 41.62       | 25.72       | 33.17       | 36.40       | 32.44      | 36.81       | 35.94       | 36.86      |
| An | 11.48       | 9.57        | 5.73        | 6.69        | 9.14         | 4.32         | 2.41        | 0.69        | 1.78        | 2.02        | 2.85        | 2.47         | 2.24        | 1.27        | 3.94        | 5.67        | 7.76        | 19.00       | 12.90      | 4.14        | 2.67        | 3.81       |
| Di | -           | -           | -           | -           | -            | -            | -           | -           | -           | -           | -           | -            | -           | -           | -           | -           | -           | 0.33        | 0.13       | -           | -           | -          |
| En | 2.66        | 2.20        | 1.87        | 1.60        | 2.21         | 1.18         | -           | 0.22        | -           | -           | 0.17        | -            | 0.10        | 0.22        | 0.49        | 1.53        | 1.04        | 6.83        | 0.43       | 0.15        | 0.30        | -          |
| Ms | 2.58        | 0.05        | -           | -           | 1.01         | -            | -           | -           | -           | -           | -           | -            | -           | -           | -           | -           | -           | 3.23        | -          | -           | -           | -          |
| Hm | 0.19        | 2.00        | 1.80        | 1.88        | 1.15         | 1.51         | 1.26        | 0.98        | 1.42        | 1.40        | 1.20        | 1.58         | 0.92        | 0.67        | 1.17        | 1.94        | 1.80        | -           | 1.72       | 1.00        | 0.70        | 0.91       |
| Il | 0.92        | 1.04        | -           | 0.42        | 0.71         | -            | -           | -           | -           | -           | -           | -            | 0.15        | 0.08        | 0.21        | 0.15        | 0.11        | 1.38        | 0.33       | -           | -           | -          |
| Ru | -           | -           | 0.45        | 0.18        | -            | 0.39         | 0.32        | 0.11        | 0.20        | 0.22        | 0.19        | 0.55         | 0.07        | 0.16        | 0.03        | 0.37        | 0.45        | -           | 0.06       | 0.10        | 0.06        | 0.05       |
| C  | 0.72        | 0.03        | 0.84        | 0.31        | 0.50         | 0.67         | 0.96        | 1.52        | 1.15        | 1.15        | 0.57        | 0.56         | 1.25        | 0.81        | 1.26        | 1.55        | 0.33        | -           | -          | 0.82        | 0.87        | 0.77       |
|    |             |             |             |             |              |              |             |             |             |             |             |              |             |             |             |             |             |             |            |             |             | 0.79       |





values is not known although the totals are within the 1.5 to 2.0% error limit for EDA analyses. The data is plotted on conventional diagrams in Figures 13 to 22; these include Harker variation plots, AFM diagrams, and alkali metals versus  $\text{SiO}_2$ . Most of the diagrams follow the proposed classification of igneous rocks of Irvine and Baragar (1971).

### 2.6.3 Discussion of Results

It should first be noted that emphasis is placed on diagrams which include alkalis to classify the rocks and that the principle shortcoming of this is the sensitivity of the elements to changes imposed by alteration or metamorphism (Irvine and Baragar, 1971; Scott, 1971).

Typical Harker variation diagrams, Figures 13 to 15, indicate a simple differentiation trend for the rock suites and their good fit to the same line might suggest a genetic relationship. The rocks are classified as rhyolites ( $>77\% \text{SiO}_2$ ), rhyodacites ( $67-71\% \text{SiO}_2$ ), dacites ( $62-67\% \text{SiO}_2$ ) for the volcanics and granites and granodiorites for the two intrusive suites according to the divisions of Gelinas and Brooks (1974), and fall in the calc-alkaline fields of both the conventional AFM diagram (Figure 16) and total alkalis ( $\text{Na}_2\text{O} + \text{K}_2\text{O}$ ) versus  $\text{SiO}_2\%$  plot (Figure 17). The calc-alkaline affinity of the rocks is confirmed in a plot of  $\text{Al}_2\text{O}_3\%$  versus normative plagioclase composition (Figure 18),





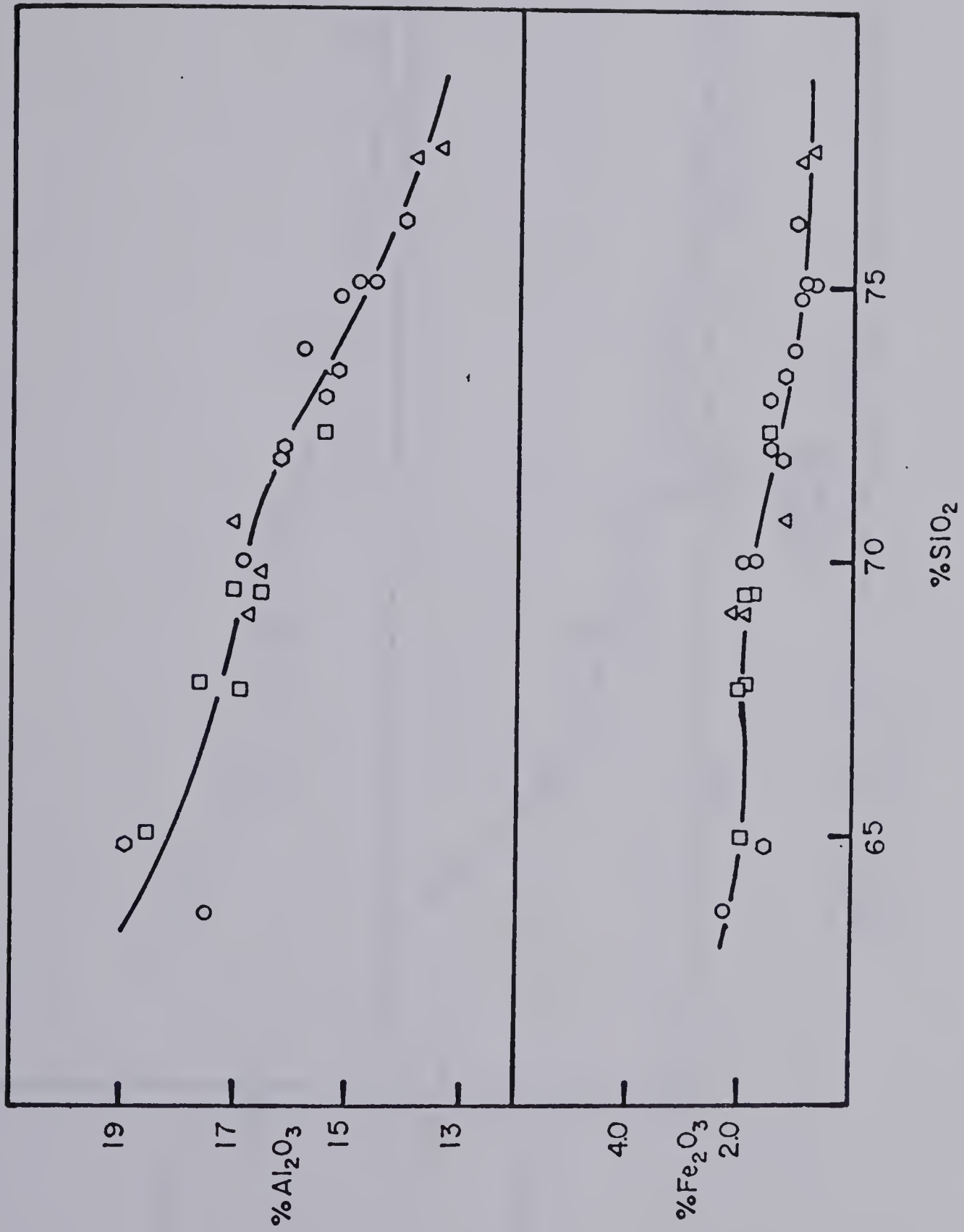
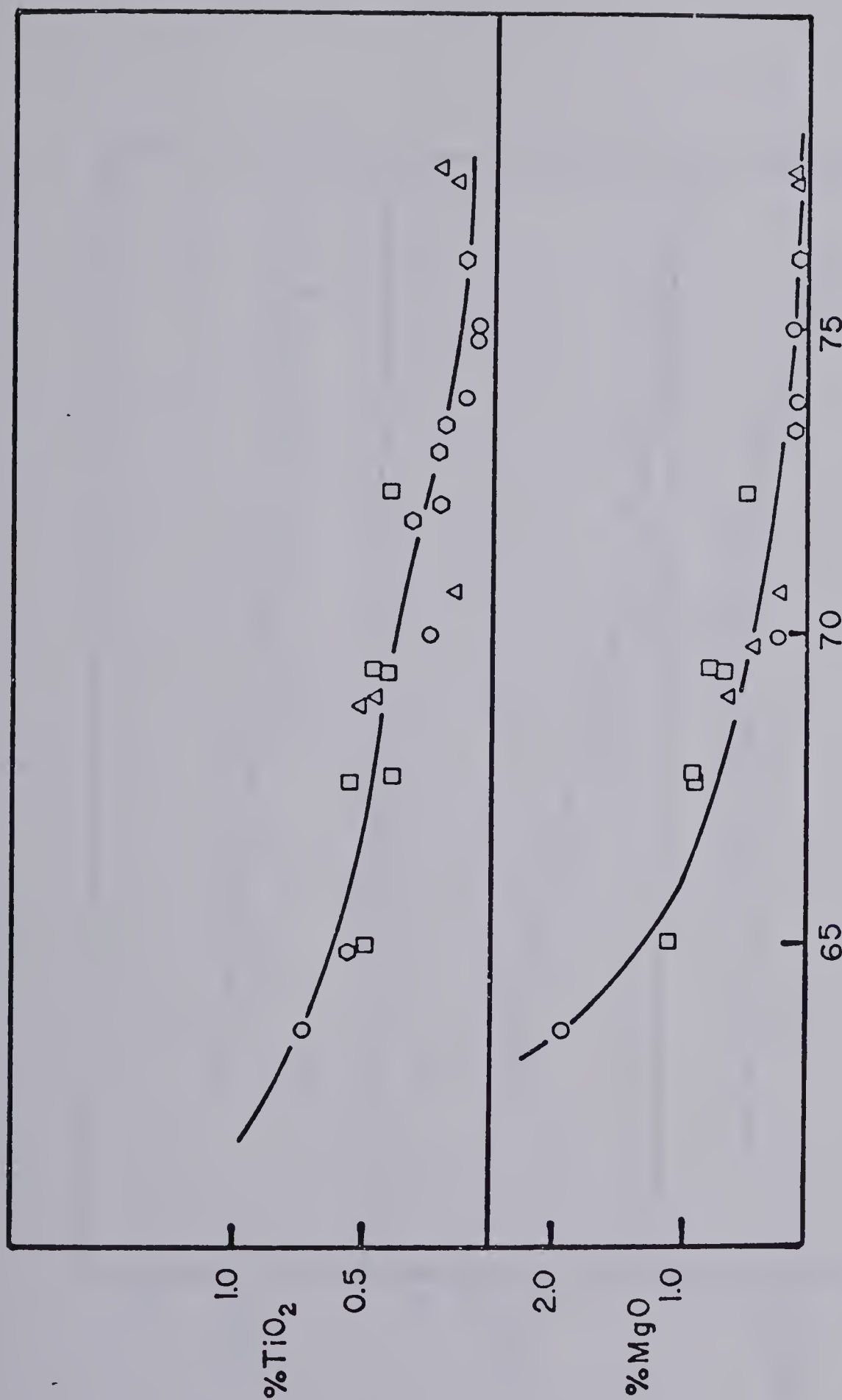


Figure 13

Weight %  $\text{Al}_2\text{O}_3$  and  $\text{Fe}_2\text{O}_3$  versus weight %  $\text{SiO}_2$  diagram for the Bruce River volcanics ○, Minisinakwa volcanics △, Walker Lake Granite □, and Otter Lake Granite ◇





%  $\text{SiO}_2$   
Figure 14

Weight %  $\text{TiO}_2$  and  $\text{MgO}$  versus weight %  $\text{SiO}_2$  diagram (symbols same as for Figure 13)



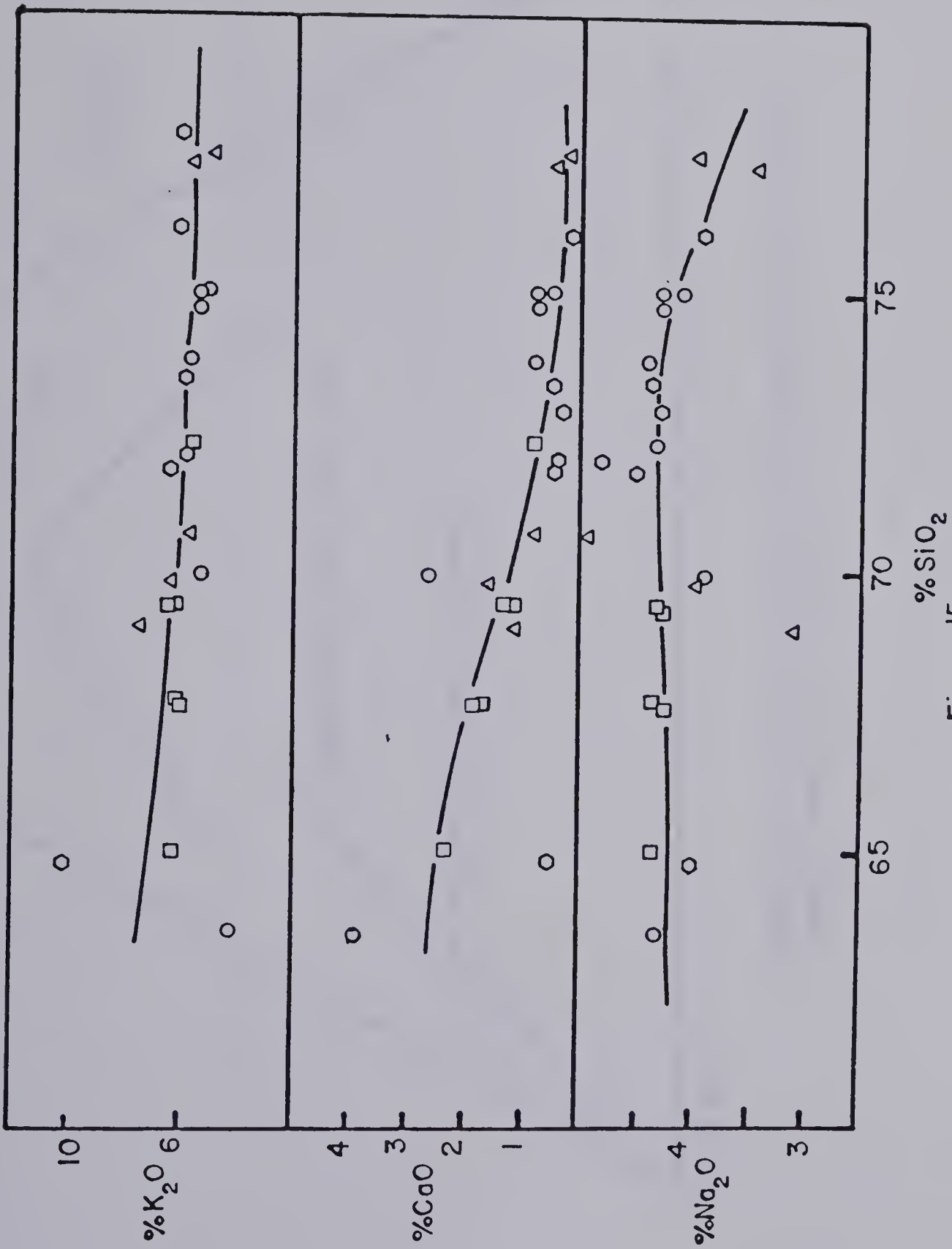
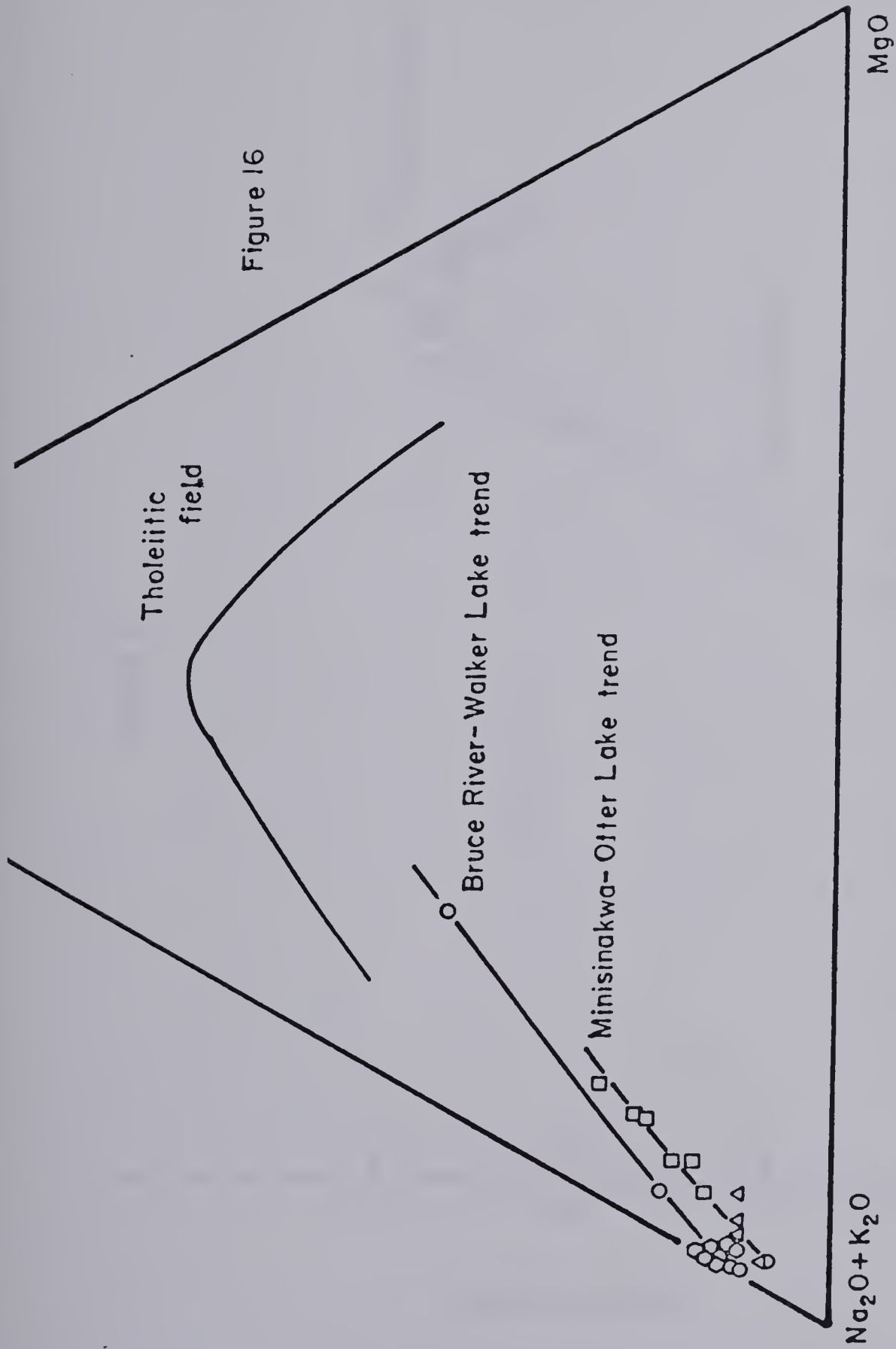


Figure 15  
Weight %  $\text{K}_2\text{O}$ ,  $\text{CaO}$ , and  $\text{Na}_2\text{O}$  versus weight %  
 $\text{SiO}_2$  diagram (symbols same as for Figure 13)



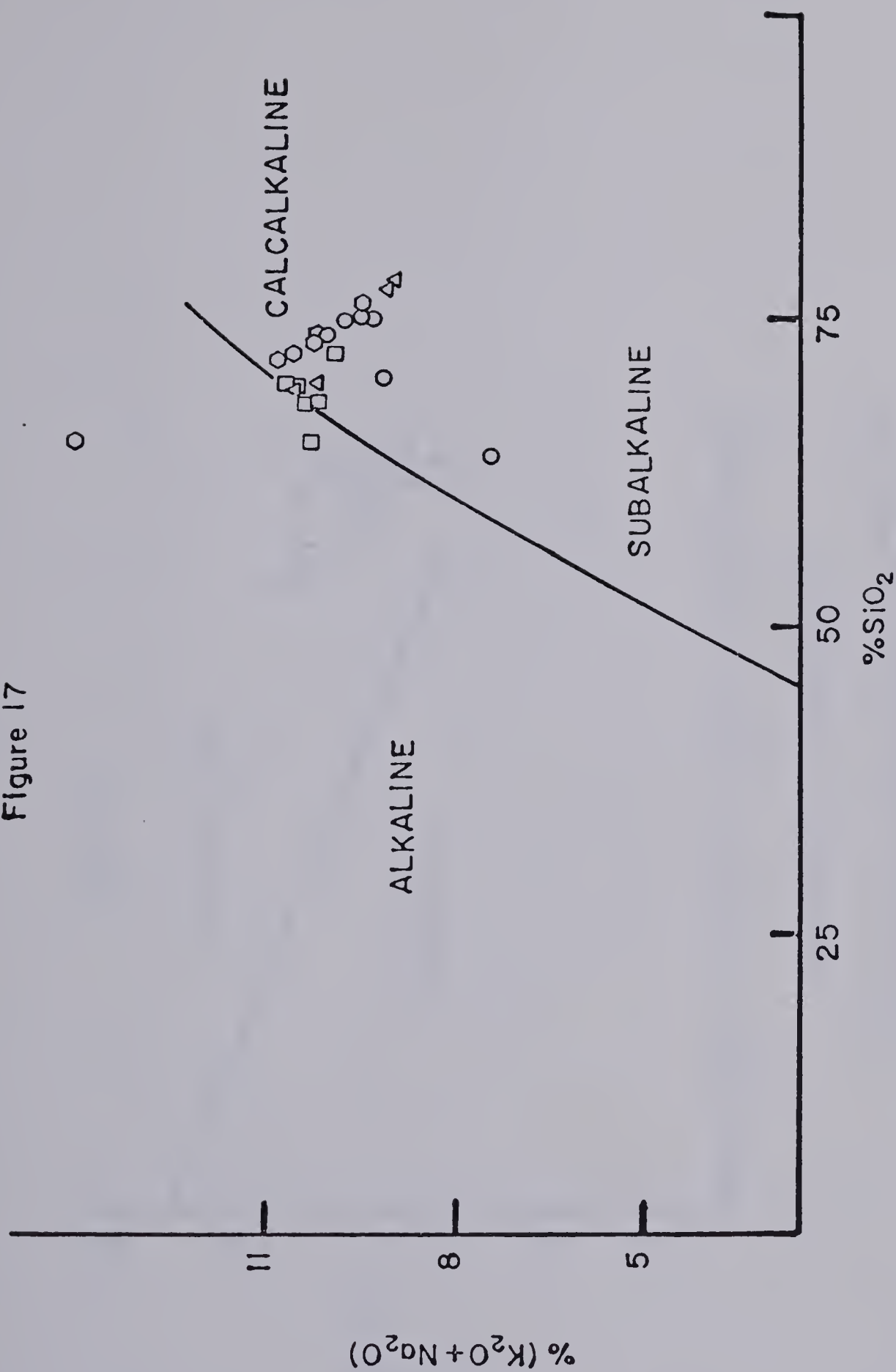




AFM diagram for rock suites of the Central Mineral Belt  
(symbols same as for Figure 13)

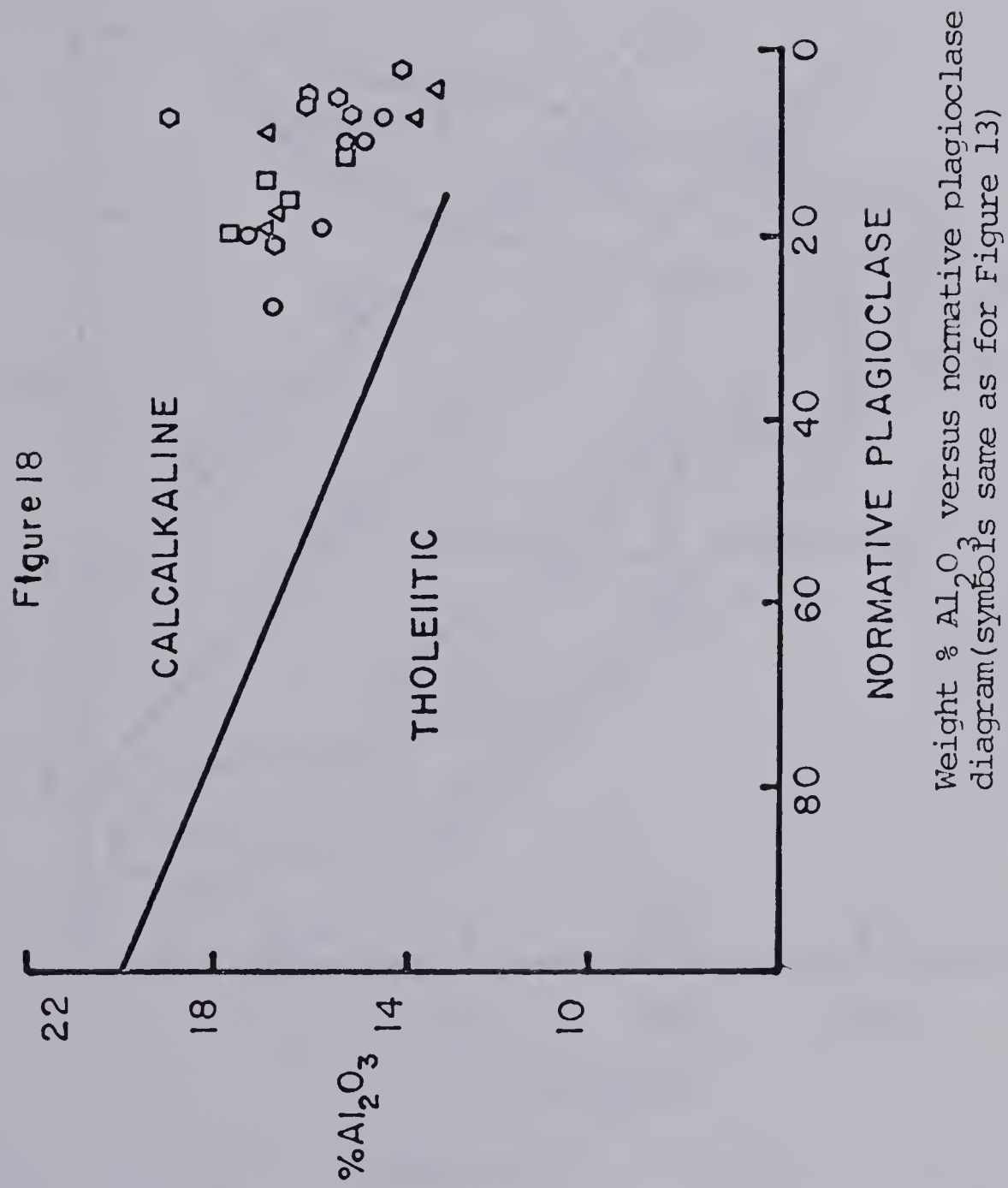


Figure 17



Weight %  $(K_2O + Na_2O)$  versus weight %  $SiO_2$  diagram  
(symbols same as for Figure 13)







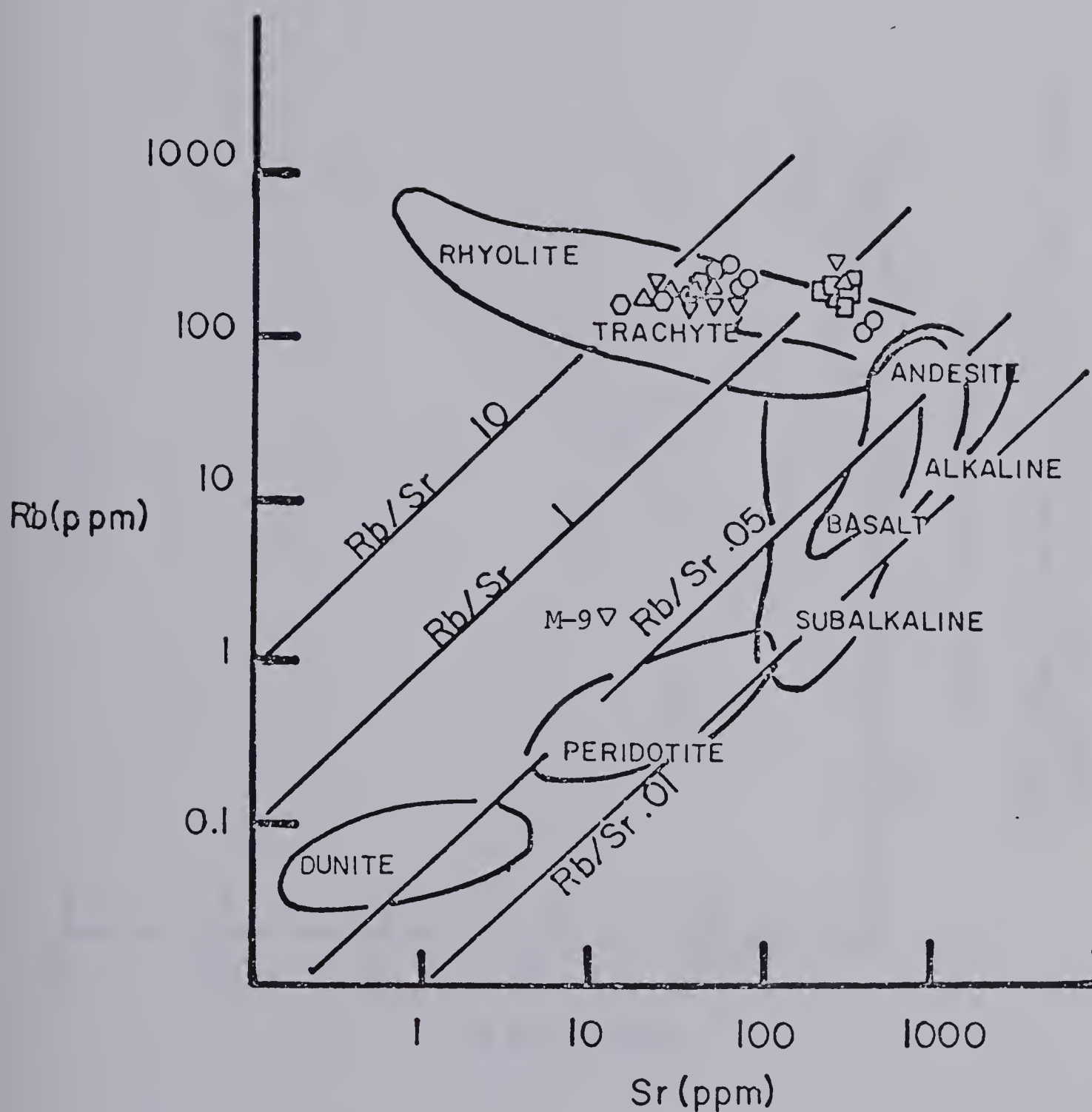
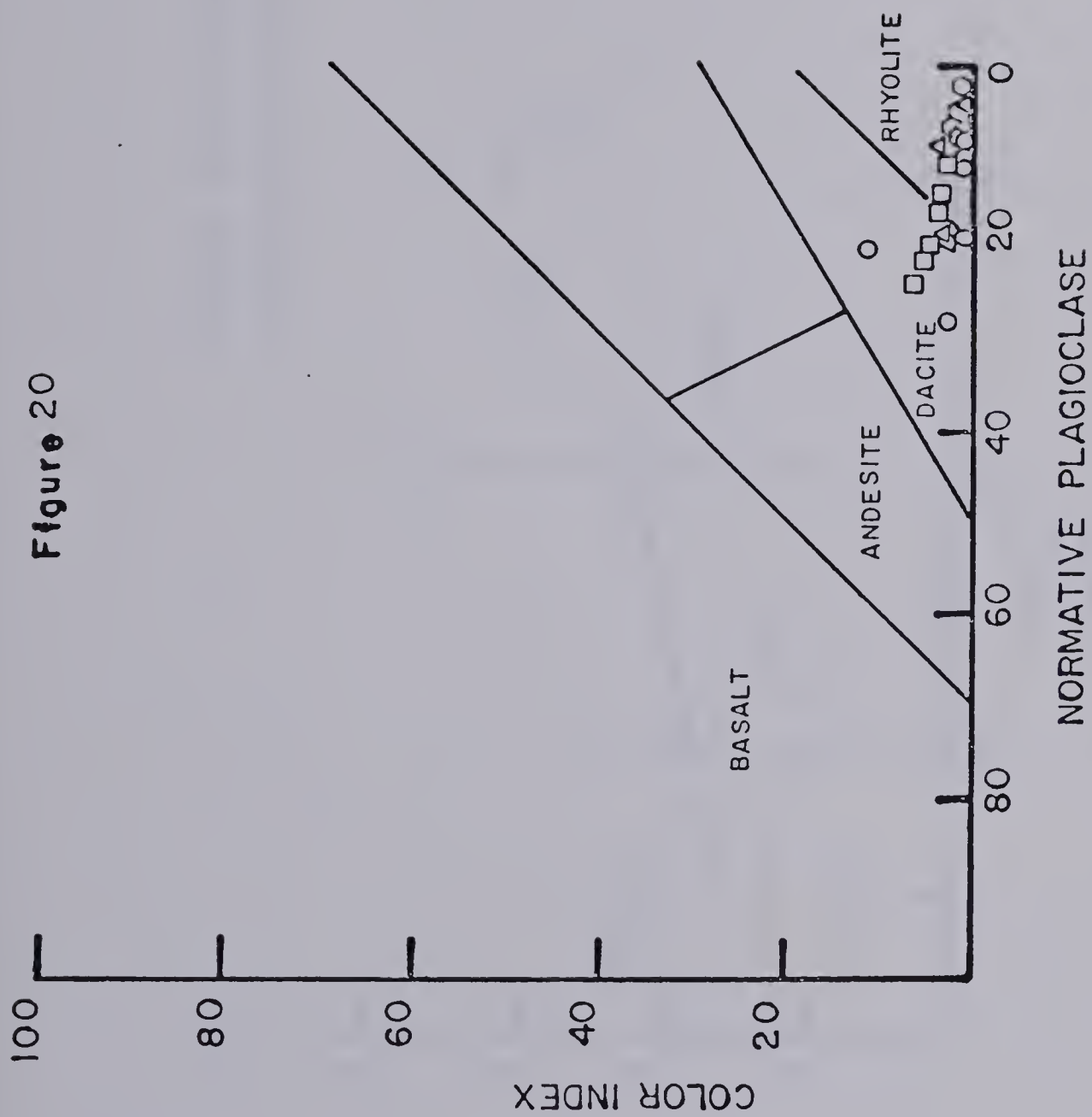


Figure 19

Rb versus Sr plot from Kistler and Peterman (1973), (symbols same as for Figure 13)







Color index versus normative plagioclase diagram (symbols same as for Figure 13)



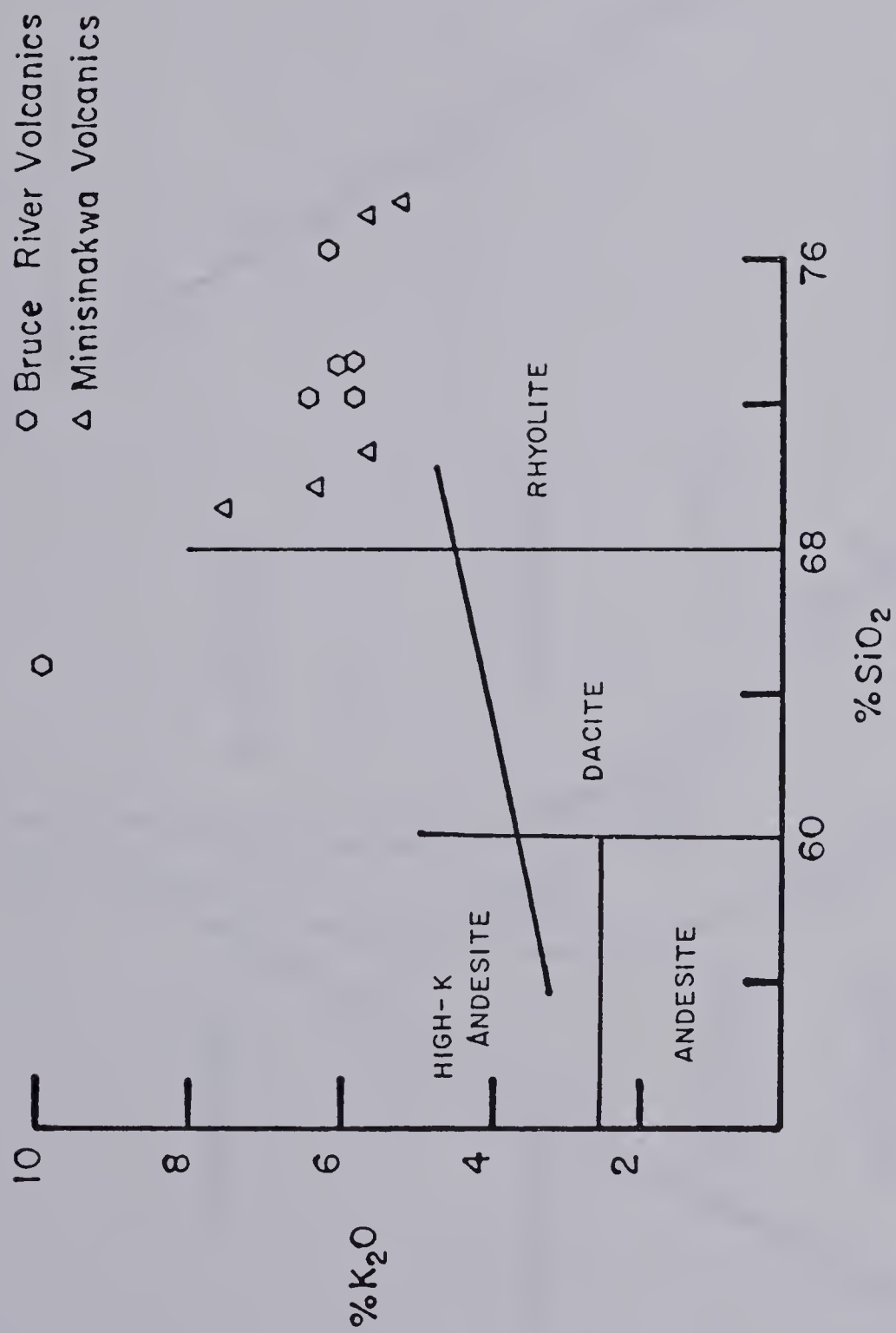


Figure 21  
Weight %  $K_2O$  versus weight %  $SiO_2$  diagram



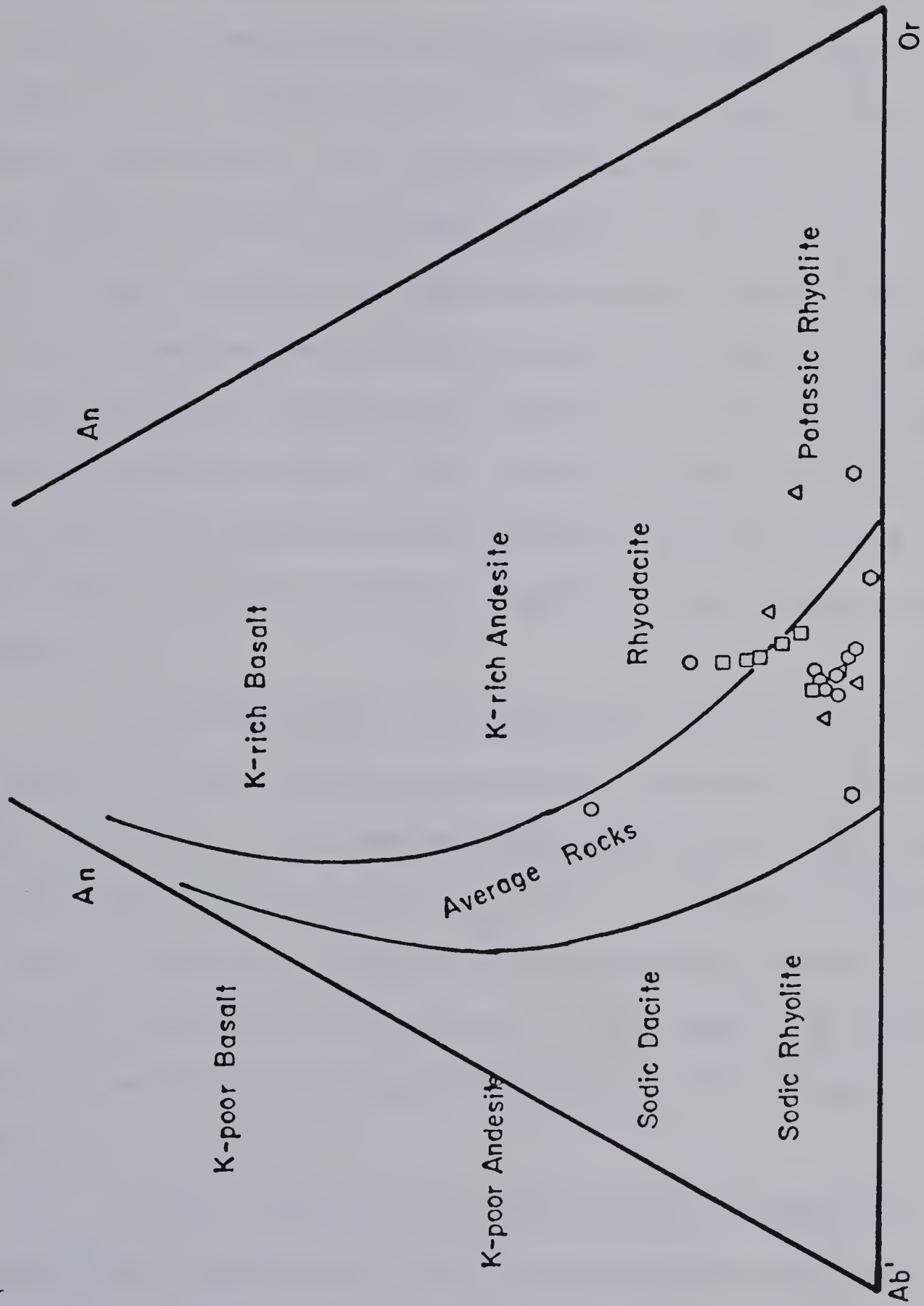


Figure 22

Normative An : Ab' : Or plot (symbols same as for Figure 13)





which also shows the highly aluminous nature of the rocks. Table 10 indicates the peraluminous nature of the rocks with the molecular proportion of  $\text{Al}_2\text{O}_3 > \text{CaO} + \text{K}_2\text{O} + \text{Na}_2\text{O}$  (Carmichael et al., 1974), this is also reflected by the presence of corundum in the normative calculations, (Table 9) and almandine garnet in thin section of the rocks. A plot of Rb versus Sr, **after** Kistler and Peterman (1973) (see Figure 19) indicates the calcalkaline nature of the rocks with most corresponding to rhyodacites (granite) and dacites (granodiorites); this diagram also indicates that the elements have not been altered by post-crystallization events, except for one point (M-9), which is important for radiometric dating.

Although Figure 20 shows that the rocks are dacitic to rhyolitic (intrusive equivalents, granites to granodiorites) in composition, anomalously high  $\text{K}_2\text{O}$  and  $\text{Na}_2\text{O}$  concentrations are reflected in Figure 17. A Peacock (1930) plot of %  $\text{Na}_2\text{O}$ ,  $\text{CaO}$  versus  $\text{SiO}_2\%$  to determine the correct alkali-lime index was useless due to the high  $\text{Na}_2\text{O}$  content, and Figures 21 and 22 show the high  $\text{K}_2\text{O}$  affinities of the suites.

With respect to the AFM diagram, Figure 16, it is interesting to note that two apparent trends are indicated; (i) a Walker Lake Granite-Bruce River volcanic trend, and (ii) Otter Lake Granite-Minisinakwa volcanic trend. The signifi-



TABLE 10

|       | CaO + Na <sub>2</sub> O + K <sub>2</sub> O<br>(Molecular Proportions) | Al <sub>2</sub> O <sub>3</sub><br>(molecular Proportions) |
|-------|---|---|
| MZ-1  | .17   | .18   |
| MZ-4  | .15   | .16   |
| MZ-7  | .14   | .16   |
| MZ-9  | .14   | .16   |
| MZ-10 | .17   | .17   |
| MZ-14 | .13   | .15   |
| Br-1  | .13   | .15   |
| Br-5  | .11   | .13   |
| Br-7  | .12   | .15   |
| Br-8  | .13   | .15   |
| Br-9  | .13   | .14   |
| Br-14 | .16   | .18   |
| Mv-1  | .10   | .13   |
| Mv-3  | .11   | .13   |
| Mv-4  | .15   | .16   |
| Mv-6  | .13   | .16   |
| Mv-9  | .14   | .16   |
| W-7   | .15   | .17   |
| W-8   | .15   | .16   |
| W-9   | .12   | .14   |
| W-11  | .14   | .15   |
| W-13  | .11   | .14   |
| W-16  | .12   | .14   |



cance of this is not known although the geographical position of these suites relative to each other in the field might support the observation. However, the Harker variation diagrams did not indicate any such trends so the validity of this possible distinction between two coeval intrusive-extrusive magmatic suites remains ambiguous.

Although the rock suites display typical calc-alkaline features, they are characterized by their high content of  $\text{Al}_2\text{O}_3$  and  $\text{K}_2\text{O}$ . A similar association of these types of rocks with calc-alkaline volcanism and shoshonitic magmatism in Papua New Guinea led MacKenzie and Chappell (1972) to extend the definition of the shoshonitic association to grade into the K-rich calc-alkaline rocks. Although the classic occurrences (Yellowstone Park and the Roman Comagmatic Province) of shoshonitic rocks are set in areas of post-orogenic stabilization of continental margins, similar rocks have been discovered in active orogenic regions, most notably the circum-Pacific belt (Morrison, 1976). The magmatic evolution of these areas usually follows the trend tholeiitic-calcaline-shoshonites-alkaline rocks (Jakes and White, 1972), corresponding to a progressive change of the subduction zone. This change of motion in the case of island arcs built on oceanic crust is attributed to rotation and fragmentation of the arc produced by oblique convergence between the adjacent lithospheric



plates (Morrison, 1976).

In the case of the Central Mineral Belt the rocks of particular interest to this study are recognized as having high potassic affinities suggesting an association with the K-rich calc-alkaline rocks of MacKenzie and Chappel (1972). Although Watson-White (1976) recognized the alkaline nature of these rocks he proposed a rifting environment to explain their petrogenesis, the present author rejects this in light of recent studies carried out on similar rocks found in present day orogenic settings such as Indonesia, Papua New Guinea, Malaysia, Japan, etc. Instead, a model is proposed whereby the tectonics of the area progressed from predominantly subduction with dip-slip motion to strike-slip motion due to failure or "flipping" of the subduction due to oblique plate convergence. Such a tectonic transition is associated with a change from calc-alkaline to shoshonitic volcanism (Morrison, 1976; Jakes and White, 1972)

It is interesting to note that the Central Mineral Belt is characterized by its unique structural pattern which is oblique to the pattern of the rest of the Nain Province and hence its recognition as the Makkovik subprovince. The reason for this change in structural pattern in the southern Nain Province has always been attributed to rotation of the area approximately  $55^{\circ}$  some 1200-1500 Ma ago (Fahrig and Roy, 1973). Perhaps rotation and fragmentation of an arc system,





which gave rise to the K-calcalkaline rocks of the Central Mineral Belt due to the oblique convergence of two plates, was also responsible for the present day discordance of the structures of the Makkovik subprovince due to rotation of the area. Also, the presence of the Letitia Lake Porphyry (Marten, 1975) and the Red Wine Alkaline Province (Currie et al., 1975) would correspond to the last part of the magmatic cycle, tholeiite-calc-alkaline-shoshonitites-alkaline rocks, of Jakes and White (1972) for the evolution of this type of tectonic model.

The anomalously high  $\text{Al}_2\text{O}_3$  and  $\text{K}_2\text{O}$  contents, fairly high  $\text{SiO}_2\%$ , presence of corundum in the norm and almandine garnet in thin section, and  $^{87}\text{Sr}/^{86}\text{Sr}$  values of 0.705 (Otter Lake Granite) and 0.707 (Walker Lake Granite) for the granites suggests that these fit into Chappel and White's (1974) S-type granitic field. Such granites originate from partial melting or fusion of crustal material enriched in K, Al, Rb, etc., versus I-type granites which originate from partial melting of mantle material immediately above subducted lithospheric (oceanic) plates (Green and Ringwood, 1968).

Although the chemical patterns displayed by the rock-suites may be explained by two different processes, the orogenic settings accompanying each are divergent to each other. In one case an active arc system is dominant while in the second case an orogenic setting is not particularly



diagnostic of S-type granites as long as fusion of crustal material is included in the model. A compromise between the two proposals is found in the north island of New Zealand where an active arc environment occurs east of continental crust corresponding to a flexure in the Tonga-Kermadec arc. Of course, if the angular discrepancy in structural style between the Nain Province and Makkovik subprovince of  $55^{\circ}$  is omitted and attributed to another process then an active system is not required in the interpretation. Instead, a stable orogenic environment analogous to the Cascades of the western United States may be the best analogy to the Central Mineral Belt.\*

## 2.7 The Isochrons obtained (Rb-Sr Geochronology)

### 1) 2.7.1 The Aillik Volcanics

An isochron plot, Figure 6, of five points (excludes point M-9) indicates an age of  $1767 \pm 4$  Ma and an initial  $^{87}\text{Sr}/^{86}\text{Sr}$  ratio of  $0.7022 \pm .0005$ . A mean square of weighted deviates (MSWD) value of 4.86 obtained from the isochron is due to sample M-12, if this point is also excluded then the four remaining points indicate an age of  $1776 \pm 2$  Ma and an initial ratio of  $0.7005 \pm .0004$  with a much better MSWD value of 0.803. However, there is no good

---

\* However, similar geologic environments displaying vast thicknesses of rhyolitic pyroclastic material (Cascades, Roman Province) are typically stable continental areas.



reason to exclude this point and the former age is accepted. Point M.9 is excluded on the basis of its altered chemistry believed to be responsible for its low Rb content relative to the other rhyolites of the same volcanic unit as indicated in Figure 19 as discussed earlier.

The 1767 Ma age for the volcanics is considered geologically reasonable. If the primary syngenetic uranium mineralization at Burnt Lake and Michelin is indeed 1770 Ma as suggested by a U-Pb concordia plot (see Chapter 4), then the calculated age for the Aillik volcanics is verified. However, when compared to the 1693 Ma age calculated by Watson-White, there is a considerable difference. In this latter case the isochron represents a regional sampling procedure and it may be that the result obtained also reflects this. If this is the case, then it would suggest a younging to the north for the volcanics and indicates a minimum time limit of approximately 80 Ma for the acid volcanism in the Aillik Group. A maximum limit for this volcanism is calculated at 120 Ma based on a K-Ar date of  $1645 \pm 46$  Ma for hornblende taken from the Walker Lake Granite (Wanless and Loveridge, 1974) which is known to cut the Aillik volcanics.

Although the initial  $^{87}\text{Sr}/^{86}\text{Sr}$  value of 0.7022 falls just outside of the field for the growth curve of  $^{87}\text{Sr}/^{86}\text{Sr}$  for rocks of mantle origin (cf. 1700 Ma age; Faure and







Powell, 1972) an origin involving crustal fusion is preferred since it agrees more with the calc-alkaline chemistry of the rock suite.

## 2) 2.7.2 Otter Lake Granite

A six point isochron plot for the Otter Lake Granite, Figure 7, indicates an age of  $1496 \pm 37$  Ma and an initial  $^{87}\text{Sr}/^{86}\text{Sr}$  ratio of  $0.7051 \pm .0013$ . A meansquares weighted deviates of 11.0 suggests that the spread is outside of analytical error and may therefore be geologically real.

From field relationships the granite is known to be younger than the Bruce River Group Volcanics which have been dated at  $1520 \pm 20$  Ma (see further on; Wanless and Loveridge, 1972) and older than the Seal Lake Group dated at  $1323 \pm 92$  Ma (Wanless and Loveridge, 1978). Therefore, the apparent age is considered to be geologically reasonable and suggests a coeval relationship between the Otter Lake Granite and the Bruce River Volcanics.

The initial ratio of  $0.7051 \pm 0.0013$  is within error of a source region deep within the mantle (Faure and Powell, 1972), although a more favorable opinion would be a crustal source. The latter would be more compatible with its calc-alkaline nature suggested from petrographic study and whole rock chemistry.



The  $1496 \pm 37$  Ma age for the Otter Lake Granite is considerably younger than the  $1645 \pm 45$  Ma old Walker Lake Granite (Wanless et al., 1974) located further to the east (Figure 2). Ryan and Harris (1978) considered these two granites to be equivalent, however, this dating does not support such a correlation. It does suggest that the two bodies may be related such that the Walker Lake Granite formed earlier on in the same geologic cycle thus implying a transgression of igneous activity towards the west with time.

### 3) 2.7.3 The Bruce River Volcanics

An "isochron" plot of six points, Figure 8, indicates an age of  $1612 \pm 34$  Ma and an initial  $^{87}\text{Sr}/^{86}\text{Sr}$  ratio of 0.6844. A mean square weighted deviates value of 346.35 and the exceptionally low initial ratio value are due to sample BR-8. A recalculation excluding this point gives an age of  $1527 \pm 39$  Ma and an initial ratio of 0.69826 with a significantly lower MSWD value of 18.4. The initial ratio value is still too low for a rock suite of 1500 my generated by normal processes but is, however, within error of a value expected if the source region were a portion of the mantle depleted in rubidium (Faure, 1977). However, considering the other rock suites of the area (i.e. Otter Lake Granite, Minisinkwa volcanics, Aillik volcanics, Petscapiskau Group volcanics) studied by the writer, Wanless and Loveridge (1972, 1978), and Watson-White (1976) and the initial ratios ob-



tained, a value of 0.702 - 0.706 would seem more reasonable for the Bruce River volcanics. Using this value as a guide an isochron plot of the same five points would give an age of 1520 Ma, agreeable with the  $1526 \pm 44$  Ma old age obtained on the same rocks by Wanless and Loveridge (1974).

#### 4) 2.7.4 The Minisinakwa Volcanics

A six-point "errorchron" plot for the Minisinakwa Volcanics, Figure 9, indicates an age of  $1449 \pm 43$  Ma with an initial  $^{87}\text{Sr}/^{86}\text{Sr}$  ratio of  $0.7150 \pm 0.0067$  and a MSWD value of 945.5. The high initial ratio and MSWD value is attributed to sample MV-5, recalculation excluding this sample indicates an age of  $1538 \pm 25$  Ma and an initial ratio of  $0.7068 \pm 0.0032$  with a MSWD value of 178.5. This latter age is considered geologically more reasonable since the volcanic rocks are intruded by the Otter Lake Granite, dated at  $1496 \pm 37$  Ma, and are thought to be equivalent to the 1520 my old Bruce River Group (Ryan, 1978). A combined plot of the data from these two volcanic suites, Figure 10, shows a good linear relationship indicating age of 1537 Ma.

The initial ratio value of  $0.7068 \pm 0.0032$  lies well outside the field for mantle derived magma (cf. 1500 Ma). The high initial ratio compared to the values obtained for the Aillik and Bruce River Volcanics and the Otter Lake Granite might suggest some contamination or fusion of a





precursor relatively more enriched in Rb.

#### 5) 2.7.5 Walker Lake Granite

A plot of six points for the Walker Lake Granite does not define an isochron, Figure 11, but instead an "errorchron." An open system must, therefore, have existed some time after the crystallization of the granite or variable amounts of contamination may have occurred during the formation of the granite, producing a phase with a variable  $^{87}\text{Sr}/^{86}\text{Sr}$  value for each subvolume of the larger phase. The points do provide some range for the age, however, this indicated age is  $1550 \pm 55$  Ma with an initial ratio of  $0.7070 \pm .0069$  with a mean square weighted deviates value of 11.4.5. Previous work indicates a hornblende K-Ar age of  $1645 \pm 46$  Ma and a biotite K-Ar age of  $1437 \pm 36$  Ma (Wanless and Loveridge, 1974).

The age of  $1550 \pm 55$  Ma is geologically reasonable based on current field evidence as an upper limit is provided by the cross cutting relationship of the granite with the Aillik volcanics, dated at ~1770 my. The relationship between the Rb/Sr ages and K-Ar ages is not known for the samples were not collected from the same locality and may, therefore, not represent the same phase of the granite

The age of  $1550 \pm 55$  Ma is tentatively regarded as a "ball park" figure for the Walker Lake Granite. More





work is required to clarify the age and nature of events responsible for the apparent scatter. Although the sampling represents two phases of the Walker Lake Granite, no distinction could be discerned between the leucogranite phase (9, 11, 13, 16) and biotite granite phase (7, 8). Petrographic study has indicated the presence of sphene and zircon so U-Pb dating of these phases may provide a more reliable date.

## 2.8 Discussion and Interpretation

The study of the Rb-Sr decay system not only permits the determination of a rock age but also permits one to look at the geochemical history of the Sr and Rb they contain. In applying the Rb/Sr dating technique to a suite of rocks formed synchronously in time a linear relationship exists between the Rb/Sr ratio of each sample and its  $^{87}\text{Sr}/^{86}\text{Sr}$  ratio such that the calculation of an isochron, a line of equal age, is possible. If the samples are all of the same age and have remained closed systems to Rb and Sr since the time of the rock formation, then all the points should lie on one isochron. If a later metamorphic event affects the rock suite of particular interest, then the original age of formation may be preserved if the system remains closed to Rb and Sr. However, an internal redistribution of Rb and Sr may occur among the minerals such that



mineral isochrons will reflect the age of the metamorphic event.

The approximate preservation of Rb-Sr systematics during a thermal event may be explained in terms of two parameters (Roddick and Compston, 1977); i) the volume throughout which Sr isotopic equilibration is effective during the event, and ii) the minimum subvolume into which the body can be divided such that each subvolume has the same mean Rb/Sr ratio as the mean Rb/Sr for the entire body. If (i) > (ii) then the system has been reset, therefore, it is important to know the scale on which Sr isotopic homogenization occurs during metamorphic events. Krogh et al., (1976) studied the contact between mafic dykes and the leucogranite they cut and found that within a few centimeters of the dyke the Rb and Sr concentrations had been altered but away from the dyke (72 cm) the leucogranite remained unaffected. In a study of Sr homogeneity in the mantle, Hofmann (1975) concluded that homogeneity was limited to tens or hundreds of metres, a view also taken by Hart and Brooks (1970), Brooks et al., (1976) and others. Hofmann and Gramert (1975) found in their study of the Phanerozoic Belt Series meta-sediments that Sr isotopic homogenization during high-grade metamorphism had occurred on a hand specimen scale and that on a larger scale of sampling isochrons reflected the age of sedimentation.



It is possible that in the case where granitic or intermediate rocks have evolved through partial melting of a precursor, that complete Sr homogenization did not occur and that an isochron plot may reflect the age of the original rock. Roddick and Compston (1977) attribute the apparently 'inherited' isochron age for the Murrembidge Batholith (Rb/Sr age of 490 Ma versus zircon U-Pb age of 426 Ma) to the fact that Sr equilibrium during partial melting of a precursor occurred on a scale smaller than their sample size. Parkhurst and Pidgeon (1976) found in a study of two Scottish granites of supposedly the same age and origin that one showed an inherited isochron and that the other gave an age agreeing with its zircon age. In the former case, the Ben Vuirich Granite, it was found that homogenization had indeed occurred but only over a few metres where as homogenization had occurred on all scales in the case of the latter, the Dumfallow Hill Granite. They attributed this difference to the fact that in the case of the latter, a more acid melt had evolved with a high fluid content as indicated by the presence of muscovite and that this permitted easier diffusion of Rb and Sr within the melt resulting in complete homogenization.

Open system behavior of rocks to Rb and Sr migration during metamorphism is also partly a function of bulk chemical and mineralogical composition. Mukhopadhyay et al.,





(1975), in their study of the geology of the Pedernal Hills area of New Mexico, found that a granitic stock showing intrusive relationships to the surrounding metasediments gave an older age ( $1471 \pm 97$  Ma) than the country rock ( $1364 \pm 27$  Ma). They attributed the younger age for the schists to be a result of Sr loss suffered during a period of cataclasis. Although this event left a marked effect on the granite it was able to retain its Sr whereas the schists, composed predominantly of phyllosilicates, lost its radiogenic Sr because there were no minerals, such as plagioclase, which could take up the element once it became mobile. In the case of fine-grained, acid volcanics open system behavior during regional metamorphism has long been suspect. Cormier (1969) found that Rb/Sr analysis of the Hercynian Cold Brook Group volcanics defined two different isochrons indicating ages of  $750 \pm 80$  Ma (initial ratio .7054) and  $370 \pm 38$  Ma (initial ratio .7135). The older age is interpreted as the time of eruption and the younger age is attributed to effects of the Acadian orogeny. Alsopp et al. (1968) found that the acid volcanics of the Onverwacht series gave an age younger than that suggested by their work and that, combined with an initial ratio of 0.716, suggested an alteration of their Rb/Sr systematics. Bell and Blenkinsop (1978) divided sixteen samples of the Cape St. John Group acid volcanics into two chemical groups which define different



isochron ages of  $520 \pm 40$  Ma and  $385 \pm 15$  Ma. The latter age is defined by the more silicious group of rocks and is attributed to their open system behavior with respect to Rb and Sr during the last thermal event which affected the area.

In the case of four of the five isochron plots (i.e. the Otter Lake Granite, the Minisinakwa Volcanics, the Bruce River Volcanics, the Walker Lake Granite) discussed the scatter observed was outside of analytical error and was believed to be related to something geologic. The scatter from linearity may be attributed to either one, or all of the following; i) incomplete homogenization of the  $^{87}\text{Sr}/^{86}\text{Sr}$  ratio. If the rock suites were formed by partial melting of a precursor, as is suggested by their calc-alkaline nature, then an incomplete resetting of Rb-Sr systematics may have resulted. In this case scatter of the points may define two isochrons between which all the points would lie. The maximum age, or isochron with the steeper slope, would represent the 'inherited' isochron and the minimum age, or isochron with the shallow slope, would indicate the true age of the rock if some of the samples analysed represented subvolumes where complete homogenization had occurred. It is interesting to note that Chappell and White (1974) state that isochrons of S-type granites show a scatter of points within a broad



envelope, reflecting variations in the initial  $^{87}\text{Sr}/^{86}\text{Sr}$  within a single pluton as a consequence of more heterogeneous source material. ii) Partial resetting of the Rb/Sr clock by some later metamorphic event. As was discussed earlier, the degree of resetting depends on the bulk composition of the rock and also on the minerals present, and their retentivity to Sr. Resetting of the Rb-Sr systems would increase the initial  $^{87}\text{Sr}/^{86}\text{Sr}$  ratio and the present Rb/Sr ratio would depend on the time elapsed since the age of the subsequent event. iii) Assimilation of older material through anatexis which would cause an increase in both the Rb/Sr and  $^{87}\text{Sr}/^{86}\text{Sr}$  ratio. The presence of Archean rocks is known in the area and incorporation of this material into the ascending magma may have occurred. Anatexis would preferentially incorporate the alkali phases enriched in Rb thus increasing the overall Rb/Sr ratio. Such a mechanism need not be homogeneous and may, therefore, cause inhomogeneity with respect to the initial  $^{87}\text{Sr}/^{86}\text{Sr}$  ratio throughout the magma.

A combined  $^{87}\text{Rb}/^{86}\text{Sr}$  versus  $^{87}\text{Sr}/^{86}\text{Sr}$  plot of all the data (30 points total) is presented in Figure 23. The 1770 Ma age is for the Aillik Group Volcanics and thus represents the oldest rocks of the suites studied. The remaining points appear to be enveloped by two quasi-linear lines. Regression of the data points to these lines indicate ages of





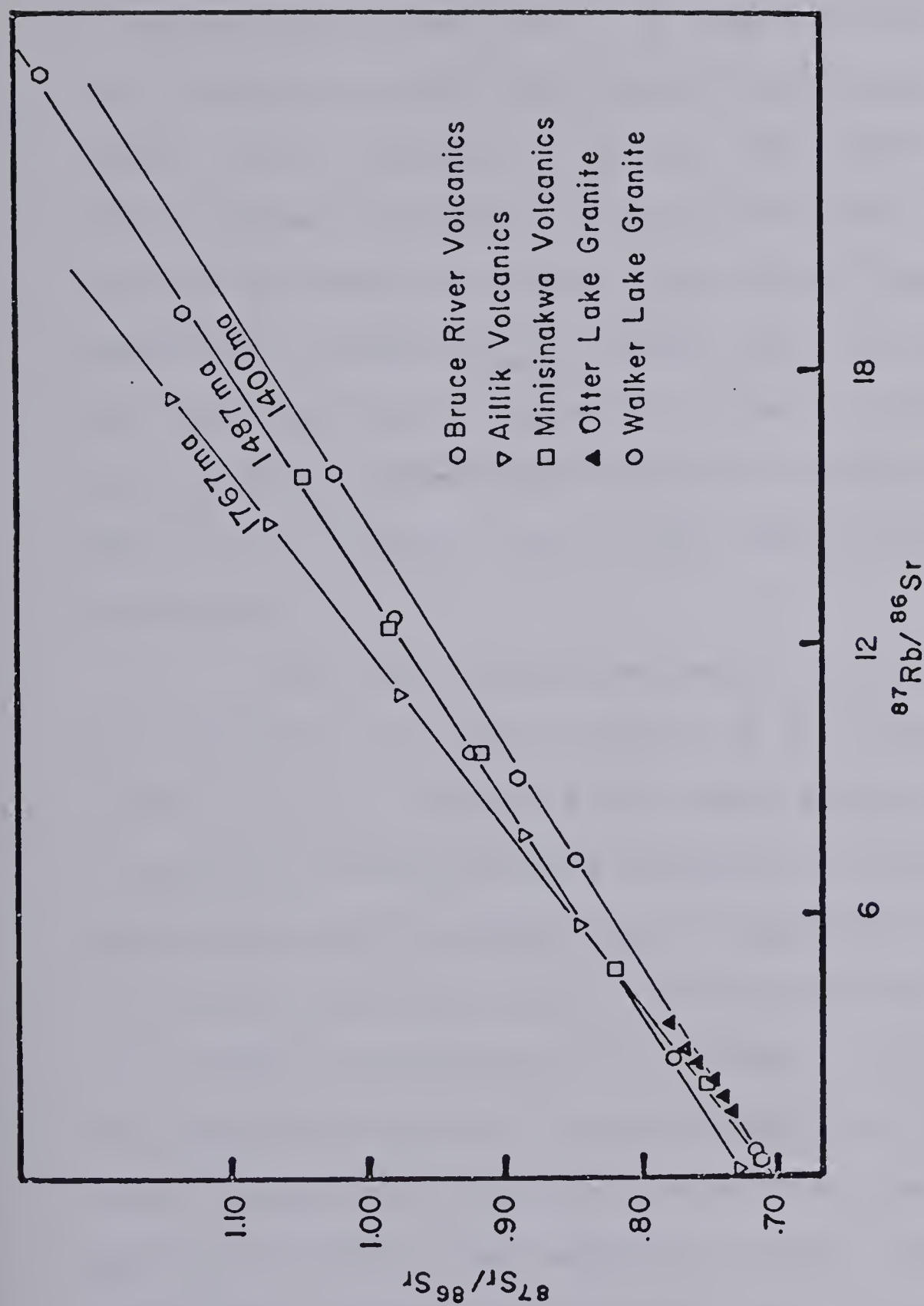


Figure 23

Combined Rb-Sr isochron plot for the Bruce River Group volcanics, Minisinkwa volcanics, Aillik Group volcanics, Otter Lake Granite, and Walker Lake Granite





1487 Ma (initial ratio of 0.7169) and 1400 Ma (initial ratio of 0.7093). What the significance of these pseudo-isochrons is remains unresolved and it is highly probable that it is just a fortuitous and coincidental phenomenon. The only comment worthy of mention is that the 1400 Ma age coincides with the Elsonian thermal event in Labrador. That resetting of Rb-Sr systems can occur at even lower greenschist facies metamorphism (Priem et al., 1978) may lend significance to this "apparent" age. However, one must realize that such plots of data representing different rock suites (although these may be related genetically) should be examined cautiously.

The range in ages of the five rock suites with the oldest in the eastern sector of the Central Mineral Belt and the youngest further to the west suggests a transgression of volcanic activity during Aphebian to Melikian time. Depending upon the orogenic setting accepted (discussed earlier) two possible explanations can be postulated. First, if an arc system is considered then it would suggest evolution of the system during time with subduction towards the west. A second explanation involves eastward movement of the continental plate over a heat source at depth, a model analogous to the formation of the Hawaiian chain of volcanic islands (Carmichael et al., 1974).



## CHAPTER 3

### THE STORMY LAKE AREA

#### 3.1 Introduction and Previous Work

The Stormy Lake uranium showing, located approximately 2.5 km (1.5 miles) northeast of Stormy Lake, Figure 4, was discovered by Piche in 1955 (Robinson, 1956) during a regional reconnaissance program. Follow-up work consisting of detailed mapping and trenching was completed during the same field season. A radioactive zone at the contact between arkosic quartzites (remapped as rhyolites) and an overlying arkosic conglomerate (Piche, 1955) was traced for 1800 feet with visible pitchblende seen in eight locations; nine chip samples from this zone void of visible pitchblende assayed at 0.0023 to 0.225%  $U_3O_8$  (Robinson, 1956). Recognizing the hydrothermal nature of the assemblage uranium, native silver, chalcopyrite and specularite hematite found at Stormy Lake, Beaven (1958) suggested a similarity to the vein deposits found in the N.W.T. around Port Radium.

Marten and Smyth (1975) were the first to recognize that the uranium mineralization at Stormy Lake was spatially related to an unconformity, i.e., the Bruce River-Seal Lake Group unconformity (first documented by Smyth et al. (1975)). They suggested that this unconformity thus offered potential in other sectors of the Central Mineral Belt. Recently Brinex and Inco. have begun exploration in the area



under a joint venture, however, no information concerning other discoveries is available.

Mapping of the Stormy Lake area was carried out during the last week of June, 1977. A grid was first constructed by pace and compass by running a 2000 foot baseline north-south through the area and then putting in offsets every 200 feet both east (1200 feet) and west (1400 feet). Lines were also run between the offsets and the remaining area tied in with pace and compass work where required. Although the mapping was concentrated over a small area, two regional traverses were made to acquaint the author with the regional geology.

### 3.2 Regional Geology

The regional geology of the Stormy Lake area, figure 24, is included in the maps of Fahrig (1959), Piche (1955), DeGrace (1969), Cotê (1970), Marten and Smyth (1975) and Ryan (1978). At the Stormy Lake showing, sedimentary rocks of the Seal Lake Group unconformably overlies porphyritic rhyolites of the Bruce River Group.

The oldest rocks in the area are the Paleohelikian Bruce River Group found to the north and northeast of the study area. They consist of massive rhyolites and ignimbrites and correspond to the uppermost division of the Bruce River Group (Smyth et al., 1975). They are typically por-





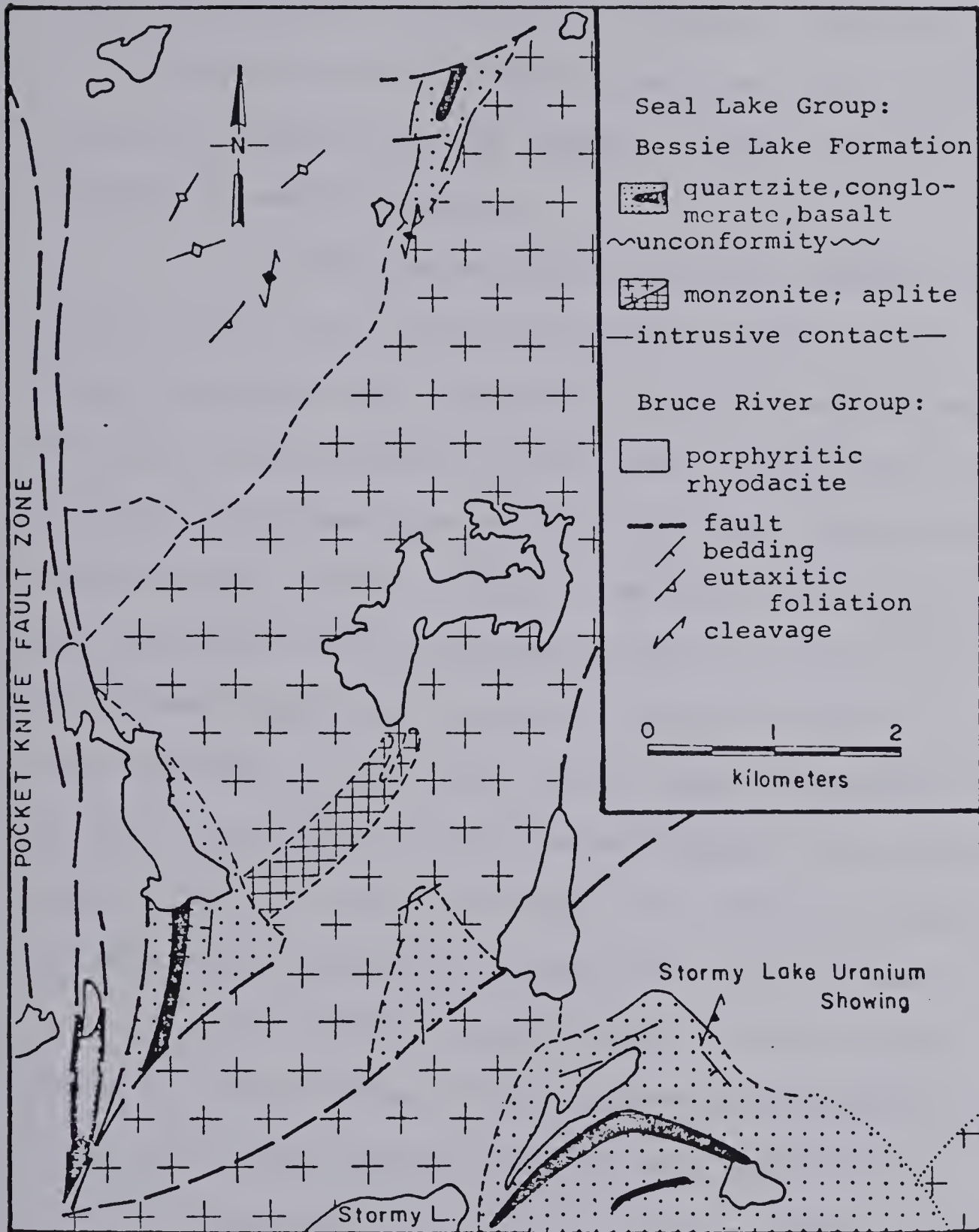


Figure 24.

Regional geology of the Stormy Lake area



phyritic in nature with up to 25-30% of feldspar phenocrysts of 3-5 mm size and 1-3% blue quartz eyes of 1-3 mm size with eutaxitic textures fairly common. Chemically they vary between rhyolites and rhyodacites.

A large batholithic body, the Otter Lake Granite, dated by the Rb/Sr method at  $1496 \pm 37$  Ma, cuts the Bruce River Volcanics and suggests a possible coeval relationship between the two suites. This body varies from monzonite to granite in composition and cut by later aplitic bodies west of Katty Lake (Ryan, 1978). Some dioritic phases occur and may represent early differentiates as in some instances dioritic xenoliths can be seen in the main granitic phase. In thin section it typically shows a hypidiomorphic granular texture consisting of K-feldspar (65-80%), plagioclase (5-15%), quartz (15-25%), biotite (1-2%) and a high accessory content of euhedral to anhedral sphene and rarely almandine garnet.

Côté (1970) shows several other intrusive bodies south of Stormy Lake in the Liorte-Gayle-Stormy Lakes area. He divides these bodies into several complexes as follows: 1) diorite-syenite; 2) Adlavik gabbro-diorite-syenite; 3) adlavik gabbro-diorite; and 4) medium grained diorite. The age relationships of these various intrusives is suggested by Côté (1970) to be : Adlavik gabbro oldest, followed by the syenite and then diorite. The age of the medium-grained granite-diorite remains ambiguous. It is believed



that most of these rocks predate the Seal Lake Group sediments (Smyth, personal communication).

Unconformably overlying the Bruce River volcanics and the Otter Lake Granite are the Bessie Lake sediments, basal member of the Neohelikian Seal Lake Group (Brummer and Mann, 1961). A zone of paleoweathering up to 30 metres thick is developed in the Otter Lake Granite below the Seal sediments (Marten and Smyth, 1975) suggesting a major time break between the Bruce River Group and Seal Lake Group. The Bessie Lake sediments consist of a basal conglomerate which grades upwards into quartzites and grits intercalated with tholeiitic basalts. The conglomerates typically display good graded bedding and the quartzites show excellent cross-bedding defined by heavy mineral laminations of magnetite.

The Stormy Lake area lies in the Grenville Foreland Belt, or more specifically the Nain Foreland Zone of Wynne-Edwards (1972). Although the Grenville Front is shown on regional maps (cf. Greene, 1972), to go through the Seal Lake-Stormy Lake area it cannot be precisely defined but is instead represented by a wide zone of northerly directed thrusting and folding.

Two periods of folding can be recognized on a regional scale in the Stormy Lake area. The first ( $F_1$ ) folds (Plate 1) are large, flat lying open folds, whose axial planes generally dip  $<30^\circ$  to the south and whose axis





dip gently to the west. The Stormy Lake uranium showing is located on the northerly limb of such an  $F_1$  synclinal fold and Côté (1970) shows this pattern of folding to continue along the eastern margin of the Seal Lake-Bruce River Group contact further to the south (i.e. synclines represented by tongues of Seal Lake Group sediments protruding easterly into the Bruce River volcanics). The second period of folding ( $F_2$ ) (Plate 2) is represented by the northerly outlier of Seal Lake sediments and volcanics, Figure 24, which has a tight closure to the north (Plate 3).

Associated with the second period of folding is the development of a regional schistosity which generally strikes northeast-southwest and dips  $45^\circ$  to the southeast. In places this has crenulated an earlier cleavage, notably in the finer grained sediments where an earlier fabric related to  $F_1$  folding was probably developed.

Two prominent directions of faulting occur within the area, a north-south and northeast-southwest set of faults. The north-south trending Pocket Knife Fault Zone is a major structural lineament that coincides approximately with the eastern limit of the Seal Lake Group. It may represent a rejuvenated crustal break, possibly a continuation of the Nain-Churchill boundary (Greene, 1974; Marten and Smyth, 1975). The northeast-southwest trending Minisinakwa Shear (Ryan, 1978) is probably related to foreland thrusting and





the closure of tight isoclinal folds (cf. the Bruce River Syncline which is bounded to the north and south by the Bruce River and Gravelly River shear zones respectively).

### 3.3.1 Local Geology (Stratigraphy)

The local geology of the Stormy Lake showing is shown in Figure 25, and Plate 4, an area approximately 0.4 km<sup>2</sup> in size. In the map area the following stratigraphy has been recognized: Bruce River Group porphyritic rhyolites unconformably overlain by a thin polymictic conglomerate bed of the Bessie Lake Formation which is overlain conformably by schistose, mafic volcanic rocks with intercalated lenses of blue-grey quartzite. This is overlain by a quartz cobble conglomerate which grades laterally and vertically into a thick unit of quartzites, grits and conglomerate.

The Bruce River Volcanics are typically porphyritic with 5-20% phenocrysts of feldspar (3-5 mm) and rarely blue quartz eyes (1-3 mm) set in a microcrystalline felsic matrix which is locally a quartz-sericite schist depending on the degree of metamorphism. A penetrative cleavage ( $S_2$ ) is pervasive throughout the unit. In thin section the rhyolites consist of approximately 5-10% of blastoporphyratic phases of K-feldspar, microcline, and plagioclase of xenoblastic shape set in an equigranular to inequigranular quartzo-feldspathic matrix. The phenocrystic phases show mortar-like





Figure 25

Local Geology of the Stormy Lake Uranium Showing.

Seal Lake Group (Bessie Lake Formation):

- 6

 Quartzites, quartz pebble quartzites, grits; 6a, quartz pebble conglomerate.
- 5

 Quartz pebble conglomerate
- 4

 Quartzites, grits; 4a, quartzites
- 3

 Mafic volcanic rocks
- 2

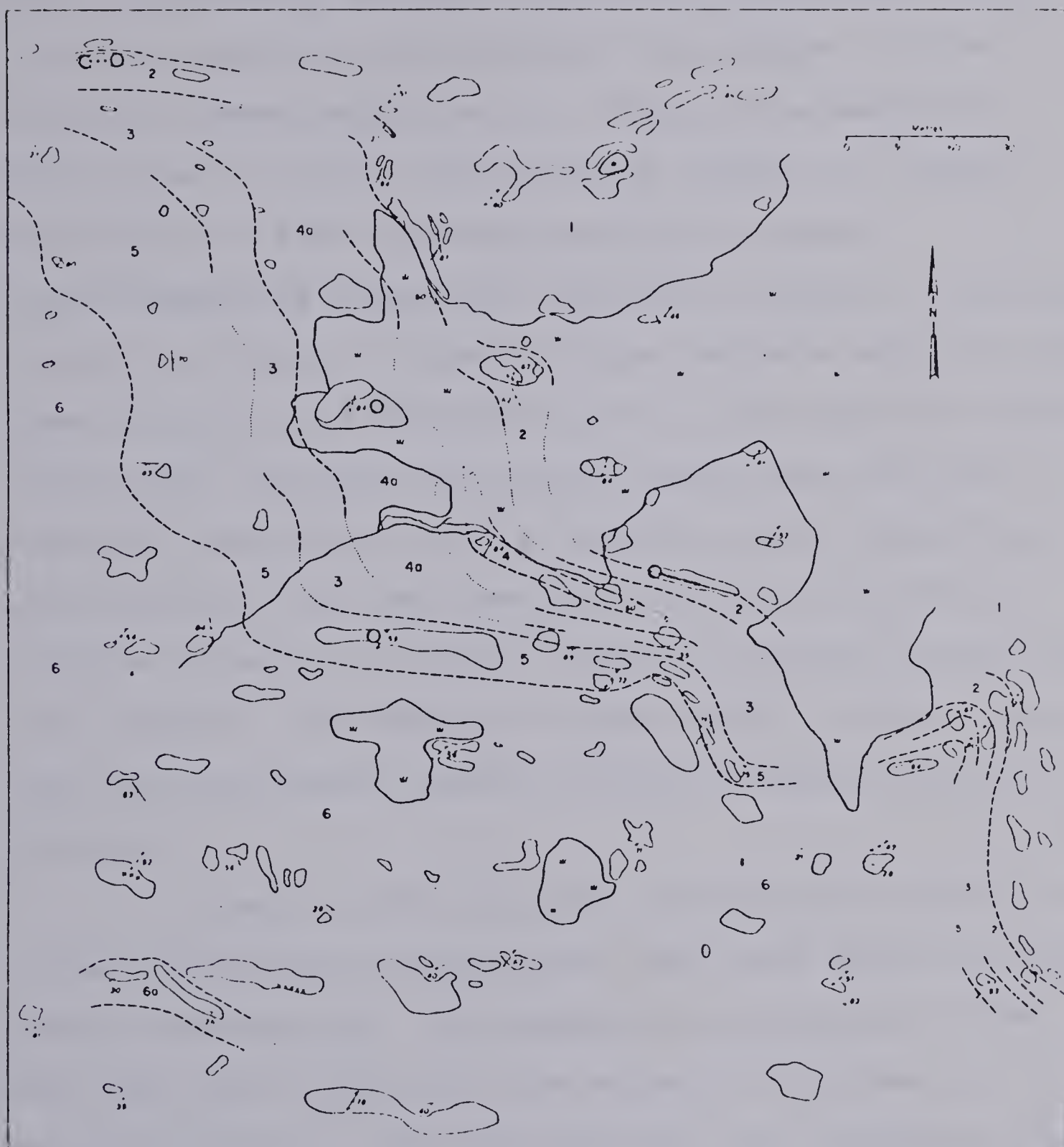
 Basal conglomerate and arkosic conglomerate

Bruce River Group:

- 1

 Feldspar porphyry with minor quartz

|   |   |
|---|---|
| Bedding (tops known, tops unknown). . . . .         |   |
| Cleavage . . . . .                                  |   |
| Geologic contact (defined, approximate, assumed). . |   |
| Uranium showing . . . . .                           | X |
| Fluid inclusion specimen (quartz) . . . . .         | ○ |
| Outcrop . . . . .                                   |   |
| Swamp . . . . .                                     |   |







structures with recrystallization having occurred along their margins with the associated development of muscovite  $\pm$  epidote. Fracturing, undulose extinction, development of deformation lamellae, and conversion of K-feldspar to microcline are common indicating the effects of metamorphism. Quartz eyes are rarely preserved but instead have recrystallized to a finer grained aggregate of quartz grains displaying granoblastic-polygonal texture. The matrix consists of lenses of recrystallized pumiceous material composed of quartz and K-feldspar, set in a finer grained quartz and feldspar aggregate with lesser plagioclase and minor carbonate, muscovite, epidote, sphene, zircon, magnetite, and fluorite. The matrix may show either a granoblastic elongate or polygonal texture, sometimes varying within the same section. Any schistose texture within the rock usually parallels any primary igneous banding suggesting isoclinal folding.

Overlying the volcanics unconformably (Plate 5) is a basal, polymictic conglomeratic unit which grades into an arkosic conglomerate. The polymictic conglomerate varies from less than a metre to a few metres in thickness and is typically infolded with the volcanics. It consists of round cobbles and boulders of quartzite, jasper, granitic material, and feldspar porphyry set in a sand and gravel size matrix. The material is poorly sorted and the matrix seldomly accounts for more than 15-20% of the rock. This basal unit is



overlain by an arkosic conglomerate which is highly indurated and whose components are commonly stretched due to subsequent deformation. The components are mainly pebble in size consisting predominantly of quartz with jasper, and rock fragments forming the remainder set in an arkosic matrix, covered by a hematitic stain. This unit hosts most of the radioactive occurrences and where mineralization occurs the development of chlorite, massive and specular hematite, red and white carbonate and sericite are noticeable. In thin section the rock consists of recrystallized quartz pebbles exhibiting mortar textures set in a matrix composed of quartz, feldspar, muscovite, magnetite, and the accessory minerals sphene and zircon, all coated by a hematitic stain. The overall texture would best be described as cataclastic.

The overlying unit consists of blue-grey, well cross-bedded quartzites which are intercalated with chlorite schists believed to be mafic volcanics. The quartzites are typically blue in color and contain very little of anything else except for magnetite which defines the cross-bedding (Plate 6) and some sericite which locally imparts a good fabric to the rock. In thin section the rock consists of >90% quartz which shows a granoblastic-polygonal texture, idiomorphic cubes of magnetite, and lenses concentrated with the accessory minerals sphene and zircon comprising 50-75% of the section in places (Plate 7). Muscovite is present in



some sections defining a lepidioblastic texture.

The chlorite schists contain a well developed fabric in hand specimen and in a few instances possible crenulation surfaces were noted indicating two periods of deformation. In thin section they consist predominantly of chlorite and intensely altered feldspar which is sericitized and sausseritized. Carbonate alteration is pervasive and in some cases may locally compose 75% of the section. Although quite thin and of no lateral extent, in the surrounding area some very thick units of similar chlorite schists were seen on regional traverses. Brummer and Mann (1961) also report the presence of thin basaltic flows in the Bessic Lake Formation. Baragar (1974) reports that they are of tholeiitic composition and are typical plateau-type basalts.

The blue quartzites are overlain quite sharply by a quartz cobble conglomerate (Plate 8). This unit, which is 75 metres thick in the centre of the map area, pinches out along strike both to the northwest and southeast. It grades upwards from a quartz cobble conglomerate composed of 90% quartz, 5% dark grey chert, and 5% matrix of grit to a quartz pebble conglomerate. The percentages stay the same until the upper part of the unit where the matrix of grit increases to 25-30% of the rock and in this instance a fabric is developed. The quartz grains are usually elliptical in shape and have been rotated such that they plunge  $35^{\circ}$  to  $65^{\circ}$





towards the west or southwest.

The quartz pebble conglomerate grades both laterally and vertically into a thick unit composed predominantly of cross-bedded, blue-grey quartzites and coarse-grained grits with lesser amounts of quartz pebble and cobble conglomerate, and pelites. The quartzites are similar to the ones already described with the cross-bedding being defined by heavy mineral laminations of magnetite which occur as idio-blastic octahedra. The pelites are a dark grey or black rock with a well developed cleavage and in thin section consist predominantly of sericite with carbonate alteration and minor amounts of sphene and zircon occurring in bands parallel to the fabric. Magnetite occurs as irregular streaks within the sections parallel to the fabric. The sandstones are quartz-rich and in thin section individual grains can be seen to have recrystallized and to be granulated on their margins. Feldspar also occurs as sandsize grains of anhedral shape and are quite fresh, and are usually fractured and infilled by matrix material and show undulose extinction. The matrix has an inequigranular texture which has recrystallized into a granoblastic elongate aggregate of quartz and minor feldspar with local development of muscovite and some epidote, again accessory minerals are present.

### 3.3.2 Local Structure

In the vicinity of the Stormy Lake showing two phases of Grenville age deformation ( $D_1$  and  $D_2$ ) can be recog-

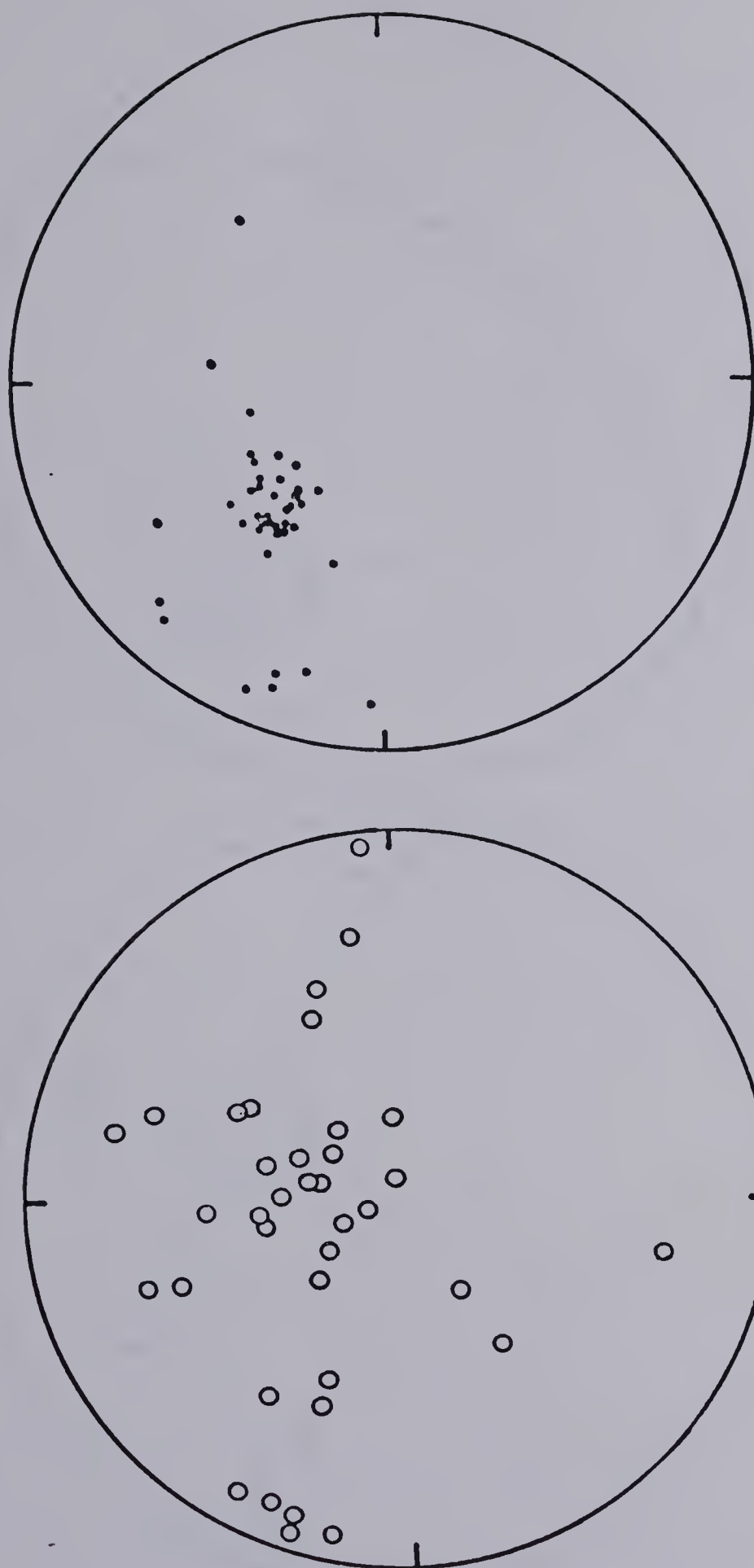




nized. The first phase was responsible for the folding of the lithologies into a large, flat lying **syncline** overturned to the south and plunging gently to the west or southwest. This period of deformation is only recognized in the area from regional mapping as explained earlier and because of the presence of a crenulation cleavage seen in the chlorite schists and some local erratics.

The second phase of deformation produced isoclinal folds plunging steeply to the south or southwest with an associated penetrative cleavage. A B plot of the poles to bedding, Figures 26 and 28, show that the general trend and plunge of the fold axes for these  $F_2$  structures is N-S and  $30^\circ @ 193^\circ$ . Although the distribution of the points on the stereogram suggests a box-type of folding this is believed to be due to an inadequate number of points plotted plus the fact that if the folds are isoclinal then statistically there would be more readings taken on the limbs and crests than the shoulders of the folds. A  $\pi$  plot of the poles to the cleavage, Figures 27 and 29, shows that the general trend of the fabric is N  $36^\circ$  E, dips  $50^\circ$  SE. Also associated with this second phase of deformation is the local development of numerous folds, particularly at the unconformable contact between the rhyolites and basal conglomerate (Plate 9), and the rodding of the quartz cobbles and pebbles in unit 5. The quartz grains generally plunge  $30-60^\circ$  to the west or south-



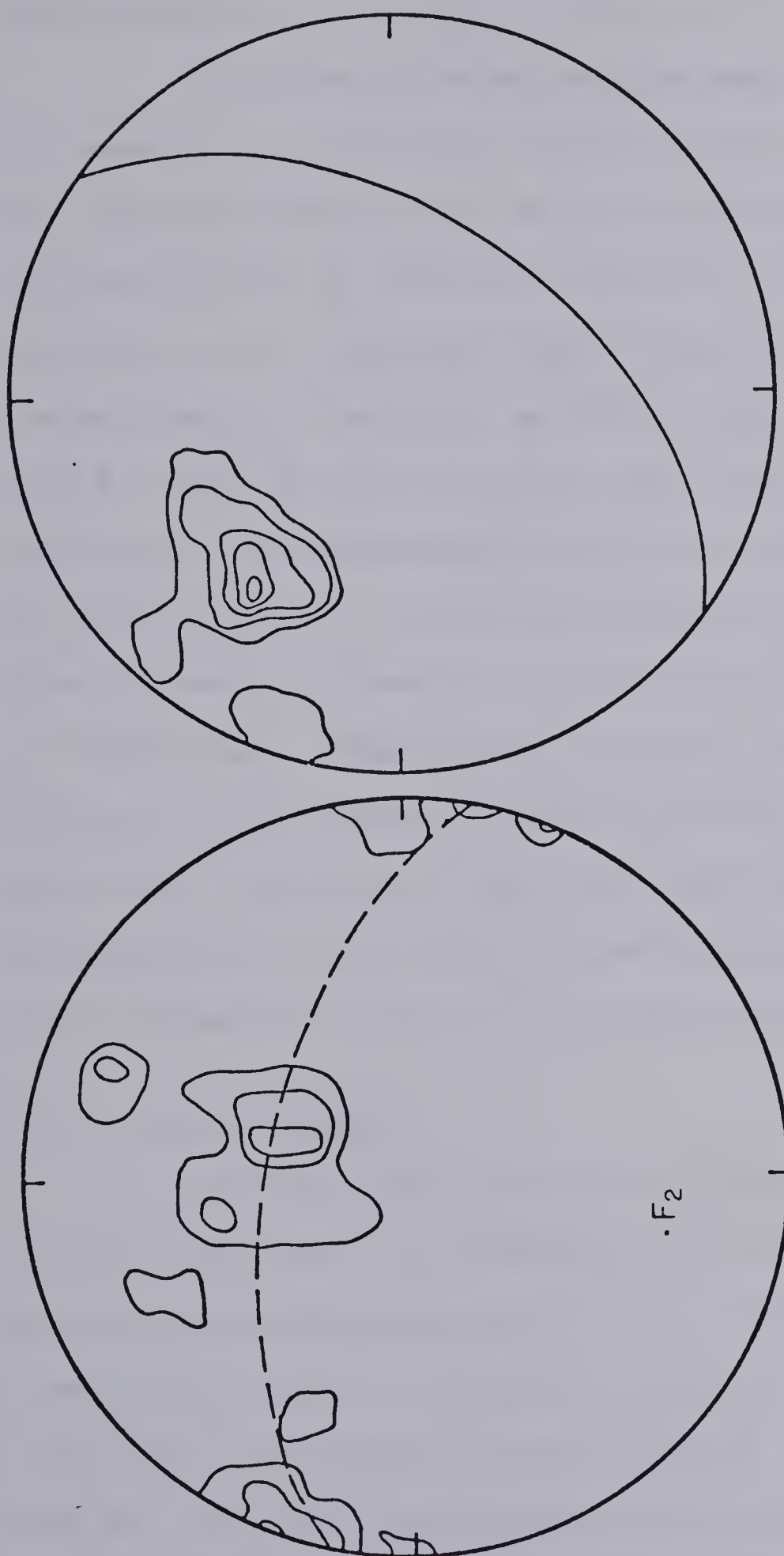


Plot of poles to bedding(38 measurements)      Plot of poles to cleavage(43 measurements)

Figure 26      Figure 27

Structural data for the Stony Lake (uranium deposit) area





1% equal-area projection of poles to bedding; contour interval 3,6,9%

1% equal-area projection of poles to cleavage; contour interval 5,10,20,30,40%

Figure 28

Figure 29

Structural data for the Stormy Lake (uranium deposit) area





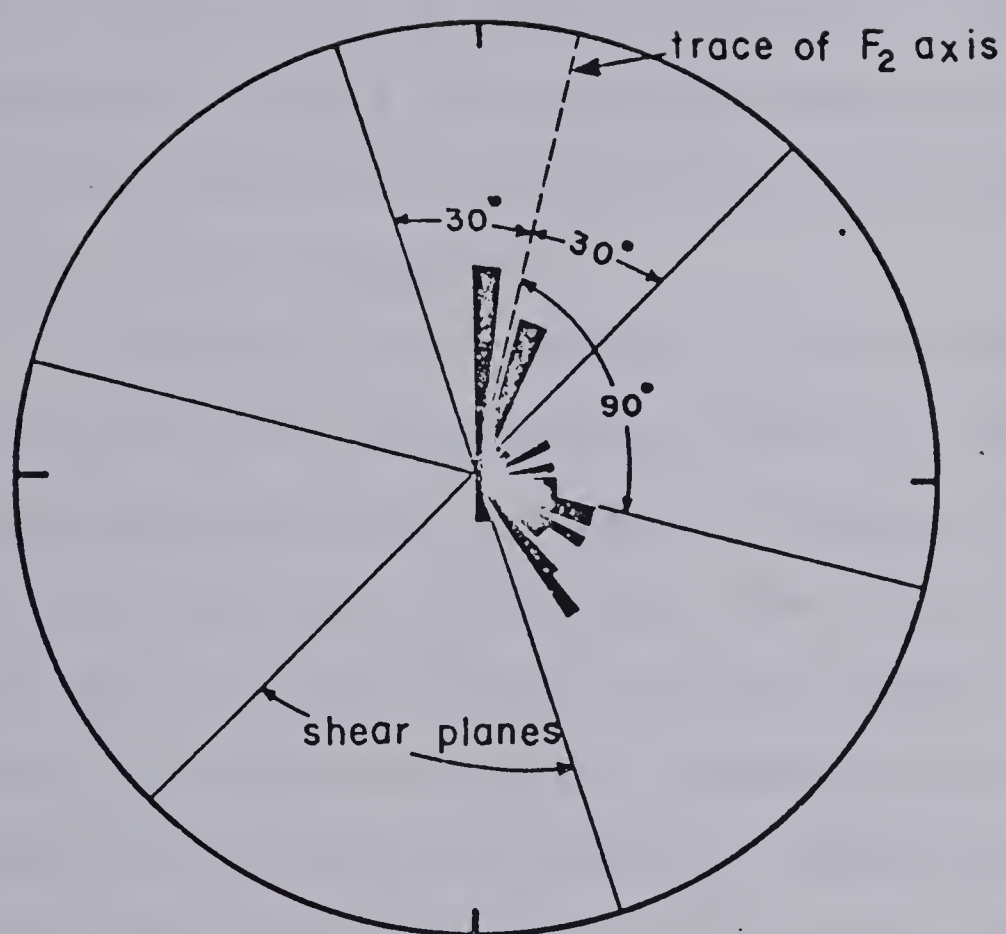
west and lie in the plane of the local fabric.

Fracturing is quite prominent in the area and since it seems to control the uranium mineralization it is important to understand the origin of these structures. Figure 30 shows a rosette plot of fractures taken in the map area with two prominent sets developed which trend  $005-020^{\circ}$  and  $110-140^{\circ}$  respectively. The trace of the  $F_2$  fold axis, when superimposed on the diagram suggests that the first set may be radial or tensional features and the second set are related to shear planes. A third less prominent set at  $\sim 115^{\circ}$  may have formed as a result of tension parallel to the direction of the stress. Thus, both of these fracture patterns can be related to the second phase of deformation. It should be noted that there are other less prominent fracture patterns developed but these were of limited extent and accounted for only a fraction of the total number measured.

### 3.3.3 Metamorphism

The metamorphism in the Stormy Lake area is generally of low grade, corresponding to Winkler's (1974) low-grade facies characterized by the assemblage chlorite + zoisite/clinozoisite  $\pm$  actinolite  $\pm$  quartz. The only rocks of the area which are helpful in determining the grade of metamorphism are the mafic volcanics, now chlorite schists. As previously stated these consist predominantly of chlorite and epidote





Rosette plot of joints and fractures showing their relationship to  $F_2$  fold axis.

Figure 30



with minor **sericite** after feldspar, magnetite, and carbonate alteration. This assemblage is usually referred to as greenschist. The other rocks of the area offer little assistance being characterized by the presence of muscovite and sometimes minor amounts of epidote, but mostly they consist of recrystallized quartz with minor K-feldspar. Where muscovite is present it is usually found rimming feldspar grains thus suggesting that it formed from **clay** alteration products of the feldspars.

However, the textures of the sediments and felsic volcanics do offer some information concerning the past history of metamorphism. Granoblastic elongate aggregates of quartz and feldspar in the matrix and mortar textures of the quartz grains suggest high pressure, dynamic metamorphism. This is also suggested by the feldspar grains in both the volcanics and sediments which show **undulose** extinction, deformed twin lamellae, fracturing, exsolution twin lamellae, and some inversion of orthoclase to microcline. Where quartz grains have recrystallized arrested grain boundaries are indicated by lobate textures suggesting that equilibrium conditions were not everywhere attained. However, the extensive development of a granoblastic-polygonal texture, most common in monomineralic layers, suggests that both equilibrium was attained and that post-tectonic recrystallization occurred. At this time the numerous quartz veins seen





in the area were probably formed, this is supported by plate 10 showing one of these quartz veins containing a piece of country rock which exhibits crenulation cleavage. Thus it was probably during the waning stages of metamorphism that large quantities of fluid were released with the decrease of pressure permitting the development of granoblastic-polygonal textures in the rocks and the formation of numerous quartz veins.

### 3.4 Mineralization

Uranium mineralization at the Stormy Lake showing is located in two zones, the first and most important is located at the unconformity between the Paleohelikian Bruce River volcanics and Neohelikian Bessie Lake sediments. The second is located approximately 275 metres (800 feet) stratigraphically above the unconformity in quartzites and quartz pebbly quartzites.

The uranium mineralization in the first zone is confined to north-south fractures (Plate 11) and quartz veins in an arkosic conglomerate unit immediately above the unconformity. Five of the seven occurrences seen were within this zone and four had visible pitchblende. In three cases uranium mineralization was noted to be in the form of rods aligned along fractures, generally plunging to the south at  $30^{\circ}$  to  $50^{\circ}$ . Several erratics showed this phenomenon best





(Plate 12) where uranium mineralization as pitchblende formed on an original fracture surface as long slender rods. The rods were the full length of the boulders varying from 15-30 cm. In other instances pitchblende was seen to form within quartz veins, the best example of this being found at the far northwest corner of the map area where the arkosic conglomerate has been invaded by numerous north-south trending quartz veins. It may be significant to note that the veins were not seen to extend into the underlying volcanics.

The second zone of radioactivity was void of visible, primary uranium mineralization, but secondary yellow and orange uranium oxides were seen. Mineralization appeared to be confined to vertical fractures generally aligned northwest-southeast. The zones of radioactivity gave scintillometer readings of 5-10 times background values.

The composition of four pitchblende samples used for dating, as determined from isotopic dilution analysis, is presented in Table 11. Except for samples S-8 and S-8<sup>1</sup> the uranium content is quite low due to surface weathering and therefore leaching of the uranium. Semiquantitative microprobe analysis were also performed and the same phenomenon prevailed as illustrated in a chart recording of an EDA spectrum, Figure 31. The high lead peak is due entirely to radiogenic lead as no galena was present. In general, the ratio of U/Pb (counts) over 400 second periods varied from 1.0 to

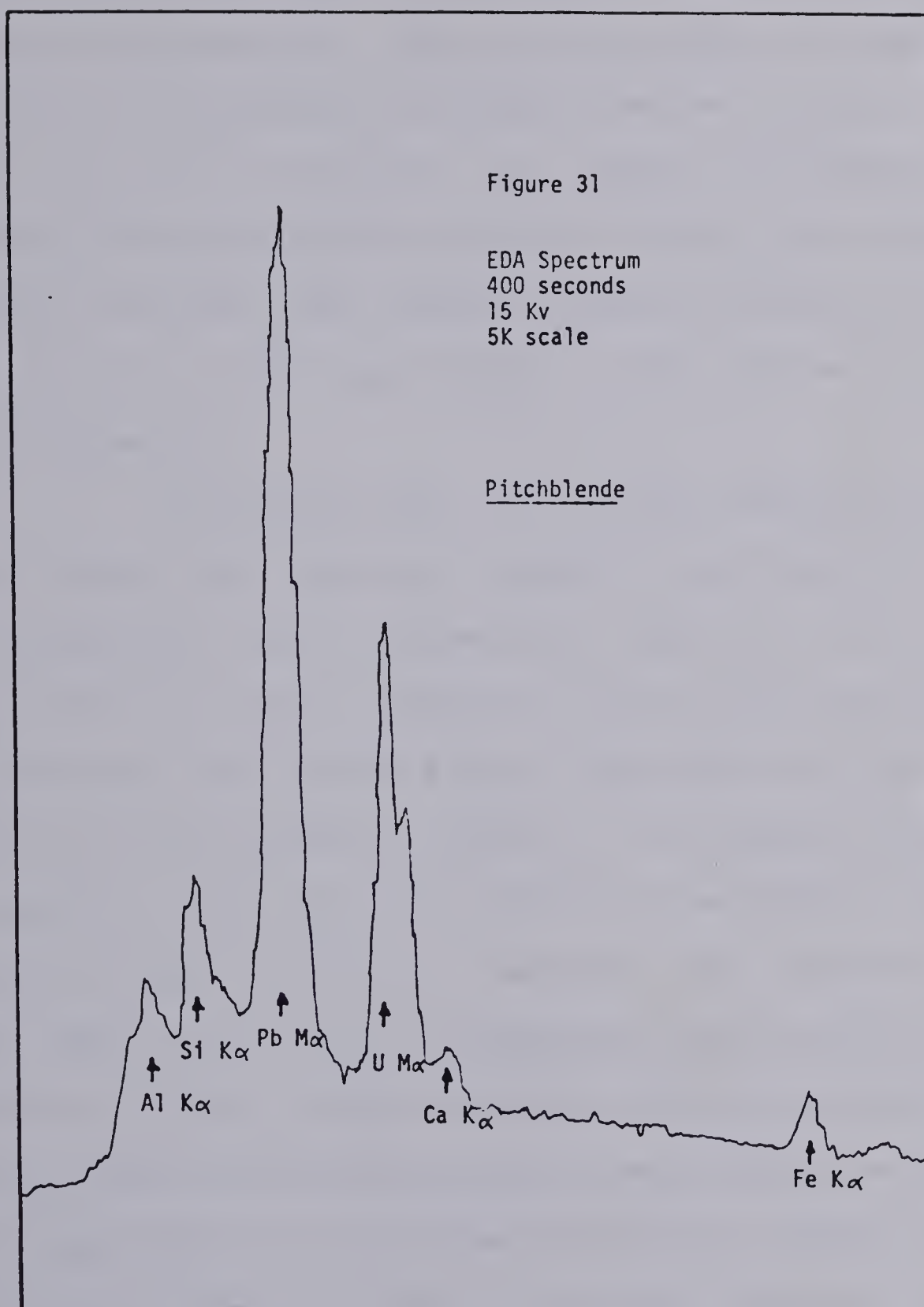


TABLE 11

## Uranium-Lead Data, Stormy Lake

|                  | $^{238}\text{U}$<br>ppm | $^{235}\text{U}$<br>ppm | $^{206}\text{Pb}$<br>ppm | $^{207}\text{Pb}$<br>ppm | $^{208}\text{Pb}$<br>ppm | $\frac{^{207}\text{Pb}}{^{206}\text{Pb}}$ | $\frac{^{206}\text{Pb}}{^{238}\text{U}}$ | $\frac{^{207}\text{Pb}}{^{235}\text{U}}$ | $\frac{^{206}\text{Pb}}{^{238}\text{U}}$ |
|------------------|-------------------------|-------------------------|--------------------------|--------------------------|--------------------------|---|--|--|--|
| S-8              | 437246                  | 3131                    | 69241                    | 4712                     | 7174                     | 860 Ma                                    | 1083 Ma                                  | 1.7082                                   | 0.183                                    |
| S-8 <sup>1</sup> | 207138                  | 1483                    | 58694                    | 2810                     | 9527                     | 990 Ma                                    | 1260 Ma                                  | 2.503                                    | 0.2158                                   |
| S-40-1           | 20091                   | 144                     | 5315                     | 204                      | 458                      | 640 Ma                                    | 1125 Ma                                  | 1.6072                                   | 0.1906                                   |
| S-40-2           | 27256                   | 195                     | 10434                    | 854                      | 2006                     | 1230 Ma                                   | 2263 Ma                                  | 4.725                                    | 0.4205                                   |





EDA spectrum for pitchblende mineralization  
from the Stormy Lake uranium deposit





0.2 for several different samples analyzed.

The abundance of thorium was found to be insignificant from field work by the use of a McPhar TV-1 discriminating scintillometer. Thus isotopic dilution analysis to determine the abundance of thorium and to obtain a  $^{232}\text{Th}/^{208}\text{Pb}$  age was felt unwarranted. The absence of thorium was confirmed from microprobe analysis, however, the high  $^{208}\text{Pb}$  values obtained from isotopic dilution contradict this unless it is not of radiogenic origin. This problem will be discussed elsewhere.

Associated with the uranium mineralization in varying amounts were specular hematite, red and white carbonate, chalcopyrite, pyrite, malachite, fluorite, chlorite and quartz. In addition to this, Robinson (1956) also reported a vein of chalcocite with native silver and Marten and Smyth (1975) mention the presence of galena. The specular hematite usually occurred as large (1-2 cm), tabular rhombohedral crystals in quartz veins (Plate 13). Hematite also occurred in a dendritic form, as massive, fine-grained specularite coating fractures or at the contact between quartz veins and the country rock, and in polished specimens small blades of hematite can be seen intergrown with the pitchblende (Plate 14). Fluorite is fairly ubiquitous next to specular hematite and occurs either as fine-grained bands parallel to the local schistosity in the sediments and volcanics (Plate 15), or as cubic crys-



tals up to 0.5 cm in size in veins. It is characterized by its dark purple color, a color often attributed to the presence or near-proximity of uranium.

### 3.5.1 Fluid Inclusions (Introduction)

Previous studies of fluid inclusions pertaining to uranium mineralization are few due to the fact that many of the fluid inclusions are hosted by minerals which were not deposited contemporaneously with the uraniferous phases (Rich et al., 1977). In the Stormy Lake area uranium mineralization is intimately associated with quartz veining thus permitting a study of this sort to be undertaken and provide information concerning the nature of the ore bearing fluid. Being such a controversial point (cf. Gabbelman, 1977; Rich et al., 1977) it was hoped that the study would elucidate more about the nature of the ore fluids, their composition, and lend information towards solving the genesis of the Stormy Lake uranium mineralization.

### 3.5.2 Previous Work as Applied to Uranium Deposits

Roedder (1963, 1967, 1977) discusses the application of fluid inclusion research to the study of ore deposits in general and Rich et al. (1977) speak of fluid inclusions with specific reference to "hydrothermal" uranium deposits and vein-type deposits respectively.

The temperature of homogenization for hydrothermal



uranium deposits generally falls in the range 100-200°C. Kostov et al. (1971) and Rogovo et al. (1971) found the temperature of formation for hydrothermal U-Mo deposits to be around 200°C, however, Barsukov et al. (1971) gave a temperature of formation of 112-145°C for a U-Mo deposit. Studies by Leroy and Poty (1969) and Poty et al. (1974) indicate temperatures in excess of 300°C for the "uranium stage" for the deposits of Limousin, France. Of course, all these values are dependent on the salinity of the solutions and depth of formation and in all cases the appropriate corrections may not have been applied. With the notable exception of the data of Leroy and Poty, filling temperatures for the deposition of hydrothermal deposits are <190°C and the majority are less than 150°C (Rich et al., 1977).

Although the majority of fluid inclusions contain only two phases, Poty et al. (1974), Rugova et al. (1971) and Morton et al. (1978) have analyzed inclusion containing a third phase, CO<sub>2</sub>, and in high concentrations (cf. 100 g CO<sub>2</sub>/Kg H<sub>2</sub>O). The presence of such a phase in the temperature range 100-200°C possibly permitted greater amounts of uranium to be carried in the ore solution (Poty, 1979).

### 3.5.3 Procedure

Six samples from five quartz veins and one fluorite erratic were prepared and analyzed in the conventional manner as described by Roedder (1963, 1967). Specimens were cut to





approximately 3 mm thickness and then polished on both sides down to 1 $\mu$  diamond paste while being taken to a final thickness of  $\sim 0.5$  mm. The specimens were then studied petrographically to determine the phases present before proceeding with the heating and freezing experiments. The freezing and heating was carried out on a Chaixmeca microthermometry apparatus, capable of a temperature range of  $-200$  to  $+600^{\circ}\text{C}$ . The apparatus consists of a heating and freezing stage, mounted on a Leitz microscope; a console with temperature readout either manually or mechanically controlled; and apparatus for temperature exchange and cooling. The cooler consists of a dewar flask which houses a copper coil leading to the freezing stage. The flask is filled with liquid nitrogen and gaseous nitrogen passed through the copper coil into the stage causing depression of the temperature. The heating is carried out by heating resistance ( $18\text{V} - 8.5\text{A}$ ). For temperature determinations, the sensor is a platinum resistor ( $100$  ohms at  $0^{\circ}\text{C}$ ) connected to a linear bridge and then to a four-digits temperature readout. Resolution is  $\pm 0.1^{\circ}\text{C}$ . Calibration of the stage was carried out by Mawer (1977) and for any particulars other than described above, the interested person is referred to him.

### 3.5.4 Analysis and Results

Six specimens were studied in all, five quartz and



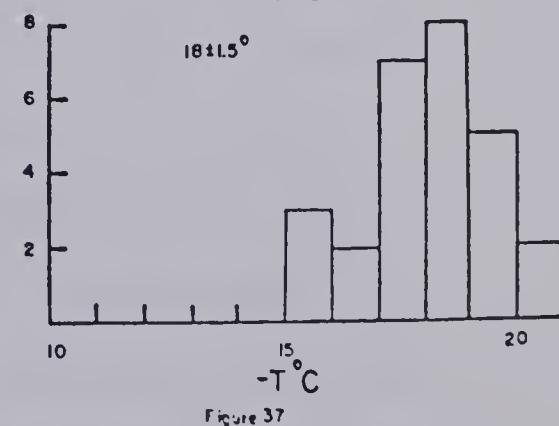
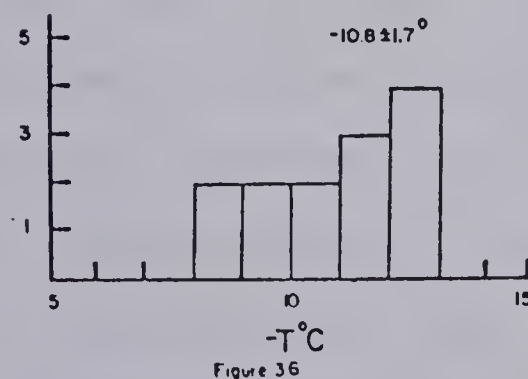
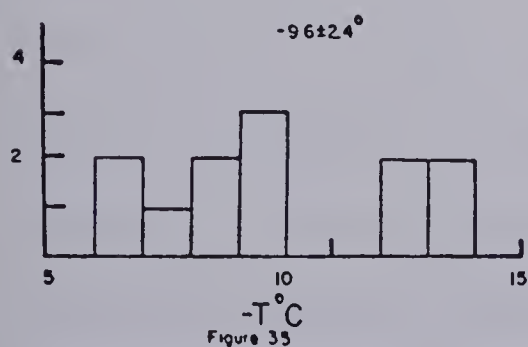
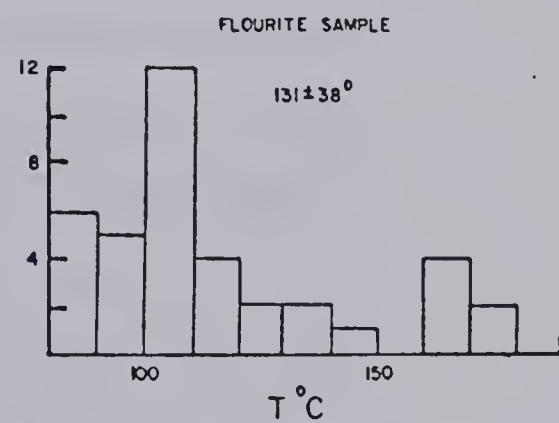
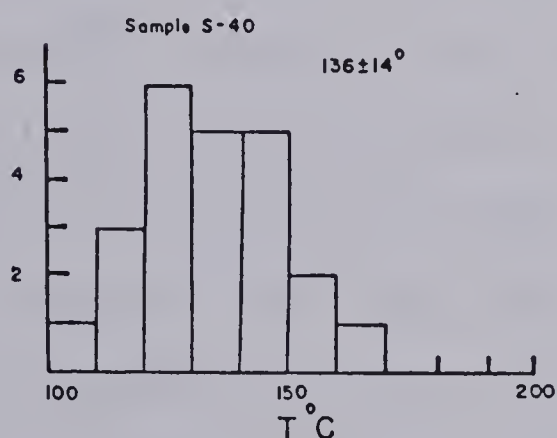
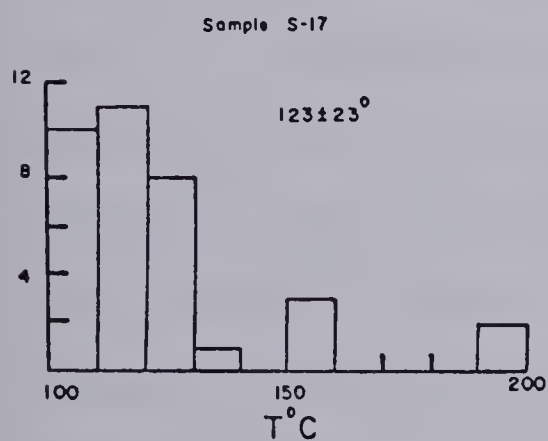
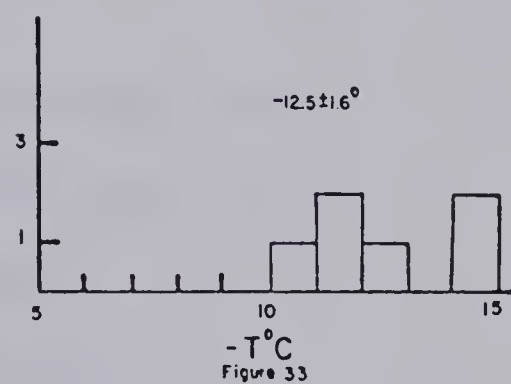
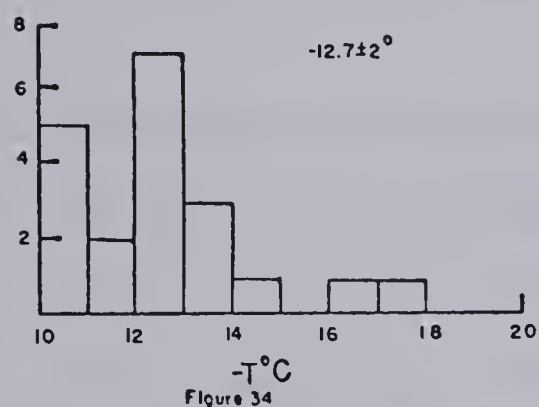
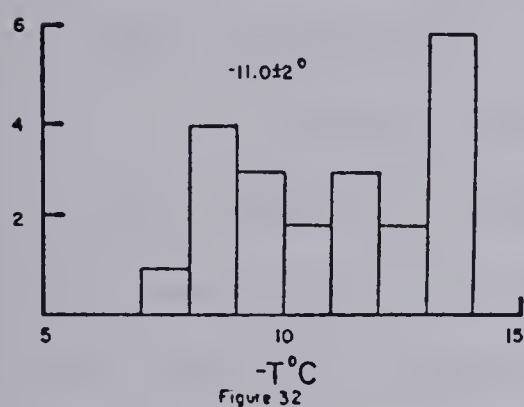
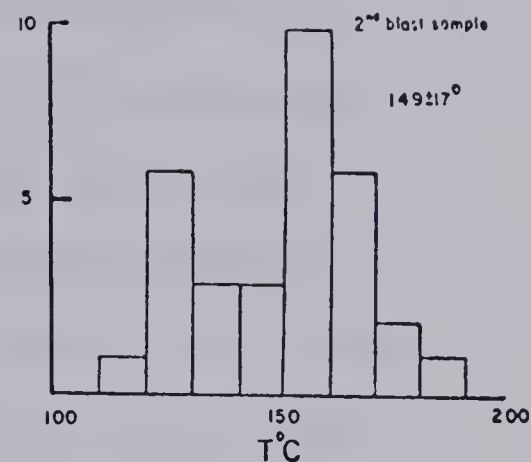
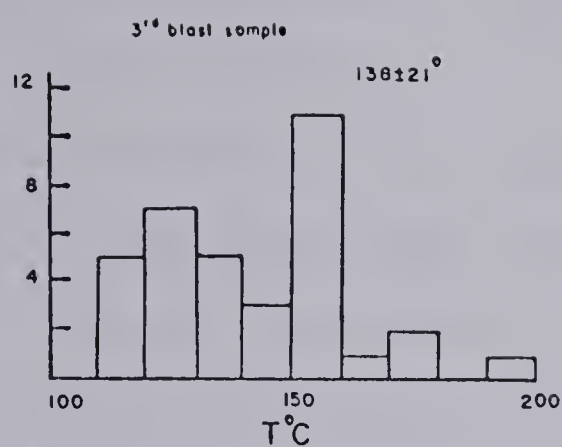
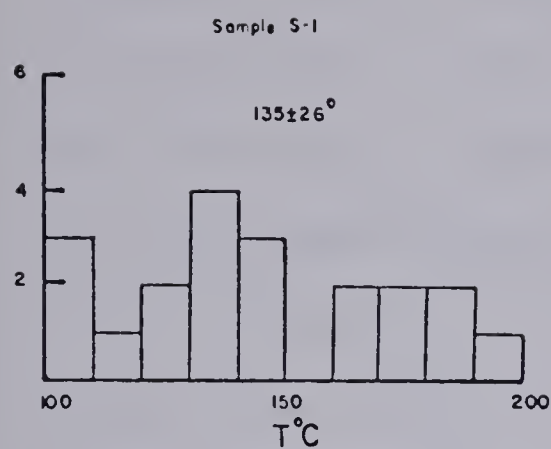


one fluorite. The localities are shown in Figure 25 for the specimens; the fluorite was from an erratic boulder found by a trench where uranium mineralization is known to occur.

The primary fluid inclusions (Plate 16) consisted of two phases: an aqueous brine and a vapor phase, and were ubiquitous in all specimens analyzed. In a few instances a third phase, a long acicular solid was observed in the inclusions in the quartz specimens (possibly a sulfate), and in the fluorite a cubic phase, possibly halite, was seen (plate 17). Their shapes varied from elliptical, rectangular and rounded to good negative crystal shapes. The inclusions in the fluorite tended to be larger on the average (100-200 microns) as compared to the inclusions in the quartz samples. The ratio of the volume of liquid to vapor phase was constant in the quartz specimens, thus negating any possibility of effervescence having occurred. However, in the fluorite specimen, evidence was observed suggesting that boiling had occurred as the ratio of the volume of liquid to vapor phase varied substantially (i.e. from 15-20:1 to 1:5).

Results of the freezing experiments are presented as histograms in Figures 32 to 38. Referring to Figure 30 from Roedder (1962) one can determine the corresponding salinity as a result of the depression of the freezing point caused by the salt concentration in the fluid phase. One assumes that the majority of the salt is NaCl, which is





Heating and freezing temperatures for quartz  
(Figures 32-36) and fluorite (Figure 37) fluid  
inclusions from Stormy Lake



thought to be an acceptable generality. The corresponding concentration for the quartz samples is 14-16 wt% equivalent NaCl and for the fluorite specimen 21 wt% equivalent NaCl. The high concentration of equivalent NaCl in the fluorite fluid inclusions, up to 23% for some of the inclusions, would support the previously stated observation of halite in some of the inclusions.

Results of the heating experiments are presented as histograms in Figures 32 to 36 and a combined plot of all the quartz data in Figure 38. Examined separately specimens S-40 and S-17 appear to have a univariant distribution and the filling temperatures for the two localities agree within error at approximately 130°C. Each of the remaining quartz specimens show a bimodal distribution which is better illustrated in the combined plot showing two peaks at 120-130°C and 150-160°C. It was thought that the rather broad distribution of homogenization temperatures for S-1 may have indicated a history of boiling but re-examination of this specimen provided no evidence to support this hypothesis. The data for the fluorite, Figure 37, specimen shows a univariant distribution around a low temperature with a few results distributed towards higher temperatures. This tight distribution would proscribe against there having been any boiling, however, this will be discussed in greater detail later.





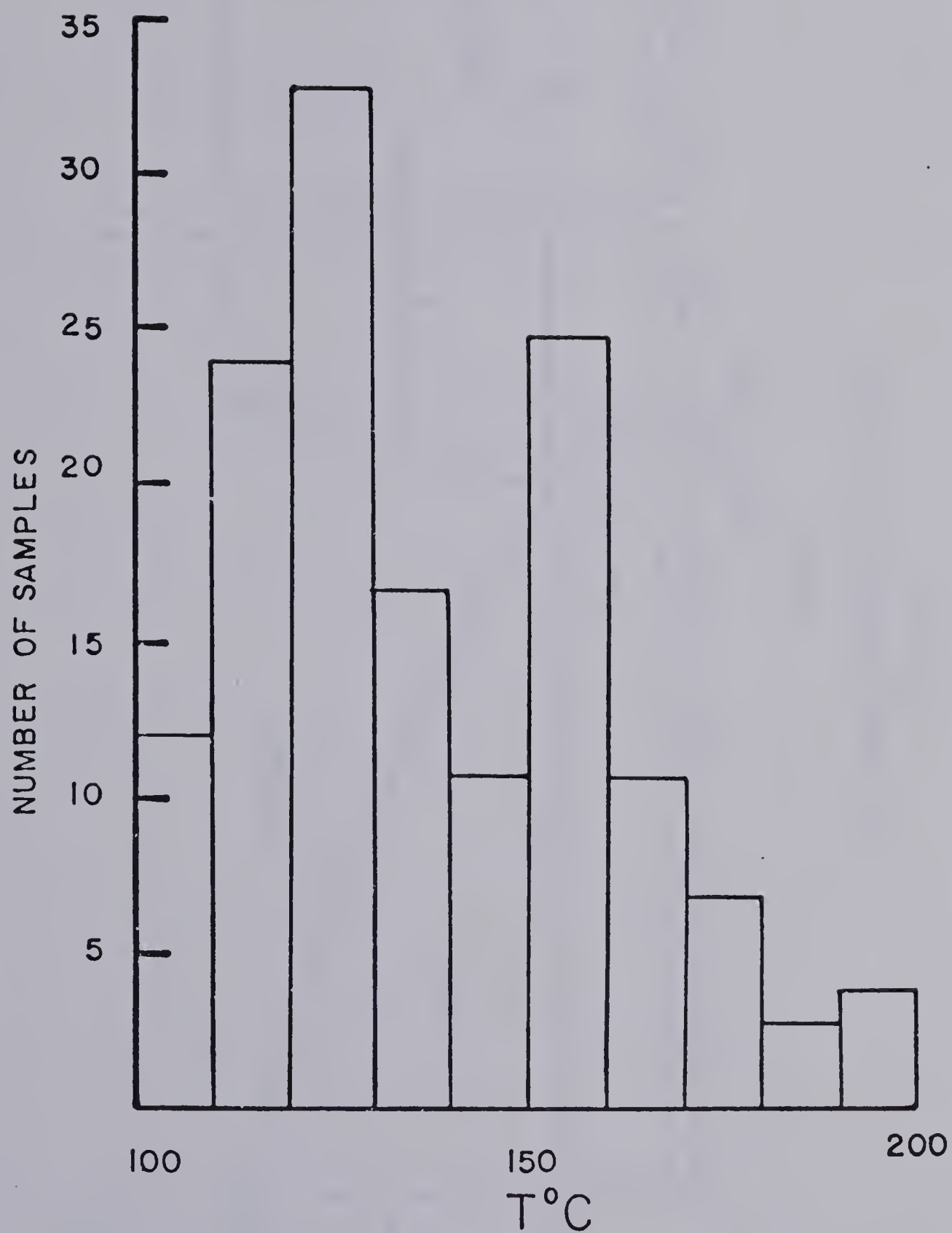
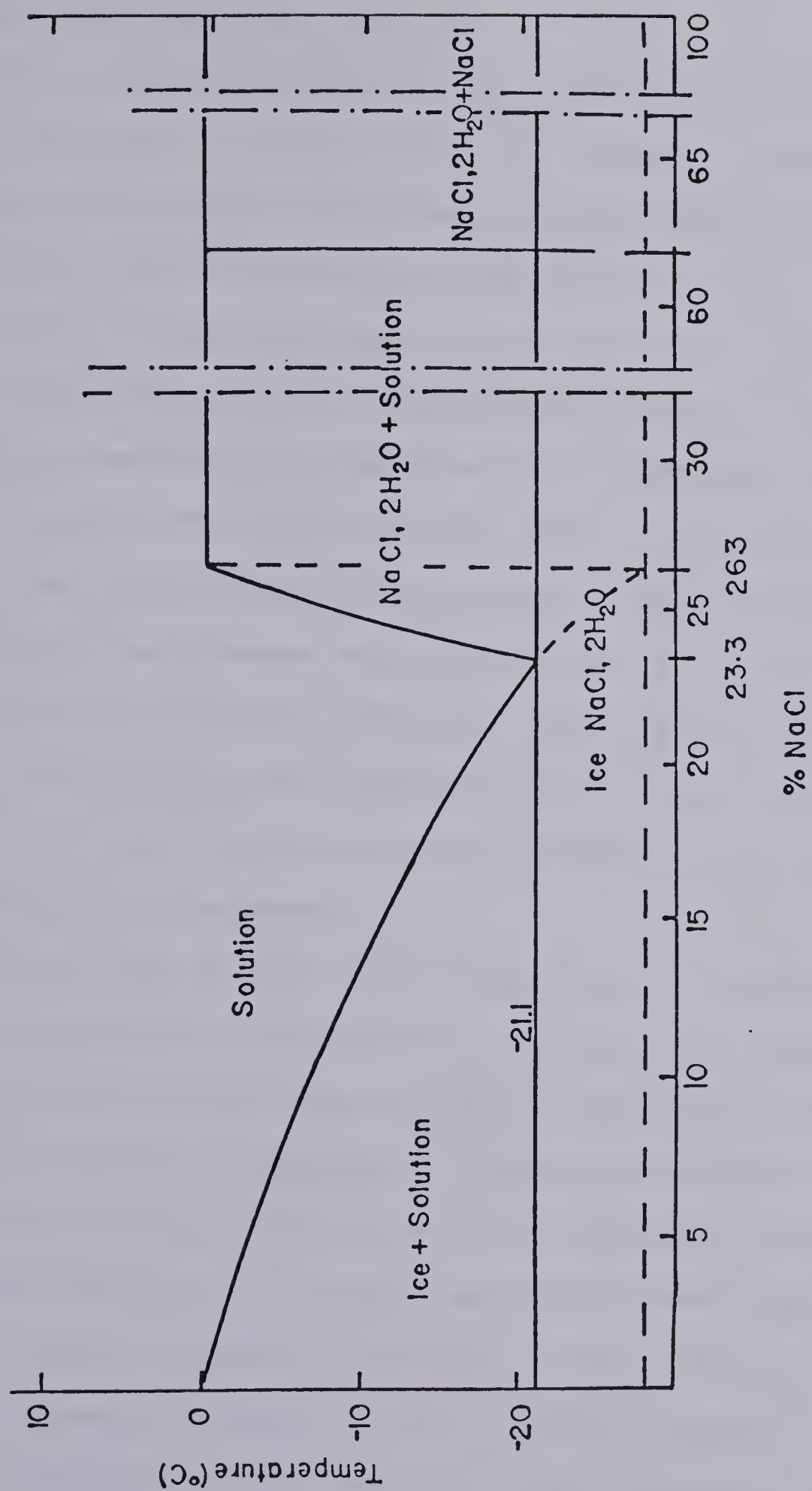


Figure 38 Combined histogram plot of homogenization temperatures for quartz fluid inclusions from Stormy Lake. A bivariate distribution of the data suggests two filling temperatures of 125°C and 150°C





The system  $\text{H}_2\text{O}-\text{NaCl}$  (in Roedder, 1962)

Figure 39



### 3.5.5 Discussion and Interpretation

Homogenization temperatures in fluid inclusions have long been recognized as representing the minimum temperature of entrapment for the contained fluid (Sorby, 1857 in Roedder, 1977). However, this is only true provided the lithostatic pressure did not exceed the vapor pressure of the solution. In circumstances where this is not the case, then an appropriate temperature correction based upon the volumetric properties of the solution in the fluid inclusion is required to obtain the true temperatures of entrapment. Potter (1977) has compiled data to produce such diagrams as in Figure 40 for a solution containing 15 wt% NaCl. Knowing the composition of the fluid inclusions obtained from freezing experiments, and the pressure at the time of entrapment the appropriate correction can be made.

In the case of the Stormy Lake area, no information was available to calculate the lithostatic pressure during the formation of the quartz veins and the fluid inclusions and without this data no temperature correction could be applied. To solve this problem the oxygen isotopic composition of quartz and hematite, found together in the veins, was obtained in order to estimate a temperature of formation independent of pressure (Taylor, 1967). Oxygen isotopic data on the quartz-hematite pairs from the Stormy Lake area suggest a temperature of formation of  $150^{\circ}\text{C}$  for the quartz veins, thus



indicating that the veins formed very near the surface and that only a minimal temperature correction for lithostatic pressure is required.

Data from the heating experiments suggested two homogenitization temperatures at  $125^{\circ}\text{C}$  and  $150^{\circ}\text{C}$ . The latter temperature would be obtained if vein formation occurred at or near the surface, however, if the fluid was trapped at  $\sim 500$  metres depth the filling temperature would be depressed  $\sim 25^{\circ}\text{C}$  (Figure 40 ). Thus, the bimodal distribution of the homogenization temperatures may reflect a two-stage history in the crystallization of the vein solution.

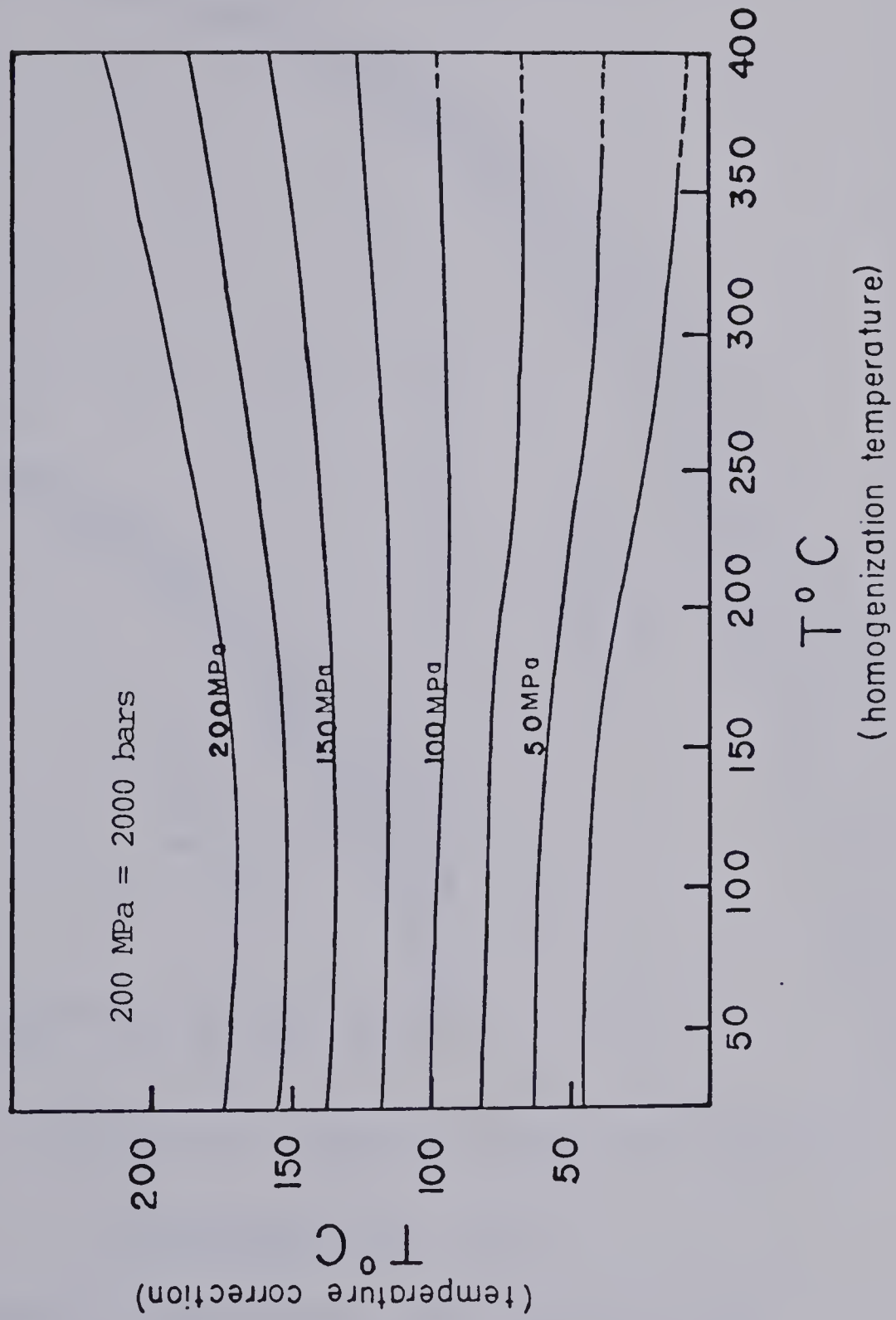
Referring to Figure 41 from Haas (1971) for boiling point curves for  $\text{H}_2\text{O}$  liquids with varying brine compositions one notices that for a brine of  $\sim 15$  wt% NaCl, approximately what the Stormy Lake samples are, boiling occurs at  $\sim 30$  metres depth for a temperature of  $150^{\circ}\text{C}$ . From petrographic study we concluded that little evidence existed to support a past history of boiling for the vein solutions, thus the minimum depth of vein formation must have been between 30-40 metres. However, taking errors into account and considering the close proximity to the surface it is possible that some solutions may have ascended to shallower depths and mixed with solutions of lower salt concentration permitting some boiling to occur resulting in a broad distribution of filling temperatures as in specimen S-1. Oxygen studies also suggest that mixing of





Figure 40

Temperature correction diagram for a 15 per-cent NaCl solution as a function of homogenization temperature and pressure(after Potter, 1977)





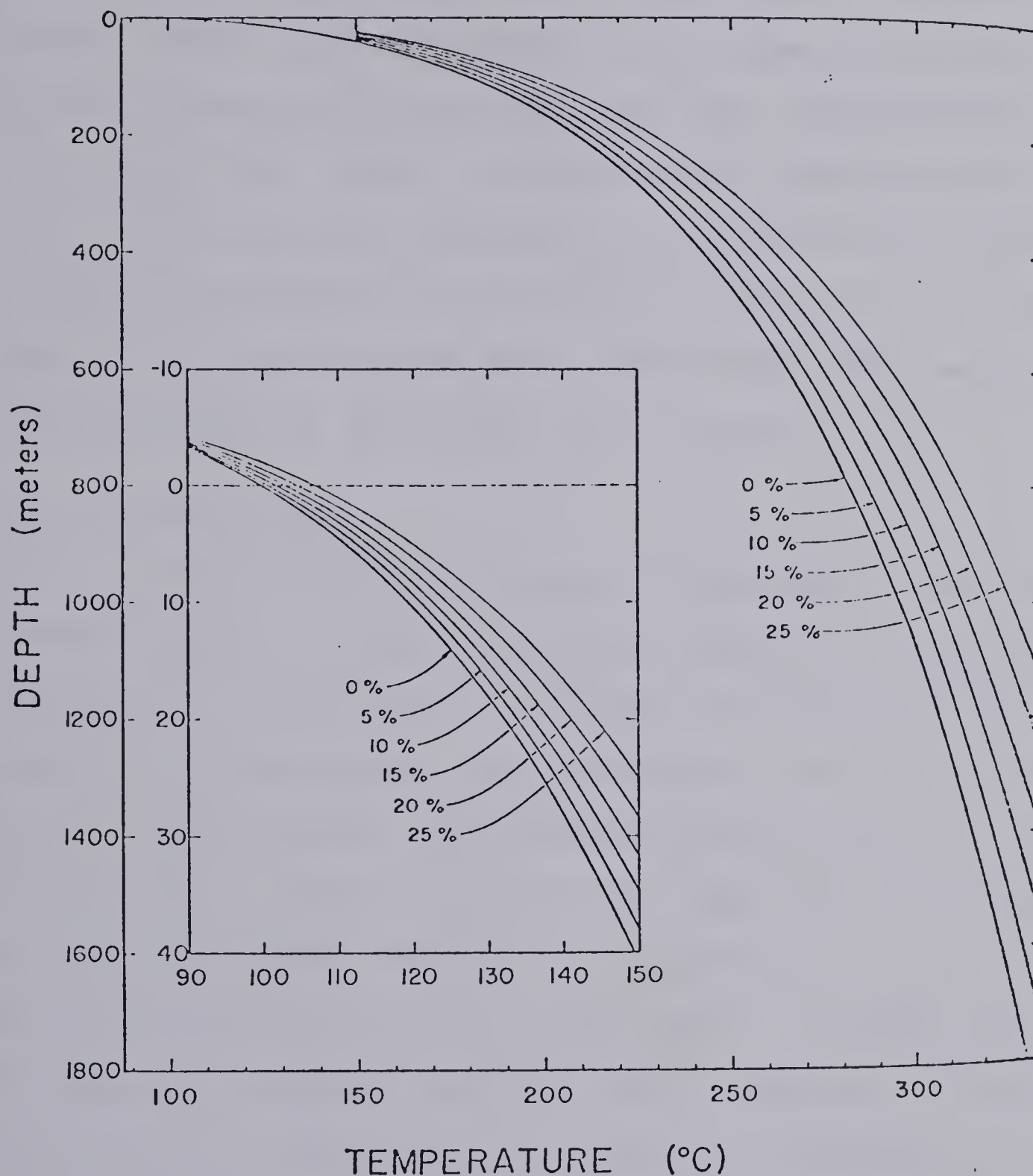


Figure 41 Boiling-point curves for  $H_2O$  liquid (0 wt.%) and for brine of constant composition given in wt.% NaCl. Insert expands the relations between  $100^{\circ}C$  and  $150^{\circ}C$



meteoric water and metamorphic water occurred (see later).

The relative position of the fluorite sample with respect to the quartz specimens is not known from field work. However, combining the knowledge that the concentration of salts is ~21 wt% and the temperature of homogenization is  $\sim 130 \pm 38^{\circ}\text{C}$ , and that the system was boiling would suggest a depth of formation of ~75 metres. The few filling temperatures at the upper end of Figure 37 for the fluorite may represent the effects of boiling in the system.

### 3.5.6 Conclusions

Fluid inclusion studies of five quartz veins and one fluorite erratic suggest a two-stage sequence of vein formation which is reflected in a bimodal distribution of the homogenization temperatures. Vein solutions, containing approximately 14-16 wt% NaCl, first began to crystallize at a depth of 300 metres. Final mineralization apparently was effected at shallower depths. Knowing the composition of the vein solution, and that boiling did not occur, a minimum depth of 30 metres is suggested for final vein formation. A lower temperature of homogenization, higher salt concentration (~21 wt% NaCl), and petrographic evidence supporting boiling suggests that the fluorite specimen represents a shallower level of crystallization of ~75 metres, but this does not reflect the range indicated by the filling temperatures and is





considered only an approximation.

### 3.6 Oxygen Isotope Study

An oxygen isotope study was undertaken to augment the fluid inclusion investigation carried out on the Stormy Lake quartz veins associated with the uranium mineralization. From the isotopic composition of mineral pairs analyzed it is possible to calculate the paleotemperatures, demonstrate whether equilibrium between minerals was obtained, and gather information on the origin, nature, and amount of fluid which participated in the ore-forming process (Taylor, 1967). The theoretical basis for oxygen isotope geothermometry was given by Urey (1947) and Bigeleisen and Mayer (1947) and its application to ore genesis and the ore fluid was reviewed by Taylor (1967).

When a solid phase is crystallized in a hydrothermal process in local equilibrium the isotopic composition of the mineral in that phase will depend on (i) the overall isotopic composition of the system of fluid and crystals in equilibrium with it; (ii) the chemical nature and relative amounts of the fluid and of the other solid phases; and (iii) the temperature of the system (Clayton and Epstein, 1961). Knowing the temperature of the system, obtained either from oxygen isotopic analysis of mineral pairs or fluid inclusion studies, and the isotopic composition of the mineral phase one can calculate the isotopic composition of the fluid phase



provided the fractionation factor ( $\alpha$ ) between the mineral phase and water is available. For example, in the case of quartz-water.

$$1000 \ln \alpha_{\text{qtz} - \text{H}_2\text{O}} = AT^{-2} \times 10^6 + B$$

$$\text{where } \alpha = \frac{{}^{18}\text{O} / {}^{16}\text{O}_{\text{qtz}}}{{}^{18}\text{O} / {}^{16}\text{O}_{\text{H}_2\text{O}}} \quad (\text{Clayton \& Epstein, 1961})$$

and the value of  $T^{\circ}\text{C}$  is obtained from either the fluid inclusion study or mineral pairs (quartz-hematite) and paleotemperatures obtained from oxygen isotopic analysis ( $T = 150^{\circ}\text{C}$ ).

Several samples were analyzed from different localities in the Stormy Lake area and the results are presented in Figure 42. Only in sample S-3B was a paleotemperature calculated as it was the only instance where the two phases analyzed were in equilibrium with each other, in this instance a temperature of  $150^{\circ}\text{C}$  was obtained, Figure 43, for  $\Delta_{\text{quartz-hematite}} = 21.6$ . The values obtained for the different minerals are quite anomalous in some instances; for example, the quartz  $\delta^{18}\text{O}$  values are very heavy,  $+13.5$  to  $+14.5\%$ , for hydrothermal vein deposits but they compare to similar results obtained for quartz from Port Radium (Taylor, 1967), Eldorado, Martin Lake, and the Tazin area (K. Hattori, personal communication, 1979). It is interesting to note that Taylor and Epstein (1962a) reported  $\delta^{18}\text{O}$  values of  $\sim 10\%$  for quartz from several igneous complexes, much lighter than the Stormy







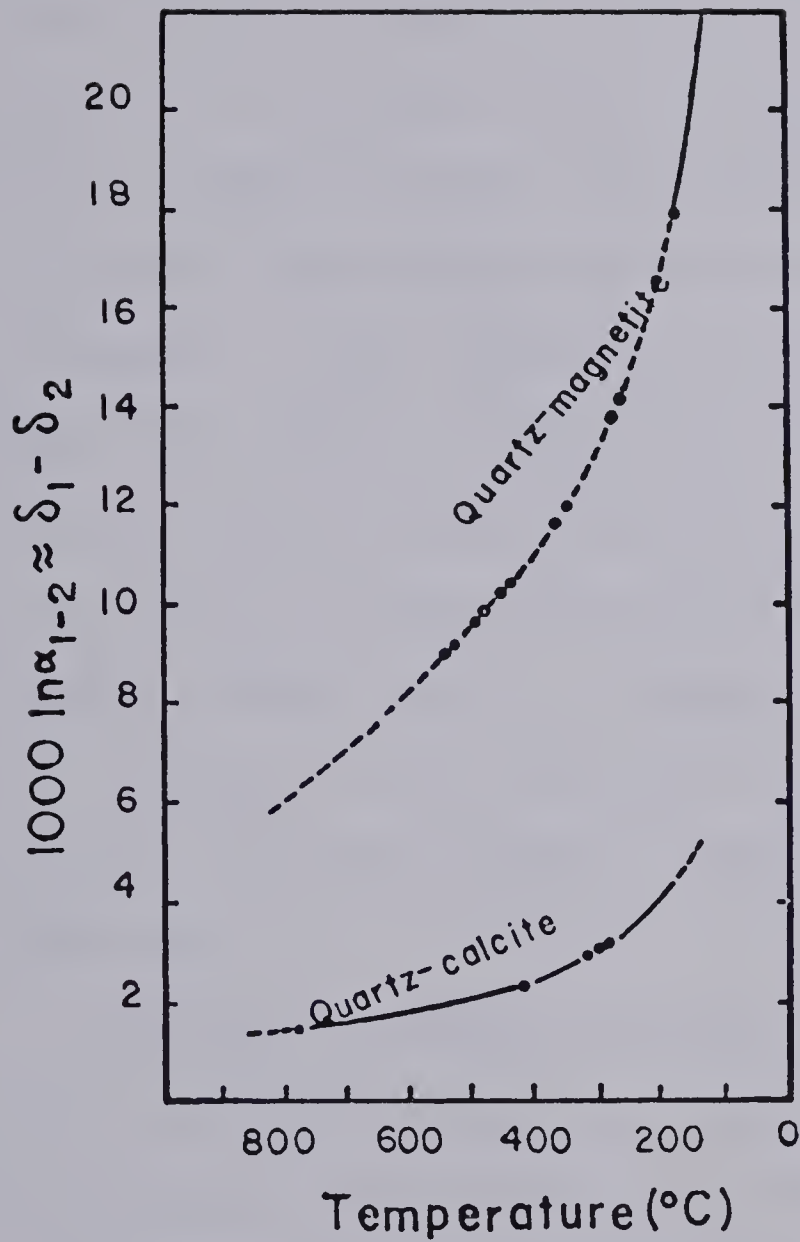


Figure 43  $1000 \ln \alpha_{1-2}$  versus Temperature diagram for quartz-magnetite and quartz-calcite pairs from Taylor (1967). Note that the quartz-magnetite curve has been extrapolated above  $1000 \ln \alpha_{1-2} = 18$





Lake values, but that Clayton and Epstein (1958) report analysis of quartz from hydrothermal veins with even heavier  $\delta^{18}\text{O}$  values.

Calculations of the  $\delta^{18}\text{O}$  values of the participating fluids were calculated using the data of Clayton et al. (1972) for quartz and the data of Rye and O'Neil (1964) for calcite. The results in Table 12 show a very narrow range indicating little change in the composition of the ore fluid suggesting a large reservoir. The values of  $\sim -1$  to  $-2\%$  are however much lighter than those usually obtained for hydrothermal deposits and are heavier than values of metamorphic regions. Instead the values are more typical of meteoric or connate fluids (Taylor, 1967), but , Hattori (personal communication, 1979) points out that such  $\delta^{18}\text{O}$  enriched moderate temperature fluid is very unusual in the terrestrial environment at the present time.

Although the oxygen isotopes suggest a moderate temperature for mineralization at Stormy Lake ( $\sim 150^\circ\text{C}$ ), they lend little help in determining the origin of the ore-forming fluids.  $\delta^{18}\text{O}$  values obtained on quartz are anomalously enriched in  $^{18}\text{O}$  compared to magmatic and metamorphic values and the  $\delta^{18}\text{O}$  values calculated for the ore forming fluid are well outside the range usually observed for hydrothermal fluids (i.e.  $7.5-9\%$ ). Instead, the values obtained are more akin to those for connate or meteoric waters suggesting that



TABLE 12

Calculated  $\delta^{18}\text{O}$  of the hydrothermal solutions  
from which quartz and calcite precipitated

| Quartz<br>sample  | T°C | $\alpha$ | $\delta^{18}\text{O}$ quartz<br>(‰)  | $\delta^{18}\text{O}$ water<br>(‰) |
|-------------------|-----|----------|--------------------------------------|------------------------------------|
| 2nd blast         | 150 | 1.0156   | +14.5                                | -1.0                               |
|                   |     |          | +14.2                                | -1.3                               |
| 3rd blast         | 150 | 1.0156   | +14.6                                | -0.9                               |
| SL-17             | 150 | 1.0156   | +13.9                                | -1.6                               |
| S4-1              | 150 | 1.0156   | +13.5                                | -2.0                               |
| SL-40             | 150 | 1.0156   | +14.0                                | -1.5                               |
| Calcite<br>sample | T°C | $\alpha$ | $\delta^{18}\text{O}$ calcite<br>(‰) | $\delta^{18}\text{O}$ water<br>(‰) |
| 2nd blast         | 150 | 1.0134   | +11.1                                | -2.17                              |
| SL-40-1           | 150 | 1.0134   | +13.5                                | +0.23                              |



supergene fluids may have participated in the ore forming process with a slight increase in their  $S^{18}O$  content due to increased temperatures at depth, and also their mixing with heavier metamorphic fluids.

### 3.7 Uranium-Lead Dating

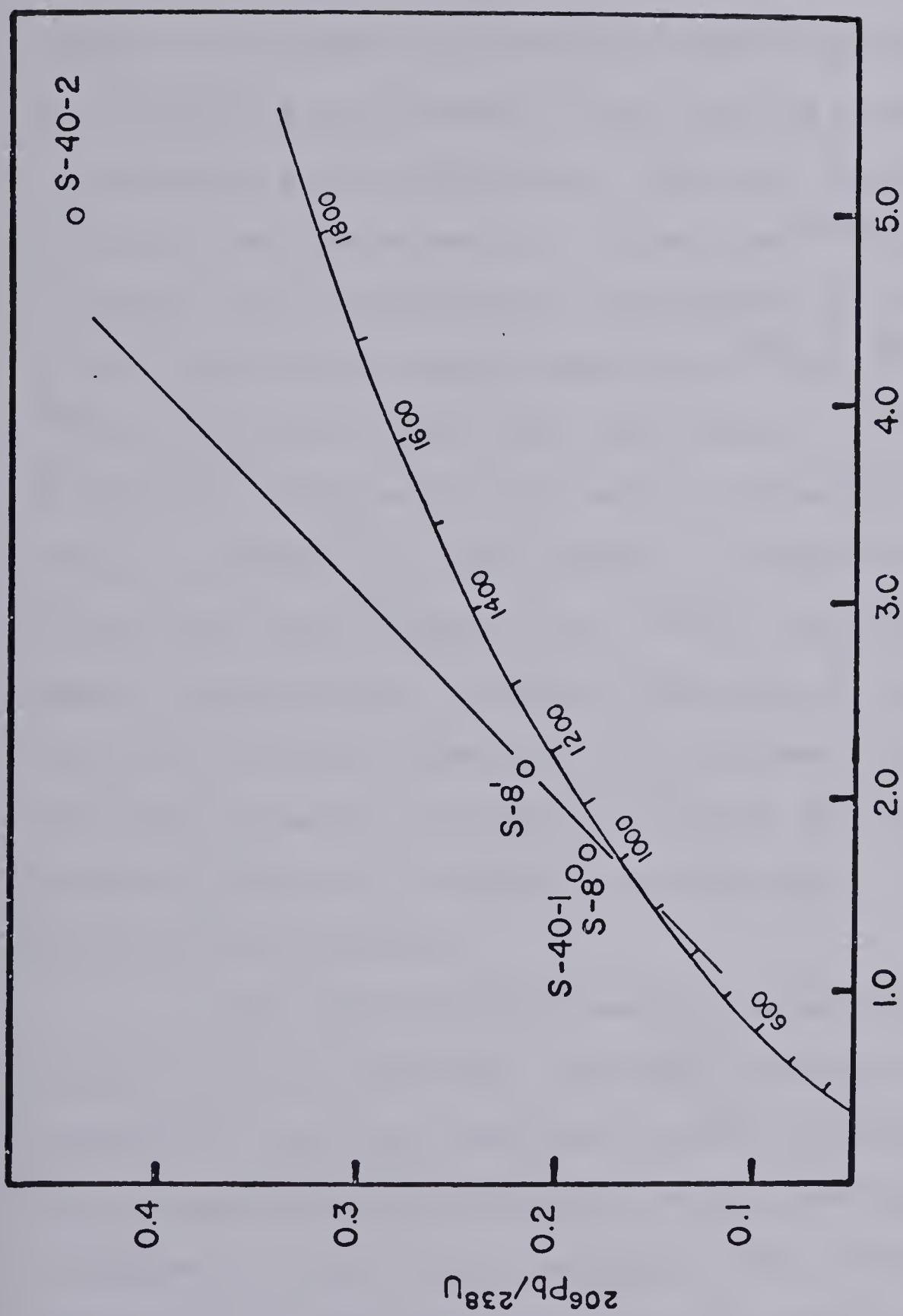
Four specimens were selected for U-Pb dating of the Stormy Lake showing. The procedure is described in Appendix I and the results are presented in Table 11 and plotted on a concordia diagram in Figure 44. As can be seen from the concordia plot the points do not show a simple linear relationship but instead scatter above the concordia curve indicating either loss of uranium and/or gain of lead. Although the points do scatter a reference line of 950 Ma has been included as this is the age of mineralization suggested from geological data.

The  $^{207}Pb/^{206}Pb$  ages of the four samples range from 640-1230 Ma, however, the two intermediate ages given by samples S-8 (860 Ma) and S-8 (990 Ma) are believed to be more reliable. They have higher uranium contents, 43.7% and 20.7% respectively, suggesting less weathered specimens and the spread of the  $^{206}Pb/^{235}U$ ,  $^{207}Pb/^{234}U$  and  $^{207}Pb/^{206}Pb$  ages is less or in other words the points are more concordant.

Examination of the Pb-I.R. ratios for  $^{206}Pb/^{204}Pb$  indicate surprisingly low values ranging from 80 - 156,







$^{207}\text{Pb}/^{235}\text{U}$

Figure 44

Concordia diagram for Stormy Lake U-Pb data



very atypical of a vein-type deposit. Also peculiar about the analyses is the presence of  $^{208}\text{Pb}$ , as thorium was thought to be absent in the pitchblende mineralization since low readings were obtained on the thorium channel of a self-discriminating scintillometer. This was confirmed by micro-probing as mentioned earlier. Thus the  $^{208}\text{Pb}$  is interpreted as normal lead, representing a period of isotopic modification of the pitchblende during which time  $^{208}\text{Pb}$ ,  $^{207}\text{Pb}$ ,  $^{206}\text{Pb}$ , and  $^{204}\text{Pb}$  were incorporated into the system. A  $^{207}\text{Pb}/^{204}\text{Pb}$  versus  $^{206}\text{Pb}/^{204}\text{Pb}$  isochron plot of the pitchblende samples is presented to Figure 45. The scatter of some of the I.R. and I.D. values for single samples (i.e. S-40-1) may be related to sample inhomogeneity, perhaps reflecting i) surficial weathering of the mineralization, ii) subsequent modification of the U-Pb system by an event post dating the original mineralization, and/or iii) original heterogeneity at the time of uranium mineralization.

The quasi-linear trend of the data in Figure 45 indicates an age of 490 Ma. Although no significance can be attached to this date one can interpret the Figure as indicating a multistage growth model for the U-Pb system(s) (i.e. a minimum of three stages to account for the data). This suggests that at some time post original mineralization an unknown amount of common lead was added to the radiogenic lead(s) changing the position of the point(s) on the lead growth curve. In an attempt to determine the timing of this event values for



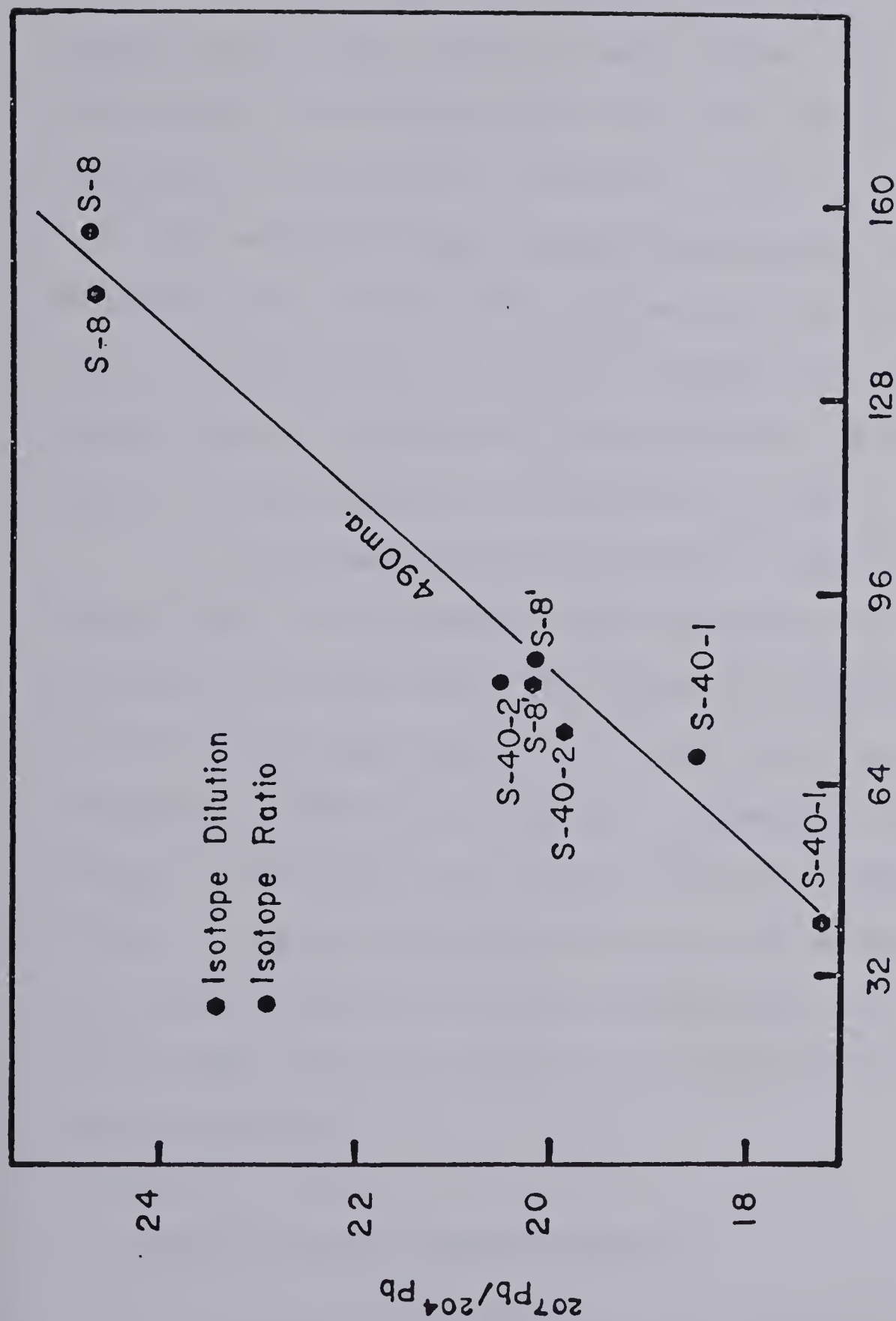

 $^{206}\text{Pb}/^{204}\text{Pb}$ 

Figure 45

$^{207}\text{Pb}/^{204}\text{Pb}$  versus  $^{206}\text{Pb}/^{204}\text{Pb}$  plot for Stormy Lake U-Pb data



$^{207}\text{Pb}$  and  $^{206}\text{Pb}$  concentrations were calculated for different times assuming i) that the  $^{208}\text{Pb}$  in the samples was nonradiogenic (i.e. not from the decay of thorium), ii) that the same amount of lead was added to each system, and iii) using the appropriate  $^{204}\text{Pb}:$  $^{206}\text{Pb}:$  $^{207}\text{Pb}:$  $^{208}\text{Pb}$  ratios at each time. However, the points scattered in a pattern far more sporadic than before the recalculations perhaps indicating that the addition of normal lead to the U-Pb systems was not homogeneous. If this was the case then it would render the apparent age indicated from the quasi-linear relationship of the points in Figure 45 meaningless as mentioned earlier.

In summary vein-type uranium mineralization at Stormy Lake was generated some time before 900 Ma age during an event associated with the Grenville orogeny. Contamination of the uranium-lead system by normal lead is suggested by the presence of  $^{208}\text{Pb}$  (i.e. absence of Thorium) and a  $^{207}\text{Pb}/^{204}\text{Pb}$  versus  $^{206}\text{Pb}/^{204}\text{Pb}$  plot which indicates a meaningless age of 490 Ma. This net effect of this period of contamination with recent weathering of the pitchblende was to move the points above the concordia curve and scatter them in a non-linear fashion.

### 3.8 Discussion and Interpretation

The vein-type uranium mineralization at Stormy Lake shares many similarities with the recently discovered deposits





of northern Saskatchewan (Beck, 1977), Australia (Ryan, 1977), the long established Beaverlodge area (Beck, 1969; Koeppel, 1968), and the Goldfields area of Saskatchewan (Robinson, 1956; Christie, 1953). The most important characteristic shared by these areas is the spatial relationship of vein-type uranium mineralization to major unconformities, all of which are Proterozoic in age. This relationship between mineralization and an unconformity led Derry (in Beck, 1977) to coin the term "unconformity-type deposit" and with it came two divergent schools of thought, each professing their ideas on the genesis of these new deposits. The supergene or per-descendum school (Langford, 1974; Knipping, 1974; Smith, 1974; Robertson and Lattanzi, 1974; Dalkamp, 1976) believes that mineralization is related to extensive periods of deep weathering during which time uranium was leached from local basement terrain and redeposited in structurally prepared sites at or near unconformities. The hypogene or hydrothermal school (Beck, 1977; Ryan, 1977; Koeppel, 1968; Robinson, 1956; Morton, 1976) believes that ascending fluids, possibly of metamorphic or diagenetic origin, carried uranium from Archean sediments into new areas favorable for uranium concentration with unconformities acting as physio-chemical boundaries helping to initiate mineralization.

Uranium mineralization at Stormy Lake corresponds to the "simple monomineralic type" characterized by pitchblende



$\pm$  pyrite, galena, quartz and carbonate (Bastin, 1939), as opposed to the "complex type" where associated mineralization included Ag, Ni, Co, arsenides, selenides, and tellurides. Everhart and Wright (1953) noted that the "simple type" was more commonly hosted by felsic intrusives and the latter by metasediments. However, Badham's (1974) U  $\pm$  Co, Ni, Ag association is characteristic of calcalkaline intrusive-volcanic terrains and the unconformity-type deposits may be either the complex type (cf. Baker Lake, Key Lake, Mid West, Cluff Lake) or simple mineralogical type (Rabbit Lake).

The low thorium contents of the uranium mineralization at Stormy Lake suggests a remobilized nature although it is not characteristic of either hypogene or supergene processes. Analysis of five pitchblende samples from Goldfields gave maximum thorium values of 0.0097% (Collins et al., 1954),

but , Knipping (1974) interpreted the simple mineralogy and absence of REE, Co, Ni, Ag and thorium at Rabbit Lake to indicate a low temperature supergene origin. Langford (1974) states that the high temperature assemblage of Ni, Cu, As, Se, Co, etc., characteristic of the unconformity-type of deposits (i.e. Cluff Lake, Mid West, Key Lake) are hypogene in origin but that the pitchblende is later and occurs as coatings on the earlier minerals, and the origin of the uranium is supergene. However, the intense calcareous, chloritic, hematitic and sericitic alteration immediately adjacent to the



veins at Stormy Lake certainly lend themselves to a hypogene rather than supergene origin as Koeppel (1968) also favored for the Beaverlodge area.

For most of the "unconformity related" deposits the uranium mineralization rarely extends for more than a few hundred metres below the unconformable surface (Langford, 1974; McMillain, 1977; Smith, 1974). The extent of the uranium mineralization at depth for the Stormy Lake area is not known, however, the above is not considered to be a deterrent in future exploration in the area. Also the above is not considered to favor either a hypogene or supergene origin for it can be interpreted in either context. What is of importance is that the structural traps hosting the mineralization continue to sufficient depth to have permitted economically viable concentrations of ore to have precipitated. For the Stormy Lake area this is quite likely, considering the structures are an effect of regional deformation. However, it should be noted that fluid inclusion and oxygen isotope studies indicated an extremely shallow depth for the formation of the quartz veins so that in the Stormy Lake area subsequent denudation may have eroded away much of the mineralization. Nevertheless, folding of the area may have buried some of the unconformity making synclinal structures better targets.

Transport of the uranium phase (i.e. the uranium ore fluid) prior to deposition was probably as a uranylcarbon-





ate (Hostetler and Garrels, 1962) or a uranylfluoride complex (Gabbelman, 1977), since both carbonate and fluorite are associated with the uranium mineralization. As to which of these was the dominant species is difficult to say for the literature contains contradictory arguments. Hostetler and Garrels (1962) showed the importance of uranium solubility in aqueous media containing dissolved  $\text{CO}_2$  but noted that the uranyl carbonate complexes become increasingly unstable at temperatures greater than  $120^\circ\text{C}$ . This was confirmed by other workers who showed that uranium solubility in carbonate solutions diminishes by a factor of about 100x between  $100$ - $200^\circ\text{C}$  (Rafalsky, 1959; Miller, 1958).

Poty (1977) documented uranium formation from a  $\text{CO}_2$ - $\text{H}_2\text{O}$  fluid phase at  $345^\circ\text{C}$  at Limousin, France, and Morton et al. (1978) found similar results for uranium mineralization in the Rexspar deposit, British Columbia. It is interesting to note that in the latter case Preto (1978) reports the association of purple fluorite with uranium mineralization. However, with respect to uranylcarbonates, Romberger (1978) concluded from solubility studies up to  $300^\circ\text{C}$  that carbonate complexing was less important at elevated temperatures for the transport of uranium and that in deposits containing fluorine, uranylfluoride complexes are most important. This agrees with Gabbelman's (1977) conclusion that for the temperature range  $200$ - $400^\circ\text{C}$   $\text{UF}_4$  is the stable transporting complex. For the



Stormy Lake showing, no conclusive answer can really be obtained concerning the complexing agent although it is believed to be one of either uranylcarbonate or uranylfluoride, or perhaps both.

The association of uranium mineralization with quartz veins cutting crenulated schists indicates that the mineralization occurred during the waning stages of regional metamorphism (i.e. Grenville Orogeny). Yermolayev (1973) noted that regional metamorphism often terminates with a regressive stage associated with the onset of local hydrothermal activity accompanied by an influx of radio elements. This may well have been the case in the Stormy Lake area. Whether the uranium is of local or regional origin is not known, although the arkosic conglomerates of the Bessie Lake Formation, basal member of the Seal Lake Group, are known to have anomalous radioactive zones regionally (Baragar, 1969; Côté, 1970). The felsic volcanics of the Bruce River Group also contain radioactive horizons at the Boundary Lake showing (Robinson, 1956) and the Madsen Lake showings (Piche, 1956), both located a few kilometres from Stormy Lake. It may be significant that in the latter two cases uranium is associated with fluorite in the felsic volcanics. If the uranium was derived from the volcanics then this might indicate transport as uranylfluoride complexes rather than as uranylcarbonate complexes.

Fluid inclusion and oxygen isotopic studies suggest a moderate temperature (i.e.  $150^{\circ}\text{C}$  for the ore forming pro-



cess with the ore fluid enriched in salts ( $\sim 15$  wt% NaCl) and a connate or meteoric component participating. Also a rather shallow depth was indicated for the formation of quartz veins intimately related to the uranium mineralization. What component of uranium may have been contributed from the supergene process indicated here is not known but it is important to realize that it may have been substantial although no concrete evidence is presented to favor either a super- or hypogene source.

In summary, the Stormy Lake showing is an "unconformity-type" vein deposit corresponding to the "simple type" with pitchblende and chalcopyrite, pyrite, quartz, carbonate and minor fluorite, and also traces of silver. Structural data indicates the mineralizing event occurred during the waning stages of the Grenville orogeny during decreasing temperatures and pressures and that structural traps related to  $D_2$  deformation were important in localizing mineralization. Fluid inclusion studies suggest a fluid enriched in salts and combined with oxygen isotope results indicate a moderate temperature of formation ( $150^{\circ}\text{C}$ ), shallow depth, and a fluid composed of both a supergene and metamorphic component.





## CHAPTER 4

### THE BURNT LAKE AREA

#### 4.1 Introduction and Previous Work

The Burnt Lake Uranium showing is located on the northwest side of Burnt Lake (Figure 3) within felsic volcanics of the Aphebian Aillik Group. Several showings were found within this area by Brinex in 1967 (Gandhi et al., 1973), but only the main, or north showing, was mapped and examined in detail.

The area was previously mapped in detail by Barua (1969) and Gandhi et al. (1976) and was included in the regional maps of Watson-White (1971; 1976), Stevenson (1970), Krajewski (1976), and Bailey (1978). During the summer of 1977 Brinex carried out detailed mapping and geophysics concentrated around the north showing and this was followed by a drilling and trenching program. A mapping program was also undertaken by Brinex within this area during the 1978 field season.

Mapping of the Burnt Lake north showing by the author was carried out during the latter part of July and the first half of August, 1977. Inclement weather prevailed the entire length of the mapping program. Mapping of the north showing was restricted to an area  $0.2 \text{ km}^2$  in size and also to another showing further to the west, approximately 2500 metres, of nearly the same size. Regional mapping of the





area at a 1:5000 scale was also attempted but insufficient time prevented drafting of a map as the geology of the area was not understood adequately to permit valid interpretations to be made.

#### 4.2 Regional Geology

The Burnt Lake area, Figure 3, consists predominantly of felsic volcanics and sediments of the Aphebian Aillik Group in the north and is underlain by a large Hudsonian (?), granite body in the south. The volcanics are of rhyolitic composition (Bailey, 1978) dominated by a feldspar porphyritic character with varying amounts of elliptical, blue quartz crystals. The volcanic textures vary from welded to nonwelded and in the former case may display eutaxitic textures suggestive of an ignimbritic or pyroclastic origin (Ross and Smith, 1961). Watson-White (1976) describes textures within these volcanic rocks further to the west which suggest a past history of devitrification, metasomatism and replacement caused by alkaline hydrothermal fluids, of either magmatic or meteoric origin. The sediments are typically massive, pink, gray and white, arkosic - and quartzitic - sandstones. In some places heavy mineral laminations define original sedimentary structures such as cross-bedding and planar-bedding (Bailey, 1978).

The volcanics are intruded by a monzonitic-to-granitic body, part of a large complex batholith termed the Walker



Lake Granite, dated by the Rb/Sr method at  $1550 \pm 50$  Ma (?). Within the Burnt Lake area the intrusion is composed predominantly of leucocratic phases of monzonite, quartz monzonite and granite with a lesser amount of biotite granite occurring south of Stevens Lake. Xenoliths of dioritic material are frequently found within the body and Bailey (1978) reports that some dykes of leucocratic granite cut the granodiorite phases.

Cutting both the volcanic-sedimentary pile and the plutonic rocks are northeast trending gabbroic dykes. These dykes are part of the Michael Gabbro (Fahrig and Larochelle, 1972) and have been dated by the K-Ar method at 1000 Ma (Gandhi et al., 1969).

The area has been subjected to tight isoclinal folding and to reverse faulting. The folds are synclinal with the anticlinal folds being faulted off due to extreme compression. The axial planes strike northeast and dip steeply to the south. The folds have wavelengths of approximately 1 km and an associated northeast-southwest trending fabric is recognizable in the field. Bailey (1978) suggests that the presence of slickenslides and L-fabric mineral lineations show that the faults are of the reverse type and very steep. Although there are few major faults or shear zones within the area, numerous splays are seen and locally shear zones are developed in the rocks sometimes altering the original composition and texture to that of a mylonite.



#### 4.3.1 Local Geology (Stratigraphy)

Mapping of the local geology of the north showing covered an area of approximately  $0.2 \text{ km}^2$ , Figure 46. Within the map area the following stratigraphy can be recognized; the western part of the map is underlain by an undifferentiated unit consisting of quartz porphyry, feldspar porphyry, and quartz feldspar porphyry. These are overlain by the mineralized unit characterized by a green banding (layer of pyroxene and amphibole) in a felsic tuff; overlying the mineralized unit in the east is a feldspar porphyry unit. The volcanics are intruded by a leucogranite in the east and both of these units are in turn cut by lamprophyre dykes.

The oldest unit outcrops in the western and northern parts of the map area and consists of several different subunits, all of which are discontinuous. These include tuffs, welded tuffs, quartz porphyries, feldspar porphyries, quartz feldspar porphyries, lapilli tuffs, and fragmental units. The quartz phenocrysts (1-4 mm) are characterized by their blue color and elliptical habit. The K-feldspar phenocrysts (3-8 mm) are anhedral to subhedral with rectangular and sub-rounded shapes. The lapilli tuffs consist of elliptical, white fragments of 1-3 cm size which comprise approximately 75-80% of the rock, set in a fine-grained greenish colored matrix (plate 18). In thin section the rocks show anhedral feldspars and recrystallized quartz eyes set in a granoblastic












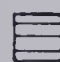


Figure 46








Local Geology of the Burnt Lake Uranium Showing

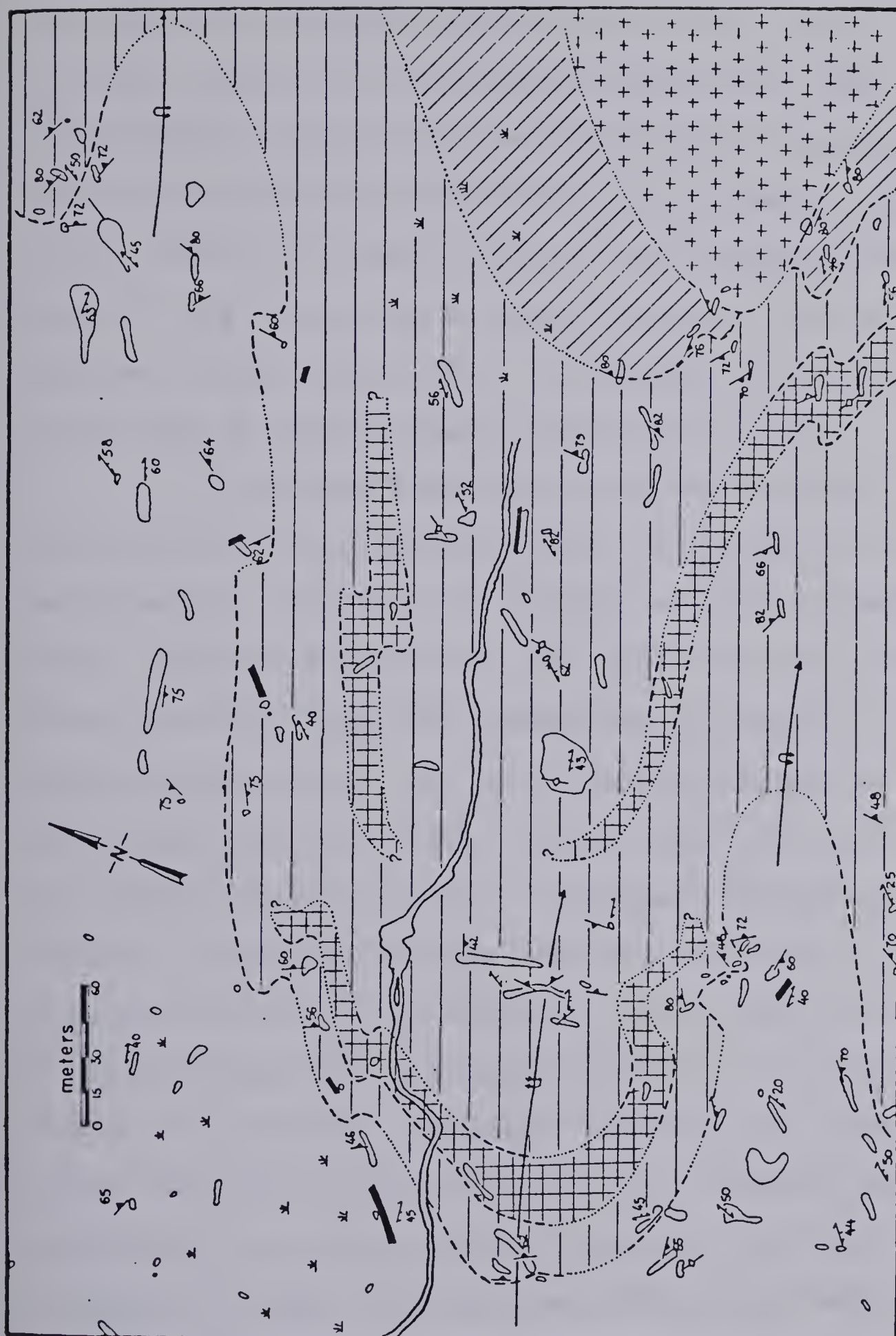
Intrusive rocks

-  Lamprophyre dykes
-  Burnt Lake Granite

Aillik Group

-  Feldspar porphyry with minor quartz
-  Mineralized unit including feldspar porphyry, lapilli tuffs, tuffaceous horizons (in parts disrupted);
-  quartz-feldspar porphyry
-  Undifferentiated (includes quartz porphyry, feldspar porphyry, and quartz-feldspar porphyry)

|  |   |
|--|---|
| Geological boundary (defined, approximate, assumed). . |  |
| Igneous banding (vertical) . . . . .                   |  |
| Cleavage ( $S_1$ , $S_2$ ) . . . . .                   |  |
| Antiform (overturned) . . . . .                        |  |
| Synform (overturned) . . . . .                         |  |
| Outcrop . . . . .                                      |  |
| Swamp . . . . .  |  |





polygonal to elongate, quartz-feldspathic matrix. Original welding textures are represented by coarser lenses of quartz and feldspar displaying good triple point development and which wrap themselves around phenocrysts where present. Minor amounts of aegerine augite and seldomly riebeckite, biotite and chlorite are present in the matrix but never forming a major constituent. A cleavage is developed in the rocks and is easily recognizable in the field.

Overlying the undifferentiated unit is the "mineralized unit," so termed because it contains the uranium mineralization. Although it consists of lapilli tuffs, porphyries, massive tuffs, etc. This unit is characterized by a mafic banding (Plate 19) consisting of aegirine-augite and magnesioriebeckite, this was originally mapped as a chloritic alteration (Kontak, 1978). Within this unit are three lenses of quartz feldspar porphyry, feldspar porphyry and massive welded tuffs which do not show the mafic banding. The mafic banding, typically 0.5 cm thick, can be seen to wrap itself around feldspar and quartz phenocrysts in a eutaxitic-like texture (Plate 20). Abundant red hematitic alteration is also quite pervasive throughout this unit, probably resulting from oxidation of magnetite which is present as finely disseminated octahedra (1-2%). Intercalated within this unit are fragmental units containing angular fragments of fine-grained, dark material whose origin was not resolved, as none of it was seen





in situ within the area. Also, pegmatite like veinlets of massive, fine-grained quartzo-feldspathic material were seen cutting across the banding discordantly (Plate 21), these have been interpreted as representing the remnants of underlying massive tuffs which were disrupted and incorporated in overlying flows.

Several thin sections were examined to determine the nature and origin of the mafic banding. It should be noted that a similar type of banding has been noted by Minatidis (1976) in the Michelin area and by Adamek (1976) in the Kopparasen greenstone belt, Sweden. In thin section the mafic bands can be seen to consist predominantly of acmite and aegirine-augite which occur as bands, aggregates, and disseminated grains. A blue-green amphibole, magnesioriebeckite, is sometimes present but in smaller quantities and in places appears to be replacing earlier pyroxene. The areas containing these minerals are separated from the rest of the section by discrete contacts (Plate 22) and the bands are parallel to what are believed to be primary igneous textures. The identification of these two phases was confirmed by electronmicroprobe studies, the results of which will be discussed later.

The mafic minerals occur in quartzo-feldspathic rocks typically of porphyritic character and of tuffaceous origin. Porphyritic phases (0.5-5 mm) consist of quartz,





orthoclase, microcline, plagioclase, and anorthoclase set in a fine-grained quartz-feldspar matrix, which displays a well developed granoblastic polygonal or elongate texture. In the latter case the microfabric parallels the mafic banding except in a few instances, the implications of which will be discussed under structure. The quartz phenocrysts, typically blue elliptical grains, have recrystallized and now consist of an aggregate of quartz grains showing either a granoblastic, polygonal texture or lobate intergrowths of the quartz grains. In some cases the quartz eyes have recrystallized into a fine-grained aggregate indistinguishable from the matrix. Where original quartz phenocrysts have survived recrystallization or are only partially broken down they are badly corroded and show undulatory extinction. Feldspar phenocrysts consisting of several varieties are present and these show both primary and secondary features, the latter being due to replacement and are typical of pyroclastic volcanics (Ross and Smith, 1961; Smith, 1960). Orthoclase occurs as anhedral grains, often showing granulated margins and invasion by the matrix along fractures. Perthitic varieties are quite common, the variety occurring is string perthites. Where un-twinned orthoclase has recrystallized along its margins it is common to find a cross-hatched, twinned feldspar, (most likely microcline). This same feature was also noted by Watson-White (1976) and attributed to secondary replacement.



Orthoclase is usually quite fresh with only minor secondary alteration products. Plagioclase occurs as anhedral, primary oligoclase and andesine, and also as chessboard albite which replaces the former in varying amounts. Oligoclase and andesine are quite fresh with secondary development of carbonate and epidote occasionally found in the centres of the grains. It is not uncommon to find overgrowths of K-feldspar mantling plagioclase phenocrysts or find K-feldspar as patches within plagioclase grains. However, the most common replacement<sup>of</sup> plagioclase occurs as chessboard albite either entirely or partially replacing an earlier phase.

Microcline was seen as phenocrysts only rarely, occurring most often in the matrix or as an alteration product of orthoclase and was distinguished from chessboard albite by staining. The presence of anorthoclase was suggested by the 2V value of  $50^{\circ}$  in some feldspars and its presence seems reasonable considering the sodium-rich nature of the volcanic rocks (see later).

The matrix of the volcanic rocks consist predominantly of quartz and K-feldspar with lesser amounts of plagioclase, microcline, mafic minerals (pyroxene, amphibole, biotite), magnetite and accessory zircon and apatite. A granoblastic polygonal texture is well developed and pervasive in all the sections examined. Notable was the absence of any coarser bands of quartz and feldspar which is typical of the





units bounding the mineralized unit and suggestive of remnant pieces of flattened pumiceous material. The absence of such a feature may suggest that unit was essentially nonwelded in character.

In one section fragments (1-15 cm) of granitic material were seen, these contained quartz (10-15%), plagioclase (30-40%), K-feldspar (10%), pyroxene (30-35%), amphibole (5-10%) with minor pitchblende associated with the pyroxene. As in the volcanics the pyroxene is aegerine-augite and the amphibole a blue green variety, riebeckite. The plagioclase is the dominant phase occurring as coarse (3-4 mm), subhedral grains of andesine composition, with alteration to epidote only very slight. Quartz occurs as finer grained, granulated grains forming a matrix for the plagioclase and glomeroporphyritic aggregates of pyroxene and amphibole. In some fragments invasion of the granitic clast by the volcanic matrix has occurred. No apparent reaction rim enveloping the fragments was observed. The presence of these fragments containing the alkali minerals aegerine-augite and riebeckite and associated uranium mineralization suggest a coeval relationship with the volcanics and also a possible high level, sub-volcanic intrusive relationship.

Bounding the mineralized unit to the east and further to the south is a porphyry unit, dominated by feldspar phenocrysts and by minor quartz phenocrysts. This unit is





similar to the undifferentiated unit described earlier with feldspar phenocrysts in a granoblastic polygonal matrix of quartz and feldspar with minor plagioclase and microcline. Coarse lenses of quartz and feldspar attest to the welded character of the volcanics. In one section three euhedral to subhedral grains of almandine garnet were seen.

Intruding the volcanic pile, and outcropping in the southeastern part of the map area, is a leucogranite which corresponds to unit 5b (fine-medium grained, grey and pink leucogranite and quartz monzonite) on Bailey's (1978) regional map. Along the contact with the volcanics, several pegmatite dykes can be seen cutting the rhyolites, they are composed of quartz and feldspar and are coarse-grained (1-1.5 cm).

The leucogranite consists of quartz (40-45%), K-feldspar (30-35%) and plagioclase (20-25%) and has a hypidiomorphic, granular texture. The quartz is typically recrystallized and granulated into finer grained aggregates, forming a matrix for the rest of the rock. It frequently shows undulatory extinction. The K-feldspar is orthoclase with a perthitic variety common. It is typically anhedral to subhedral and occurs as separate grains or rimming plagioclase and is slightly altered to sericite with undulose extinction common. The plagioclase is andesine in composition and is frequently zoned on its outer margins. Twinning is by the albite and carlsbad laws and less commonly pericline twinning is



developed. It is very fresh with only minor amounts of epidote alteration and is commonly replaced by K-feldspar, particularly along the margins and less often in the centres of grains where both K-feldspar and plagioclase have begun to break down to finer grained aggregates along their margins. Textures are typically lobate indicating arrest before equilibrium was attained. Accessory zircon, epidote, and apatite are present but no mafic minerals. In one section, which showed the contact between the granite and volcanics, no chilled margin was developed in the granite suggesting that the intrusion was into a heated volcanic pile, permitting slow crystallization of the granite. Again a close association in time between the volcanics and granite is likely.

The youngest igneous event in the map area is represented by lamprophyre dykes which cut both the volcanics and the granite. They are classified as vogesites (Harker, 1968) due to the dominance of riebeckite (50%) over brown biotite (10%). Other components are orthoclase (20-25%), plagioclase (15%) and quartz (5%) and opaques (2-3%). In one section the feldspars occurred as coarser phases along with the amphiboles but in another the feldspars and quartz formed a finer grained matrix. In the latter case the rock showed evidence of multiphase deformation, so the original texture may have been altered by subsequent recrystallization. The feldspars are all badly altered to sericite and epidote and



have corroded rims. Plagioclase compositions determined varied between An<sub>30</sub> to An<sub>38</sub> and the grains are commonly mantled by orthoclase.

#### 4.3.2 Structure

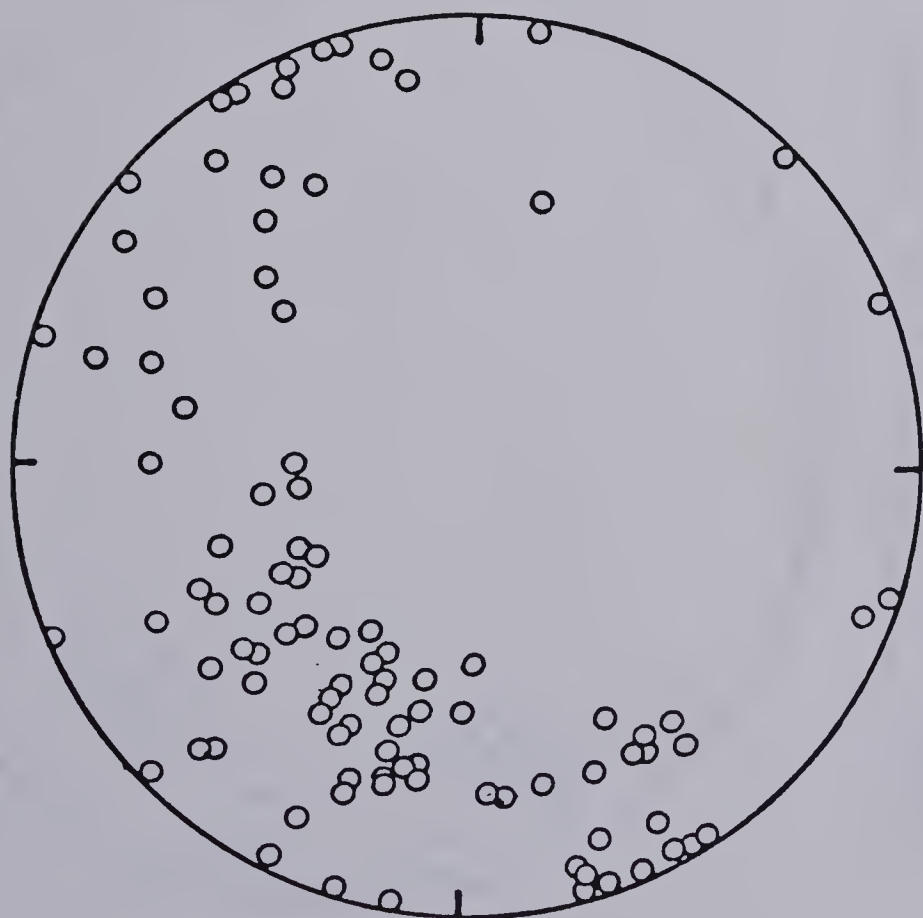
The Burnt Lake area has undergone polyphase deformation, although within the map area, Figure 46, only one phase predominates. The map shows the area to be generally highly folded into anticlines and synclines plunging steeply to the southeast with minor folds on the limbs. This structure was defined by mapping the mafic banding as a planar fabric thought to represent primary igneous banding.

A plot of the poles to bedding is shown in Figure 47, this includes the mafic banding described earlier and also igneous banding as defined by eutaxitic textures in metaignimbritic units. The measurements, total of 101, were collected from both the north showing and the surrounding area. The poles are contoured on a one percent equal area projection, Figure 49, which indicates that the beds have been folded fairly symmetrically about a fold axis which trends  $105^{\circ}$  and plunges  $70^{\circ}$ SE.

A plot of the poles to cleavage is shown in Figure 48, the measurements, total of 143, were again from the north showing and surrounding area. As can be seen from this diagram there is some scatter, but a broad cluster is apparent in the northwestern hemisphere. The poles are contoured on

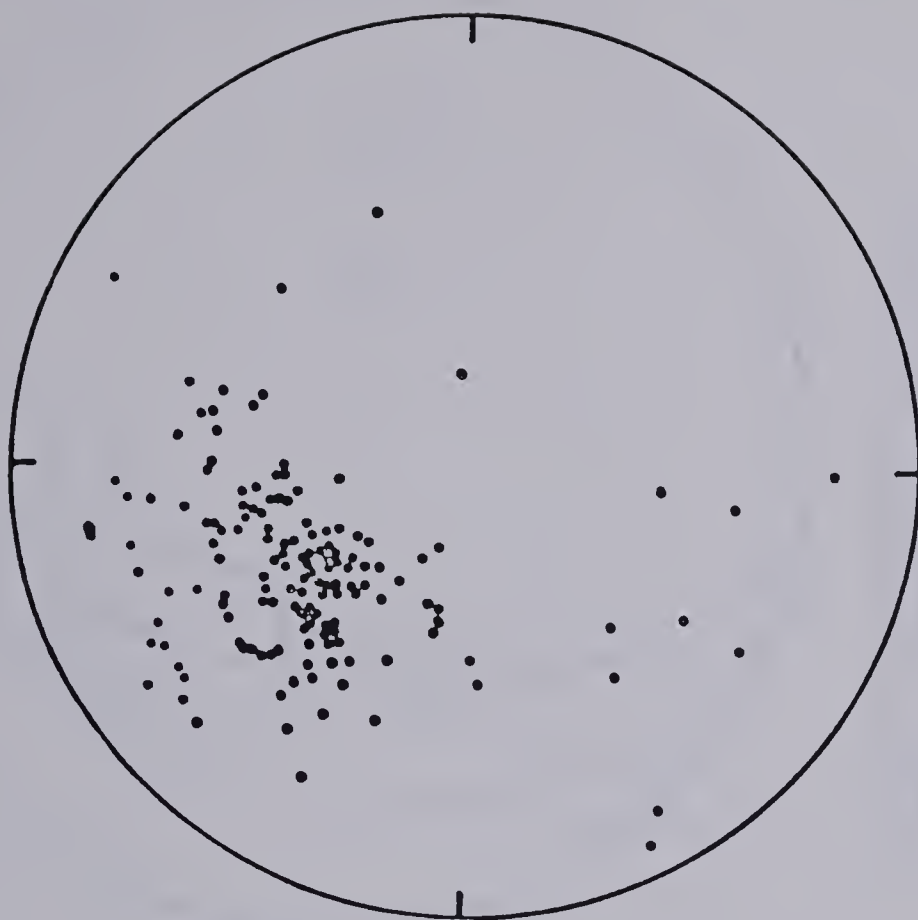






Plot of poles to bedding(101 measurements)

Figure 47



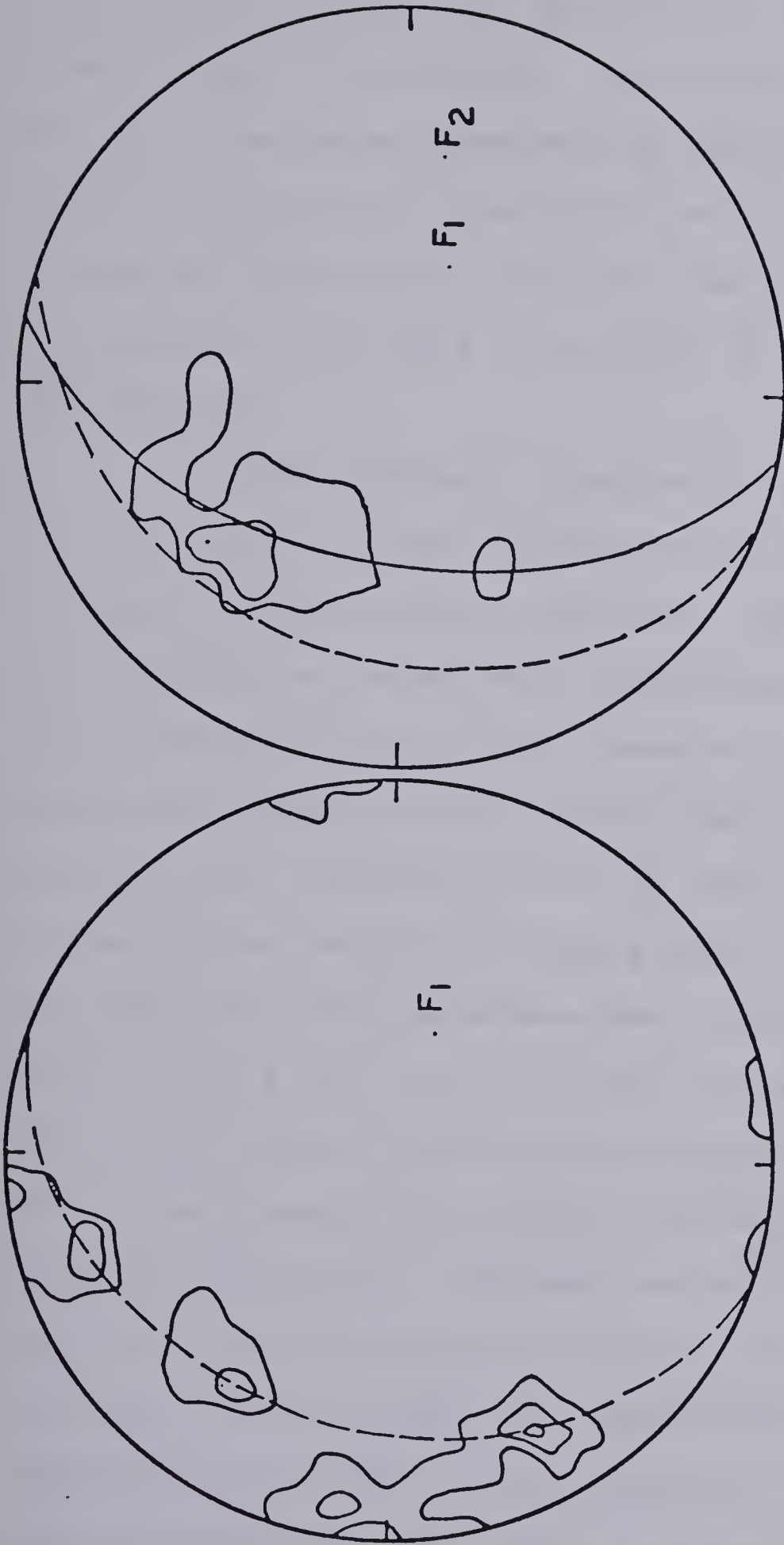
Plot of poles to cleavage(143 measurements)

Figure 48

Structural data for the Burnt Lake(uranium deposit) area







1% equal-area projection of poles to igneous banding; contour interval 3,5,7%

1% equal-area projection of poles to cleavage; contour interval 5,10,15%

Figure 49

Figure 50

Structural data for the Burnt Lake (uranium deposit) area



a one percent equal area projection, Figure 50, and again the same pattern is indicated. The cluster represents an average for the cleavage measurements of  $048/70^{\circ}\text{S}$ . Figure 46 shows that this cleavage is generally not axial planar to the folding of the beds as the trace of the cleavage only contains the plunge of the fold and not the trace of the fold axis from the map.

Although the  $\pi$  diagram defines the general trend of the cleavage, quite a broad scatter is evident. If this scatter is attributed to refolding of the area then the axis of this folding trends  $099^{\circ}$  and plunges  $38^{\circ}\text{E}$ . From the map of the area one can see that some of the cleavages do not follow the general NE-SW trend, thus it is suggested that this may have been the result of refolding. It is also possible that an earlier developed fabric has been folded during the same event that produced the local folding since the two axis of  $70^{\circ} @ 105^{\circ}$  and  $38^{\circ} @ 99^{\circ}$  correspond fairly closely. The earlier fabric may be an axial planar cleavage of folds with a much larger wavelength than the area mapped and therefore not detectable. Although several crenulation cleavages were seen in the lamprophyre dykes most of these were in erratics, where in situ the crenulations generally had an attitude of  $090/78^{\circ}\text{N}$ . Smyth (personal communication, 1978) also reported that the area is refolded as indicated by additional mapping carried out by Brinex during 1978.



Evidence of refolding was sought in thin sections as the development of an  $S_2$  fabric should cut the mafic banding, but , the only sections which showed such a relationship happened to be in the noses of the  $F_1$  folds and the schistose fabric in this case is probably  $S_1$ .

Although it is believed that polyphase deformation has affected the area, it is unknown whether both of these events are related to the Hudsonian Orogeny or if the latter may be related to the Grenville event. However, it should be noted that polyphase deformation of Hudsonian age is recorded in rocks of the lower Aillik Group further north (Marten, 1972; Clark, 1971).

#### 4.4.1 Amphibole and Pyroxene Analyses

Analyses of amphibole and pyroxene were performed to determine precisely their composition and correct classification. Grains were separated (60-120 mesh fraction) and mounted in an epoxy-resin and polished for electron microprobe analysis. An ARL (applied research laboratories) "EMX" microprobe was employed using the Energy Dispersive System (Smyth, 1976) for analyses of both amphibole and pyroxene. Standards were probed for a total of 400 seconds which consisted of eight fifty-second counts on random positions covering the grains. In order to monitor and correct drift effects, a willemite standard was run before and after the analysis of the samples. For the amphibole analyses the elemental abundances of Na, Mg, Al, Si, K, Ca, Ti, Mn, Fe, Zn and Cr were







calculated by comparing counts on the samples to counts obtained from the standards, plagioclase (Ca, Al, Na), Kaersutite (Si, Ti, Fe, Mg) and garnet (Mn, Cr). For pyroxene the elemental abundances of Na, Mg, Al, Si, Ca, Cr, Ti, Mn, Fe were calculated and the standards employed were willemite (Zn, Mn), plagioclase (Na), kaersutite (Fe, Ti, Si, Mg, Cr, K). The compositions of the standards used in the study are given in Table 13.

#### 4.4.2 Amphiboles

Six different amphibole grains, taken from two rock specimens which contained a high amount of uranium mineralization (XRF analysis indicate 1800 ppm and 2200 ppm), were analyzed. The results in oxide wt. percent are given in Table 14 along with their calculated structural formulae based on 23 oxygen. Although the probe is not presently capable of differentiating between ferrous and ferric iron (and thus calculates total Fe) the analyses presented do distinguish between the two. This was done by assuming an  $\text{Fe}^{2+}:\text{Fe}^{3+}$  ratio of 1:4 which is typical of amphiboles of these compositions (Deer et al., 1969) and thus proportioning the total Fe content accordingly.

The amphiboles analysed belong to the glaucophane-magnesioriebeckite series (Appleman et al., 1966) where the X site of the amphibole structural formula  $(\text{A}_{0-1}\text{X}_2\text{Y}_5\text{Z}_8\text{O}_{22}(\text{OH},\text{O},\text{F},\text{Cl})_2)$  is filled mostly by Na. The general formula for this series is,



TABLE 13

Standards used for microprobe analysis of  
pyroxene and amphibole grains

|                                | <u>†Willemite</u> | <u>††Kaersultite</u><br><u>639-34</u> | <u>†Wicks Garnet</u><br><u>639-1</u> | <u>†Ab-20 Plagioclase</u><br><u>EPS6-5</u> | <u>†Ab-80 Plagioclase</u><br><u>EPS6-2</u> |
|--------------------------------|-------------------|---------------------------------------|--------------------------------------|--|--|
| SiO <sub>2</sub>               | 28.07             | 40.37                                 | 39.04                                | 48.07                                      | 63.39                                      |
| TiO <sub>2</sub>               |                   | 4.82                                  | 0.38                                 |  |  |
| Al <sub>2</sub> O <sub>3</sub> | 0.04              | 14.91                                 | 21.65                                | 33.37                                      | 23.05                                      |
| FeO                            | 0.03              | 10.92                                 | 1.53                                 |  |  |
| MnO                            | 4.82              | 0.09                                  | 0.61                                 |  |  |
| MgO                            | 0.12              | 12.80                                 | 0.02                                 |  |  |
| CaO                            |                   | 10.30                                 | 36.58                                | 16.32                                      | 4.23                                       |
| Na <sub>2</sub> O              |                   | 2.60                                  |                                      | 2.25                                       | 9.34                                       |
| K <sub>2</sub> O               |                   | 2.05                                  |                                      |  |  |
| H <sub>2</sub> O               |                   | 0.98                                  |                                      |  |  |
| ZnO                            | 66.87             |                                       |                                      |  |  |
| <hr/>                          |                   |                                       |                                      |  |  |
| † pyroxene                     |                   |                                       |                                      |  |  |
| †† amphibole                   |                   |                                       |                                      |  |  |

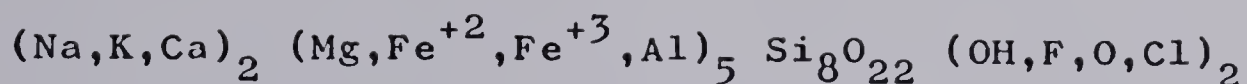


Table 14

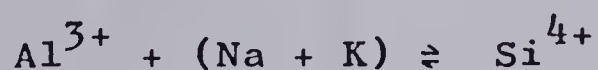
Microprobe Analyses (weight%) and Structural Formulae of Amphibole,  
Burnt Lake,

| Sample                         | B-54-1      | B-54-2      | B-54-3      | B-54-4      | A-1         | A-2         |
|--------------------------------|-------------|-------------|-------------|-------------|-------------|-------------|
| SiO <sub>2</sub>               | 53.99       | 54.11       | 54.65       | 54.21       | 52.90       | 52.81       |
| Al <sub>2</sub> O <sub>3</sub> | 0.96        | 0.92        | 0.82        | 0.91        | 1.39        | 1.44        |
| FeO                            | 4.23        | 4.28        | 4.34        | 4.31        | 4.14        | 4.17        |
| Fe <sub>2</sub> O <sub>3</sub> | 14.09       | 14.27       | 14.47       | 14.36       | 13.79       | 13.91       |
| MnO                            | 1.28        | 1.25        | 1.10        | 1.31        | 1.88        | 1.91        |
| MgO                            | 12.95       | 12.74       | 12.62       | 12.61       | 12.31       | 12.06       |
| TiO <sub>2</sub>               | 0.16        | 0.18        | 0.12        | 0.10        | 0.06        | 0.12        |
| ZnO                            | 0.25        | 0.24        | 0.18        | 0.23        | 0.12        | 0.09        |
| Cr <sub>2</sub> O <sub>3</sub> | --          | --          | --          | --          | --          | 0.05        |
| Na <sub>2</sub> O              | 7.00        | 7.08        | 7.02        | 6.96        | 6.71        | 6.77        |
| K <sub>2</sub> O               | 0.74        | 0.66        | 0.66        | 0.59        | 0.58        | 0.58        |
| CaO                            | <u>2.15</u> | <u>2.03</u> | <u>1.84</u> | <u>1.95</u> | <u>2.94</u> | <u>2.89</u> |
| Total                          | 97.80       | 97.76       | 97.82       | 97.54       | 96.82       | 96.80       |
| Si                             | 7.791       | 7.808       | 7.854       | 7.829       | 7.726       | 7.722       |
| Al <sup>iv</sup>               | 0.156       | 0.156       | 0.138       | 0.156       | 0.246       | 0.246       |
| Al <sup>vi</sup>               | --          | --          | --          | --          | --          | --          |
| Fe <sup>+2</sup>               | 0.511       | 0.520       | 0.518       | 0.521       | 0.509       | 0.510       |
| Fe <sup>+3</sup>               | 1.525       | 1.543       | 1.571       | 1.562       | 1.510       | 1.529       |
| Mn                             | 0.156       | 0.156       | 0.138       | 0.165       | 0.237       | 0.237       |
| Mg                             | 2.782       | 2.739       | 2.701       | 2.717       | 2.678       | 2.627       |
| Ti                             | 0.018       | 0.018       | 0.018       | 0.009       | 0.009       | 0.018       |
| Zn                             | 0.026       | 0.026       | 0.017       | 0.026       | 0.009       | 0.009       |
| Cr                             | --          | --          | --          | --          | --          | 0.006       |
| Na                             | 1.958       | 1.976       | 1.950       | 1.944       | 1.896       | 1.916       |
| K                              | 0.138       | 0.122       | 0.120       | 0.104       | 0.106       | 0.106       |
| Ca                             | 0.329       | 0.312       | 0.285       | 0.304       | 0.465       | 0.457       |
| Σy-site                        | 5.018       | 5.002       | 5.125       | 5.000       | 4.952       | 4.936       |
| Σx-site                        | 2.425       | 2.410       | 2.355       | 2.352       | 2.467       | 2.479       |





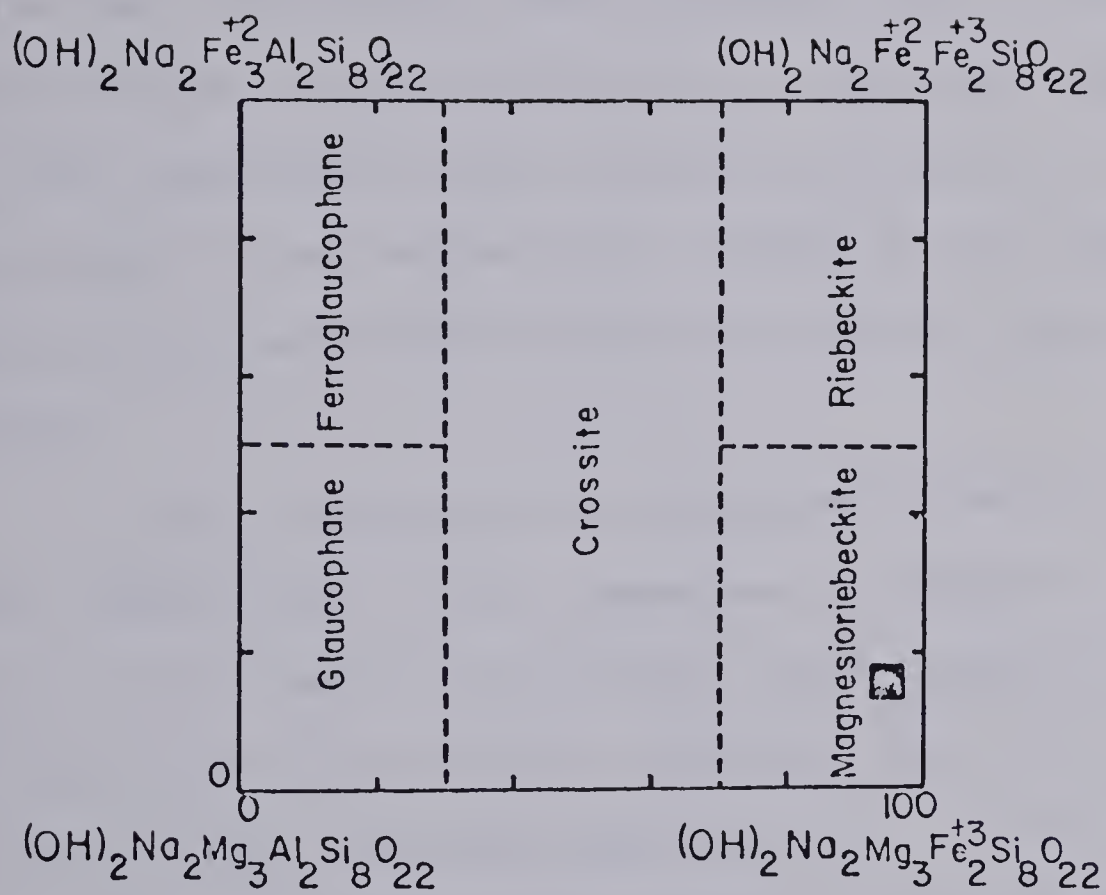
with the Al-rich varieties corresponding to glaucophane and the Mg rich varieties magnesioriebeckite; illustrated in Figure 51 from Ernst (1962). The analyses do not have to conform to the composition of the ideal end-member and quite often the sum of the X+Y ions may be less than seven (i.e. crocidolites) or in excess of seven (i.e. riebeckites) (Deer et al., 1969). The latter appears to be the general case here. Some of the alkalis probably belong in the A site due to the substitution of  $\text{Al}^{+4}$  for Si which creates a charge deficiency compensated by extra alkali cations in the A sites. This is represented by the reaction,



Magnesioriebeckite (Plate 23) occurs as slender acicular crystals in thin section and rarely as sections cut perpendicular to the C crystallographic axis which display the characteristic cleavage pattern. The grains are strongly pleochroic from lavender-blue (B) or blue ( $\gamma$ ) to colourless ( $\alpha$ ). In some sections cut perpendicular to X ( $\infty$ ) the grain remains blue during rotation of the stage. Values of 2V are characteristically low approaching  $0^\circ$  and the optic sign is (-). Refractive indices were not measured and the extinction angles are usually  $<10^\circ$ . The latter physical parameters are variable depending on the  $\text{Po}_2$  and Ernst (1962) proscribes their being used in attempting to derive the chemical composition







Compositional range and classification of the glaucophane-riebeckite amphiboles.

■ Amphiboles from Burnt Lake

Figure 51



of Fe-bearing amphiboles from their optical properties.

Magnesioriebeckite can be seen to be replacing aegerine-augite and also being replaced by it, in addition to it being altered to biotite. The biotite is characterized by its very dark brown color, probably due to its high Fe content which resided previously in the amphibole. In general the amphibole is not ubiquitous except in lamprophyre dykes where it may account for 15-20% of the mode or in the granite fragments found in volcanics where its content was 15-20%.

The occurrence of magnesioriebeckite and the other alkali amphiboles is not common and is thought to result from (i) hypersodic and subcalcic bulk compositions, or (ii) through physical conditions different from those commonly attained during regional metamorphism. In the case of magnesioriebeckite it is most commonly found in schists or low-grade metasediments. However, Ernst (1962) has shown that magnesioriebeckite is actually stable over very broad temperature and pressure ranges which covers a large part of regional metamorphic conditions. For example, White (1962) reports the presence of magnesioriebeckite in schists from New Zealand which fall in the almandine-amphibolite facies and Milton and Engster (1959) report the presence of authigenic magnesioriebeckite in the Green River Formation sediments. Thus, it is more likely that the development of magnesioriebeckite is



controlled by bulk composition of the host rock (Ernst, 1962; White, 1962) or possibly by the introduction of metasomatic fluids rich in the alkali elements, rather than regional metamorphism.

In the case of the occurrence of magnesioriebeckite at Burnt Lake an origin related to metasomatism is favored where fluids rich in alkalis were introduced into felsic tuffs not known to be of unusual bulk composition (i.e. hypersodic or subcalcic). Evidence supporting this contention is discussed under whole rock geochemistry.

#### 4.4.3 Pyroxene Analyses

Nine different pyroxene grains were analyzed, some of which were taken from the same specimens that were used for the amphibole analysis. The analyses in oxide wt. percent are given in Table 15 along with their calculated structural formulae based on 6 oxygens. The iron content was assumed to be all ferric although the ferrous ion may be present as indicated by the list of analyses given by Deer et al. (1969), but , this ratio varied too much to permit a valid approximation to be made.

The pyroxenes analyzed belong to the aegerine-augite class characterized by their high Na and  $\text{Fe}^{3+}$  contents due to the principal reaction of replacement,







Table 15

Microprobe Analysis (weight%) and structural formulae of Pyroxene,  
Burnt Lake.

| Sample                         | A-1         | A-2         | A-3         | A-4         | B-54-1      | B-54-3      | B-54-2      | B-59-1      | B-59-2      |
|--------------------------------|-------------|-------------|-------------|-------------|-------------|-------------|-------------|-------------|-------------|
| SiO <sub>2</sub>               | 51.83       | 51.98       | 51.87       | 52.14       | 52.18       | 51.94       | 52.38       | 52.30       | 51.64       |
| Al <sub>2</sub> O <sub>3</sub> | 0.68        | 0.79        | 0.54        | 0.59        | 0.81        | 0.70        | 0.88        | 0.94        | 0.46        |
| Fe <sub>2</sub> O <sub>3</sub> | 27.54       | 27.06       | 28.86       | 29.06       | 27.88       | 28.19       | 28.28       | 31.53       | 31.71       |
| MnO                            | 0.83        | 0.99        | 0.66        | 0.68        | 0.77        | 0.82        | 0.76        | 0.37        | 0.37        |
| MgO                            | 2.47        | 2.76        | 2.02        | 2.66        | 3.03        | 2.83        | 3.02        | 1.30        | 1.43        |
| TiO <sub>2</sub>               | --          | 0.06        | 0.06        | 0.01        | 0.10        | 0.11        | 0.09        | 0.06        | 0.01        |
| Cr <sub>2</sub> O <sub>3</sub> | 0.25        | 0.24        | 0.23        | 0.07        | --          | 0.07        | 0.05        | 0.07        | 0.06        |
| Na <sub>2</sub> O              | 10.93       | 10.50       | 11.42       | 11.47       | 10.95       | 11.05       | 11.17       | 12.39       | 12.26       |
| CaO                            | <u>5.12</u> | <u>5.84</u> | <u>4.00</u> | <u>4.46</u> | <u>5.21</u> | <u>5.23</u> | <u>5.21</u> | <u>2.83</u> | <u>2.85</u> |
| Total                          | 99.65       | 100.22      | 99.66       | 101.13      | 100.93      | 100.94      | 101.84      | 101.79      | 100.79      |
|                                |             |             |             |             |             |             |             |             |             |
| Si                             | 1.983       | 1.975       | 1.987       | 1.958       | 1.970       | 1.954       | 1.965       | 1.967       | 1.967       |
| Al <sup>iv</sup>               | 0.017       | 0.025       | 0.013       | 0.027       | 0.030       | 0.032       | 0.035       | 0.033       | 0.023       |
| Al <sup>vi</sup>               | 0.015       | 0.012       | 0.010       | --          | 0.006       | --          | 0.006       | 0.008       | --          |
| Fe <sup>+3</sup>               | 0.795       | 0.776       | 0.833       | 0.821       | 0.791       | 0.801       | 0.797       | 0.895       | 0.911       |
| Mn                             | 0.028       | 0.032       | 0.021       | 0.023       | 0.023       | 0.027       | 0.025       | 0.011       | 0.012       |
| Mg                             | 0.140       | 0.158       | 0.115       | 0.149       | 0.170       | 0.158       | 0.169       | 0.072       | 0.082       |
| Ti                             | --          | 0.003       | 0.003       | --          | 0.003       | 0.003       | 0.003       | 0.003       | --          |
| Cr                             | 0.009       | 0.009       | 0.009       | 0.005       | --          | 0.005       | 0.003       | 0.005       | 0.001       |
| Na                             | 0.808       | 0.772       | 0.848       | 0.906       | 0.816       | 0.878       | 0.812       | 0.904       | 0.906       |
| Ca                             | 0.209       | 0.237       | 0.163       | 0.180       | 0.211       | 0.210       | 0.210       | 0.115       | 0.117       |
| Σy-site                        | 0.987       | 0.990       | 0.991       | 0.998       | 0.993       | 0.994       | 1.003       | 0.994       | 1.006       |
| Σx-site                        | 1.017       | 1.009       | 1.011       | 1.086       | 1.027       | 1.088       | 1.022       | 1.019       | 1.023       |

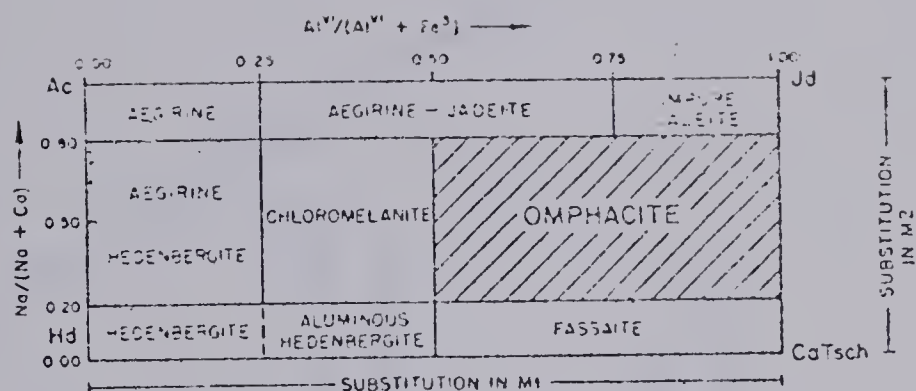


The analyses suggest that this reaction did not go to completion due to the relatively high contents of Ca and Mg which are present, approximately 5% and 2.5% respectively, except for two analyses. This would either have been due to a deficiency in the amount of sodium available or a change in  $PO_2$  causing the reaction to switch to the right.

The pyroxenes analyzed fall in the aegirine field for the pyroxene quadrilateral plot acmite - jadeite - hedenbergite - Ca tschermak (Figure 52). This plot points out both the high sodium and ferrous contents and also the very low aluminum contents. Note that a small change in the ferrous:ferric ratio will not move the points very far on the diagram. In figure 53 the pyroxenes analyzed plot in the iron-rich part of the aegirine field about an isotherm which indicates a temperature of formation of approximately  $900^{\circ}C$ . This field is bounded to the right by hymatite which is formed from the incongruent melting of aegirine at  $990^{\circ}C$  (Bowen and Schairer, 1929). It should be noted that these temperatures of crystallization are necessitated by the properties of dry melts used in the experiments and in corresponding natural magmas there would be a lowering of the temperature due to the presence of volatiles.

In thin section the pyroxenes (Plate 2<sup>4</sup>) are usually brownish-green to green in color, showing a distinct pleochroism. The grains are usually elongate parallel to the





|  |  |  |
|--|--|--|
|  |  |  |
|  |  |  |
|  |  |  |

Figure 52 Composition and classification of alkaline pyroxenes from the Burnt Lake area (diagram after Currie et al., 1975)

| Range for pyroxene analyses from Table 15



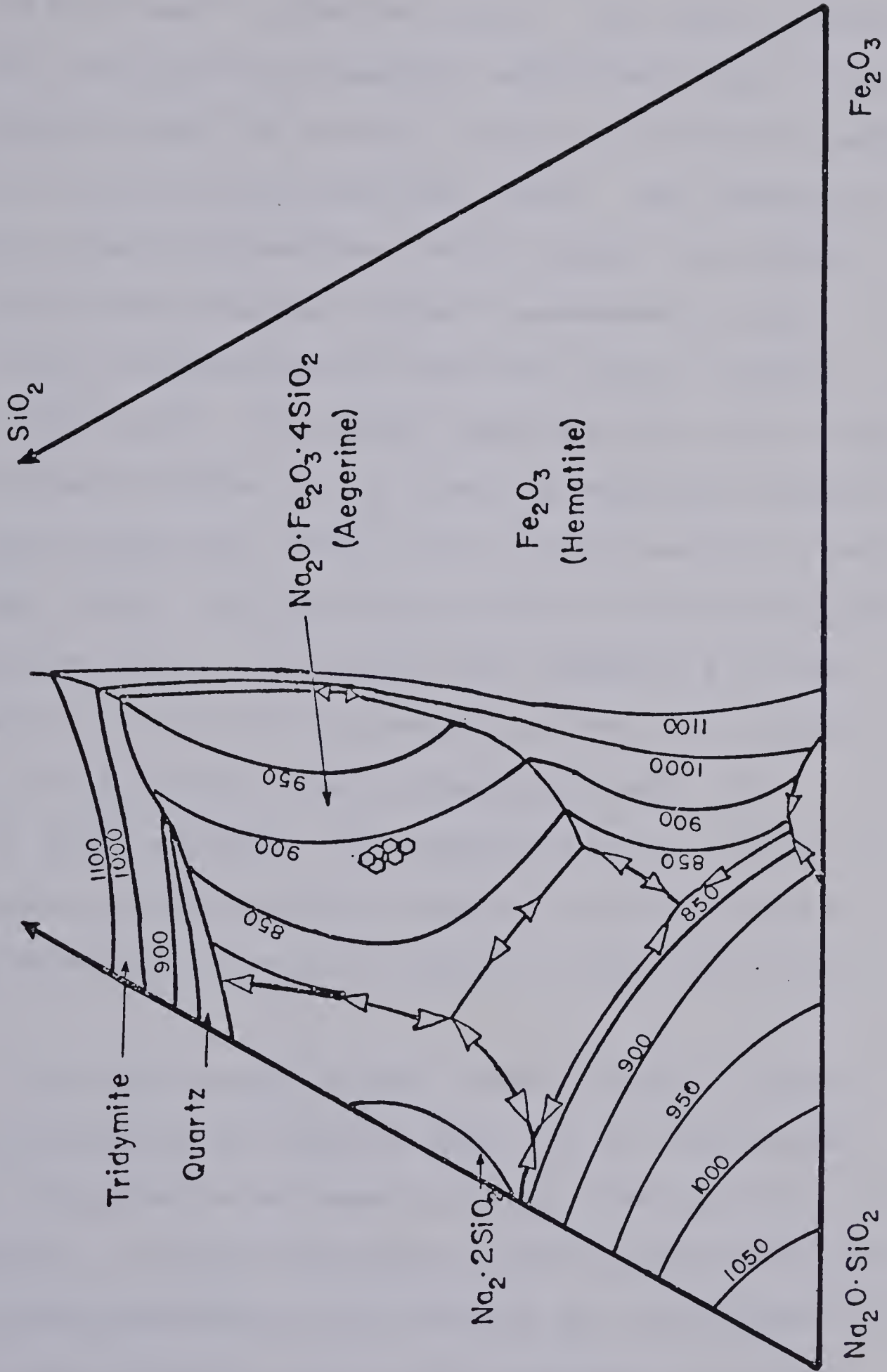


Figure 53

Phase diagram of the system  $\text{Na}_2\text{O} : \text{SiO}_2 : \text{Fe}_2\text{O}_3$  showing the aegirine field (after Bowen et al., 1930) and analyses of alkali pyroxenes from Burnt Lake





C-axis and have small extinction angles. The high birefringence, and also the high dispersion exhibited by most of the grains suggests that the dominant orientation would be perpendicular to B (or b crystallographic axis). The grains are more often found as aggregates forming bands a few millimetres thick rather than as single disseminated grains.

Other clinopyroxenes identified include augite, aegirine, and acmite. The latter was identified by its distinctive brownish color and was found in acid tuffs outside of the mineralized zone, there was no alkali amphibole seen in the same slide. Aegirine was seen in a few sections and was associated with a blue-green alkali-amphibole and was characterized by its strong pleochroism from yellow-green to green or yellow and very small extinction angle ( $<10^{\circ}$ ). Neither of these pyroxenes approached the total amount of aegirine-augite seen and their presence is attributed to small differences in the local chemical conditions of the rocks.

Aegirine-augite is most commonly found in late-stage differentiates of alkaline magmas or in areas which have been subjected to metasomatism (i.e. fenitization). It is interesting to note that Suzuki (1934) attributed the action of sodametasomatism to have caused the development of bands of aegirine-augite in some metamorphosed quartzose rocks from Hokkaido, Japan. However, White (1962) believed



that original chemical differences in the supracrustal rocks resulted in a banding of the mafic alkali minerals aegerine and riebeckite and that this banding ". . . could be taken as evidence against metasomatism . . . ."

In the Burnt Lake area the development of aegerine-augite is believed to be a synvolcanic process related to metasomatic fluids originating from the volcanic centre. Although aegerine was noted to be present in all the rocks of the area it is most common in the mineralized unit composing 10-15% of the mode. The reason for the sudden increase in the percent of the pyroxene is not known although it is probably related to the evolution of the magma with hypersodic conditions.

#### 4.5 Major and Trace Element Geochemistry

Major and trace element geochemical analyses were performed on both mineralized and unmineralized units to determine what processes were responsible for the differences in character of the respective units. Similar studies by Watson-White (1976), Minatidis (1976), and Bailey (personal communication) on both mineralized and unmineralized units in the area indicated that sodium metasomatism was responsible for altering the whole rock geochemistry where uranium mineralization occurs. However, it should be noted that alkali exchange during devitrification and hydration of glasses in ignimbritic cooling units is a common phenomenon (Scott, 1971).





Frequently associated with this is an inverse alkali relationship (Scott, 1966) in which either Na or K increases at the expense of the other. This relationship is usually related to alteration of the volcanic unit by an aqueous fluid whereby ion exchange occurs during decreasing temperatures (Orville, 1963). It is during this period of hydrothermal alteration of the volcanics that uranium may be released from crystalline material and enriched in the aqueous phase (Rosholdt et al., 1971).

#### 4.5.2 Major Elements

Analysis of major elements was performed in the same manner as described earlier under the section dealing with whole rock geochemistry for the Rb/Sr sample suites. Unfortunately many of the samples proved to be too siliceous and light colored to permit melting with the image furnace apparatus and consequently only three analyses could be performed, Table 16. Samples B-41 and B-59 both contained good mineralization and sample B-42 contained very little.

Although inconclusive it is interesting to note that the two mineralized rocks contain higher than normal contents of  $\text{Na}_2\text{O}$  and lower than average  $\text{K}_2\text{O}$  (compare to Table 9 for regional whole rock chemistry). According to Bailey (personal communication), this relationship is typical for mineralized rocks of the Burnt Lake area with the combined  $\text{Na}_2\text{O} + \text{K}_2\text{O}$





TABLE 16

Whole rock chemistry of mineralized rhyolites,  
Burnt Lake

|                                 | <u>B-41</u> | <u>B-42</u> | <u>B-59</u> |
|---------------------------------|-------------|-------------|-------------|
| Na <sub>2</sub> O               | 7.16        | 3.33        | 8.91        |
| MgO                             | 0.17        | 9.62        | 0.15        |
| Al <sub>2</sub> O <sub>3</sub>  | 14.39       | 15.50       | 13.42       |
| SiO <sub>2</sub>                | 70.12       | 53.53       | 69.53       |
| K <sub>2</sub> O                | 3.20        | 2.31        | 0.55        |
| CaO                             | 0.49        | 8.56        | 0.59        |
| TiO <sub>2</sub>                | 0.54        | 0.85        | 0.28        |
| MnO                             | 0.06        | 0.10        | 0.10        |
| Fe <sub>2</sub> O <sub>3</sub>  | 4.01        | 8.01        | 6.03        |
| H <sub>2</sub> O <sup>-</sup>   | 0.25        | 0.41        | 0.20        |
| H <sub>2</sub> O <sup>+</sup> } | 0.44        | 0.77        | 0.38        |
| Other }                         |             |             |             |
|                                 | <hr/>       | <hr/>       | <hr/>       |
|                                 | 100.83      | 102.98      | 100.14      |



content always approximating 10%. The low alkali content and high CaO, MgO, and  $\text{Fe}_2\text{O}_3$  content in B-42 may be accounted for by mafic phases (i.e. pyroxene and amphibole), however, this cannot be confirmed as a thin section of the sample was not made.

#### 4.5.3 Trace Elements

Analyses of sixteen samples for fourteen trace elements (Nb, Zr, Y, Sr, Rb, U, Th, Ce, La, Zn, Cu, Ni, Cr, Pb) included both mineralized and nonmineralized felsic volcanics and one granite sample. The analyses were performed by Dr. G. Holland, at the University of Durham, England, and the procedure employed was the same as that described by Lambert et al. (1974). The results are listed in Table 17.

It was hoped that the analyses could have been used to classify the volcanics, using the "immobile elements" as proposed by Floyd and Winchester (1975, 1978), but the inability to obtain major elements, for the reasons mentioned earlier, prevented the construction of the proper diagrams (cf.  $\text{Zr}/\text{TiO}_2$  versus Nb/Y;  $\text{Zr}/\text{TiO}_2$  versus Ce;  $\text{SiO}_2$  versus  $\text{Zr}/\text{TiO}_2$ ). However, the data do indicate some interesting relationships as seen in Figures 54, 55, and 56. The plot of Rb-Sr, Figure 56, indicates depletion of Rb in the mineralized samples, a similar pattern was also found by Minatidis (1976) for the Michelin deposit. It also indicates that the rocks are basically calcalkaline in composition for those



Table 17

Trace element geochemistry of mineralized and unmineralized rhyolites, Burnt Lake.

| <u>No</u>  | <u>ppm</u> | <u>Nb</u> | <u>Zr</u> | <u>Y</u> | <u>Sr</u> | <u>Rb</u> | <u>U</u> | <u>Th</u> | <u>Ce</u> | <u>La</u> | <u>Zn</u> | <u>Cu</u> | <u>Ni</u> | <u>Cr</u> | <u>Pb</u> |
|------------|------------|-----------|-----------|----------|-----------|-----------|----------|-----------|-----------|-----------|-----------|-----------|-----------|-----------|-----------|
| B1         |            | 26        | 212       | 49       | 8         | 221       | 11       | 23        | 186       | 89        | 13        | 3         | 3         | 3         | 26        |
| B4         |            | 28        | 130       | 15       | 39        | 158       | 5        | 37        | 33        | 18        | 7         | 6         | 2         | 3         | 22        |
| B6         |            | 34        | 202       | 46       | 8         | 333       | 4        | 33        | 163       | 73        | 21        | 6         | 3         | 12        | 29        |
| B14        |            | 20        | 270       | 31       | 9         | 1         | 5        | 43        | 206       | 97        | 21        | 4         | 4         | 11        | 19        |
| B18        |            | 36        | 305       | 58       | 30        | 230       | 5        | 28        | 157       | 68        | 7         | 4         | 4         | 2         | 20        |
| B23A       |            | 40        | 304       | 46       | 18        | 169       | 585      | 27        | 205       | 92        | 152       | 4         | 1         | 30        | 222       |
| B32        |            | 38        | 486       | 21       | 12        | 2         | 134      | 35        | 218       | 102       | 54        | 51        | 1         | 22        | 53        |
| B33        |            | 42        | 86        | 15       | 47        | 211       | 10       | 17        | 19        | 16        | 9         | 4         | 4         | 8         | 30        |
| B38        |            | 48        | 374       | 64       | 6         | 8         | 403      | 35        | 173       | 71        | 16        | 2         | 7         | 11        | 145       |
| B40        |            | 23        | 461       | 35       | 4         | 1         | 24       | 18        | 194       | 90        | 35        | 10        | 5         | 27        | 36        |
| B41        |            | 51        | 432       | 30       | 14        | 78        | 642      | 32        | 144       | 72        | 50        | 8         | 1         | 61        | 189       |
| B54        |            | 60        | 595       | 76       | 13        | 29        | 1769     | 22        | 83        | 30        | 67        | 382       | 2         | 89        | 547       |
| B57        |            | 23        | 470       | 60       | 14        | 3         | 223      | 32        | 321       | 151       | 126       | 4         | 6         | 31        | 101       |
| B58B       |            | 19        | 314       | 85       | 8         | 120       | 139      | 22        | 235       | 108       | 218       | 15        | 3         | 28        | 118       |
| PS5        |            | 19        | 207       | 34       | 97        | 181       | 6        | 13        | 98        | 59        | 26        | 2         | 6         | 4         | 29        |
| A          |            | 77        | 394       | 93       | 15        | 46        | 2232     | 31        | 125       | 47        | 58        | 845       | 8         | 41        | 795       |
| ppm        |            |           |           |          |           |           |          |           |           |           |           |           |           |           |           |
| St'd error | 2          | 2         | 1         | 1        | 1         | 1         | 2        | 2         | 4         | 4         | 2         | 2         | 1         | 1         |           |

ppm



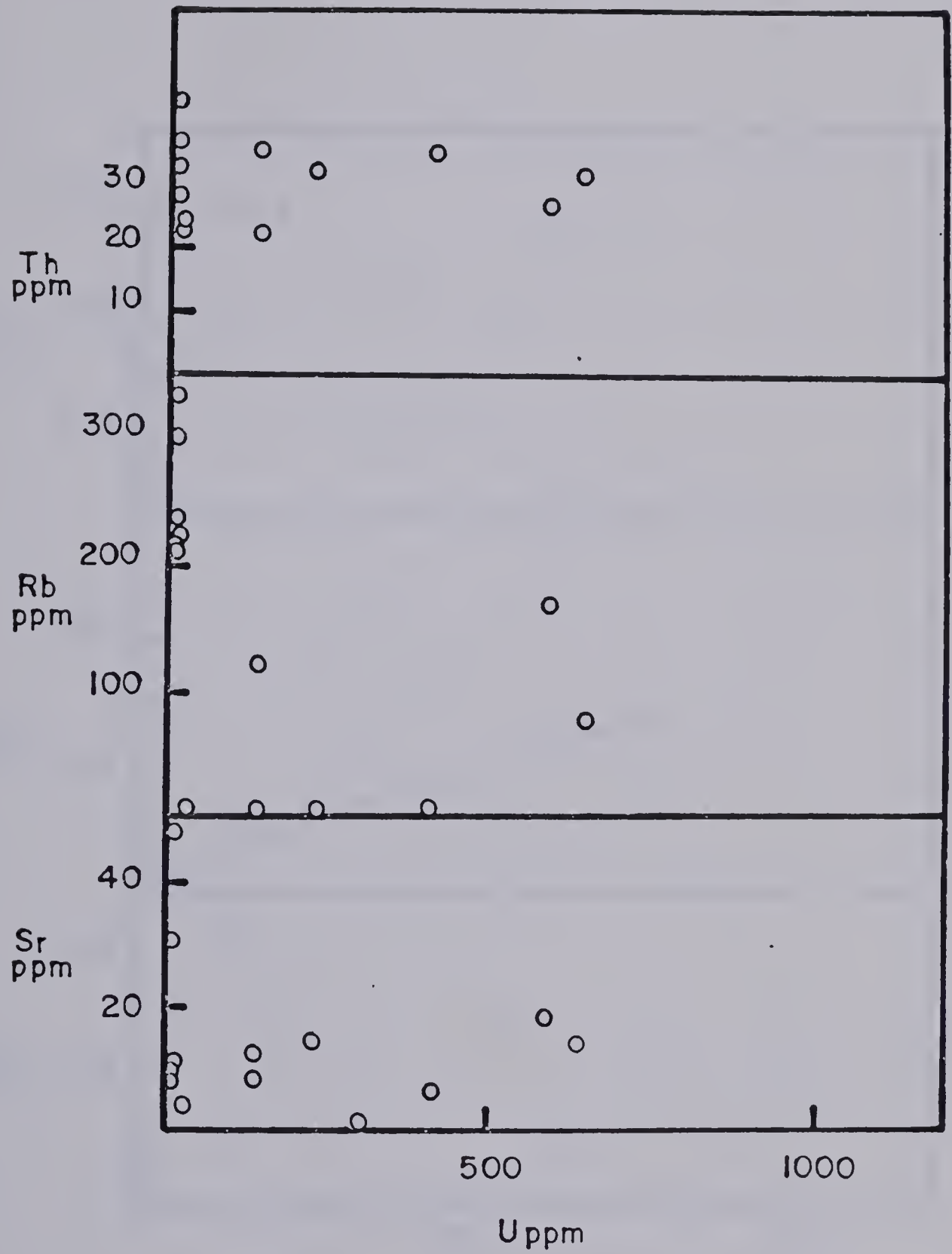


Figure 54 Th, Rb, and Sr versus U diagram





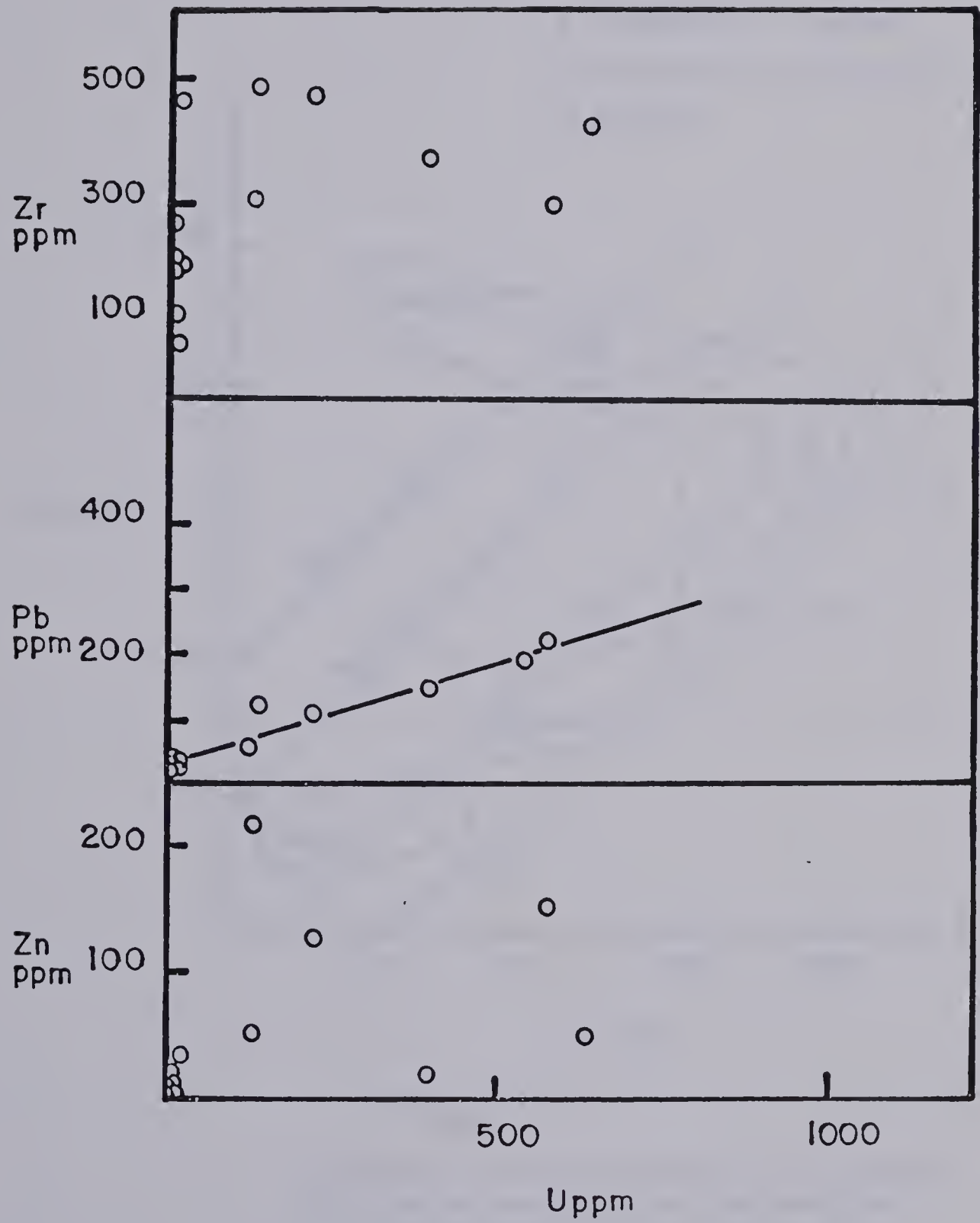


Figure 55 Zr, Pb, and Zn versus U diagram



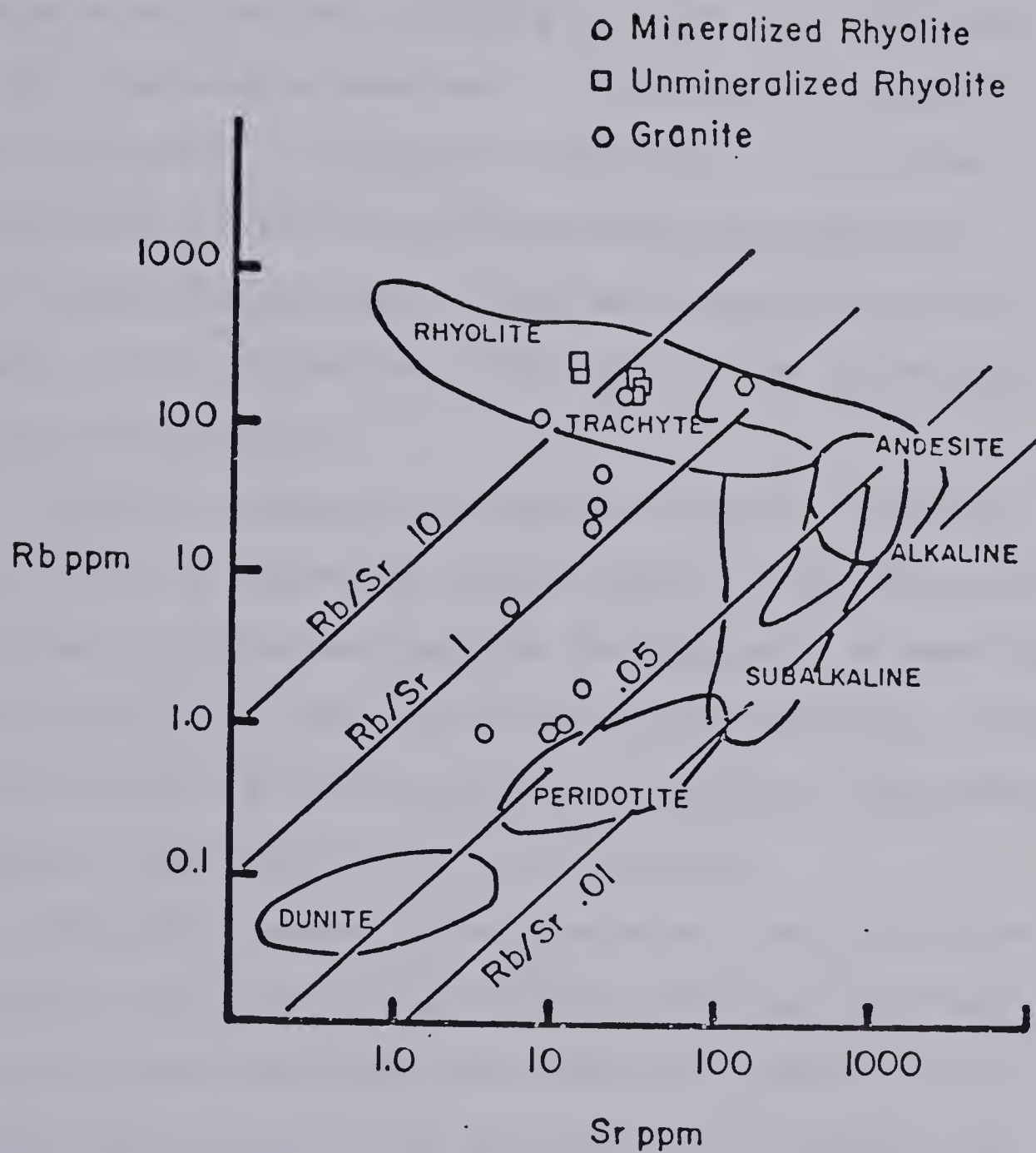


Figure 56

Rb versus Sr diagram(Kistler and Peterman, 1973) for mineralized and unmineralized rhyolites and granite from Burnt Lake uranium deposit



without the Rb depletion. Plots of U versus Rb and Sr, Figure 54, suggest possible depletion again where uranium mineralization occurs. It was shown earlier that depletion of  $K_2O$ , with a concomitant increase in  $Na_2O$ , was characteristic of the mineralized samples. A relationship between K, Rb, and Sr depletion is suggested from thin section also where replacement of both orthoclase and plagioclase by chessboard albite can be seen. Such an alteration process would result in the depletion of Ca, Sr, K, and Rb and subsequent enrichment of Na.

A positive correlation exists between U and Pb, Figure 55. This is important for it suggests that the lead is of radiogenic origin and negates the presence of nonradiogenic lead associated with the uranium mineralization. The presence of the latter would seriously influence the isotopic composition of lead required for U-Pb dating.

Plots of U versus Zr and Zn show a broad scatter but do suggest that some uranium may be tied up in zircon and that some associated zinc mineralization could be present. From thin section study the presence of zircon was confirmed and although it was usually clear some pleochroic grains, typically of fairly large size (up to 0.5-1mm), were seen suggesting a uraniferous content. Some fine grained sphalerite was seen in hand specimen. The plot of U versus Th, Figure 54, shows no well defined linear trends between





the two elements with thorium values remaining low even for very high uranium analysis. This relationship suggests that the main uraniferous phase identified as pitchblende lacks any significant amount of thorium.

#### 4.6 Uranium Mineralization

Uranium mineralization at the Burnt Lake North showing is confined to a unit characterized by a mafic banding with the mineralization found mostly within the mafic bands. Radioluxograph studies (Plates 25 and 26) confirms this and reveals the close association between uranium and the mafic portions of the rock. The extent of the mineralized unit is outlined quite well in Figure 57 which is a contour map of a radiometric survey done on the outcrops within the map area using a McPhar TV-1 scintillometer. By comparing the geological map of the area to this map one can see the remarkably good overlap.

In the field the highest scintillometer counts on outcrop were usually obtained in areas where intense red hematitic alteration accompanied the mafic banding (Plate 27). Such a relationship would suggest that the following reaction,



may have been important in localizing uranium mineralization. However, Gandhi et al., (1973) also report that high uranium values were obtained in areas where hematic alteration was



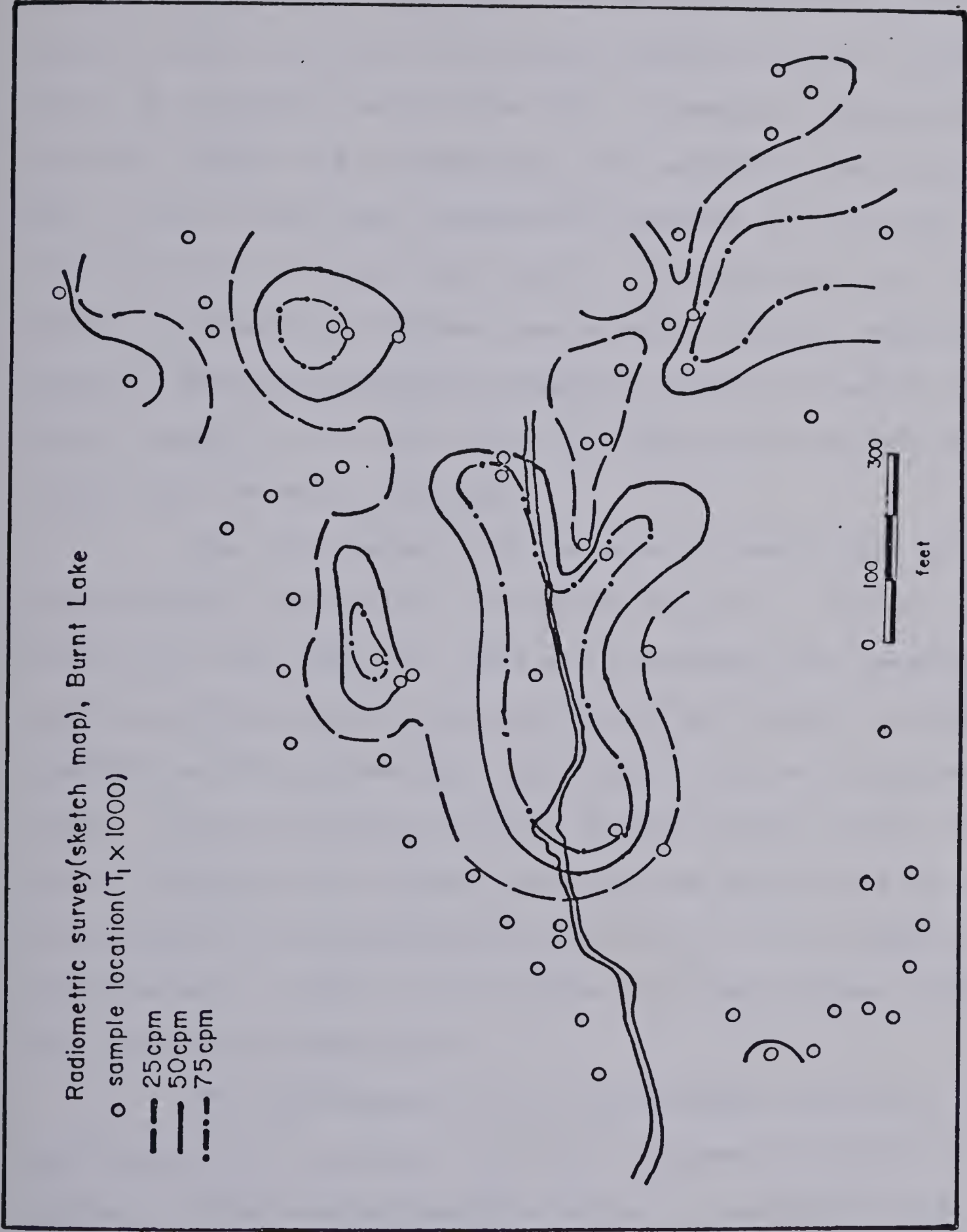


Figure 57



absent. On a smaller scale the uranium mineralization can be seen to occur as either individual uraninite cubes or aggregates of uraninite cubes (Plate 28), commonly associated with pyroxene (Plate 24) or sometimes with amphibole, but rarely was it seen within the leucocratic portions of the rock. Mineralization in thin section, easily recognized by the development of pleochroic haloes, was seen in volcanic tuffs, lamprophyre dykes, and granitic fragments within a volcanic matrix. In all cases the uranium mineralization was invariably associated with the mafic minerals.

The uraniferous phase present at Burnt Lake was identified as uraninite consisting chiefly of uranium and little, if any, thorium. This was confirmed from qualitative studies on the electron microprobe and by isotopic dilution analysis of the pitchblende, the latter will be discussed later. Yellow secondary uranium mineralization can be seen quite frequently on outcrops and this was identified as cuprosklodowskite  $[\text{Cu}_2(\text{UO}_2)_2(\text{SiO}_3)_3(\text{OH}) \cdot 5\text{H}_2\text{O}]$ , it is usually associated with a light to dark green secondary copper mineral not positively identified.

The geochemistry of the pitchblende (obtained from isotope dilution analyses for five specimens) is given in table 18. The results show the effect of weathering and subsequent uranium loss for three of the specimens. However, from whole rock trace element analyses the plot of U versus





TABLE 18

## Uranium-Lead Data, Burnt Lake

|      | <u>238U<br/>ppm</u> | <u>235U<br/>ppm</u> | <u>206Pb<br/>ppm</u> | <u>207Pb<br/>ppm</u> | <u>208Pb<br/>ppm</u> | <u>207Pb<br/>206Pb</u> | <u>206Pb<br/>238U</u> | <u>207Pb<br/>235U</u> | <u>206Pb<br/>238U</u> | <u>207Pb<br/>235U</u> |
|------|---------------------|---------------------|----------------------|----------------------|----------------------|------------------------|-----------------------|-----------------------|-----------------------|-----------------------|
| B-59 | 54 9505             | 3955                | 136288               | 14807                | 53                   | 1770 Ma                | 1624 Ma               | 1688 Ma               |                       | 4.2717                |
| B-55 | 1869                | 13                  | 14721                | 2000                 | 61                   | 2170 Ma                | 14907 Ma              | 5219 Ma               |                       | 169.65                |
| B-61 | 88085               | 631                 | 156079               | 16175                | -                    | 1680 Ma                | 7183 Ma               | 3457 Ma               |                       | 29.111                |
| A    | 115825              | 829                 | 423162               | 49394                | 2709                 | 1900 Ma                | 10654 Ma              | 4293 Ma               |                       | 67.605                |
| B-54 | 32709               | 234                 | 10585                | 1198                 | 13                   | 1840 Ma                | 2048 Ma               | 1947 Ma               |                       | 5.8058                |
|      |                     |                     |                      |                      |                      |                        |                       |                       |                       | 0.3739                |
|      |                     |                     |                      |                      |                      |                        |                       |                       |                       | 0.2865                |
|      |                     |                     |                      |                      |                      |                        |                       |                       |                       | 9.0991                |
|      |                     |                     |                      |                      |                      |                        |                       |                       |                       | 2.0472                |
|      |                     |                     |                      |                      |                      |                        |                       |                       |                       | 4.221                 |





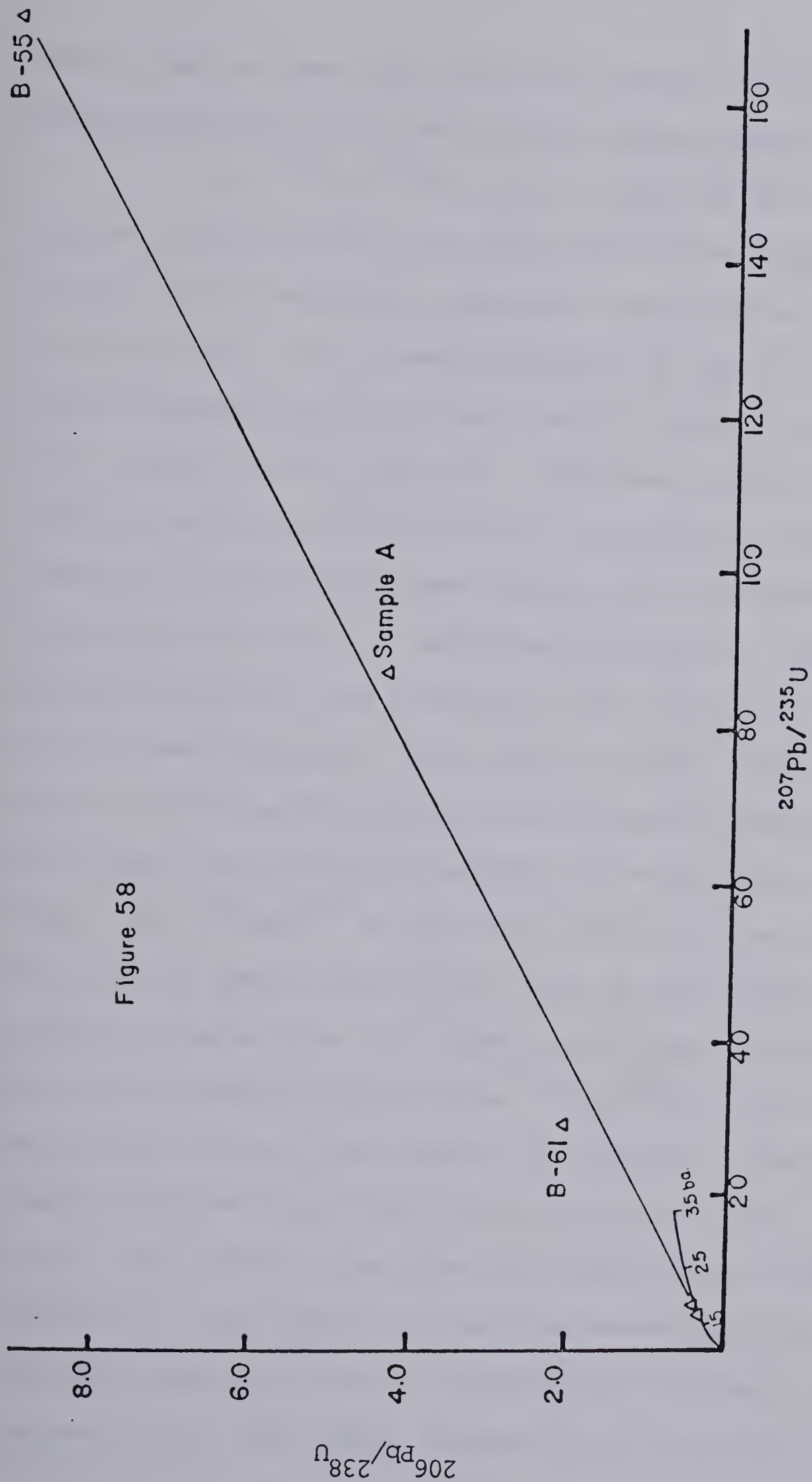
Pb does not show this relationship but instead a fairly good linear relationship. Perhaps this suggests that the uraniferous phase may have been leached but that the uranium was reprecipitated locally and that this process occurred on a very small scale. The low  $^{208}\text{Pb}$  values confirm the low thorium content of the uraniferous phase.

Associated mineralization includes sphalerite, magnetite, hematite, chalcopyrite, covellite, chalcocite, bornite, fluorite and galena. The latter is believed to be of radiogenic origin and in polished specimens can be seen to be intimately associated with the pitchblende (Plate 28). It should be noted that microprobe studies of plagioclase grains adjacent to mineralized portions of the specimens were pure albite in composition, again indicative of metasomatic processes active during mineralization.

#### 4.7 Uranium - Lead Dating

Five pitchblende samples were dated from the Burnt Lake north showing and the results are presented in Table 18 and plotted on a concordia diagram in Figure 58. Three of the samples (B-35, B-61, A) lie well above the concordia curve indicating loss of uranium or gain of lead. Of the two remaining points, B-59 is considered the most reliable due to its high uranium content (55%) and more concordant ages. It should also be noted that sample B-59 was obtained from drill core recently recovered from diamond drilling, whereas the







other samples came from surface trenches which in many instances showed yellow secondary uranium minerals.

The  $^{207}\text{Pb}/^{206}\text{Pb}$  ages of 1770 Ma for B-59 and 1680 Ma for A agree quite well with the 1770 Ma Rb/Sr age obtained on the Aillik volcanics collected approximately 15 km west of Burnt Lake. The close agreement of the two ages for the mineralization and host rocks would strongly suggest a syngenetic origin for the uranium. Geochronological data for uranium mineralization from other occurrences similar in many respects to the Burnt Lake showing are included in a concordia plot, Figure 59. The Michelin deposit, and Emben and John Michelin showings are hosted by acid volcanics of the Aphebian Aillik Group (Gandhi, 1976; Bailey, 1978, 1979) and in the case of the Michelin deposit the uranium mineralization is associated with aegerine-augite and riebeckite as at Burnt Lake. The  $^{207}\text{Pb}/^{206}\text{Pb}$  ages for mineralization at the Michelin deposit and Emben showing are 1264 Ma and 1386 Ma respectively, notably younger than the Burnt Lake mineralization, and for the John Michelin deposit the  $^{207}\text{Pb}/^{206}\text{Pb}$  age of 1774 Ma approximates closely the age at Burnt Lake. However, the concordia diagram shows that these five points all fall on a single line which intercepts the concordia at ~1800 Ma and ~1100 Ma. This suggests that the mineralization at these various localities may be genetically related. Following the episodic lead loss model proposed by Wetherill (1956) it





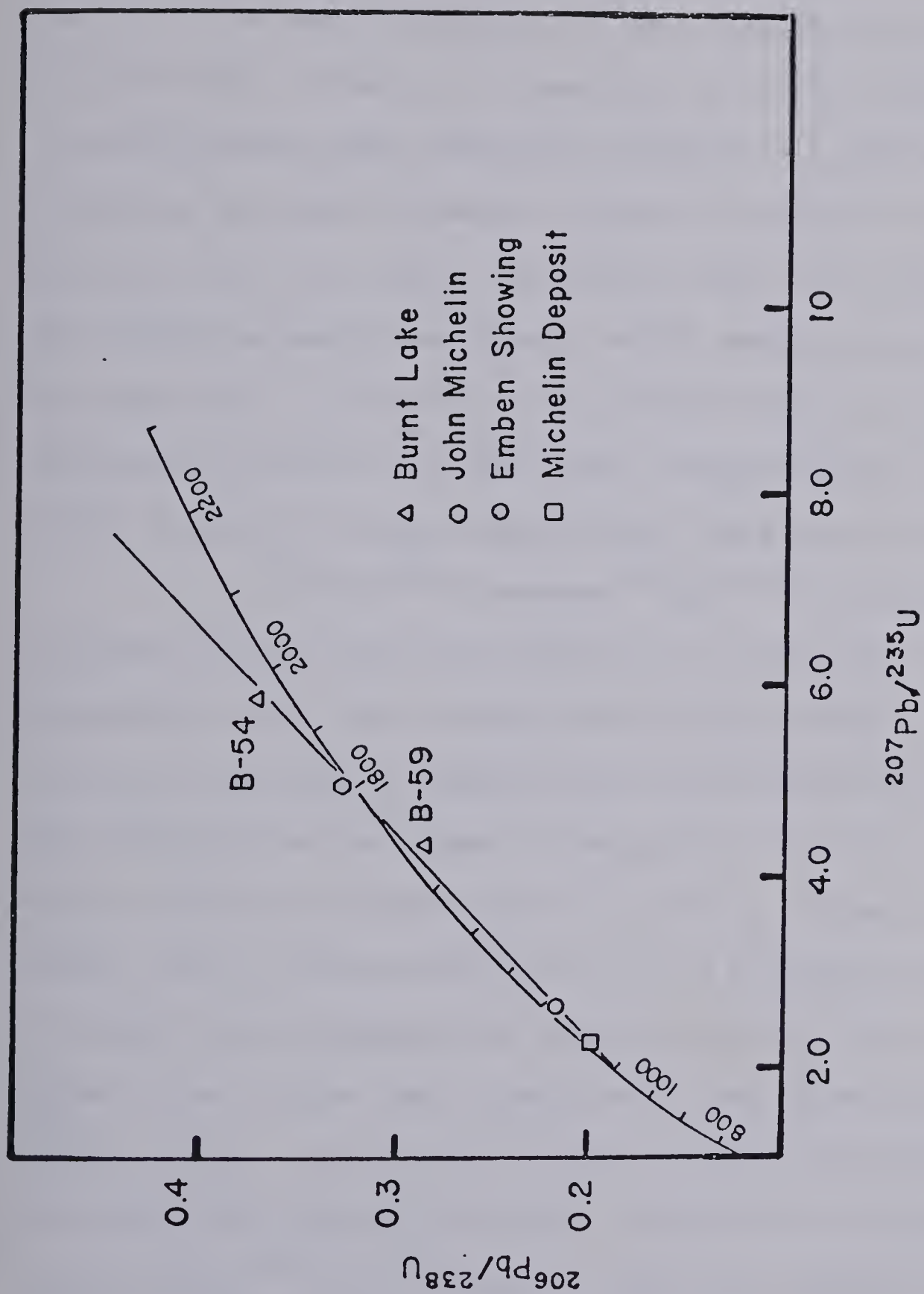


Figure 59

Concordia diagram for U-Pb data from the Burnt Lake, John Michelin, Emben, and Michelin uranium deposits



would appear that uranium mineralization formed syngenetically (?) in acid volcanics of the Aillik Group ~1800 Ma ago and that subsequent resetting of the uranium-lead clocks occurred during the Grenville orogeny at ~1100 Ma ago in the Michelin and Emben showing. Recent mapping of the area by Bailey (1978) has shown that both these localities are cut by Grenville-age shear zones, which would account for the younger ages. However, at the Burnt Lake and John Michelin showings no such event has been recognized and thus the original period of mineralization has been preserved.

A  $^{207}\text{Pb}/^{204}\text{Pb}$  versus  $^{206}\text{Pb}/^{204}\text{Pb}$  isochron plot (Figure 60) of the data indicates a scatter of the points suggesting that the isotopic system has not had a simple history involving a single stage of mineralization. Instead, the high content of lead in samples A and B-61 relative to their uranium contents would suggest an influx of nonradiogenic lead. The position of B-61 in Figure 60 would indicate a rather high component of normal lead for this sample as it lies close to the lead growth curve and also has a low  $^{206}\text{Pb}/^{204}\text{Pb}$  ratio. Using points B-61 and B-59 (believed to be the most reliable point with only radiogenic lead since it has such a high  $^{206}\text{Pb}/^{204}\text{Pb}$  ratio and high uranium content) as guides a  $^{207}\text{Pb}/^{206}\text{Pb}$  slope age of 1770 Ma was calculated, which agrees with the age obtained from the concordia diagram.



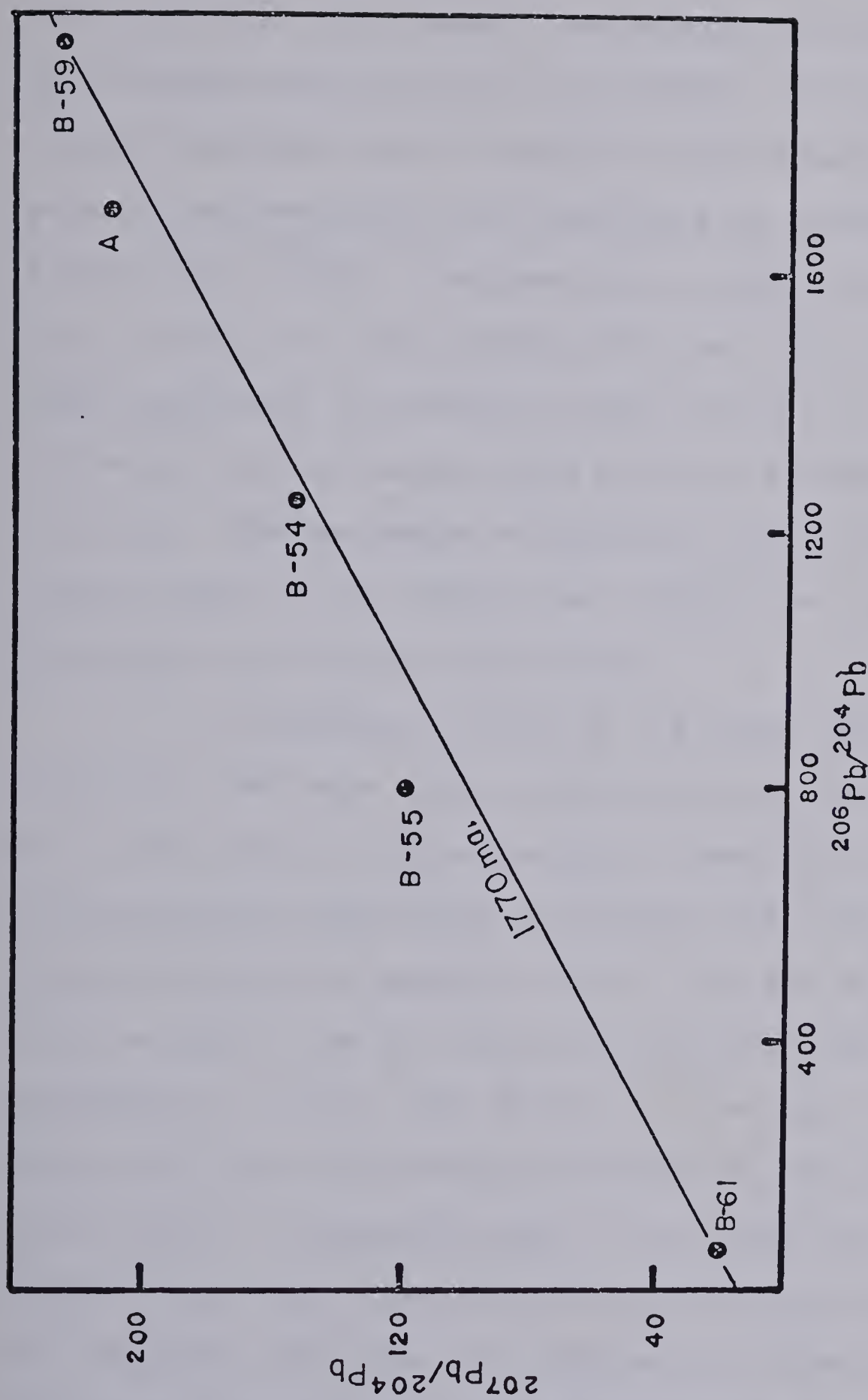


Figure 60

$^{207}\text{Pb}/^{204}\text{Pb}$  versus  $^{206}\text{Pb}/^{204}\text{Pb}$  plot for U-Pb data from the Burnt Lake uranium deposit



Assuming this represents a noncontaminated slope line then the relative positions of points B-55 and A suggest that the normal lead must have resided in older material since the points lie above the line indicating an increase in  $^{207}\text{Pb}$  rather than  $^{206}\text{Pb}$ . A minimum age of 2200 Ma is approximated from a slope age using points B-61 and B-55, however, an older parentage of probably Archean origin is believed to be the source of the normal lead since it is known to underlie the area. The mechanism responsible for selectively contaminating some of the samples may perhaps be related to either Hudsonian or Grenville tectonics.

In summary, dating of the Burnt Lake uranium mineralization indicates that a complicated history involving gain of Pb and loss of uranium occurred, probably due to recent weathering and subsequent tectonics, but that unweathered and uncontaminated samples indicate an age of approximately 1770 Ma (B-59) for the uranium mineralization. This age corresponds to a whole rock Rb/Sr isochron age of  $\sim 1770$  Ma obtained for acid volcanics equivalent to the host rocks at Burnt Lake. A concordia plot of the Burnt Lake data and additional data for other deposits exhibiting similar features to the Burnt Lake area (i.e. Michelin, Emben, John Michelin) define an episodic lead loss line giving an upper intercept of  $\sim 1800$  Ma, and a lower intercept of  $\sim 1100$  Ma. The older age is interpreted as the time of original uranium minerali-





zation in acid volcanics of the Aillik Group and the younger age is interpreted as a time of resetting corresponding to Grenville tectonics known to have affected these areas.

#### 4.8 Discussion and Interpretation

Uranium mineralization associated with felsic volcanics, as in the case of Burnt Lake, is a common phenomenon occurring in rocks of all ages around the world. However, alkali volcanism is probably the best source of uranium due to the concentration of the radioelements in the final stages of the magmatic cycle (Gabbleman, 1977; Sorensen, 1970; Armstrong, 1974; Boshe et al., 1974). In addition uranium is usually concentrated in the matrix and glassy portions of these volcanics (Sorensen, 1970; Dostal et al., 1977) rather than in the major mineral phases. This characteristic of uranium permits subsequent remobilization of the radioelements (Rosholdt et al., 1971; Zielinski, 1977; Zielinski et al., 1977) leading to its reprecipitation often in higher grade concentrations as the roll-type deposits of the southwestern states (Finch, 1967). Studies of uranium contents in obsidian, perlites and felsites (Zielinski, 1977; Zielinski, et al., 1977; Rosholdt et al., 1971; Rosholdt and Nobel, 1969) have shown that the radioelement content of nondevitrified volcanic material is normal for felsic rocks but that for devitrified components there is an 80% depletion of uranium. Such mobilization is believed to have been an important con-



trol in the localization of uranium mineralization of Burnt Lake.

Commonly associated with anomalous concentrations of uranium in felsic igneous rocks (i.e. intrusive and extrusive) is alkali metasomatism (Adamek, 1971; Smirnov, 1977; Mitterperger, 1970) frequently reflected by the presence of aegirine-augite and riebeckite as in the albite-riebeckite granites of Nigeria and the Soviet Union (Sorenson, 1970) and in areas of contact metasomatism around granitic intrusives in the Soviet Union (Smirnov, 1977). This association also occurs in the Burnt Lake area, at the Michelin deposit (Minatidis, 1976), and was noted during regional surveys conducted in the Central Mineral Belt (Krajewski, 1975; Gandhi and Guiton, 1975). Trace element geochemistry also reflects the metasomatic process with mineralized zones characterized by high Mo, F, REE, Be, Zn, Nb, etc. and Sr and Ba depletion (Bain, 1977). However, Schrider and Furbish (1977) reported high uranium assays that correlated with Co and Cu but did not show an equivalent association with Mo, Li, and Pb. Although trace element analyses were obtained on mineralized samples from Burnt Lake nothing very conclusive resulted. Enrichment of Zr, Pb and perhaps Zn were noted along with strong depletion of both Rb and Sr. Molybdenite and fluorite were observed in hand specimen indicating Mo and F associated with uranium mineralization. Bain (1977) points out that





depletion of these elements usually indicates depletion of the host rocks perhaps suggesting nearby enrichment of the remobilized uranium.

Walton (1978) favors subaerial pyroclastic rocks as hosts of uranium deposits rather than those formed in subaqueous environment. Whole rock analyses indicate little or no long distance migration of uranium occurs following its release from glass shards in submarine deposits due to the lack of a complexing agent. He speculates that reaction of calcium and other alkalis with  $\text{CO}_2$  depletes all the available dissolved  $\text{CO}_2$  leaving none to form uranylcarbonate complexes. However, in subaerial flows this phenomenon is not critical and uranium can be easily transported. The rocks of the Burnt Lake area are subaerial flows and Bailey (personal communication) believes most of the western part of the Aillik Group represents an area of subaerial deposition, as opposed to submarine in the east around Makkovik. However, where fluorine is present this could act as a complexing agent (Romberger, 1978), thus volcanic rocks deposited subaqueously should not be completely neglected as potential exploration targets.

The ultimate source of the uranium which formed the mineralization was probably igneous, but during pitchblende formation two contributors are envisaged. Uranium was probably partly derived from glass shards and from the matrix





of the volcanic rocks, and also from volatile-rich fluids emanating from a nearby vent. Thus, an active coeval, volcanic-plutonic association is envisaged similar to models proposed by Konstantinov and Yakumin (1973) and Bain (1977) for volcanic-intrusive magmatic complexes. Watson-White (1971) noted the close proximity between uraniferous volcanic horizons and intrusive contacts in the Walker Lake-McLean Lake area, and Bailey (1978) suggests a close association between uranium mineralization in volcanics and the granite in the Michelin deposit. However, the mineralization at Burnt Lake is considered stratiform and to represent syngenetic processes, rather than an epigenetic event, with the mineralizing solutions coeval with the volcanism. It is important to note that these areas adjacent to granitic contacts should offer good potential for epigenetic deposits if local fracture systems were present prior to the intrusion. The aerial extent of provinces showing the effects of metasomatism and subsequent enrichment of uranium can vary from local horizons covering a large area (Bain, 1977), or single isolated occurrences (Yermolayev, 1973), to large areas ( $\times 1000 \text{ km}^3$ ) where anomalous uranium concentrations pervade the entire terrain (Smirnov, 1977; Mittempergher, 1970).

In summary, uranium mineralization at Burnt Lake is confined to felsic volcanic horizons characterized by mafic bands composed of aegerine-augite and magnesioriebeck-



ite. The stratiform nature of the mineralization, intimately associated with the alkali mafic minerals and zones of red hematitic stain, and its age of 1750–1800 Ma which approximates closely the 1770 Ma age of the host rocks suggests a syngenetic origin. Although the ultimate source of the uranium was igneous, two contributors are considered for the local formation of pitchblende, these are the glass shards and matrix of the felsic tuffs, and the volatile-rich fluids emanating from a nearby vent, thus implying a model involving a coeval volcanic-intrusive magmatic complex. Such complexes are noted for uranium mineralization associated with alkali metasomatism (Sorenson, 1970; Smirnov, 1974; Bain, 1977; Konstantinov and Yakumin, 1973) and a similar model is proposed for Burnt Lake; this is supported by the presence of granitic fragments in volcanic tuffs which contain pitchblende associated with aegerine-augite and riebeckite. Localization of the uranium in certain horizons is considered to be a reflection of porosity, those horizons of welded nature did not permit the influx of mineralizing solutions whereas the porous horizons were more amenable to the fluids. The metasomatism, mineralization and growth of the mafic minerals is considered to have occurred during this process.



## CHAPTER 5

### THE MORAN LAKE AREA

#### 5.1 Introduction

The Moran Lake uranium showings lie southeast of Moran Lake. Figure 61, in an area underlain by the Heggart Lake Formation, the basal member of the Paleohelikian Bruce River Group. Three showings occur and are referred to informally from east to west as the A, B, and C zones (Bernazeaud, 1965). Of interest to this study were the latter two, the B and C zones, also referred to as the Montague 1 and Montague 2 (Ellingwood, 1958), with the A zone examined only briefly out of interest. The B and C zones were both mapped in detail during July, 1977 and shall be discussed separately, even though they may be genetically related (Kontak, 1978).

#### 5.2 Regional Geology of the Moran Lake Area



The Regional geology of the Moran Lake area (Figure 61), was included in the maps of Williams (1970), Smyth et al. (1975), Ryan (1977), and Smyth and Ryan (1977). The oldest rocks in the area are Archean granites and gneisses which outcrop north of Moran Lake and form part of a much more extensive basement terrain which also includes metavolcanic and metasedimentary units (Ryan, 1977). Overlying the Archean basement and cropping out in the western part of the map area is the Aphebian (Williams, 1970) Moran Group (Smyth et al., 1975) which consists of black and grey laminated mudstones,









Figure 61Regional Geology of the Moran Lake area (after Smyth and Ryan, 1977)

## Intrusive Rocks (post Bruce River Group)



-  Gabbro, diorite
-  Feldspar porphyry

## Bruce River Group


-  Porphyritic dacite, minor sandstone
-  Massive mafic flows, agglomerate
-  Tuffaceous sandstone
-  Heggart Lake Formation: conglomerate, sandstone; minor mafic flows and breccia

~~~~~U/C~~~~~

## Moran Group

-  Pillowed mafic flows
-  Slate, dolostone

## Archean

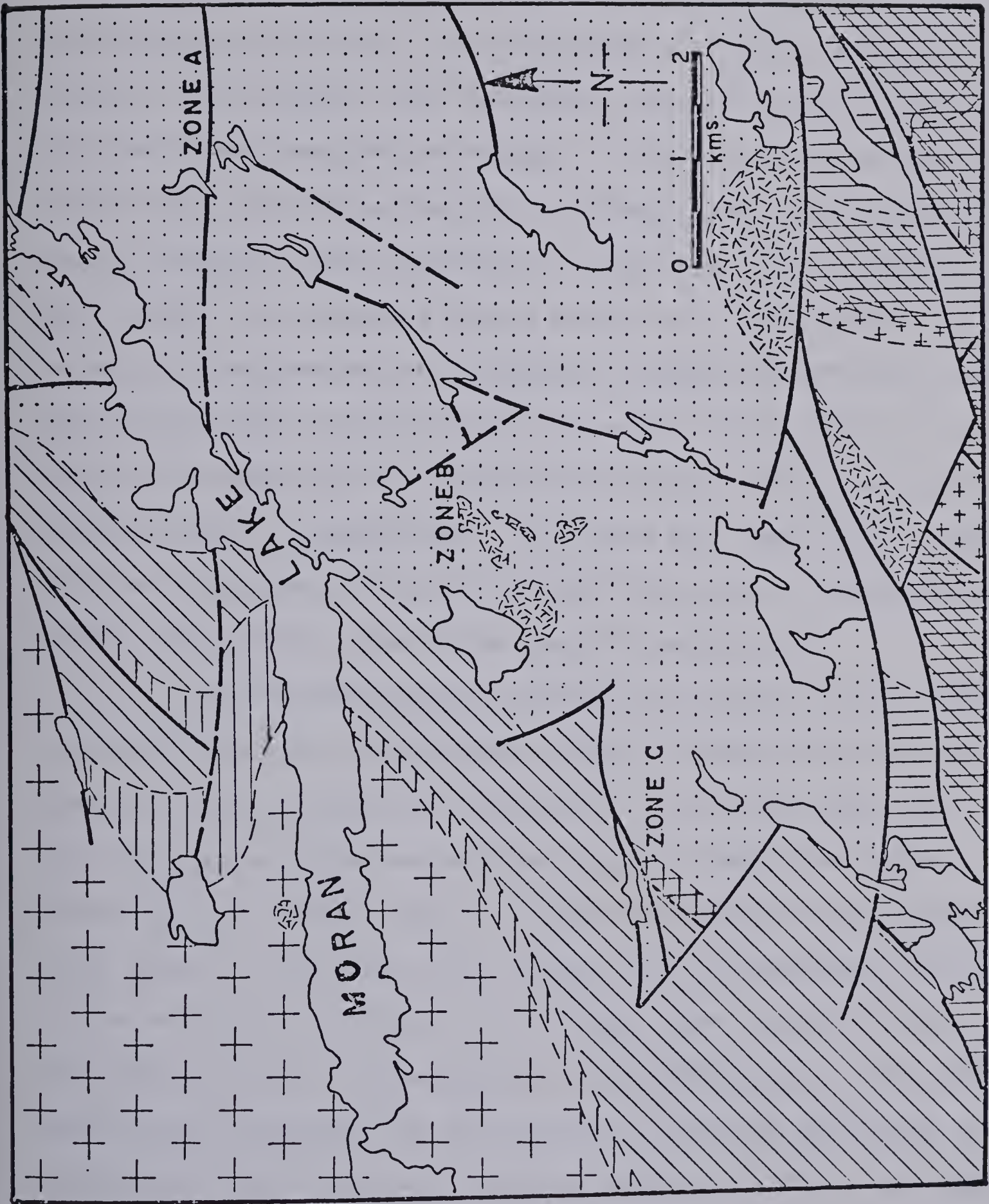
-  Foliated granite and gneiss

Fault (defined or approximate, assumed) . . . . . //

Zone (A, B, C) . . . . . uranium showing









with minor chert and dolostone overlain by massive and pillowed mafic volcanics. Unconformably overlying the Moran Group is the Heggart Lake Formation, the basal member of the Paleohelikian Bruce River Group. It consists of red and pink sandstones, quartzites and grits intercalated with cobble to pebble conglomerates and mafic to felsic volcanics (Smyth et al., 1975). The Heggart Lake Formation is overlain to the south by a succession of tuffaceous sandstones of red, maroon, and green color which contain some minor mafic flows. The uppermost member of the Bruce River Group consists of acid volcanics and ignimbrites. The area has been cut by both feldspar porphyry and mafic bodies, the ages of which are unknown, but are believed to be post Paleohelikian.

No detailed studies of the structure of the Archean basement have been undertaken, but in outcrop it is evident that polyphase deformation occurred. The Moran Group has also undergone polyphase deformation, at least two phases (Smyth et al., 1975), prior to the deposition of the Bruce River Group. The Bruce River Group has been deformed further to the south and southeast into large, open upright folds plunging gently to the southwest. Modification of the local geology has occurred due to Grenville faulting developed in north-south and east-west trending patterns. These are high-angle reverse faults and have juxtaposed older basement rocks against the younger Bruce River Group rocks as seen in the





area of the Moran Lake C Zone uranium showing (Ryan, 1977).

### 5.3 Moran Lake 'B' Zone: Introduction and Previous Work

The Moran Lake 'B' Zone, discovered by Brinex during the summer of 1957 (Ellingwood, 1958), lies east of Lake Louis in the Heggart Lake Formation where anorthositic dykes are found cutting red sediments. The area was originally worked by Brinex until 1964 at which time Mokta acquired a concession on the area and later took out a development license, subsequently dropped in 1975. At present the area is held by Commodore Mining Ltd. who has optioned the area to Shell Canada Ltd.

The area was mapped in detail (Figure 62) during early July, 1977, utilizing a grid put in by Shell Ltd. Previous work in the area included detailed mapping by Ellingwood (1958), Mann and Collins (1957), Bernazeaud (1965) and Smyth and Ryan (1977).

### 5.4 Local Geology of the 'B' Zone

The local geology of the 'B' Zone is shown in Figures 62 and 63, the latter one is taken from Ellingwood (1958). The area mapped by the writer corresponds to the area immediately adjacent to the biotite gabbro found southeast of Lake Louis on Ellingwood's map. Thus, the sedimentary units in figure 62 represent what Ellingwood refers to as the lower conglomerate and lower quartzite. These two rock types





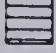

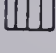







Figure 62

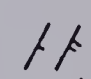
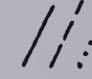
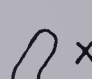

Local Geology of the Moran Lake 'B' Zone Uranium Showing

**Intrusive Rocks**

-  Mafic differentiate (dunite to syenite)
-  Feldspar-pyroxene porphyry
-  Feldspar porphyry with trachytic matrix
-  Fine-grained trachytic dyke
-  Fine- to medium-grained anorthosite (plagioclase laths are accicular)
-  Coarse-grained anorthosite

**Bruce River Group (Heggart Lake Formation)**

-  Polymictic conglomerate
-  Red to mauve, fine- to medium-grained sandstone; minor tuffaceous sediments

- Bedding (tops known, tops unknown) . . . . . 
- Geological contact (defined, approximate, assumed) . 
- Outcrop (large, small) . . . . . 
- Swamp . . . . . 

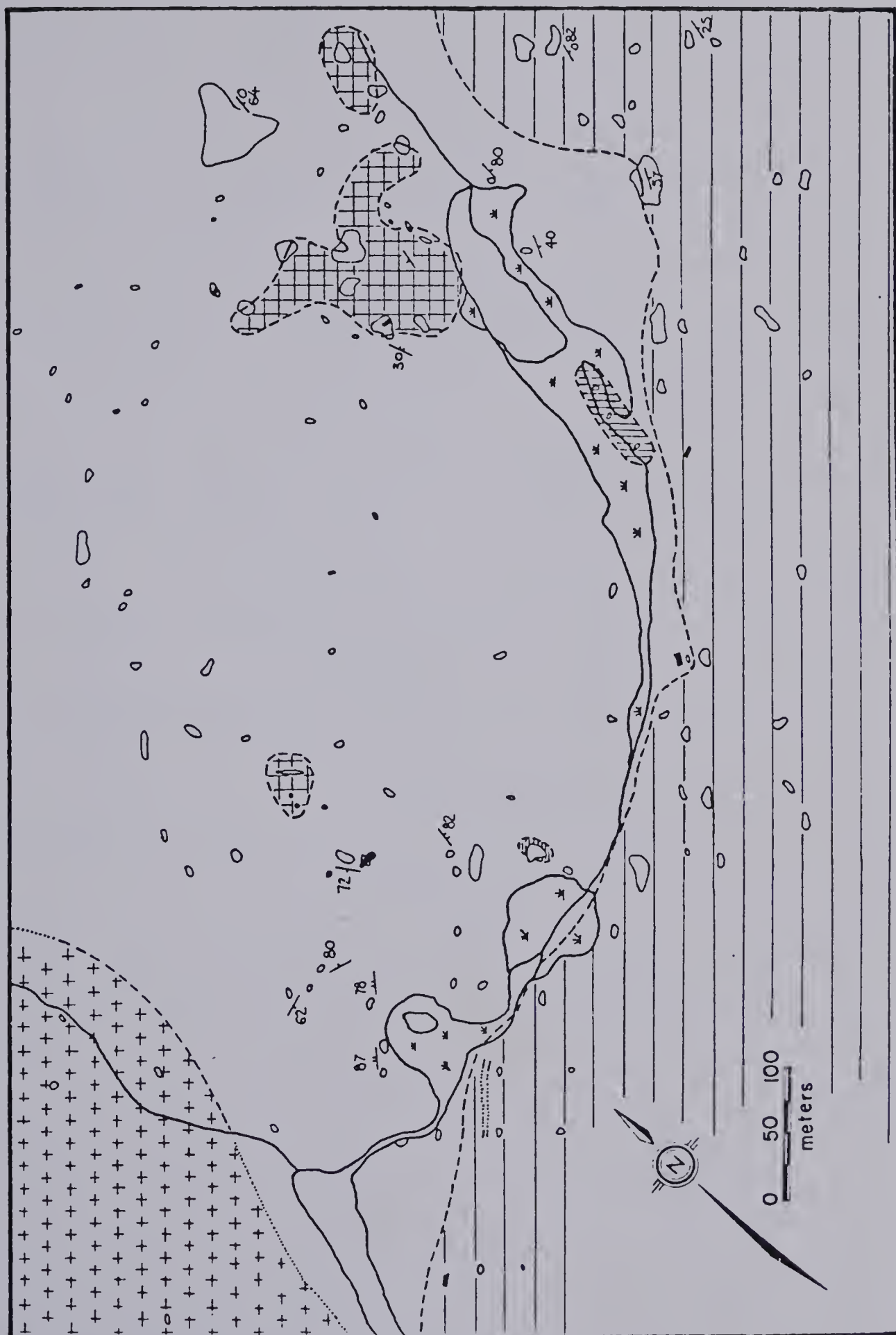


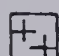


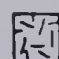


Figure 63

Local Geology of the Moran Lake 'B' Zone (after Ellingwood, 1958)

Intrusive Rocks


 Gabbro to syenite

 Gabbroic dykes


Bruce River Group

(Sedimentary Rocks of Heggart Lake Formation)


 Upper conglomerate

 Middle quartzite; fine-grained grey quartzite

 Lower conglomerate

 Lower quartzite; feldspathic sandstones and quartzites

Moran Lake Group

 Mafic volcanics

Fault or shear . . . . . 

Bedding (inclined, vertical) . . . . . 







underlie the area and form part of the Heggart Lake Formation which has been cut by numerous dykes, small anorthositic bodies and a large ultramafic stock of unknown age.

#### 5.4.1 Sedimentary rocks

The oldest unit of the area is composed of fine-grained red sediments, typically sandstones and siltstones, which are usually massive and display very few sedimentary features. In the field most of the rocks appeared to be quartz-rich with feldspar the next major component. Sometimes the feldspar content may approach 75%, suggesting a possible volcanogenic origin, which was confirmed in the western portion of the map area where similar feldspathic sandstones exhibited textures suggestive of a pyroclastic origin (cf. eutaxitic texture). The sediments are usually intensely fractured and in some cases secondary alteration is associated with these, especially where minor movement has occurred or where mafic dykes are present. The alteration is usually a combination of hematite, chlorite, and red and white carbonate, these areas are frequently radioactive. In two outcrops salt or pyrite casts (?) were seen in mudstones. These were cubic or pentagonal in outline and averaged 3-6 mm in size. Although only a few sedimentary features were seen such as planar- and trough cross-bedding, scour and fill structures and current ripples they indicated tops to the north. In one area on the southwest side of Lake 202, the best outcrop of the red beds



occur where abundant sedimentary structures are visible.

In the vicinity of the dykes, particularly in the eastern part of the map area, soft sediment deformation structures were seen and were originally thought to indicate intrusion of the dyke-like bodies into unlithified, wet sediments (Kontak, 1978).

In thin section the sediments are quite variable in composition with varying amounts of quartz, K-feldspar, magnetite, and plagioclase as the detrital components and carbonate, hematite, and penninite as secondary alteration products. The detritals are typically angular to subrounded with quartz forming the largest percent and feldspar and plagioclase, commonly andesine or high oligoclase, varying in amounts but nearly always fresh and unaltered. The grains are commonly corroded indicating reaction with a fluid, probably during diagenesis. The amount of matrix, consisting mainly of feldspar, varies but in one section composed 50% of the rock. The amount of alteration is variable, for example, one slide contained 50-60% carbonate and another had no carbonate but instead hematite coatings on the grains and penninite. The samples examined in thin section would best be called arkosic grits.

A thin section of a pyroclastic rock from the western portion of the map area confirmed its igneous origin. An eutaxitic texture is defined by magnetite banding and





this is paralleled by sericite and quartz bands. Minor amounts of feldspar phenocrysts (< 1%) and biotite (2-3%) are the only coarse phases with the remainder of the rock composed of quartz and K-feldspar with minor plagioclase and microcline.

Overlying the red sediments disconformably is a polymictic, pebble to cobble conglomerate (Plate 29). This conglomeratic unit can be seen to cut large channels (commonly 10-12 metres) into the underlying finer-grained red sediments. The conglomerate unit may be up to 900 metres (2800 feet) thick (Ellingwood, 1958) and Mann and Collins (1957) recognized these different types of conglomerate referred to informally as (i) conglomeratic quartzite, (ii) fractured conglomerate, and (iii) conglomerate. The conglomerate interfingers with the red sediments in the western part of the map area forming two tongues which protrude westwards before pinching out, Figure 63. Finer-grained sandstone and siltstone lenses may occur within the conglomerate indicating periodic changes in the energy of the environment of deposition.

The conglomerate commonly contains angular to sub-rounded pebbles and cobbles, and frequently boulders (>256 mm), of varying composition. Towards the bottom where it rests on sediments, fragments of the same material may dominate and the matrix may be feldspathic. However, further up the section fragments of smoky quartz, red jasper, granite, and





gneiss are dominant with lesser amounts of red sandstone, greenstone, porphyritic rhyolites, andesites, and mafic intrusives. The fragments usually constitute up to 60-70% of the rock with the matrix composed of a greenish grey grit, typically quartz dominant. Locally conglomerate may show shearing and faulting and in these secondary alteration consisting of hematite and chlorite may be present.

#### 5.4.2 Dyke Rocks

Cutting the sediments in the map area are several different types of dykes. Based on their texture and mineralogy a minimum of five types may be recognized. The dykes are believed to have entered along fractures previously developed in the sediments, the dominant directions of these being  $55-75^{\circ}$ ,  $125-135^{\circ}$ ,  $140-150^{\circ}$ , and  $180-200^{\circ}$  (Mann and Collins, 1957). From the map one can see that most of the dykes trend between  $55-75^{\circ}$  and may have thus been controlled by one of the dominant structures in the area. However, several of the bodies have irregularly defined ameboid-like outlines on the surface, exactly what their relationship is at depth is unknown. From field work the dykes were seen cross-cutting the larger bodies providing some idea of the chronological order of events, however, the exact order of intrusion of the different types of dyke-like bodies remains unknown.

The five types of dykes recognized are (i) coarse-grained anorthosite dominated by plagioclase, which represent



the largest percent of the dykes present; (ii) medium-grained anorthosite with acicular plagioclase laths exhibiting a trachytic-like texture; (iii) fine-grained trachytic dykes; (iv) feldspar porphyries which have a trachytic matrix; (v) and feldspar-pyroxene porphyry dykes with a trachytic matrix. From field work (iii) is known to cross cut (ii) and possibly (i).

(i) coarse-grained anorthositic bodies:

In outcrop these bodies may be red (hematitic staining), green (chloritic alteration), or dark grey to black in color (Plate 30). Sometimes one can observe ophitic textures where the outcrop surface has been weathered. Grain-size usually varies from 2-5 mm and the major component is always plagioclase laths with carbonate accounting for the remainder of the rock composition. Minor amounts of pyrite, chalcopyrite, and bornite were also observed, although infrequently. These bodies account for approximately 75-80% of the dykes in the map area and usually form as large ameboid-like bodies although one dyke of 3 metre thickness is included in this group.

In thin section these rocks typically consist of plagioclase (A 30-38; 80%), K-feldspar (10%), and penninite (5-10%) with minor amounts of opaques (1-3%) and accessory sphene, zircon, rutile, and anatase. They are invariably altered to carbonate and this alteration can vary from less



than 5% to in excess of 75-80% of the thin section. Where carbonate alteration is less significant the texture is typically idiomorphic with equigranular, tabular plagioclase laths accounting for the majority of the composition (plate 31). They are frequently fractured, bent and exhibit undulatory extinction and are twinned by the albite and carlsbad laws. Sericite alteration is present in variable amounts. K-feldspar occurs as subhedral, rectangular crystals, and are usually of similar grain size as the plagioclase. Kaolinization is present in variable amounts but is nearly always observable. Penninite occurs as irregularly shaped patches and was not seen as a pseudomorph although it is likely that it may have been an alteration product of some mafic phase, probably pyroxene. It may also occur as veinlets cutting the rock.

(ii) medium-grained anorthositic bodies:

These bodies crop out in the eastern part of the map area and have been grouped together into one pod-shaped body trending in a northerly direction. In outcrop they are buffish in color, possibly due to limonitic staining and carbonate weathering, and exhibit a brecciated texture. In thin section they consist predominantly of acicular plagioclase laths (0.5-1 mm) of  $An_{26-30}$  composition (Plate 32), with lesser amounts of tabular plagioclase (1-2 mm) and magnetite





and accessory sulphides. Hematitic staining is usually pervasive, as also is carbonate alteration (~95% of one thin section). The rocks are usually cut by numerous veinlets of carbonate, penninite, plagioclase, and opaques suggesting a complicated history of continued brecciation.

(iii) fine-grained trachytic dykes:

These bodies were seen cutting units (i) and (ii) in the field as narrow (20-50 cm), aphanitic green dykes. In thin section they consist of plagioclase (80-85%), chlorite (10-15%), and opaques (3%) with a notable absence of carbonate alteration except as veinlets cutting the rocks, but not pervasive throughout. The texture is trachytic with fine-grained plagioclase laths (0.1 mm average) arranged in a log-jam-like orientation with the chlorite and cubic magnetite infilling the interstitial voids. Although no definitive composition could be determined on the plagioclase using conventional optical methods (i.e. Michael Levy method) it is believed to be around An<sub>30</sub> as its  $N > \text{balsam}$  and the extinction angle is 13-17°.

(iv) feldspar-porphyry dykes:

Two dykes of this composition were seen in the field (late 33) where they are typically aphanitic, green rocks with 10-20% coarser phenocrysts of feldspar. In thin section they consist of subhedral to euhedral phenocrysts of K-feldspar





ranging from 2-5 mm in size set in a fine-grained matrix (<0.1 mm) consisting of plagioclase laths, penninite, and magnetite exhibiting a trachytic texture; in one section 2-3% biotite also occurred in the matrix. The matrix is typically altered to both sericite and carbonate. The phenocrysts are invariably altered to carbonate (Plate 34) but shows textures suggesting that the alteration may have originated at depth. In one thin section the phenocrysts consisted of coarse carbonate and plagioclase but the surrounding matrix was not altered and the boundary between the phenocryst and the matrix was very sharp. In other cases the outline of the phenocryst was diffuse suggesting that the alteration to carbonate was post intrusion.

(v) feldspar-pyroxene porphyry dykes:

Only two outcrops of this type of dyke were seen and they were on strike suggesting they were part of one intrusion as indicated on the map, western portion. In hand specimen the dyke consists of 15-20% phenocrysts of feldspar (1-4 mm) and 5-10% phenocrysts of a mafic phase (1-3 mm), in a fine-grained, green aphanitic matrix. In thin section one can see that the feldspar grains are euhedral to subhedral in outline and are typically altered to sericite and kaolinite. There are approximately equal amounts of K-feldspar and plagioclase (An<sub>24-26</sub>). The mafic phase is actinolite but remnant patches of pyroxene are present, probably augite (Plate 35).



The matrix is composed of plagioclase, chlorite, and magnetite, again exhibiting a trachytic texture.

#### 5.4.3 Gabbro Stock

Cutting the sedimentary sequence in the western portion of the map area is a syenitic-gabbroic stock which ranges in composition from peridotite to syenite. It was seen cross-cutting fine-grained, green aphanitic dykes in the field thus suggesting that it is the youngest lithological unit in the area. Three thin sections were examined and will be described separately.

M-104) Wehrlite to Dunite -- composed of olivine (80-85%), clinopyroxene (3-4%), biotite (2-3%), plagioclase (5-10%) and magnetite (1-2%). The rock consists predominantly of olivine (0.5-1 mm), iron rich fayalite ( $Zv = 40-50^0$ ) variety, which has altered to serpentine. The pyroxene is augitic and is anhedral to subhedral in outline and is typically finer-grained than the olivine. Large flakes of biotite (2-3 mm) occur and exhibit a cumulate texture. It is iron rich (i.e. deep reddish orange color) and is commonly being replaced by magnetite selvages. The plagioclase,  $An_{36-40}$ , is also of cumulate origin and is very fresh with little alteration present. Magnetite may occur as single cubes, veinlets cutting olivine and serpentine, as selvages in the biotite, or as rims bordering olivine grains.





(M-110) Gabbonorite -- composed of plagioclase (40-50%), hypersthene (25-30%), augite (25%), biotite (1-2%), olivine (1%), magnetite and accessory chlorite, rutile, and zircon. The texture is hypidiomorphic ophitic with the mafic minerals all being anhedral and badly corroded, the grain size averages 0.5-1.5 mm. The plagioclase is typically euhedral, is around An<sub>40</sub> in composition and is unaltered. Twinning occurs by the albite, carlsbad, and pericline laws. Hypersthene is distinctly pleochroic from green to red and has straight extinction, it is not uncommon for it to be partially altered to either biotite or chlorite around its margins. Augite, commonly twinned, is also altered along its margin and is usually more corroded than is hypersthene, it may also occur as coarse crystals up to 2-2.5 mm in size and frequently envelops plagioclase laths. Biotite occurs as an alteration product of pyroxene with no primary phases seen.

M-111 Quartz Monzonite:

Composed of quartz (15-20%), K-feldspar (40%), plagioclase (40% to 45%), penninite (2-3%), minor magnetite and accessory zircon. The texture is hypidiomorphic granular with the grain size about 1 mm. Quartz occurs as anhedral, ameboid shaped grains free of inclusions and does not exhibit undulatory extinction. Plagioclase, averaging An<sub>30</sub> composition, is typically subhedral and is altered (5-10%) to sericite. Orthoclase occurs as anhedral to subhedral grains and is





unaltered. The only mafic phase is penninite which is characterized by containing numerous inclusions of zircon surrounded by pleochroic haloes.

#### 5.5 Uranium Mineralization

Uranium mineralization at the Moran Lake 'B' Zone is confined mainly to coarse grained anorthositic dykes (type i) and medium grained anorthositic dykes (type ii), and feldspar porphyry dykes (type iv). Uranium mineralization was found within the sediments adjacent to the dykes, but also in areas where no dykes were observed. In the latter case this may indicate the presence of dykes immediately below the surface.

Uranium mineralization is predominantly encountered in type (i) dykes where carbonate and hematitic alteration are most abundant. This was confirmed from radioluxograph studies which show that the uranium mineralization corresponds to these parts of the sample containing hematitic alteration (Plates 36 and 37), and also where veinlets cut the rock and have caused alteration due to the subsequent passage of ore fluids. Where mineralization is found within sediments, it is confined to fractures where chloritic, hematitic, and carbonate alteration are most intense. Staining of the carbonate phase found in both the dykes and sediments indicated the presence of dolomite, ferroan dolomite, ankerite, white calcite and red calcite. There was no consistency noted as to



the occurrence of any particular type of carbonate.

A radiometric survey (Figure 64) was attempted in the map area but the results were disappointing and no correlation could be made with the geology. The reason for the failure could possibly be attributed to the amount of overburden in the area which is further covered by a layer of damp moss. Ellingwood (1958) also reported little success in a similar type survey even where the interval spacing was cut to ten metres and then two metres.

From thin-section studies one can see that the uranium phase is commonly associated with large euhedral sphene crystals (Plate 38) up to 0.5-1 mm in size and exhibiting strong pleochroism. From qualitative electron microprobe studies and reflected-light studies it was noted that uranium mineralization was also associated with anatase and rutile. Also noted was that the plagioclase associated with these parts of the rock containing uranium mineralization were commonly albitic in composition (with either very little or no calcium content). Identification of the uranium phase indicated the uranium mineral was brannerite ( $UTiO_3$ ) (Plate 39). A chart recording of an EDA spectrum of the mineral is presented in Figure 65.

The chemical analyses of four uranium phases dated is presented in Table 19. Analysis of thorium was not attempted as a self-discriminating scintillometer had previously



Figure 64

## Radiometric Survey, Moran Lake

'B' Zone

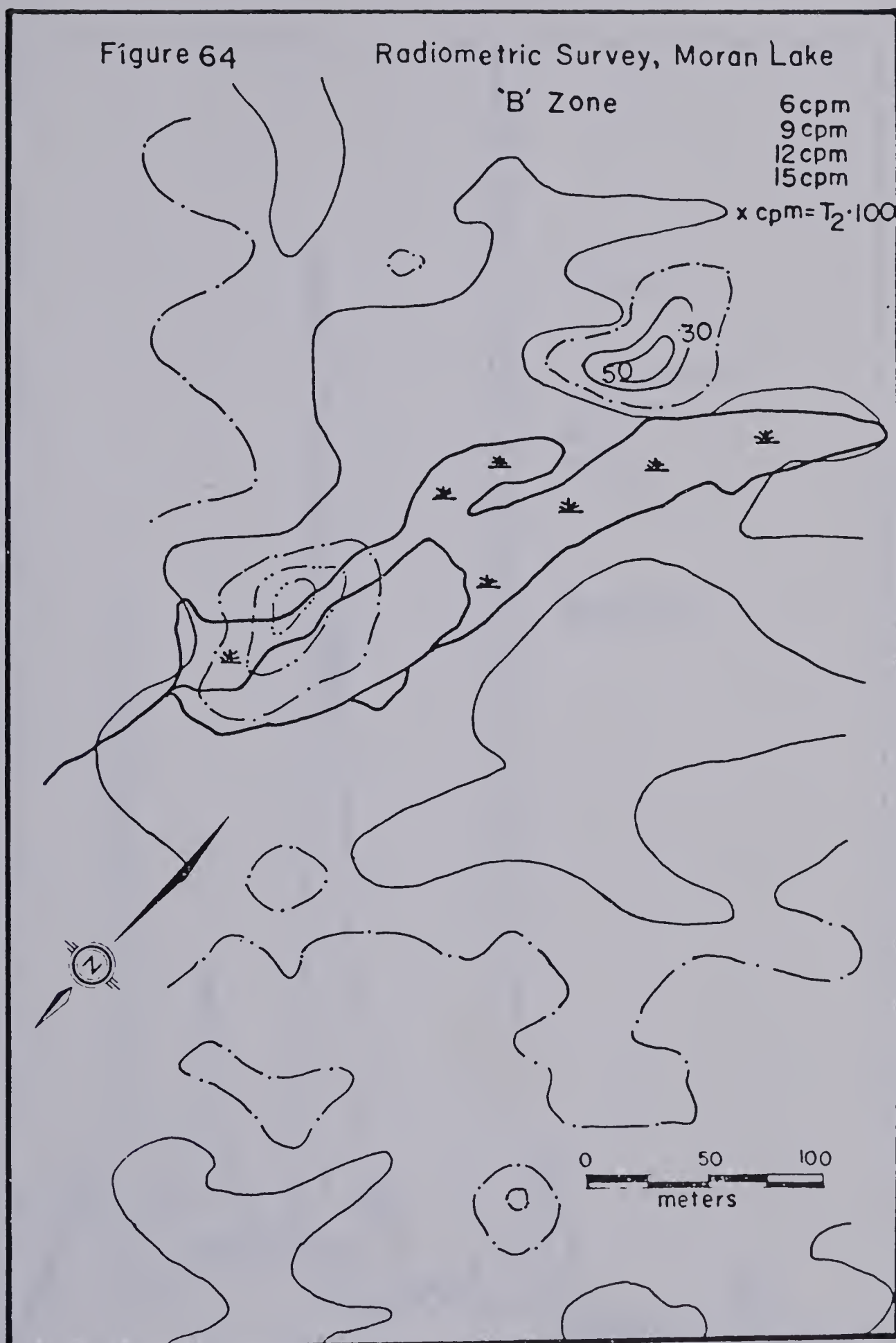
6cpm

9cpm

12cpm

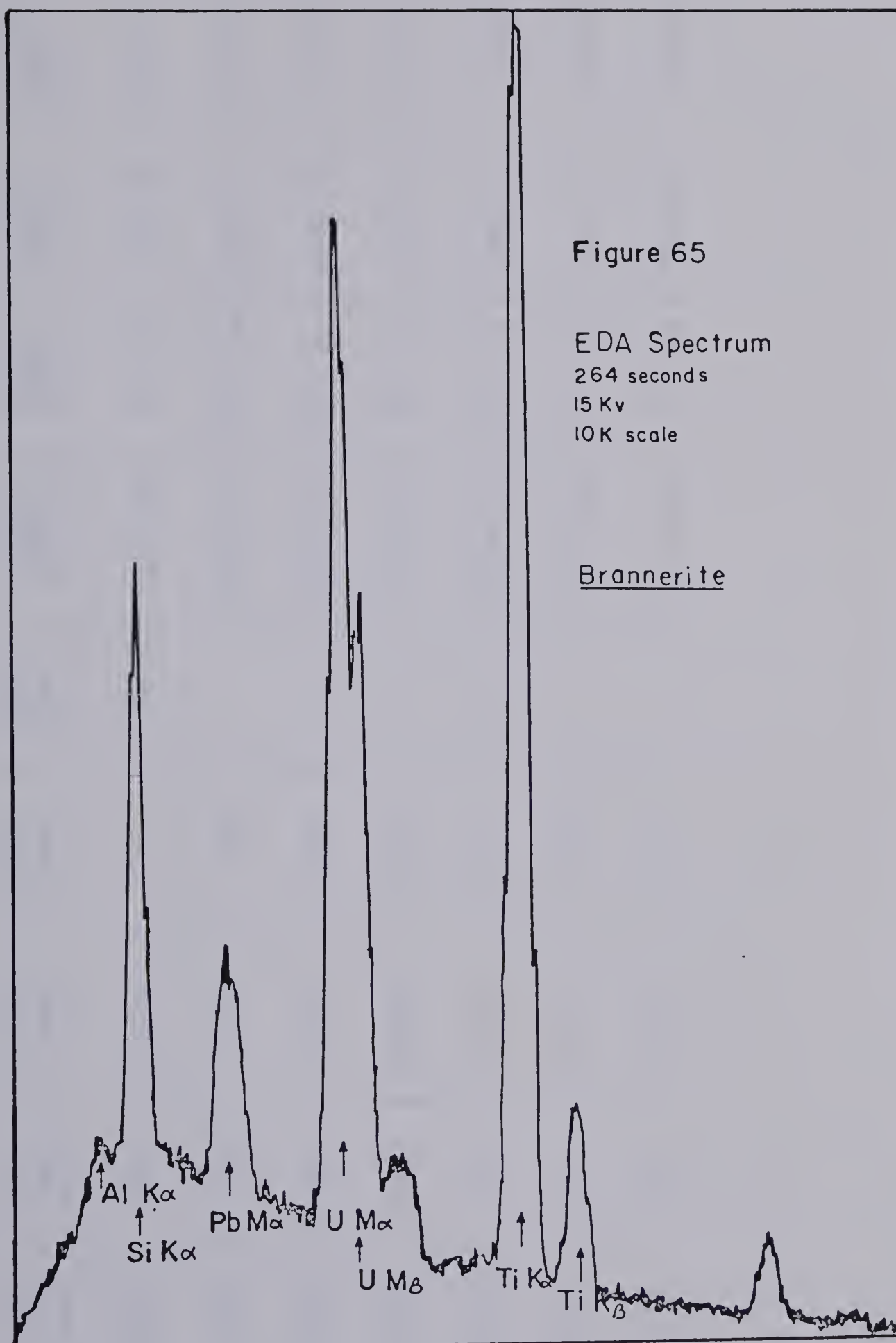
15cpm

$$x \text{ cpm} = T_2 \cdot 100$$









EDA spectrum for brannerite mineralization  
from the Moran Lake 'B' Zone uranium deposit





TABLE 19

## Uranium-Lead Data, Moran Lake

|       | $\frac{238\text{U}}{\text{ppm}}$ | $\frac{235\text{U}}{\text{ppm}}$ | $\frac{206\text{Pb}}{\text{ppm}}$ | $\frac{207\text{Pb}}{\text{ppm}}$ | $\frac{208\text{Pb}}{\text{ppm}}$ | $\frac{207\text{Pb}}{206\text{Pb}}$ | $\frac{206\text{Pb}}{238\text{Pb}}$ | $\frac{207\text{Pb}}{235\text{U}}$ | $\frac{206\text{Pb}}{238\text{U}}$ |
|-------|----------------------------------|----------------------------------|-----------------------------------|-----------------------------------|-----------------------------------|-------------------------------------|-------------------------------------|------------------------------------|------------------------------------|
| M-86e | 37059                            | 265                              | 4234                              | 391                               | .01                               | 1470 Ma                             | 799 Ma                              | 998 Ma                             | 0.132                              |
| M-896 | 6240                             | 45                               | 1596                              | 154                               | -                                 | 1550 Ma                             | 1669 Ma                             | 1615 Ma                            | 0.2955                             |
| M-87  | 133107                           | 953                              | 21993                             | 2132                              | -                                 | 1560 Ma                             | 1126 Ma                             | 1283 Ma                            | 0.1909                             |
| M-30  | 418364                           | 2996                             | 54083                             | 5297                              | -                                 | 1580 Ma                             | 897 Ma                              | 1118 Ma                            | 0.1494                             |
| M-48  | 70826                            | 507                              | 13032                             | 1350                              | 3                                 | 1650 Ma                             | 1243 Ma                             | 1402 Ma                            | 0.2126                             |
| M-61  | 447694                           | 3206                             | 81741                             | 7773                              | -                                 | 1520 Ma                             | 1234 Ma                             | 1343 Ma                            | 0.2109                             |
| M-120 | 374846                           | 2684                             | 99005                             | 10615                             | -                                 | 1740 Ma                             | 1758 Ma                             | 1752 Ma                            | 0.3136                             |



indicated that the radioactivity was due to uranium only and that thorium was absent or only present in trace amounts. Ratios of  $^{208}\text{Pb}/^{204}\text{Pb}$  also indicated that thorium was absent, with ratios typical of normal lead ( $\sim 35$ ), and the low  $^{208}\text{Pb}$  content confirms the absence of thorium. The analyses indicate a high uranium content for three of the four samples (40% versus 7%), this is reasonable for brannerite which may contain 26.5-43.6% U (Hounslow, 1976), except for sample M-48. In this latter case leaching of the uranium during weathering may have resulted in uranium loss.

Uranium mineralization in the Moran Lake "B" Zone is mainly found in anorthositic dykes displaying the following characteristics;

- 1) high content of accessory titanium minerals sphene, anatase and rutile;
- 2) associated with dykes which have undergone brecciation and subsequent alteration by ore forming fluids;
- 3) hematitic alteration;
- 4) carbonate alteration;
- 5) chloritic alteration.

Where mineralization is found in sediments, similar alteration is developed and it is assumed that the ore fluids have originated in the adjacent dykes.

Associated mineralization includes minor amounts of the sulphides pyrite, chalcopyrite, bornite, covellite



and chalcocite. It should be noted that some yellow, secondary uranium stains were observed where uranium mineralization was found.

## 5.6 Uranium - Lead Dating

Four samples were selected for dating from the 'B' Zone at Moran Lake and the results are presented in Table 19 and plotted on a concordia diagram in Figure 66. The  $^{207}\text{Pb}/^{206}\text{Pb}$  ages range from 1520-1740 Ma with the latter age being fairly concordant. On the concordia plot they define a linear trend suggesting an age of 1700-1750 Ma for the mineralization with subsequent lead diffusion from the samples. The negligible  $^{208}\text{Pb}$  contents indicate the absence of any thorium, as mentioned previously, thus precluding a magmatic source for the uranium but implying instead a past history of remobilization. A  $^{207}\text{Pb}/^{204}\text{Pb}$  versus  $^{206}\text{Pb}/^{204}\text{Pb}$  plot (Figure 67) indicates an age of 1785 Ma suggesting a simple, single mineralizing event for the 'B' Zone.

Although the age appears reasonable and the high uranium content of the samples and precision of the analyses would verify the results, the age of mineralization conflicts with the assumed age of the host rocks. The anorthositic dykes containing the mineralization cut the Paleohelikian Heggart Lake Formation (Smyth et al., 1975) which would





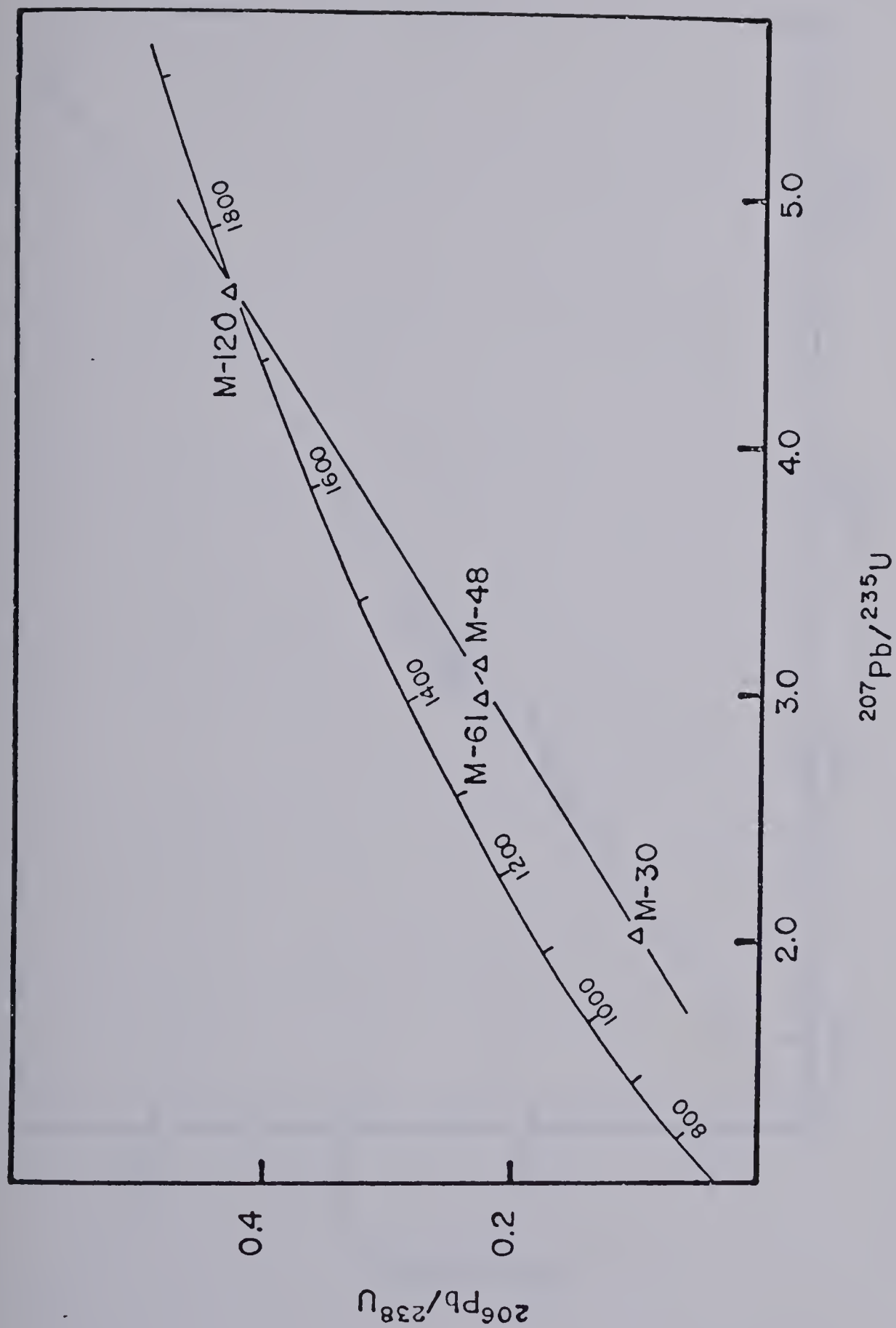


Figure 66

Concordia diagram for U-Pb data from the Moran Lake  
'B' Zone uranium deposit



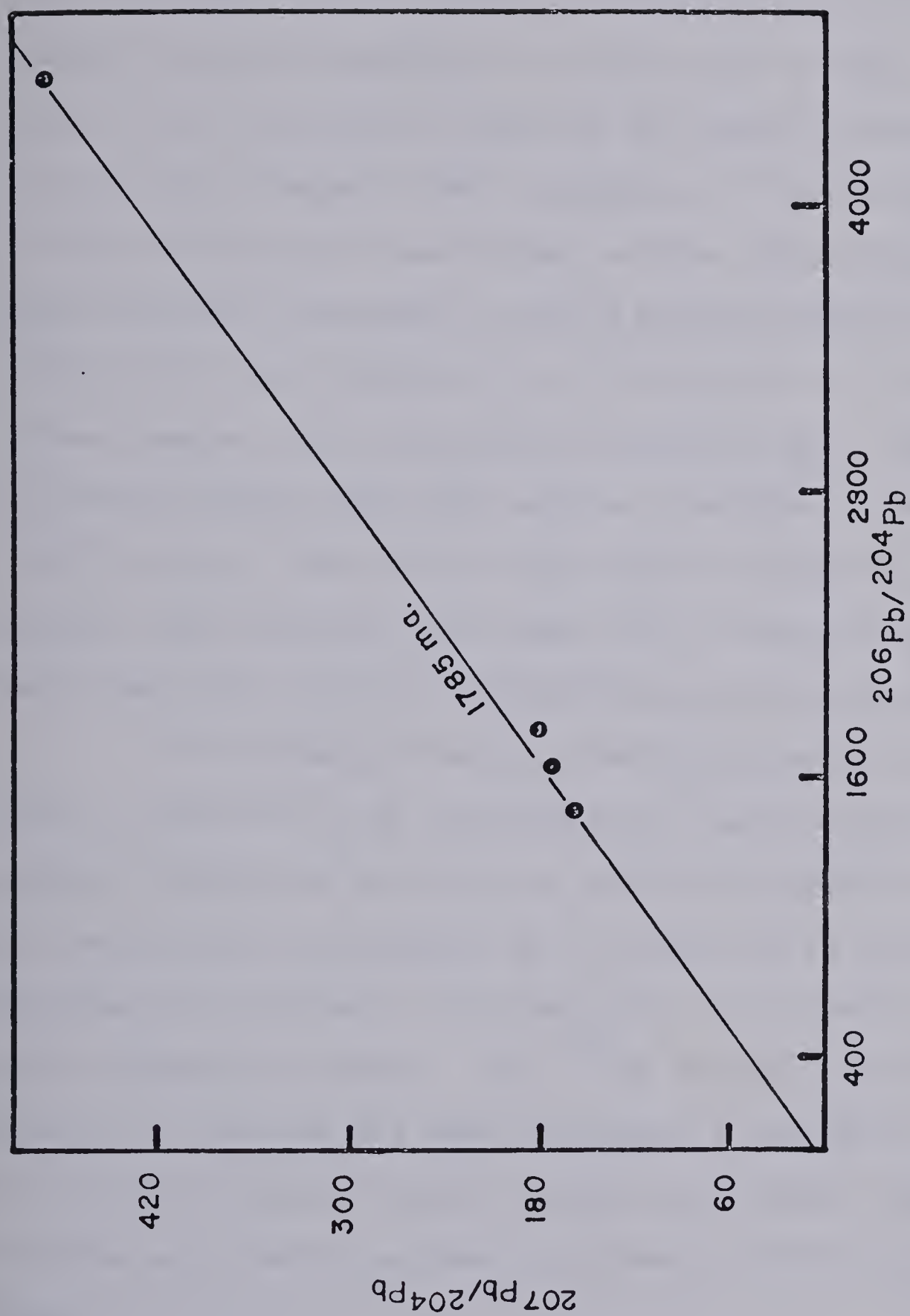


Figure 67

$^{207}\text{Pb}/^{204}\text{Pb}$  versus  $^{206}\text{Pb}/^{204}\text{Pb}$  plot for U-Pb data from the Moran Lake 'B' Zone uranium deposit



have a maximum age of ~1650 Ma according to Stockwell (1964). However, the only geologic criteria used for this classification is the unconformity between the Aphebian Moran Group and the overlying Heggart Lake sediments. If the Moran Group is a time stratigraphic equivalent to the lower Aillik Group which contains epigenetic uranium mineralization dated at 1750-1770 Ma (see Chapter 6) at Kitts, and is cut by the Long Island Gneiss dated at 1840 Ma (Gandhi et al., 1969), then the Moran Group could very well be overlain by sediments of ~1750 Ma age. Thus, if an older age is assigned to the Heggart Lake Formation then the age of mineralization at the Moran Lake 'B' Zone of 1700-1750 Ma is reasonable.

In summary, the age of mineralization at the 'B' Zone is believed to be 1700-1750 Ma, based upon four uranium samples dated (one of which is nearly concordant). This age is geologically reasonable if an older age is assigned to the Paleohelikian Heggart Lake Formation which hosts the mineralized anorthositic dykes. Low  $^{208}\text{Pb}$  contents indicate the absence of thorium and thus precludes a magmatic source for the uranium mineralization, suggesting instead that the uranium was remobilized and incorporated in the ascending dykes.

## 5.7 Discussion and Interpretation

The association of uranium mineralization with



mafic dykes is not a common phenomenon and usually one associates it with the more felsic phases of igneous rocks (Larsen et al., 1955; Boshe et al., 1974) although Page (1960 in Beck, 1970) has compiled a considerable amount of evidence to show that, to the contrary, pitchblende deposits may in fact be related to basic igneous rocks. However, in many cases the association of uranium mineralization with mafic igneous rocks does not necessarily imply that the source of the uranium was the parent magma. For example, lamprophyre dykes cutting granite or meta-gneiss at Theano Point, Ontario (Working Group Report No. 4, 1970) are believed to have remobilized earlier uranium concentrated in the felsic rocks they cut; lamprophyre dykes cutting Helikian arkoses at Baker Lake (Miller and LeCheminant, 1978) are believed to have remobilized Ag-Cu-U mineralization from the host sedimentary rock; diabase dykes in the Athabasca region contain uranium mineralization (Beck, 1970); and mafic dykes (porphyritic basalt) are described by Piche (1955) cutting felsic volcanics of the Bruce River Group at Madsen Lake; in this latter case assays indicated 0.44-2.01%  $U_3O_8$ , probably remobilized out of the volcanics. In all of the cases cited above the uranium was probably remobilized out of host rocks. The same mechanism is thus envisaged for the Moran Lake 'B' Zone.

Uranium mineralization in the 'B' Zone is believed to have been remobilized out of the Moran Group metasediments





at depth and incorporated in the ascending magma. Since the Moran Group is probably a correlative of the lower Aphebian Aillik Group, a sequence known to contain numerous uraniferous occurrences, it is quite likely that it also contains uranium. Not only did the ascending magma incorporate uranium but it may very well have assimilated dolomitic material which forms thin beds within the lower part of the Moran Group (Smyth et al., 1975), thus explaining the abundant carbonate alteration. The lack of thorium in the deposit would favour a remobilized origin for the mineralization rather than magmatic, although one should not rule out the possibility of a component being contributed by the Heggart Lake sediments also. The presence of a carbonate component may suggest that uranium might have been transported as a uranylcarbonate complex even at these elevated temperatures although contrary to the work of Rich et al. (1977), Kimberley (1978), and Romberger (1978), but in accordance with Poty et al. (1974) and Poty (1977).

The relationship between the various types of dyke-like bodies and the differentiated stock remains vague. Whether all these bodies are genetically related or represent several independent phases of intrusion remains to be solved although it is likely that they are part of a single event with perhaps the small stock representing a younger period of intrusion (Elsonian ?). What is of more concern to this



study is why some dykes contain mineralization and others are barren. The only consistent correlation between uranium mineralization and the type of rock hosting it is that the dyke is typically coarse-grained, and contains a high accessory content of sphene, with which the brannerite is associated.

Although the age obtained on the mineralization, ~1750 Ma, is somewhat higher than expected, it may be geologically feasible as discussed earlier. Perhaps dating of the sphene by the U-Pb method would solve this apparent discordancy. However, at present the age is believed to reflect the true time of mineralization.

In summary, uranium mineralization at the Moran Lake 'B' Zone is found within anorthositic dykes, part of a small dyke swarm found south of Moran Lake, characterized by their coarse-grained, brecciated nature, carbonate and hematite alteration and high accessory content of sphene. Low thorium contents, or its virtual absence, suggests that the source of the uranium was not magmatic but instead implies that it was probably remobilized out of a previous host. Uranium is believed to have been originally concentrated in metapelites and metacarbonates of the Moran Group before being remobilized and incorporated into ascending magmas. The age of this event has been dated at ~1750 Ma. It should be noted that native gold is sometimes associated with brannerite minerali-





zation (Steacy and Kaiman, 1978), however, the writer is not aware of the identification of gold in the 'B' Zone or even if it has been assayed.

#### 5.8 Moran Lake 'C' Zone: Introduction and Previous Work

Uranium mineralization at the Moran Lake 'C' Zone was found by the prospectors A. Montague and L. Montague in 1957 (Corriveau, 1958). Subsequently, the area was held by Mokta Ltd. (Bernazeaud, 1965) and then by Commodore Mining Ltd. who optioned it to Shell Company Ltd. in 1976. At present the area is still under investigation by Shell.

The 'C' Zone, located on the south side of Lake 202 (Figure 68), was mapped in detail during the middle of July, 1977 utilizing the grid set up by Shell, part of which was developed by Brinex and Mokta during their earlier investigations. Uranium mineralization occurs in two areas within the 'C' Zone, one hosted by brecciated Moran Group mafic volcanics on the north shore of Lake 202 and the second hosted by a volcanic breccia, part of the Heggart Lake Formation, located just to the south of the Lake. The latter Zone is more important and was the focus of the study in the 'C' Zone, however, the other was studied but only in a cursory fashion and shall be discussed as such.

Previous work in the area is included in the reports of Corriveau (1958), Ellingwood (1958), Bernazeaud (1965), and















Figure 68

Local Geology of the Moran Lake 'C' Zone Uranium Showing

Intrusive Rocks

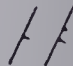


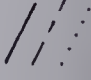


 Gabbroic dykes

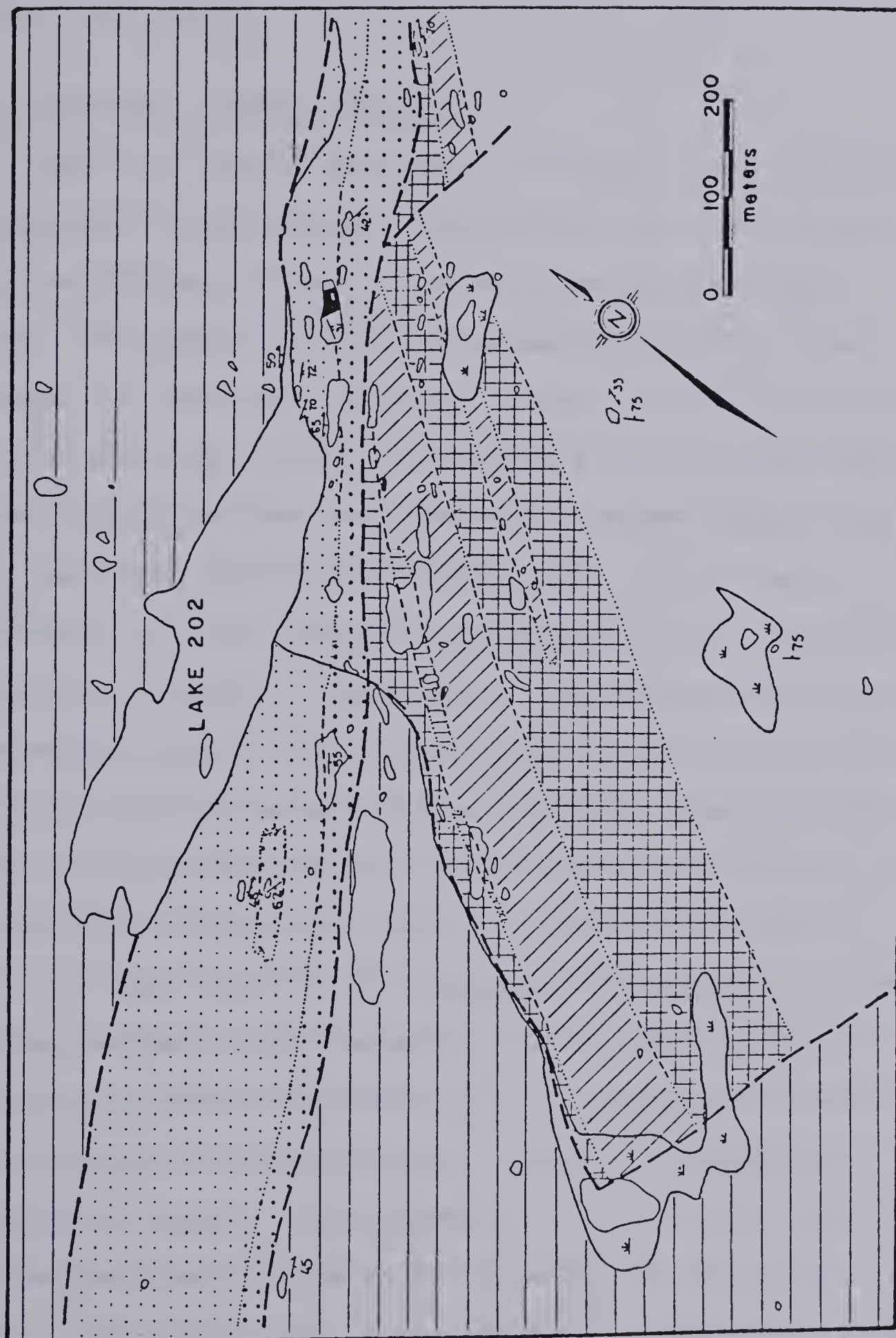
Bruce River Group (Heggart Lake Formation)

-  Polymictic conglomerate with intercalated, red-brown feldspathic sandstone lenses.
-  Green mafic volcanics
-  Volcanic breccia
-  Red, highly indurated intermediate volcanics
-  Green mafic volcanics (sheared towards the base)
-  Oligomictic (intraformational) and polymictic conglomerates
-  Red-brown arkose, mudstones and siltstones

Moran Lake Group

 Mafic volcanic rocks (massive and pillowed)

- Bedding (tops known, tops unknown) . . . . . 
- Cleavage . . . . . 
- Fault . . . . . 
- Geological contact (defined, approximate, assumed) . 
- Outcrop . . . . . 
- Swamp . . . . . 





Smyth and Ryan (1977).

### 5.9 Local Geology of the 'C' Zone

The 'C' Zone is underlain by Heggart Lake Formation sedimentary and volcanic rocks, bounded to the north and west by upfaulted blocks of Moran Group mafic volcanic rocks, Figure 68. The Aphebian Moran Group mafic volcanics, the oldest rocks in the area, are olive green, massive to pillowed volcanics (Plate 40). They are typically void of any fabric except where faulting has occurred and in these places, such as along the north shore of Lake 202, they are intensely sheared and brecciated and have subsequently been veined by red and white carbonate. Staining of the carbonate has shown it to be mostly calcite with minor ankerite and ferroan dolomite, this is associated with minor sulphide mineralization. The sliver of volcanics in the western portion of the map area forms a prominent ridge and another is developed north of Lake 202. In thin section the volcanics consist of pyroxene (10%), plagioclase (1-2%) and minor olivine set in a fine-grained matrix composed predominantly of plagioclase laths (50%) and chlorite (50%) with minor amounts of magnetite. The pyroxene is augite and is anhedral in shape with corroded borders and is usually altered to chlorite and magnetite. The rock is typically massive but may be brecciated and veined by calcite in sections examined from specimens proximal to





shears.

Near the south shore of Lake 202 the Heggart Lake Formation consists of weakly cleaved, reddish-brown, medium-grained, feldspathic quartzites and arkoses, which form a lengthy unit trending northeast-southwest across the map area. The sediments may vary somewhat and outcrops of white quartzite and red, siliceous mudstones were also seen locally. Typically the sediments are void of sedimentary structures but occasionally small-scale cross bedding and scour and fill structures were observed indicating tops to the south. Generally, the attitude of the beds was  $060^{\circ}/50^{\circ}\text{S}$  but this steepened in the direction of the fault contact with the Moran Group volcanics. Coinciding with this was the development of a cleavage thus suggesting that it is related to faulting. It was not uncommon to find conglomeratic bands within this unit and a relatively thick lens (25-30 metres) of conglomerate is found in the western portion of the map area. It consists predominantly of sedimentary clasts, probably derived from the underlying sediments, which are angular to subrounded in shape and flattened in the plane of bedding in an imbricate-like manner. They are from 2-12 cm in size and vary in composition from red siliceous mudstones, red quartzose sandstones, arkoses and fine-grained feldspathic siltstones with a few clasts of granite and rhyolite, all set in a matrix of coarse arkosic sandstone.





Overlying this unit is a conglomeratic horizon which consists of two different types of conglomerate. Immediately above the medium-grained sandstones is an oligomictic conglomerate (Plate 41) similar to the one just described. It consists of sedimentary clasts generally of rectangular shape with the majority between 6-8 cm in size and arranged in an imbricate-like fashion. As above, the clasts probably originated from the underlying sediments as they are of the same lithology (i.e. red brown sandstones, arkoses, siliceous mudstones and siltstones). The matrix, approximately 10-20% of the volume, is coarse-grained feldspathic sandstone with a high quartz content. This unit is approximately 3 metres thick and is overlain by a polymictic conglomerate. This conglomerate contrasts to the underlying one in that its source area is of regional, as opposed to local, provenance. It consists of subrounded to elliptical-shaped clasts, generally 25-30 cm by 10 cm in size, composed of quartzite, rhyolite, quartz-porphyry, andesite, granite, gneiss, red sandstones of fine to medium-grain size, and conglomerates, set in a matrix (10%) of arkose and small clasts, 1-5 cm in size and of similar composition as the coarse ones. This conglomerate contains a weakly penetrative cleavage which becomes more prominent towards the south where it is in contact with the overlying unit. This is attributed to a northeast-southwest trending fault which traverses the map area.



Overlying the polymictic conglomerate south of the east-west trending fault is a unit composed of intermediate volcanic rocks with intercalated lenses of tuff and lithic tuff. This unit has previously been mapped as an explosive breccia by Smyth and Ryan (1977), a volcanic breccia by both Ellingwood (1958) and Corriveau (1958), and a dolomitized sandstone by Bernazeaud (1965). The unit trends northeast-southwest across the map area and is fault-bounded to both the east and west with some displacement of the unit occurring in the eastern portion of the map area along an east-west trending fault. In outcrop the unit consists of three different lithologies, the most prominent being a pyroclastic unit.

The pyroclastic unit is typically buff to yellowish brown in color on weathered surfaces (approximately 0.5 cm thick) with variable amounts of fragmental material (0-50%) of 0.25-4 cm size with the majority <1 cm (Plate 42). These clasts, being more resistive to weathering, stand out above the weathered surface producing a very distinctive texture. The alignment of the clasts varies from  $50^{\circ}$  to near vertical, the steepness of this dip is what led Smyth and Ryan (1977) to their interpretation of the unit as an explosive breccia or diatrema (Smyth, personal communication). On an unweathered or fresh surface the rock shows white to pink fragments in a dark gray, blue or purplish matrix. The fragments are





usually lenticular in shape and are parallel, this has been interpreted to represent bedding (Plate 43). The rocks reacted only slightly with dilute HCl acid suggesting dolomite rather than calcite as the carbonate component. Staining of the samples with a carbonate solution (Evamy, 1963) indicates ankerite and ferroan dolomite to be more specific. The alteration is usually restricted to the matrix though, with the fragments not reacting with the staining solution except where they have been fractured and infilled by the matrix.

It was not possible to differentiate between the different pyroclastic units in the field, however, they do change their character over very short distances and in one cut specimen four distinct lithologies could be distinguished over a 5 cm length thus suggesting rapid vertical changes in the lithologies. In thin section the rocks showed remarkable similarity to one another consisting of tuffaceous size (1/16 -2 mm; Fischer, 1961) angular fragments embedded in a matrix of carbonate, plagioclase, feldspar and minor magnetite-chlorite which appears to flow around the fragments (Plate 44). The fragments have discrete boundaries and are straight rather than corroded, they frequently show invasion of the matrix along fractures. There are two types of fragments composed of either carbonate and plagioclase in varying proportions from pure carbonate to pure plagioclase or quartz, carbonate, plagioclase, K-feldspar, and magnetite. The former





type is the most common accounting for >95% of the fragments seen. In the first type the carbonate varies from 0.5-2 cm in size with the larger grains showing twin planes; the plagioclase, 0.1-0.5 mm, occurs in two forms, either as accicular laths or tabular crystals and are andesine in composition, only a few measurements could be made to determine their composition due to the absence of albite twinning. Their textures (i.e. swallow tail, rosettes, feathery, etc., Plate 45) are similar to quench textures described by Gelinas and Brooks (1974), and Pearce and Donaldson (1975) for submarine basalts. Ryan (1977) reports similar textures for mafic volcanics from the Moran Group known to underlie the area. Some of the fragments contain plagioclase (0.5-2 mm) which shows an equigranular, hypidiomorphic texture more characteristic of dyke rocks than volcanics. In some instances coarser plagioclase (1-2 mm) may be enveloped by a microlitic matrix of fine-grained plagioclase. Some of these fragments resemble the type (iii) dyke rock from the Moran Lake 'B' Zone.

The second, and less abundant, type of fragment is composed of rounded to subrounded quartz, K-feldspar, plagioclase, and minor magnetite with small carbonate crystals (<0.1 mm) scattered throughout. The fragments resemble siltstones and fine-grained sandstones in texture. These were probably derived from the underlying sediments described previously.



Some sections of the volcanic breccia showing little carbonate alteration resemble a fine-grained volcanic matrix (Plate 46) composed of 0.5-0.1 mm plagioclase laths of andesine composition. No mafic components (i.e. pyroxene) were noted other than veinlets of penninite.

The two other members of the volcanic unit are red and green fine-grained volcanics. In outcrop one can discern a volcanic texture in the green unit indicated by the parallel alignment of plagioclase laths, 1-3 mm in size, in a fine-grained matrix. The red unit is typically much finer-grained than this and was originally mapped as a fine-grained sediment (Kontak, 1978). However, in thin section the rock shows a finer-grained (.05-0.1 mm) pilotaxitic texture with coarser sections (plagioclase laths up to 1-1.5 mm in size); the only other components are carbonate and magnetite and in the green volcanics penninite, magnetite, and carbonate. In one section veinlets of plagioclase laths (0.1-0.3 mm) were seen cutting the rock (Plate 47) and they were also noted to cut across earlier veinlets of ankerite. The same section was stained for carbonate indicating that the carbonate in the matrix was ankerite and composed 30% of the rock.

Overlying the volcanic unit (Plate 48), is a polymictic conglomerate similar to that described earlier which shows a weakly developed fabric in some outcrops. This



contact was only uncovered in one spot where it was dipping to the south at  $50^{\circ}$ . The unit also contains red brown sandstones and siltstones of feldspathic character typically void of any sedimentary structures, similar to the lower sedimentary sequence.

Cutting the sediments and volcanics are fine-grained, green aphanitic dykes. Although typically 1-2 metres thick and trending east-west parallel to the local stratigraphy one dyke in the eastern portion of the map area was 30 metres wide and orientated vertically (Plate 49), trending northwest-southeast. The dykes have a microlitic texture in thin section with 1-5% coarser plagioclase laths of andesine composition. Other components include magnetite, carbonate and penninite either forming part of the matrix or as veinlets cutting the rock.

The local geology has been modified somewhat due to subsequent faulting. An early set of northeast trending high angle reverse faults have juxtaposed Moran Group volcanics against the Heggart Lake sediments and also cuts the local stratigraphic succession cutting out the mineralized zone to the east. However, from the regional mapping of Ellingwood (1958), displacement of the volcanic breccia unit with respect to the sandstones appears minor, the fault having rotated in a scissor-like fashion with the greatest amount of displacement occurring to the west. The early





faults are transected by a set of northwest-southeast trending normal faults which terminate the westward extension of the volcanic breccia and caused minor displacement in the east.

#### 5.10 Origin of the Volcanic Breccia

As mentioned previously the volcanic breccia had been mapped earlier and referred to by various authors as an explosive breccia or diatreme (Smyth and Ryan, 1977), a volcanic breccia (Ellingwood, 1958; Corriveau, 1958), and a dolomitized sandstone (Bernazeaud, 1965). The writer also classifies the unit as a volcanic breccia based on the following criteria: (i) the geometry of the unit (i.e. concordancy of the brecciated units intercalated with the mafic volcanics and their parallelism with the local geologic contacts); (ii) the existence, although rare, of mafic volcanics elsewhere in the Heggart Lake Formation (Smyth et al., 1975; Collins, 1958); (iii) the igneous textures (i.e. welded and flattened fragments) seen in thin section within the volcanic breccia; (iv) a sharp contact, dipping  $\sim 50^{\circ}$  towards the south, between a breccia lens and overlying conglomerate; (v) the microlitic textures seen in thin sections of unaltered parts of the volcanic breccia; and (vi) units which in thin section resemble typical andesites or basalts in texture showing flow alignment of the plagioclase laths.





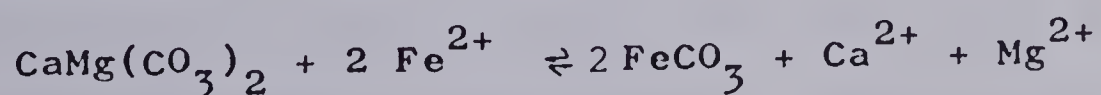
However, some of the factors may also be true if the breccia were of intrusive origin. Reinhardt (1972) describes breccia pipes controlled by faults and which have elongate outlines rather than elliptical or circular as is common for breccia pipes (Bryner, 1961). It is also common to find an igneous texture (i.e. trachytic) within the matrix of these pipes such as Reinhardt (1972) describes in the Great Slave Lake region and Shoemaker (1955) describes for diatremes in the southwestern states. However, notably lacking within the unit are the large blocks of underlying or overlying lithologies usually found within these bodies (Shoemaker, 1955) formed either as the result of the forceful injection of the body or collapse of the overlying strata as found at Garnet Ridge, Arizona (Garaschi and Kerr, 1968). Another notable difference is the size of the fragments, at Moran Lake the clasts range from 0.5 mm-4 cm as compared to tens of metres for the maximum size of blocks found within diatremes.

Thus, the evidence is interpreted to favour an extrusive origin for the breccia unit. However, this is not to rule out the possibility of finding a pipe beneath this unit. Instead, this pyroclastic unit may represent the upper part of a mature diatreme (Shoemaker, 1955) usually filled in with bedded tuff and limestone and locally with thinly laminated clay and siltstone and evaporites. Lower in the



vent these sediments give way to more massive breccia and agglomerate and ultimately to solid igneous rock. There were fragments seen in the volcanic breccia that resembled intrusive rocks, these may thus represent fragments of an underlying solid igneous body.

It is suggested then that this unit represents the upper part of a vent or pipe. The fragments it contains were derived from the underlying Moran Group volcanics and Heggart Lake sediments. A continual cycle of phreatic volcanic activity followed by a period of quiescence is envisaged as fragments similar to the breccia were seen within the unit. Extrusion was probably into a shallow water environment as suggested by the sedimentary structures in the sandstones and siltstones below the breccia and also by the pervasive carbonate alteration. The origin of the ankerite and dolomite remains vague, although it is common to associate such alteration with pipes associated with volcanic piles it is unusual to find such large quantities (i.e. up to 80-90% in some sections). Franklin et al. (1975) describe rocks from the Mattabi deposit containing 60% carbonate alteration and showed that dolomite was only developed where  $[\text{Fe}^{2+}]$  was low for temperatures around  $200^{\circ}\text{C}$ . This is defined by the following reaction:



Thin beds of dolomite outcrop as part of the Moran Group





which underlies the area, that this may have also contributed to the carbonate content of the ascending magma seems reasonable. Also it is interesting to note that Hack (1942) has suggested that much of the limestone in the Hopi Butter diatremes in Arizona is of hydrothermal origin.

The green and red volcanic members of the unit represent passive extrusion more akin to fissure-type lava flows. Perhaps these represent subaerial eruption and thus the absence of water prevented phreatic activity.

#### 5.11 Uranium Mineralization

Uranium mineralization at Moran Lake is confined to two zones, the more common occurrences being found in the volcanic breccia and the less important ones located in Moran Group volcanics. The latter were only examined in a cursory fashion with the focus of the study on the former.

Uranium mineralization in the Moran volcanics occurs on the north side of Lake 202 in intensely sheared volcanic rocks adjacent to a southeast dipping fault zone. The rocks have been invaded by white and red carbonate and accompanying sulphides (pyrite and chalco pyrite). Locally cubes of pyrite up to 3-4 mm size were seen in the carbonate veins. Radioactivity was as much as fifty times background and was attributed to uranium rather than thorium by the use of a self-discriminating scintillometer. Radioactivity was





sporadic and only occurred locally, with continuous zones recognized only along strike with the faults.

The main mineralization in the 'C' Zone occurs in a thin lens of volcanic breccia and can be traced along strike for up to 600 metres (~2000 feet). Increased radioactivity (10-15 x background) was noted on the red and green aphanitic volcanic units also but this did not approach the readings recorded on the breccia lenses. Radioactivity seemed to be higher in the lower breccia unit, for what reason is not known.

Radioluxographs (Plates 50 and 51) show that uranium mineralization occurs either at thin vein fillings orientated in numerous directions and/or as disseminated mineralization within the rock. In this latter case mineralization was usually restricted to parts of the rock characterized by either a red (hematite ?) or dark dirty brown alteration. There did not seem to be any particular pattern to this alteration and unmineralized areas were frequently seen enveloped by highly mineralized parts.

Assays reported by Corriveau (1958) on the breccia unit are listed in Table 20. The highest values obtained were 0.13%  $U_3O_8$  over distances of 24 inches and 36 inches in two localities. The best results obtained were an average of 0.11%  $U_3O_8$  over a nine foot width. He stated that the average grade for the 2000 foot long mineralized zone was



## BRITISH NEWFOUNDLAND EXPLORATION LIMITED

## SAMPLE REPORTING SHEET

267

LABRADOR  
KAIPOKOK CONCESSION - SILAS LAKE

| Sample No. | Showing  | Tr.<br>No. | Footage<br>From To |      | Spld. | U <sub>3</sub> O <sub>8</sub> | Remarks |
|------------|----------|------------|--------------------|------|-------|-------------------------------|---------|
| 901        | Mont. #2 | 1          | 8.0                | 10.5 | 2.5   | Nil                           | Breccia |
| 902        | "        | 1          | 10.5               | 12.5 | 2.0   | 0.025                         | "       |
| 903        | "        | 1          | 12.5               | 15.0 | 2.5   | 0.045                         | "       |
| 904        | "        | 2          | 3.0                | 6.0  | 3.0   | 0.065                         | "       |
| 905        | "        | 2          | 6.0                | 8.5  | 2.5   | 0.025                         | "       |
| 906        | "        | 2          | 8.5                | 11.0 | 2.5   | 0.065                         | "       |
| 907        | "        | 2          | 11.0               | 14.0 | 3.0   | 0.065                         | "       |
| 908        | "        | 3          | 2.0                | 5.0  | 3.0   | 0.045                         | "       |
| 909        | "        | 3          | 5.0                | 8.0  | 3.0   | 0.065                         | "       |
| 910        | "        | 3          | 8.0                | 11.0 | 3.0   | 0.11                          | "       |
| 911        | "        | 4          | 12.0               | 15.0 | 3.0   | 0.11                          | "       |
| 912        | "        | 4          | 15.0               | 18.0 | 3.0   | 0.09                          | "       |
| 913        | "        | 4          | 18.0               | 21.0 | 3.0   | 0.13                          | "       |
| 914        | "        | 4          | 21.0               | 24.0 | 3.0   | 0.045                         | "       |
| 915        | "        | 5          | 1.0                | 3.0  | 2.0   | 0.045                         | "       |
| 916        | "        | 5          | 3.0                | 6.0  | 3.0   | 0.065                         | "       |
| 917        | "        | 6          | 0.0                | 2.0  | 2.0   | 0.045                         | "       |
| 918        | "        | 6          | 2.0                | 4.0  | 2.0   | 0.065                         | "       |
| 919        | "        | 6          | 4.0                | 7.0  | 3.0   | 0.045                         | "       |
| 920        | "        | 7          | 4.0                | 6.0  | 2.0   | Nil                           | "       |
| 921        | "        | 7          | 6.0                | 8.0  | 2.0   | 0.065                         | "       |
| 922        | "        | 7          | 8.0                | 10.0 | 2.0   | 0.025                         | "       |
| 923        | "        | 8          | 1.0                | 4.0  | 3.0   | Nil                           | "       |
| 924        | "        | 8          | 4.0                | 6.0  | 2.0   | 0.13                          | "       |
| 925        | "        | 8          | 6.0                | 8.0  | 2.0   | Nil                           | "       |
| 926        | "        | 9          | 0.0                | 2.0  | 2.0   | Nil                           | "       |
| 927        | "        | 9          | 2.0                | 4.0  | 2.0   | 0.065                         | "       |
| 928        | "        | 9          | 4.0                | 5.5  | 1.5   | 0.025                         | "       |
| 929        | "        | 10         | 2.0                | 4.0  | 2.0   | 0.025                         | "       |
| 930        | "        | 11         | 5.0                | 8.0  | 3.0   | 0.045                         | "       |
| 931        | "        | 11         | 8.0                | 11.0 | 3.0   | 0.025                         | "       |
| 932        | "        | 11         | 11.0               | 12.0 | 1.0   | 0.045                         | "       |
| 933        | "        | 12         | 3.0                | 6.0  | 3.0   | 0.025                         | "       |
| 934        | "        | 12         | 6.0                | 9.0  | 3.0   | 0.025                         | "       |
| 935        | "        | 12         | 9.0                | 12.0 | 3.0   | 0.09                          | "       |
| 936        | "        | 1-A        | 2.0                | 5.0  | 3.0   | 0.09                          | "       |
| 937        | "        | 1-A        | 5.0                | 8.0  | 3.0   | 0.065                         | "       |
| 938        | "        | 1-A        | 8.0                | 11.0 | 3.0   | 0.045                         | "       |



0.06%. He also noted that the grade tended to fall off to both the east and the west thus concluding that ". . . the radioactive zone is dying out and most of the zone is presumably exposed." (Collins, 1958, p. 3).

Uranium geochemistry obtained from isotopic dilution analysis is presented in Table 19. The low uranium values might imply leaching of the uraniferous component and low  $^{208}\text{Pb}$  values indicate the low abundance of thorium, confirming what was assumed from the readings obtained using the scintillometer. This would thus suggest a past history during which time some process separated uranium and thorium.

Associated mineralization includes pyrite and chalcopyrite, either in carbonate veins or disseminated within the rock. The abundance of the sulphides was never noted to be very significant.

#### 5.12 Uranium-Lead Dating

Only three specimens were selected for U-Pb dating of the Moran Lake 'C' Zone uranium showing: the results are presented in Table 19 and plotted on a concordia diagram in Figure 69. The three points define a fairly good lead diffusion line which cuts the concordia curve at  $\sim 1540$  Ma, as compared to the independent  $^{207}\text{Pb}/^{206}\text{Pb}$  ages which vary from 1470-1560 Ma. This age is considered to be geologically reasonable although it is considerably younger than the time of formation





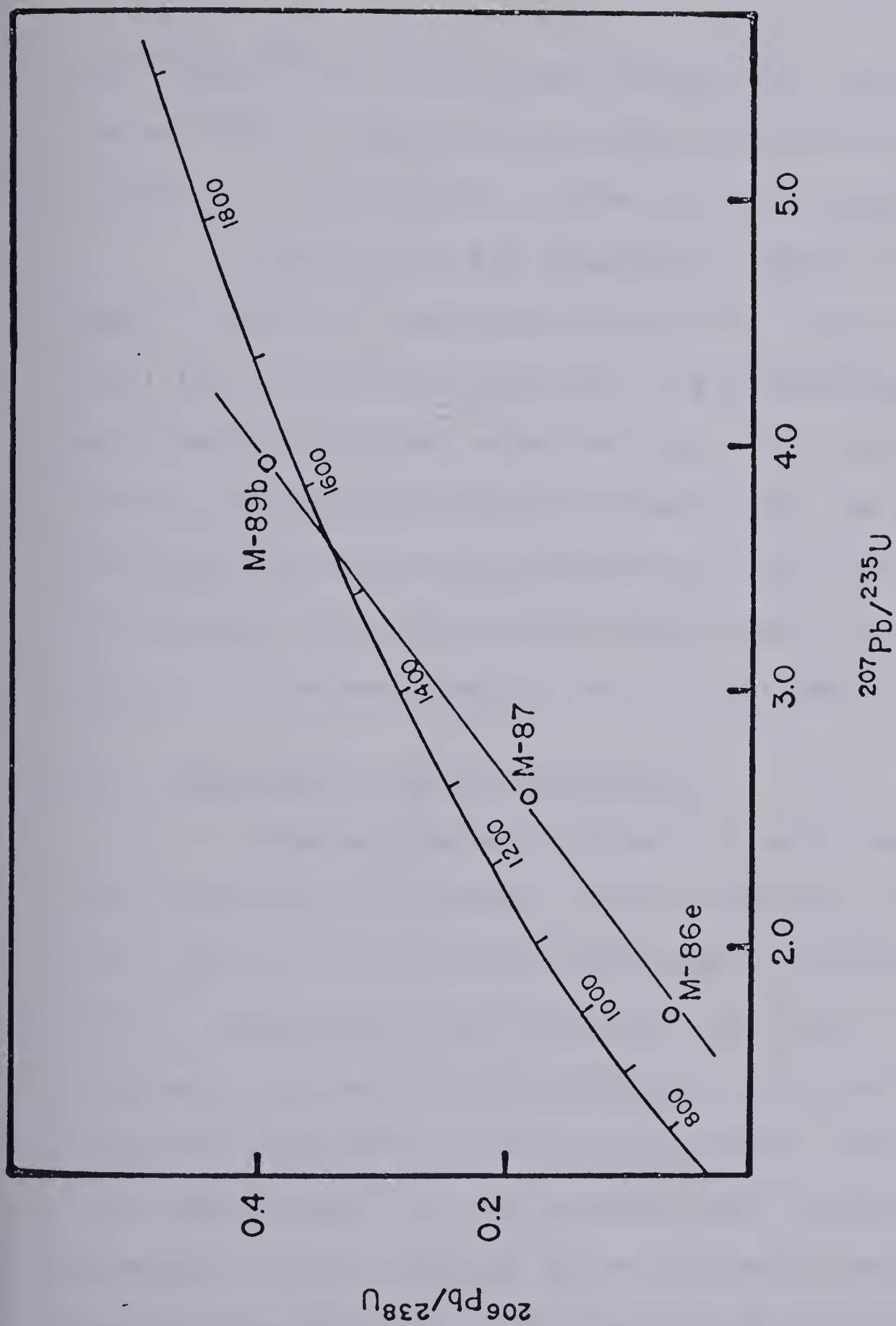


Figure 69

Concordia diagram for U-Pb data from the Moran Lake 'C' Zone uranium deposit





for the host rocks considering the results obtained on mineralization from the Moran Lake 'B' Zone. A  $^{207}\text{Pb}/^{204}\text{Pb}$  versus  $^{206}\text{Pb}/^{204}\text{Pb}$  isochron plot (Figure 70) indicates a similar age of 1590 Ma suggesting a single mineralizing event with no subsequent alteration of the isotopic system.

Although it was originally thought that the Moran Lake 'B' and 'C' Zones might be related genetically (Kontak, 1978) the results obtained from the geochronologic studies would negate any such relationship. What would be interesting, however, would be to obtain isotopic data for mineralization from the less prominent uraniferous zone north of Lake 202 in the mafic volcanics of the Moran Group to see the relationship of this mineralization to the main part of the 'C' Zone.

### 5.13 Discussion and Interpretation

Uranium mineralization in breccia horizons has long been recognized (Shoemaker, 1955; Backstrom, 1974), although very little effort has been expended to determine their origin. Gabbelman (1976) believes that most of these bodies are the result of hydraulic stoping due to ascending fluids and gases which originated in the mantle. Most breccias contain alkali basalt as the igneous phase (Shoemaker, 1955; Reinhardt, 1972) although quartz carbonate matrixes predominate in volume per cent. In the case of those which have vented, they are capped by pyroclastic units usually altered



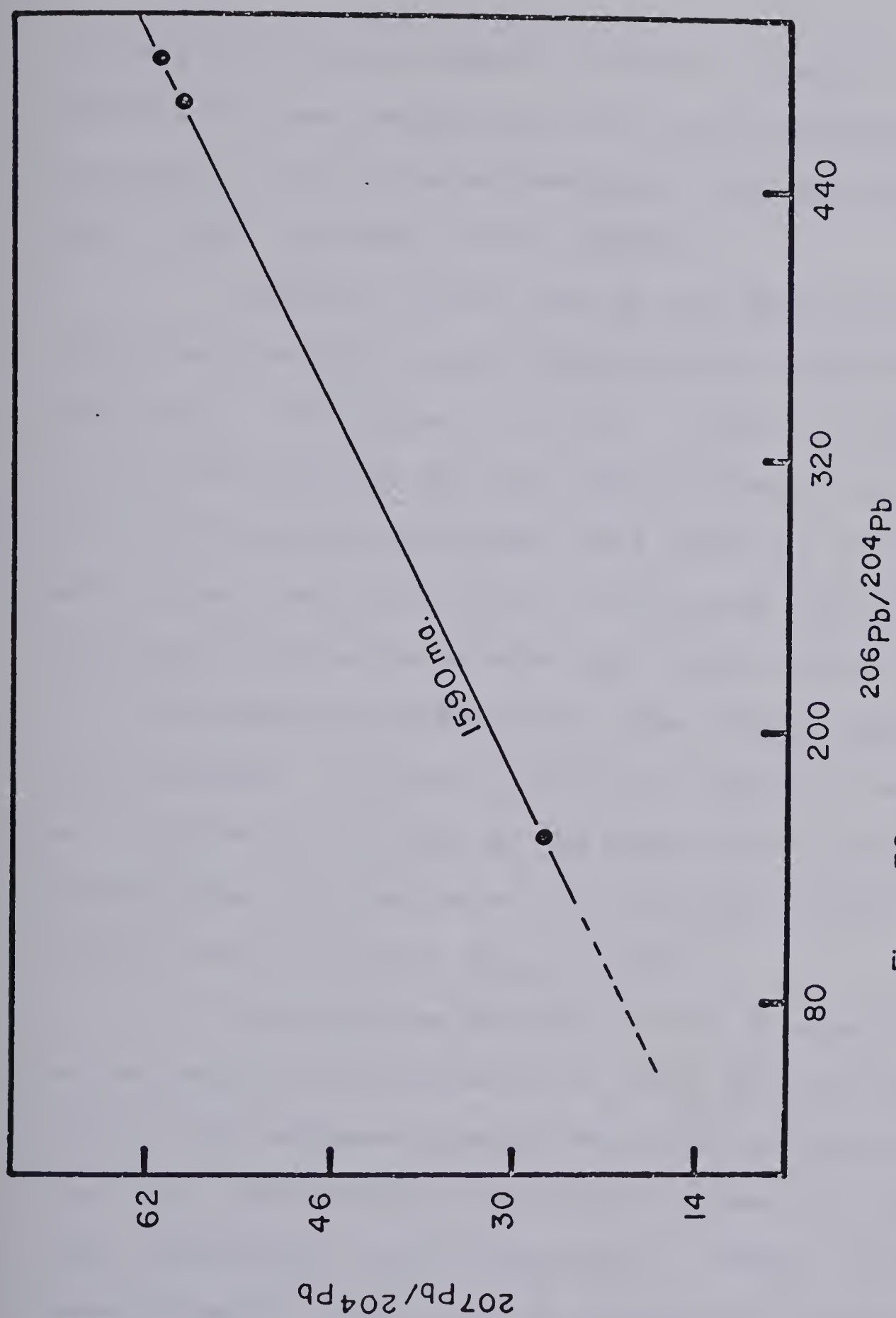


Figure 70

$^{207}\text{Pb}/^{204}\text{Pb}$  versus  $^{206}\text{Pb}/^{204}\text{Pb}$  plot for U-Pb data from the Moran Lake 'C' Zone uranium deposit



quite pervasively by quartz, carbonate, hematite and sericite; perhaps the best example of this are the stratiform breccia deposits of the Wernecke Mountains (Bell and Delaney, 1977; Bell, 1978; Laznicka, 1976a; 1976b).

However, in the case of the Moran Lake 'C' Zone, the mineralization is not believed to be related to the deposition of the volcanic breccia. Since the breccia horizon is of approximately the same stratigraphic level as the 'B' Zone the age of the volcanic unit must be  $\sim 1700$  Ma, considerably older than the  $1540$  Ma age obtained for mineralization. Instead, it is proposed that the faults located within the 'C' Zone acted as conduits for later fluids enriched in the radioelements. Volcanic activity is known to have occurred at  $1520$  Ma in the case of the Bruce River volcanics and these rocks are also known to be the host of numerous radioactive showings (Smyth et al., 1975).

Although the majority of the uranium mineralization is believed to be related to an event post dating the formation of the volcanic breccia this does not preclude the fact that some uranium mineralization may have originally been concentrated in the volcanics. Whether this type of mineralization could still be recognized by dating remains to be determined although it may have been reset isotopically by the later event at  $1540$  Ma. Mineralization in the Moran Group volcanics is probably related to this same event





although dating of the uranium would have to be undertaken to confirm this.

By using the faults in the area as conduits this requires that they are older than Grenvillian as originally proposed by Smyth et al., (1975) and Ryan (1977). They are interpreted instead to represent contemporaneous block faulting associated with the graben which developed post Moran Group deposition and which was infilled by the molasse sequence represented by the Heggart Lake Formation. However, this does not preclude the fact that later movement may have occurred along these faults associated with Grenville tectonics.

In summary, the Moran Lake 'C' Zone represents a volcanic breccia horizon, part of the Heggart Lake Formation originally classified as Paleohelikian in age (Smyth et al., 1975) but now believed to be much older (i.e. ~1700 Ma). The change from the fine-grained red sediments to massive oligomictic and then polymictic conglomerates is believed to represent instability of the area which immediately preceded the deposition of a volcanic breccia. The origin of this volcanism may be related to penecontemporaneous block faulting associated with a graben-like structure subsequently infilled by the Heggart Lake sediments, a typical molasse deposit. Later volcanism at ~1520 Ma which was associated with deposition of the Bruce River volcanics is believed to have caused



the mineralization at the 'C'Zone. Mineralized fluids derived from depth, enriched in uranium, ascended along local fault zones as in the case of the 'C'Zone mineralizing the local lithologies. Modification of the local geology may have resulted due to subsequent movement along these faults during the Grenville Orogeny.



## CHAPTER VI

### KITTS POND

#### 6.1 Introduction and Previous Work

The Kitts Pond uranium deposit is located on the south shore of Kaipokok Bay, Figure 71 within the Kitts Pond-Post Hill Belt of Aphebian volcanic-sedimentary rocks. It was discovered by Walter Kitts in 1956 (Beaven, 1958) and exploratory work since this time has delineated a deposit containing 4,056,000 lbs.  $U_3O_8$ . It is only one of several deposits within this belt of rocks with other smaller occurrences being the Inda, Gear, and Nash (Piloski, 1968).

The Kitts Pond area is included in the regional geologic reports of Kranck (1953), Douglas (1953), Gandhi et al. (1969), and Stevenson (1970). Detailed mapping of the local geology was done by Marten (1971, 1972) and at present D. Evans is studying the area as part of a Ph.D. project at Queens University. Gandhi (1976) reports one U-Pb age determination for the mineralization which gave a  $^{207}Pb/^{206}Pb$  age of 1760 Ma.

The author visited the Kitts area during the end of July, 1977 to briefly examine the local geology and to collect specimens for mineralogical and geochronological studies. No mapping of the area was undertaken and thus the geology described here is mostly the work of others, notably,,





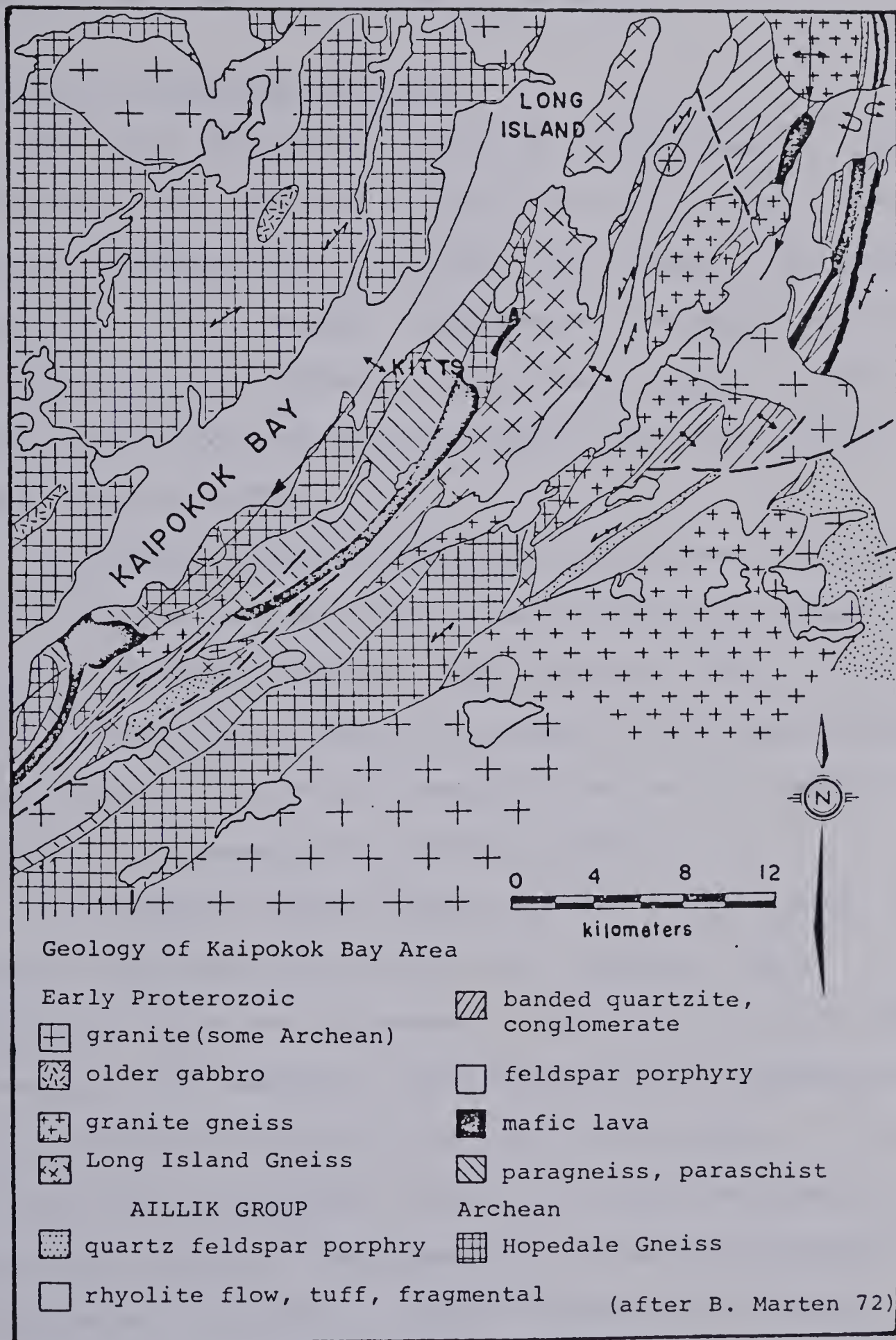


Figure 71

Regional geology of the Kitts Pond Post-hill belt





B. Marten, and will only be discussed briefly.

## 6.2 Geology of Kaipokok Bay area

The Kitts deposit is hosted by metasediments and metavolcanics of the Aphebian Aillik Group which forms a broad northeasterly trending belt along the south shore of Kaipokok Bay, Figure 71. It is bounded to the north and south by the Archean Hopedale Gneiss (Kranck, 1953; Gandhi et al., 1969) and is cut off to the east by syntectonic intrusions of Hudsonian age (Marten, 1972).

The Hopedale Gneiss represents polydeformed and reconstituted basement rocks, consisting of banded gneisses, migmatites and granites (Marten, 1971; Sutton, 1972). It formed the basement upon which the younger Aillik Group rocks were deposited with the contact modified and nearly completely obliterated during subsequent orogenic events.

The Aphebian Aillik Group consists of five main lithologies in the Kitts-Post Hill Belt, however, their stratigraphical order and thickness is difficult to ascertain because many of the boundaries have been modified tectonically and way up evidence is lacking (Marten, 1971; 1972). It is probable that mafic volcanics, often with well-developed pillow structures, forms the basal member overlain by metasediments (paragneiss), rhyolite, banded tuffaceous sediments, and conglomerate. The mafic volcanics are overlain by horizons of cherts, argillite, and tuffaceous argillite which



are associated with the uranium mineralization at Gear Lake, Inda Lake and Kitts.

Intrusive igneous rocks include prekinematic to post-kinematic suites with the majority being synkinematic. The prekinematic intrusives include the Kitts Gabbro and quartz-feldspar porphyry bodies, the latter of which intrudes the volcanics and banded tuffs. Synkinematic intrusions include the Long Island Gneiss (Gandhi et al., 1969), anatectic granites, granite and augen gneiss, pegmatites and gabbros. Post-kinematic diorite and rhyolite dykes and sheets occur cutting most of the older lithologies.

The structure of the area is quite complex. Marten (1971) recognized five periods of deformation and Clark (1971) and Sutton et al., (1971) recognized three on a more regional scale. The first two phases of deformation were developed at the basement-cover contact zone, the third represents a regional event, and structures related to the last two periods of deformation were mainly developed in schistose lithologies (i.e. metasediments).

Metamorphism of lower greenschist to amphibolite facies (Gandhi et al., 1969; Marten, 1971) occurred during  $D_1$  to  $D_3$ , with no constructive mineral growth associated with the later events (Marten, 1971; Clark, 1971). Metamorphic grade may increase adjacent to tectonic zones.





### 6.3 Local Geology of the Kitts Pond Area

The Kitts Pond area, Figure 72, is located at the contact between the basement Hopedale Gneiss and the overlying Aphebian Aillik Group. The gneiss outcrops over the eastern part of the area as banded gneiss or granodioritic phases probably representing anatectic melts. The basement-cover contact is intensely contorted and pegmatitic material frequently can be seen extending from the gneissic terrain into the metavolcanics or metasediments. The Aillik Group sequence of mafic volcanics, meta-argillites and tuffs, conglomerates and calcareous units is cut by the Kitts Gabbro, a prekinematic intrusion (Marten, 1971), sandwiched between two argillite horizons. In addition to the gabbro, dykes of diorite and quartz feldspar porphyry also cut the older lithologies. The trend of the units is generally northwest as compared to the northeasterly regional trend, the reason for this being attributed to the gabbroic intrusion.

The metapelitic unit (andalusite-garnet schist) is the most important unit locally as it hosts the uranium mineralization. It varies in hand-specimen from a black argillaceous rock to a biotite-garnet schist or less frequently a biotite-andalusite-garnet schist. It may contain up to 20-25% pyrite and pyrrhotite with minor calcopyrite forming thin (1-2 mm thickness) bands suggesting a syngenetic origin for these sulphides. The unit typically displays a fabric and












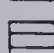
Figure 72

Local Geology of the Kitts Deposit (after Marten, 1972)

Intrusive Rocks


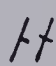




-  Gabbroic stock
-  Diorite
-  Quartz porphyry

Lower Aillik Group

-  Banded quartzite-magnetite iron formation
-  Black andalusite-garnet schist, amphibolitic "argillite"
-  Mafic pillow lava

Hopedale Complex

-  Banded gneiss and granodiorite

- Geological boundary (defined, approximate, assumed) . 
- Bedding (tops unknown; inclined, vertical) . . . . . 
- Gneissic banding . . . . . 
- Schistosity . . . . . 
- Tectonic slide . . . . . 
- Swamp . . . . . 





it is not uncommon to find this refolded into isoclinal folds plunging steeply to the south. In some specimens possible fragmental material of 1-5 mm size was seen, perhaps indicating a volcanogenic component. In thin section the unit consists of a granoblastic polygonal network of quartz and feldspar with biotite, garnet, amphibole, andalusite, chlorite, epidote, magnetite, sulphides, and carbonaceous material composing the rest of the rock. The modal contents vary depending on the specimen examined but biotite is ubiquitous in all sections with amphibole nearly always present. Where mineralization is finely disseminated throughout pleochroic haloes can be seen in the mafic minerals.

For a more detailed description of the geology the reader is referred to the publications cited which very adequately describe the individual lithologies of the area.

#### 6.4 Uranium Mineralization

Uranium mineralization at Kitts is mainly confined to the metapelitic unit, although mineralization is also found in the metavolcanic unit, in the Kitts Gabbro, the diorite dykes, and in quartz feldspar dykes. In the latter cases mineralization is usually restricted to the contact areas, where intense red, hematitic alteration is developed thus suggesting remobilization of preexisting uranium mineralization during the intrusion of the igneous bodies.





The main uranium phase, identified as pitchblende, occurs in two forms within the metapelitic unit. It occurs as coarse veinlets several centimetres in diameter, cutting across the local schistosity of the metapeletic host rock. The pitchblende is either fine- or coarse-grained, shows variable reflectivity, and the abundance of other minerals (i.e. pyrite, pyrrhotite, carbonate) is usually less than 3-5%. This type of mineralization is typical of the high-grade zones of the deposit. The second form of uranium mineralization is as finely disseminated, subrounded cubes of pitchblende in the metapelitic unit. Radioluxographs (Plate 52) show that the mineralization parallels the local fabric in the rock and also sulphide bands consisting of pyrite, pyrrhotite, and chalcopyrite. Both these forms of mineralization strongly suggest that the uranium has been remobilized during one of the several periods of deformation known to have affected the area.

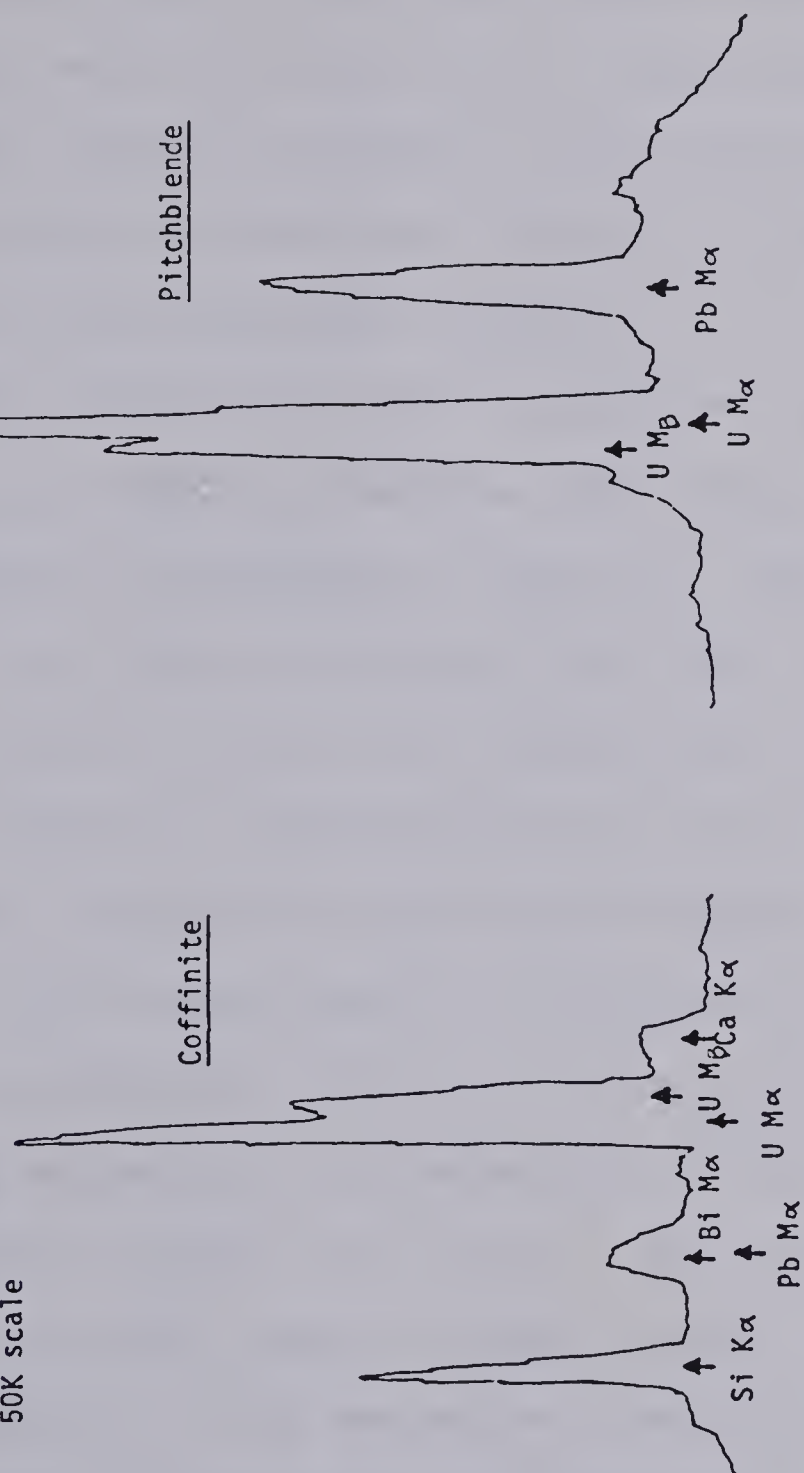
Pitchblende (Plate 53) was the main uranium phase identified with varying degrees of alteration to coffinite observed (Plates 54 and 55). Identification was made by microprobing mounted samples of ore; chart recordings of pitchblende and coffinite can be compared in Figure 73 (note the absence of thorium in both cases). Hughson (1958) attributed the high cell edge of  $5.47 \text{ \AA}$  and cubic shape of some grains to the presence of uraninite, but positive identifica-





Figure 73

EDA Spectrums  
230 seconds  
15 Kv  
50K scale



EDA spectrum for coffinite and pitchblende mineralization at the Kitts uranium deposit



tion was not confirmed. The only secondary uranium mineralization observed was in surface trenches where the metapelitic unit was badly weathered and in these cases a yellow uranium mineral coating occurred. Interstitial to pitchblende grains and infilling shrinkage cracks is galena (Plate 55), believed to be of radiogenic origin.

The geochemistry of the uranium mineralization obtained from the chemical analyses made during isotopic dating of pitchblende is presented in Table 21. Thorium was not determined as the radioactivity in the Kitts area was attributed to uranium only by the aid of a McPhar TV-1 scintillometer. However, it should be mentioned that in one instance high readings were obtained on the thorium channel for a metapelitic unit. The uranium analysis indicates the presence of high grade pitchblende with the uranium content varying from 34-75%. The absence of any detectible  $^{208}\text{Pb}$  confirmed the assumption that thorium was absent. The high  $^{206}\text{Pb}/^{204}\text{Pb}$  ratios (1600-33,000) suggest a high content of radiogenic lead and therefore a low amount of normal lead perhaps indicating that the uranium has been mobilized some time in the past.

Associated with the uranium mineralization are the sulphides pyrite, chalcopyrite and pyrrhotite, red and white carbonate, and sometimes epidote veinlets. As mentioned



previously, galena can be seen in reflected light specimens and Hughson (1958) reported the presence of molybdenite in minor amounts. Light  $\delta^{13}\text{C}$  values (-13.5 to -17.5) obtained on carbonate associated with the uranium mineralization indicate involvement of biogenic carbon, though these deposits were formed during the early Proterozoic (personal communication, Keiko Hattori, 1978).

### 6.5 Uranium-Lead Dating

Eight pitchblende samples from the Kitts deposit were dated, with six of the samples corresponding to the vein type mineralization and two representing disseminated mineralization. The procedure is described in the Appendix and the data are presented in the Table 21 and plotted on a concordia diagram in Figure 74. Additional data have been plotted on the concordia obtained from a regional geochronological study of uranium occurrences in the Aillik Group by Gandhi (1976).

The data indicate a single mineralizing event at 1750-1770 Ma corresponding to the Hudsonian Orogenic event (Stockwell, 1964). Sample K-74-3(3) gives a concordant age of 1770 Ma with other samples only giving a small range in the  $^{207}\text{Pb}/^{206}\text{Pb}$ ,  $^{206}\text{Pb}/^{238}\text{U}$ ,  $^{207}\text{Pb}/^{235}\text{U}$  ages (U-75-10(4); U-75-10(4); U-75-10(3); Kitts Dump). No systematic difference was noted for the coarse vein type of mineralization





TABLE 21

## Uranium-Lead Data, Kitts Pond

|            | 238U<br>ppm | 235U<br>ppm | 206Pb<br>ppm | 207Pb<br>ppm | 208Pb<br>ppm | $\frac{207\text{Pb}}{206\text{Pb}}$ | $\frac{206\text{Pb}}{238\text{Pb}}$ | $\frac{207\text{Pb}}{235\text{U}}$ | $\frac{207\text{Pb}}{235\text{U}}$ | $\frac{206\text{Pb}}{238\text{U}}$ |
|------------|-------------|-------------|--------------|--------------|--------------|-------------------------------------|-------------------------------------|------------------------------------|------------------------------------|------------------------------------|
| GK-2(3)    | 499062      | 3573        | 102817       | 10640        | -            | 1680 Ma                             | 1376 Ma                             | 1500 Ma                            | 3.3797                             | 0.238                              |
| GK-2(5)    | 559125      | 4002        | 142068       | 15274        | -            | 1750 Ma                             | 1659 Ma                             | 1699 Ma                            | 4.3306                             | 0.2936                             |
| K-74-3(3)  | 560322      | 4012        | 153456       | 16706        | -            | 1770 Ma                             | 1772 Ma                             | 1772 Ma                            | 4.7266                             | 0.3164                             |
| Kitts-3    | 748747      | 5361        | 194838       | 20694        | -            | 1730 Ma                             | 1694 Ma                             | 1709 Ma                            | 4.3815                             | 0.3006                             |
| Kitts Dump | 315334      | 2258        | 85099        | 9025         | -            | 1720 Ma                             | 1749 Ma                             | 1738 Ma                            | 4.5374                             | 0.3118                             |
| U-75-10(3) | 430688      | 3084        | 113958       | 12215        | -            | 1740 Ma                             | 1719 Ma                             | 1730 Ma                            | 4.4962                             | 0.3057                             |
| K-74-3(2)  | 332912      | 2384        | 84100        | 9202         | -            | 1780 Ma                             | 1651 Ma                             | 1709 Ma                            | 4.3823                             | 0.2919                             |
| U-75-10(4) | 473924      | 3394        | 128066       | 13918        | -            | 1770 Ma                             | 1751 Ma                             | 1759 Ma                            | 4.6557                             | 0.3122                             |



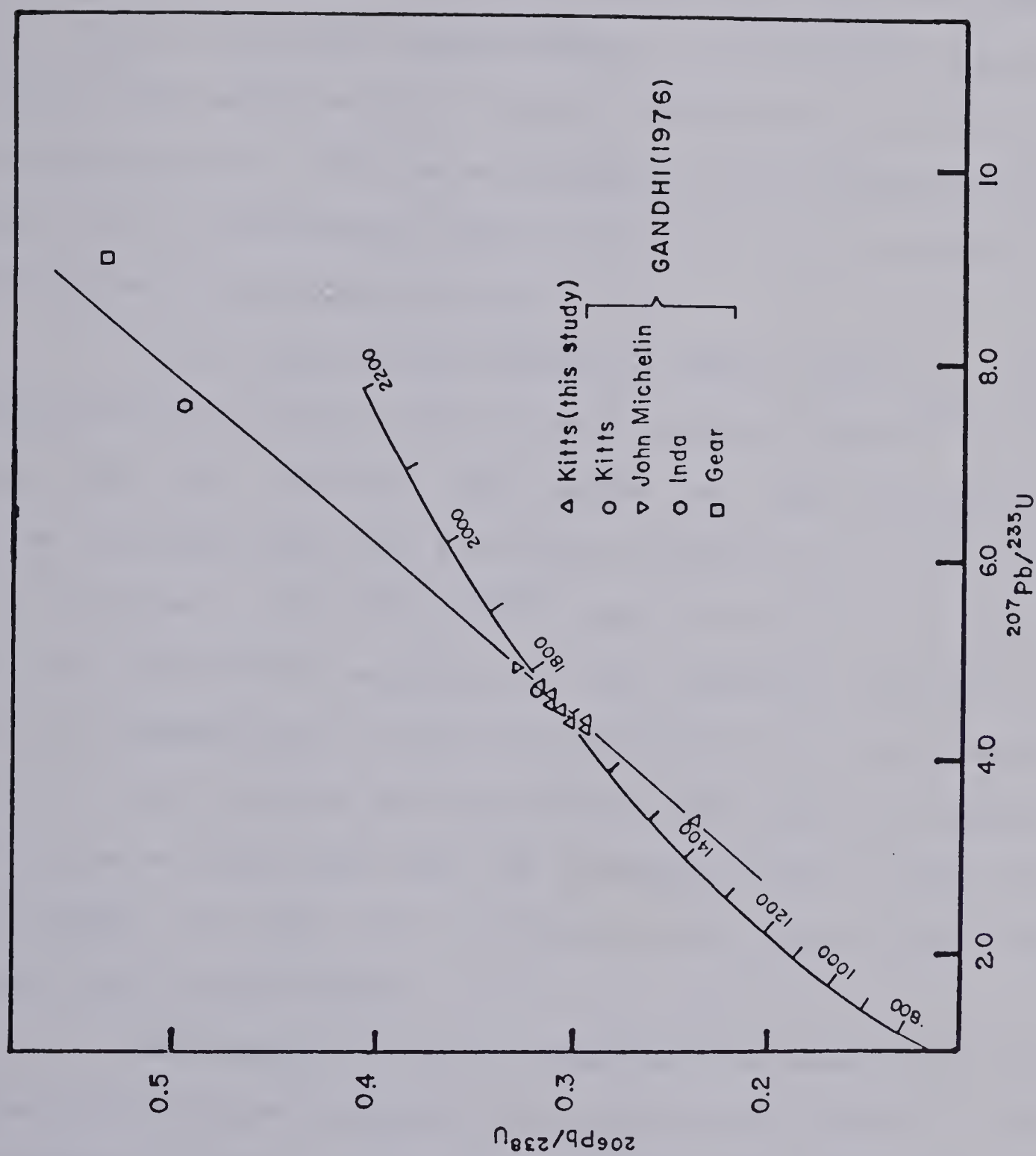


Figure 74

Concordia diagram for U-Pb data from Kitts uranium deposit



and the disseminated type of mineralization. It was originally thought that the latter type may have represented original, syngenetic uranium mineralization that was not remobilized during subsequent metamorphism. A  $^{207}\text{Pb}/^{204}\text{Pb}$  versus  $^{206}\text{Pb}/^{204}\text{Pb}$  isochron plot (Figure 75) indicates an age of mineralization of 1748 Ma confirming a single mineralizing event with no subsequent introduction of lead as noted at both Stormy Lake and Burnt Lake.

The single analysis made by Gandhi (1976) of Kitts mineralization agrees with the work reported here ( $^{207}\text{Pb}/^{206}\text{Pb}$  age = 1760 Ma). However, the results for Inda and Gear lie off a diffusion line for the Kitts mineralization drawn in as a reference. The  $^{207}\text{Pb}/^{206}\text{Pb}$  ages of the two showings, 1831 Ma and 1990 Ma respectively, may represent earlier periods of deformation and local remobilization of uranium or might in fact reflect the syngenetic deposition of uranium. It should be noted that the low uranium content (1.04%) of the sample from Inda Lake could make this analysis unreliable or at least questionable.

In summary, original syngenetic uranium mineralization concentrated in black shales was remobilized or re-concentrated as either vein-type or disseminated-type mineralization. Analyses of eight high-grade pitchblende samples cluster around the concordia indicating an age of 1750-1770



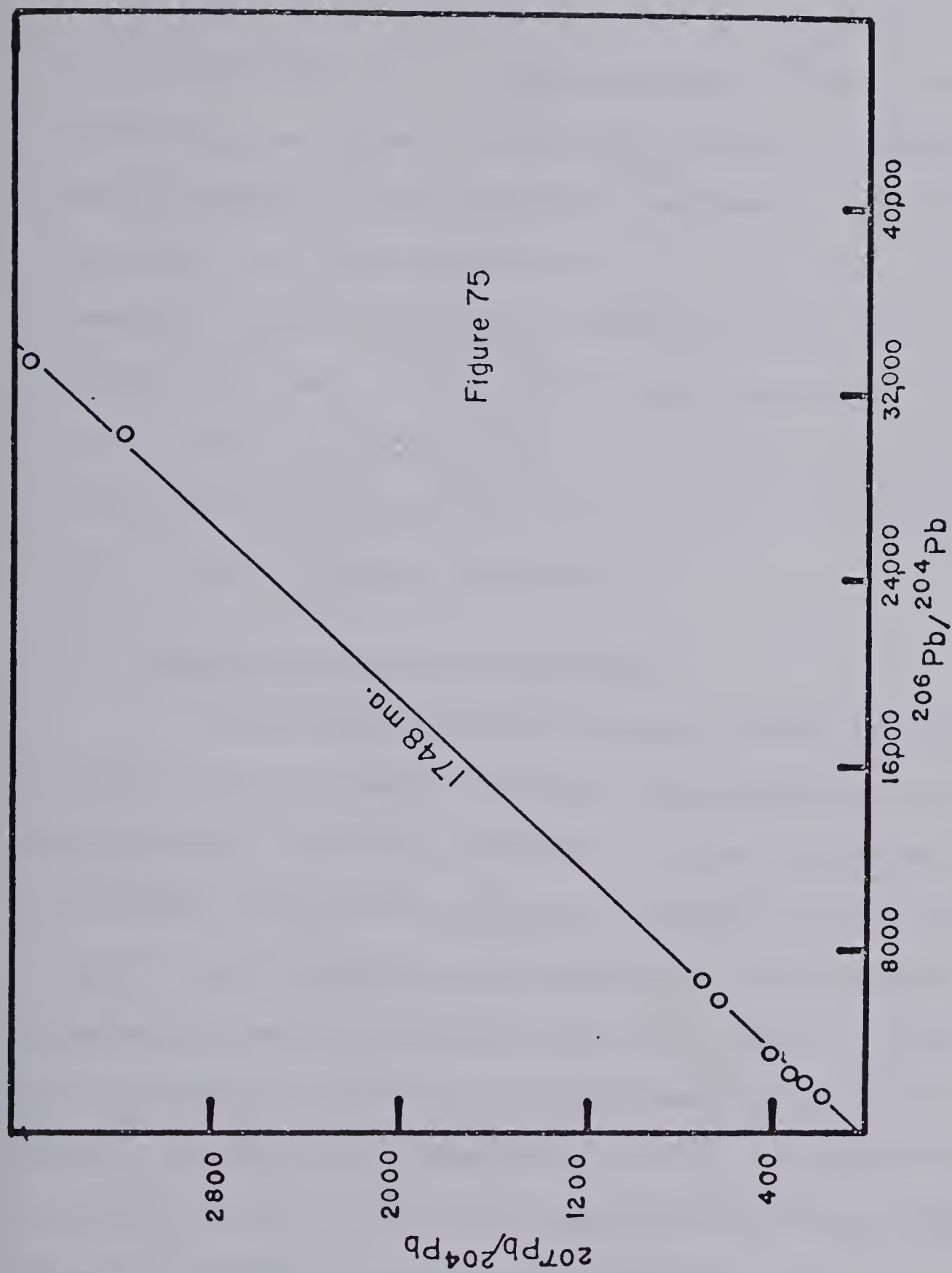


Figure 75

$^{207}\text{Pb}/^{204}\text{Pb}$  versus  $^{206}\text{Pb}/^{204}\text{Pb}$  plot for U-Pb data from the Kitts uranium deposit





Ma for this event, probably related to the Hudsonian Orogeny. High  $^{206}\text{Pb}/^{204}\text{Pb}$  ratios and negligible  $^{208}\text{Pb}$  concentrations indicating the absence of thorium, support a theory involving remobilization. Two additional analyses of similar occurrences within the Post Hill-Kitts Belt, the Inda and Gear Lakes showings, lie off the Kitts diffusion line giving older  $^{207}\text{Pb}/^{206}\text{Pb}$  ages. Although they may represent either separate periods of local uranium remobilization or original syngenetic uranium deposition, their genetic relationship to the Kitts deposit remains ambiguous.

## 6.6 Discussion and Interpretation

The occurrences of uranium mineralization in black shales is not uncommon although the high grades at the Kitts deposit are unusual, however, it does represent a remobilized event and not the original syngenetic uranium concentrations. More commonly associated with black shales are low concentrations of uranium (i.e. 50-80 ppm) in large tonnages as at Ranstad, Sweden or the Chattanooga shales of the United States (Derry, 1977; McMillain, 1977). In such cases the uranium is usually adsorbed by iron-hydroxides (Rydell and Bonatti, 1976) or hemipelagic sediments.

The stratiform nature of the uranium mineralization at Kitts strongly suggests a syngenetic origin, as proposed by Gandhi (1976), however, the source of the uranium is more



ambiguous and two possibilities exist. It was either derived from weathering of the Archean basement complex to the north and transported in solution into an adjacent basin, or the uranium may be of volcanogenic origin as there are mafic and felsic volcanics within the Aillik sequence. Bostrom and Fisher (1971) stated that the high concentration of uranium in active ridge sediments suggested that submarine volcanism is an important source of the radioelement. However, McMillain (1977), Hegge (1977), and Morton (1977) favor weathering of Archean terrains and transport of uranium into Aphebian basins where subsequent precipitation of it occurs in shelf facies sediments (i.e. black shales and calcareous rocks) with remobilization occurring during later orogenic events. Ruzicka (1975) also stated that uranium, syngenetically deposited in shales, can be remobilized and redeposited under conditions of thermal and dynamic metamorphism.

In summary, uranium mineralization at Kitts was originally deposited in black shales, part of a miogeosynclinal assemblage of Aphebian volcanics and sediments. The uranium is believed to have resulted from weathering of the Archean complex to the north although a small component may be of volcanogenic origin. Subsequent greenschist-amphibolite grade metamorphism associated with the Hudsonian Orogeny resulted in remobilization and reconcentration of the uranium as vein and disseminated mineralization 1750-1770 Ma ago.



This process is very similar to that described by Morton (1978) and McMillain (1977) for the Wollaston Fold Belt of Saskatchewan, by Hegge (1978) for the Jabiluka deposit of Australia, and by Dodson et al. (1974) for the Rum Jungle-South Alligator River Valley area of Australia.





## CHAPTER 7

### 7.1 Synthesis and Conclusions

Whole-rock geochemistry (major elements) of the Bruce River Group, Minisinakwa volcanics, Walker Lake Granite, and Otter Lake Granite indicates that the suites are (i) typically calcalkaline in composition, as indicated from various wt % oxide diagrams; (ii) are characterized by high  $\text{Al}_2\text{O}_3$ ,  $\text{Na}_2\text{O}$ , and  $\text{K}_2\text{O}$  contents indicating affinities with the high K-calc-alkaline -shoshonite suite (MacKenzie and Chappel, 1972); and (iii) may be petrogenetically related, since they share a common trend on most variation diagrams, with the possibility of a Bruce River-Walker Lake trend and a Minisinakwa-Otter Lake trend suggested by one diagram (Figure 16, AFM diagram). The anomalous chemistry of the rock suites indicating an affinity to the shoshonitic suite is indicative of orogenic environments which have changed from a dominantly dip-slip (subducting) to strike-slip regime. Such environments exhibit a progression from an early tholeiitic dominant chemistry through to calc-alkaline, shoshonitic and finally an alkaline affinity. The Central Mineral Belt displays such a pattern starting with the tholeiitic basalts of the Lower Aillik Group in the east and progressing through the series to the agpaitic alkaline rocks of the Red Wine Province found further to the west. Concomitant with this change in chemistry and lithospheric plate movement is the rotation and



fragmentation of an arc system; this may possibly explain the apparent discrepancy in structural trends ( $55^{\circ}$ ) between the Central Mineral Belt and the rest of the Nain Province.

Although the above solution is attractive, a simpler answer to explain the anomalous chemical patterns (which are similar to those found in S-type granites) involves crustal fusion of older basement rocks. Partial fusion of the Archian Hopedale Gneiss (circa 1700–1500 Ma), known to underlie the area, would result in similar chemical trends and also produce rocks with initial  $^{87}\text{Sr}/^{86}\text{Sr}$  ratios in the range of 0.7050, close to the values obtained in this study. Such an environment is more typical of a stable craton, analogous to other areas characterized by large volumes of rhyolitic to rhyodacitic pyroclastic material (i.e. Cascades, Roman Province), where an underlying heat source causes fusion of the overlying cratonic material.

A compromise between these two theories is found in the North Island of New Zealand where a stable craton is in close proximity to a flexure in the Tonga-Kermadec arc.

Five Rb/Sr isochrons, combined with previous geochronological studies and U/Pb dating performed in this study have permitted the author to resolve several of the age-relationship problems defined in the introduction, namely:

- (i) That the Aillik Group should be reclassified into



a Lower and Upper unit, with the possibility of an unconformity separating the two groups of rocks. A Rb/Sr age of  $1767 \pm 4$  for the acid volcanics of the Aillik Group, combined with a minimum age of  $1832 \pm 58$  Ma for the basic volcanics and metapelites of the Kitts-Posthill Belt of Aillik Group rocks, suggests either a diachronous relationship between the two areas, or an unconformable relationship. Dating of vein-type uranium mineralization at Kitts at 1770 Ma, believed to have formed during the Hudsonian Orogeny, implies that the area to the north was undergoing deformation and metamorphism at the same time as active volcanism was occurring further to the south, thus suggesting the presence of an unconformity between the two groups. Whether these younger rocks were deposited with an angular unconformity or disconformity on lower Aillik Group rocks, is a question which can only be resolved in the field and at present lack of outcrop in the critical area prevents this.

(ii) Dating of both the Bruce River Group volcanics (1520 Ma) and the Aillik Group acid volcanics ( $1767 \pm 4$  Ma) has shown that the two volcanic units are not time stratigraphic equivalents. However, similarities in chemistry (Bailey, personal communication), combined with other Rb/Sr dates indicate that the younger volcanics may represent a transgression of volcanic activity towards the west during





Aphebian to Helikian times.

(iii) That the Minisinakwa Volcanics ( $1538 \pm 35$  Ma) are time stratigraphic equivalents of the upper part of the Bruce River Group volcanics (1520 Ma). This conclusion is in agreement with field data, indicating similar characteristics between the two groups of rocks (i.e. feldspar porphyry sequence with minor intermediate flows, hornblende andesites, and volcaniclastic units). A combined isochron indicates an age of 1537 Ma, which agrees with the  $1526 \pm 44$  Ma age obtained by Wanless and Loveridge (1972) on the Bruce River volcanics.

(iv) That the Otter Lake Granite ( $1496 \pm 37$  Ma) represents part of a widespread intrusive event during Helikian time, possibly related to the Elsonian event (1400-1450 Ma, Stockwell, 1964) within Labrador. A less reliable Rb/Sr age of  $1550 \pm 55$  Ma (?) for the Walker Lake Granite prevents a conclusive correlation to be made between the two areas. Although mapping by Ryan (1978; 1979) and Bailey (1978; 1979) indicates that an extensive area of the Central Mineral Belt is underlain by an equigranular, leucocratic to melanocratic granite, this writer does not feel that they represent one large single intrusion but instead a composite body. For example, the Otter Lake Granite is characterized by large (0.5-1 mm) euhedral sphene crystals which are absent in the





Walker Lake Granite. Resolution of this problem will only be obtained by more mapping on a smaller scale (1:20,000), combined with geochemical, geochronological, and petrographic studies.

The results of this Rb/Sr study, combined with both earlier and more recent studies, indicate that an extensive period of acid volcanism and intrusive activity extending from 1800 Ma to 1400 Ma occurred in southern Labrador. The activity commenced in the eastern part of the study area and moved progressively westwards with the greatest amount of activity occurring during the Paleohelikian. This is represented by the acid volcanic rocks of the Bruce River Group, Minisinakwa Volcanics, Letitia Lake Porphyry and the Petscapiskan Volcanics -- a total area of  $\sim 5000 \text{ km}^2$  -- and the large area underlain by the Walker Lake and Otter Lake Granitoid bodies. In the latter case this large composite body may decrease in age from east to west, with the Walker Lake Granite dated at  $1550 \pm 55 \text{ Ma}$  and the Otter Lake Granite dated at  $1496 \pm 37 \text{ Ma}$ .

Detailed studies of five uranium deposits and showings of diverse nature throughout the Central Mineral Belt has delineated a minimum of four uraniferous subprovinces and mineralizing epochs. These are (i) the Kitts-Moran Lake subprovince, represented by the Kitts deposit and Moran Lake



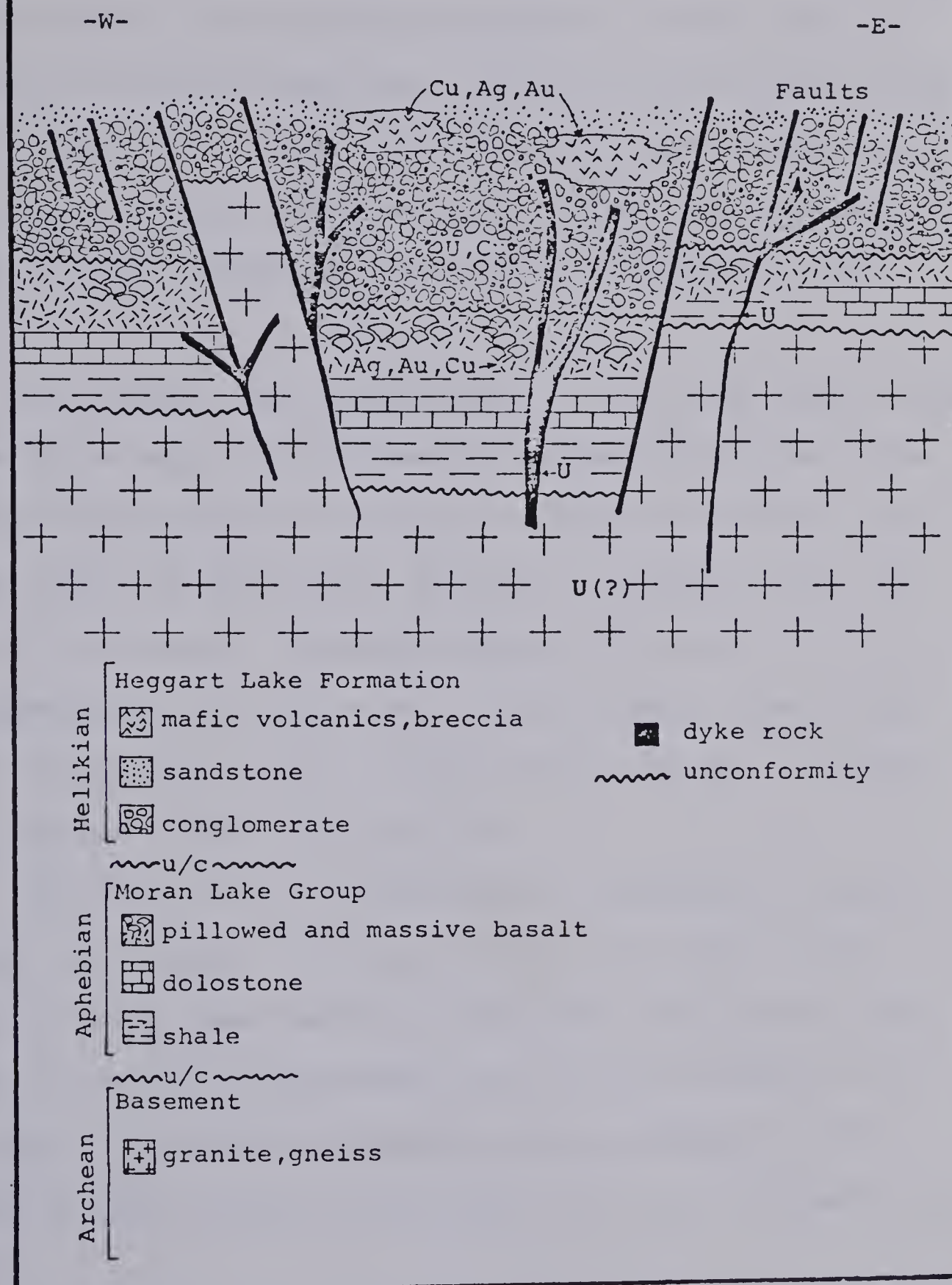
'B Zone; (ii) the Burnt Lake-Michelin subprovince, represented by the Burnt Lake showing and the Michelin deposit; (iii) the Stormy Lake subprovince, represented by the Stormy Lake showing, and (iv) the Bruce River subprovince, represented by the Moran Lake 'C' Zone. In addition to these areas several other potential targets have been recognized.

(1) The Kitts-Moran Lake subprovince: original syngenetic/diagenetic uranium mineralization concentrated in black, marine shales of the Aphebian Moran Lake Group and Lower Aillik Group was remobilized into vein-type deposits (type deposit Kitts, 1770 Ma) during the Hudsonian Orogeny. Subsequent incorporation of this upgraded mineralization by anorthositic dykes with high  $\text{PCO}_2$ , due to assimilation of carbonate, occurred in the Moran Lake 'B' Zone at 1740 Ma (Figure 76).

(ii) The Burnt Lake-Michelin subprovince: Syngenetic/diagenetic alteration and metasomatism of Aphebian felsic tuffs with contemporaneous leaching and reprecipitation of uranium in mafic-rich portions of rocks (i.e. areas rich in sodium pyroxene and amphibole) occurred during deposition of the Upper Aillik Group (type deposit Burnt Lake, 1800 Ma). The altered nature of the intrusive body at Michelin and



FIG. 76 Geologic environment for uranium mineralization at the Moran Lake 'B' Zone.









granitic fragments containing pyroxene, amphibole and uranium mineralization found in the felsic tuffs at Burnt Lake, suggest an active subvolcanic hydrothermal system enriched in alkaline solutions which participated in the mineralizing process (Figure 77). Later remobilization and reconcentration of uranium during the Grenville orogeny has increased the grade in some instances (type deposit Michelin, 1100 Ma).

(iii) The Stormy Lake subprovince: vein-type mineralization associated with the Paleohelikian-Neohelikian unconformity between Bruce River Group acid volcanics and Seal Lake Group sediments was generated during the waning stages of the Grenville Orogeny. Mineralization includes U, F, Cu,  $\text{Fe}^+\text{Ag}$  concentrated in fractures with or without quartz and calcite gangue (type deposit Stormy Lake, 900 Ma) as represented diagrammatically in Figure 78.

(iv) The Bruce River subprovince: uranium-rich solutions associated with late-stage acidic volcanism of the Bruce River Group (see Table 2) permeated along fault zones and other accessible channelways and uranium minerals were precipitated in favourable horizons (i.e. carbonate-rich volcanics at type deposit, Moran Lake 'B' Zone) as shown in Figure 79.

In addition to these favourable provinces other potential targets can be postulated by analogy to other



FIG. 77 Schematic diagram illustration Burnt Lake-Michelin type uranium environment during Aphebian time.

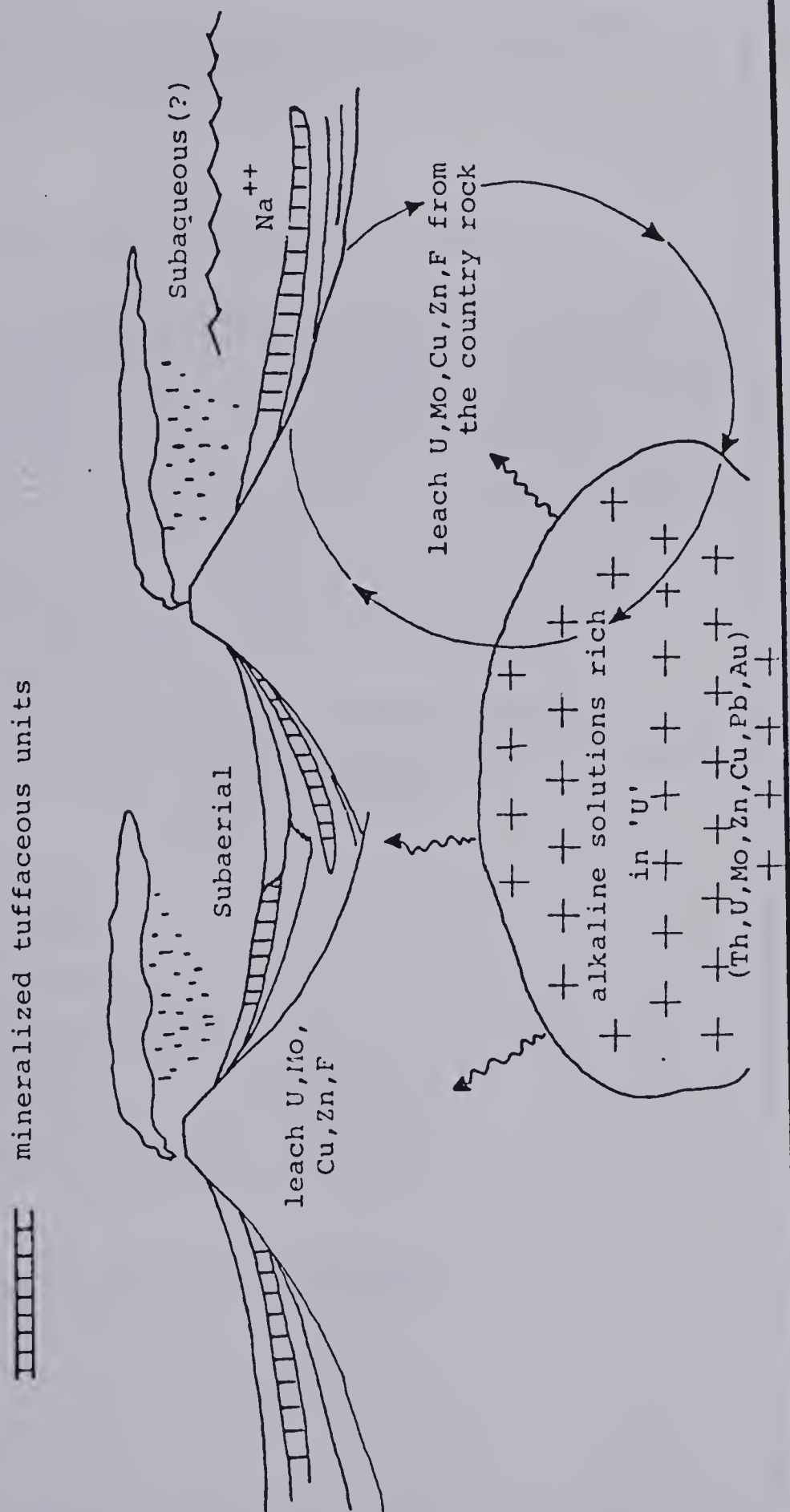




FIG. 78 Schematic diagram illustrating vein-type uranium mineralization at Stormy Lake.

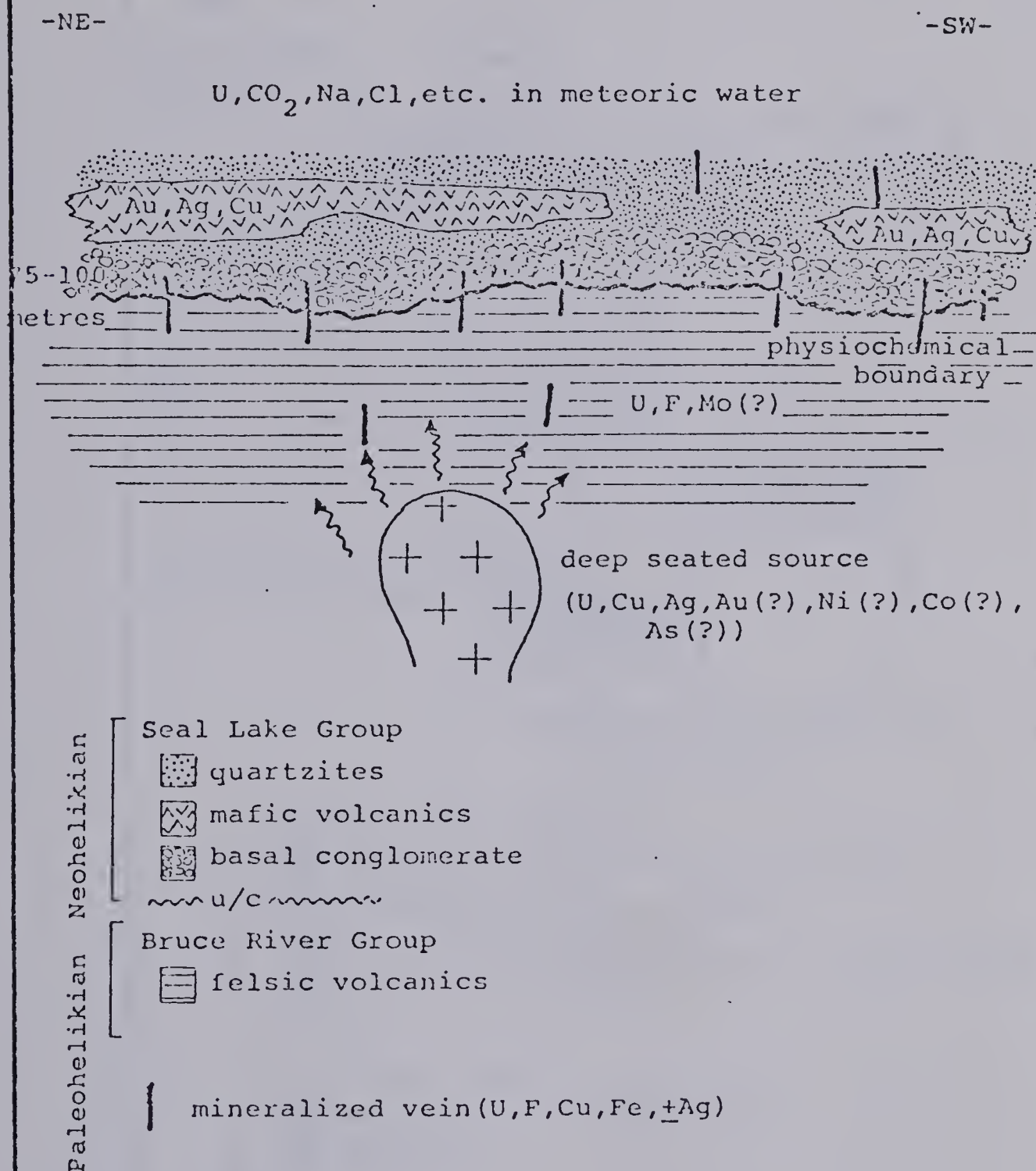
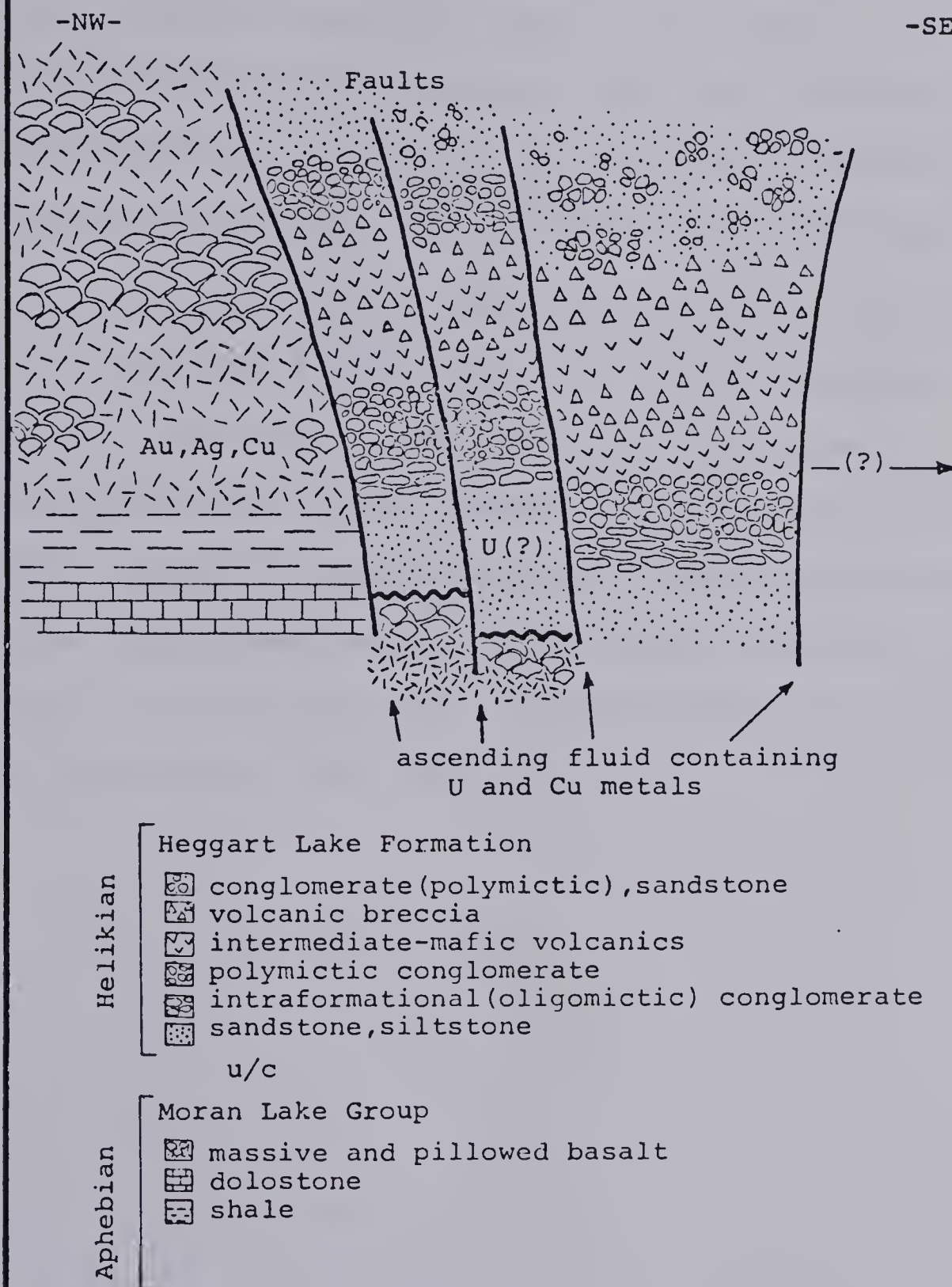






FIG. 79 Geologic environment for uranium mineralization at Moran Lake 'C' Zone







uranium districts. These include the following; i) the Archean-Aphebian unconformity between the basement gneiss terrain and the Moran Group and lower Aillik Group. This is analagous to the Beaverlodge and Wollaston Belt districts of northern Saskatchewan; ii) recent discoveries of mineralized granite boulders near Monkey Hill (assays up to 13%  $U_3O_8$ ) indicate the potential for porphyry-type uranium deposits as described by Armstrong (1974); and iii) the unconformable contact between the Paleohelikian Heggart Lake Formation and the Aphebian Moran Lake Group, identical to the relationship found in the Athabasca Basin of northern Saskatchewan where several large high-grade deposits have been discovered, constitutes the most potential for a future exploration target outside of subprovinces (i) and (ii).



## APPENDIX 1

### (Uranium-Lead Procedure)

Sampling procedure: Uranium samples were collected from exposed outcrops except for the Kitts deposit and Burnt Lake showing (samples B-59, B-61) which were obtained from drill core. As a result of this the mineralization used in the study shows some effects of recent weathering indicated by uranium loss (i.e. Burnt Lake).

Mineralization was first examined in reflected light to determine the number of phases present; in all cases only one period of mineralization was observed except for Kitts where alteration of pitchblende to coffinite occurs. Following this, samples containing uranium mineralization were crushed to -80 mesh size and the uraniferous phase handpicked with the aid of a binocular microscope. The author picked only the freshest mineralization available, free of any sulphide minerals and evidence of weathering. Some specimens did contain internal galena, however, but this Pb is believed to be of radiogenic origin and did not affect the dating (i.e. Burnt Lake and Kitts).

Approximately 200-800 ug of the uraniferous phase was used for dating except in the case of the Moran Lake 'C' Zone where ~100-150 ug was used due to a lack of good



mineralization.

Analytical procedure: The procedure employed here is a slight variation on the method described by Baadsgaard (1973) and Baadsgaard et al. (1976) for U-Pb-Th analyses of zircons, sphene and apatite. A weighed amount of handpicked uranium mineralization was first dissolved in vapor distilled  $\text{HNO}_3$  and distilled  $\text{H}_2\text{O}$ ; where a residue remained after digestion of the uraniferous phase it was weighed and an appropriate correction made to the weight of the uranium sample. Aliquots of uranium and lead spikes were added to an aliquot according to sample size after having divided the solution into I.R. (isotope ratio) and I.D. (isotope dilution) portions. The I.D. solution was evaporated to dryness and the Pb separated and purified by anion exchange (Krogh, 1973). The Pb in the I.R. solution was co-precipitated with purified  $\text{Ba}(\text{NO}_3)_2$  and the supernate solution containing U collected and evaporated to dryness before being separated by nitrate anion exchange. The I.D. Pb was co-precipitated with  $\text{Ba}(\text{NO}_3)_2$  an additional two times (to ensure purification of the Pb) before being taken up in 1.5N vapour distilled HCl and purified by an anion exchange column.

Both the Pb I.R. and I.D. samples were isotopically analyzed by the silica gel method with the Pb being taken up in 2.4N  $\text{H}_3\text{PO}_4$  and loaded on a single Re filament coated with





the gel. Uranium was loaded on a double Re filament as a nitrate. Both U and Pb were run on either a Micromass 30 automated mass spectrometer equipped with an on-line computer, or a Russell-type, 12 in. radius,  $90^\circ$  sector mass spectrometer equipped with peak switching facilities and a chart recorder.

The total Pb blank was  $< 4$  ng and the U blank  $< 1$  ng.

Treatment of data: Data obtained from the Micromass 30 was presented as computer printouts with isotopic ratios already calculated. Data from the chart recorder was hand calculated. Precision of the isotopic Pb measurements were  $< \pm 0.2\%$  and for the U  $\pm 0.2\%$ \* (see Tables 10, 17, 18 and 19). Constants employed in the study were those recommended by the IUGS subcommission on Geochronology (Steigher and Jager, 1977) and are as follows:

$$\lambda_{\text{U-238}} = 1.5513 \times 10^{-10} / \text{yr}$$

$$\lambda_{\text{U-235}} = 9.8485 \times 10^{-10} / \text{yr}$$

$$^{238}\text{U} / ^{235}\text{U} = 137.88$$

Calculation of isotopic ages and ratios was done using a computer program written by Dr. H. Baadsgaard, University

---

\* The ppm U and ppm Pb values are estimated to be precise to  $< \pm 0.5\%$ .



of Alberta. The data is presented in Tables 11, 18, 19 and 21, and plotted on conventional concordia diagrams in Figures 44, 58, 66, 69, and 74.





Plate 1 - Flat lying  $F_1$  fold in Bessie Lake Formation  
sediments. Graded bedding indicates that tops  
are up. Note refraction of slaty cleavage in  
different beds.

Plate 2 - Steeply plunging  $F_2$  folds in Bessie Lake Forma-  
tion. Folds plunge  $65^\circ$  to the SW. It is  
interesting to note that the quartz veins  
represent local remobilization of precursor  
quartz pebbles and cobbles on an outcrop scale.











Plate 3 - Large megafold of  $F_2$  age in outlier of Seal Lake sediments, looking NE. In the distance are Bruce River Volcanics and to the right the Otter Lake Granite.

Plate 4 - Aerial view of the Stormy Lake uranium showing with the Bruce River-Seal Lake unconformity sketched in.







Plate 5 - Overturned unconformity with Bruce River

Volcanics on top of Seal Lake quartz pebble  
conglomerate (photo taken in eastern part of  
the map area).

Plate 6 - Excellent cross-bedding in quartzites, defined  
by heavy mineral (magnetite) laminations.



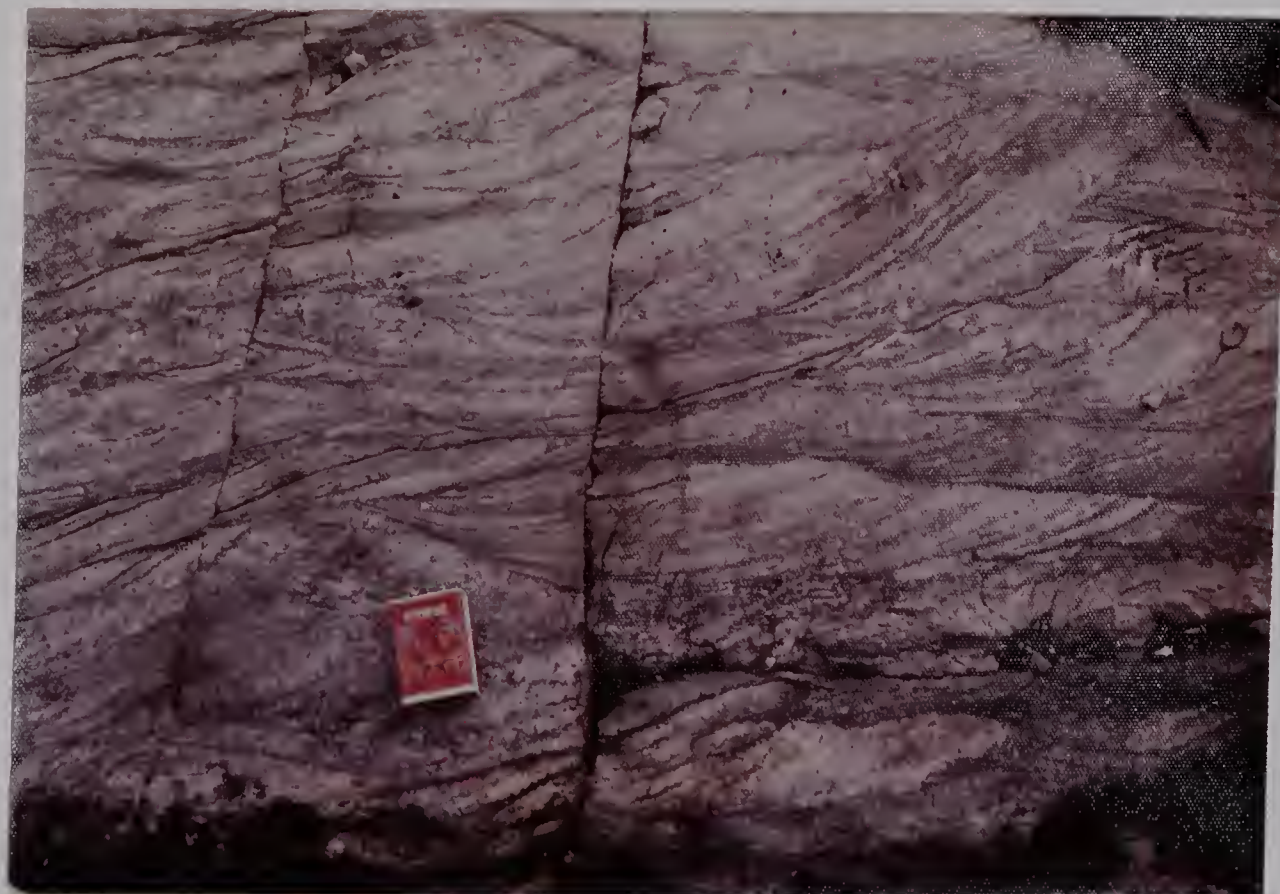






Plate 7 - Euhedral to subhedral, detrital sphene  
crystals in meta-argillite rock (plane  
polarized light, X10).

Plate 8 - Oligomictic, quartz cobble conglomerate  
unit at Stormy Lake. Note the lack of any  
matrix material and uniform grain size of  
the clasts.



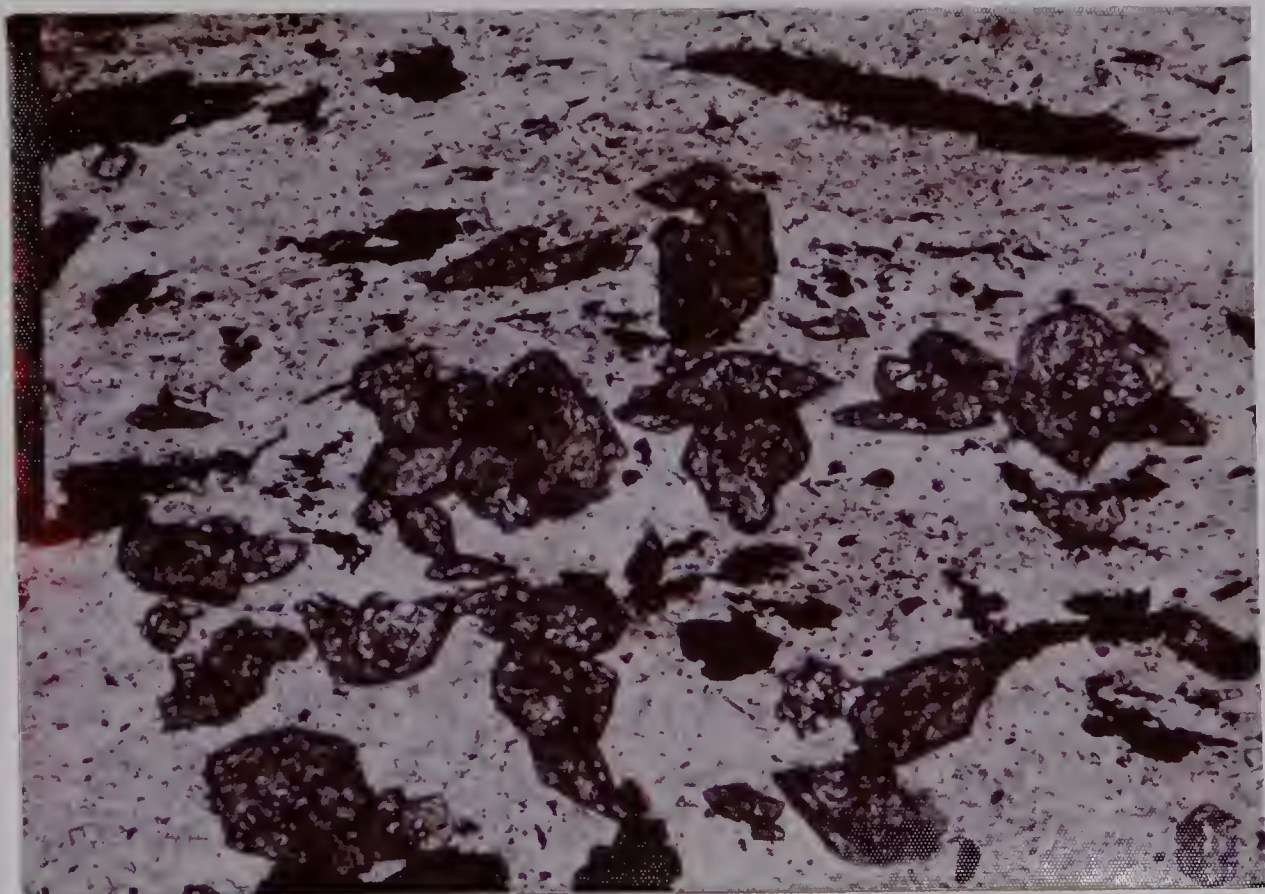








Plate 9 - Infolding of the Bruce River-Seal Lake unconformity along the main trench. Fold is  $F_2$  in age with steep plunge to the SW. The Seal Lake sediments have been eroded away leaving the empty synclinal structure. Note striations on the unconformity surface.

Plate 10 - Quartz vein containing inclusion of crenulated schist indicating two phases of deformation in the Stormy Lake area and also suggesting that quartz veining was a late stage event.







Plate 11 - Vein-type uranium mineralization (pitch-  
blende) at Stormy Lake.

Plate 12 - Local erratics with mineralized surfaces.

Note the rod-shaped habit of surfaces which  
contain uranium mineralization.











Plate 13 - Quartz vein containing rhombohedral  
hematite crystal.

Plate 18 - Lapilli tuffs in the mineralized unit,  
Burnt Lake. Note the darker matrix which  
contains alkali pyroxene and amphibole.







Plate 14 - Pitchblende mineralization containing blades of specular hematite (reflected light, X40).

Plate 15 - Metarhyolite specimen containing banded purple fluorite mineralization. In three dimensions one can see that the bands of fluorite are folded (true scale).

Plate 16 - Group of primary, two phase ( $H_2O$  + vapor) fluid inclusions in quartz (specimen S-17; plane polarized light, X40).

Plate 17 - Large primary, three phase fluid inclusion in fluorite. Note the solid phase, possibly halite, in the lower right corner of the inclusion (plane polarized light, X40).



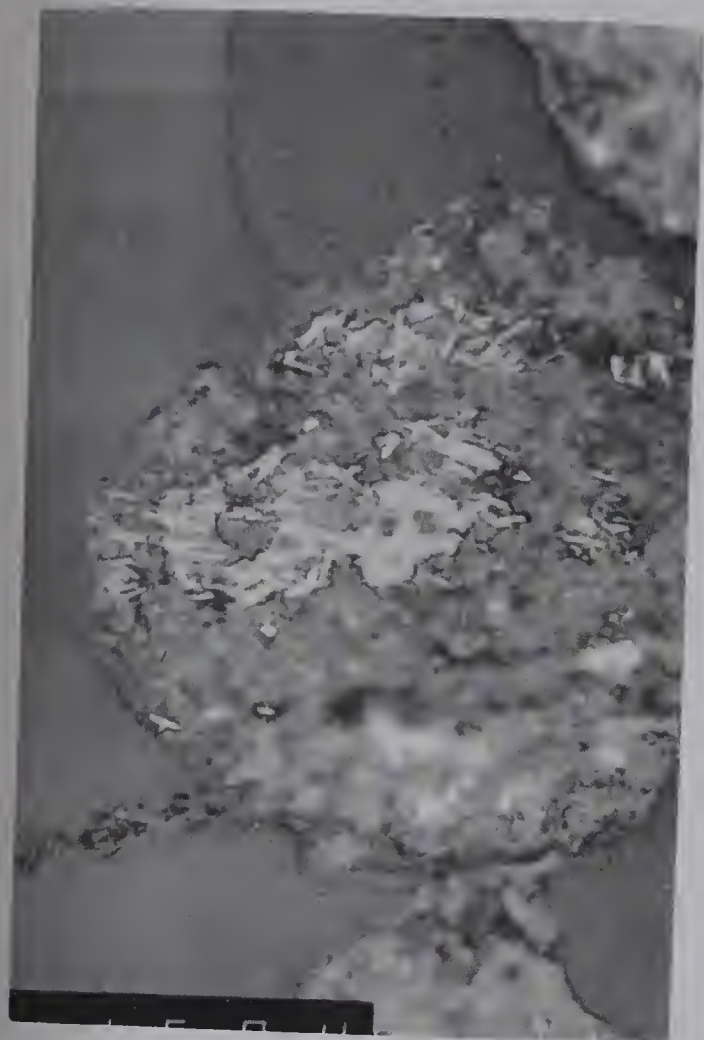








Plate 19 - Mineralized tuffs characteriaed by their  
mafic banding composed of alkali pyroxene  
and amphibole.

Plate 20 - Mineralized feldspar porphyry unit with mafic  
banding. Note how the mafic banding wraps  
itself around the feldspar crystals in a  
eutaxitic-like fashion.









Plate 21 - Large fragments of bedded felsic tuffs  
(aquagine tuffs ?) in quartz feldspar  
porphyry unit.

Plate 22 - Sharp contact between mafic rich and  
leucocratic portions of the rock (X-  
Nicols , X2.5).



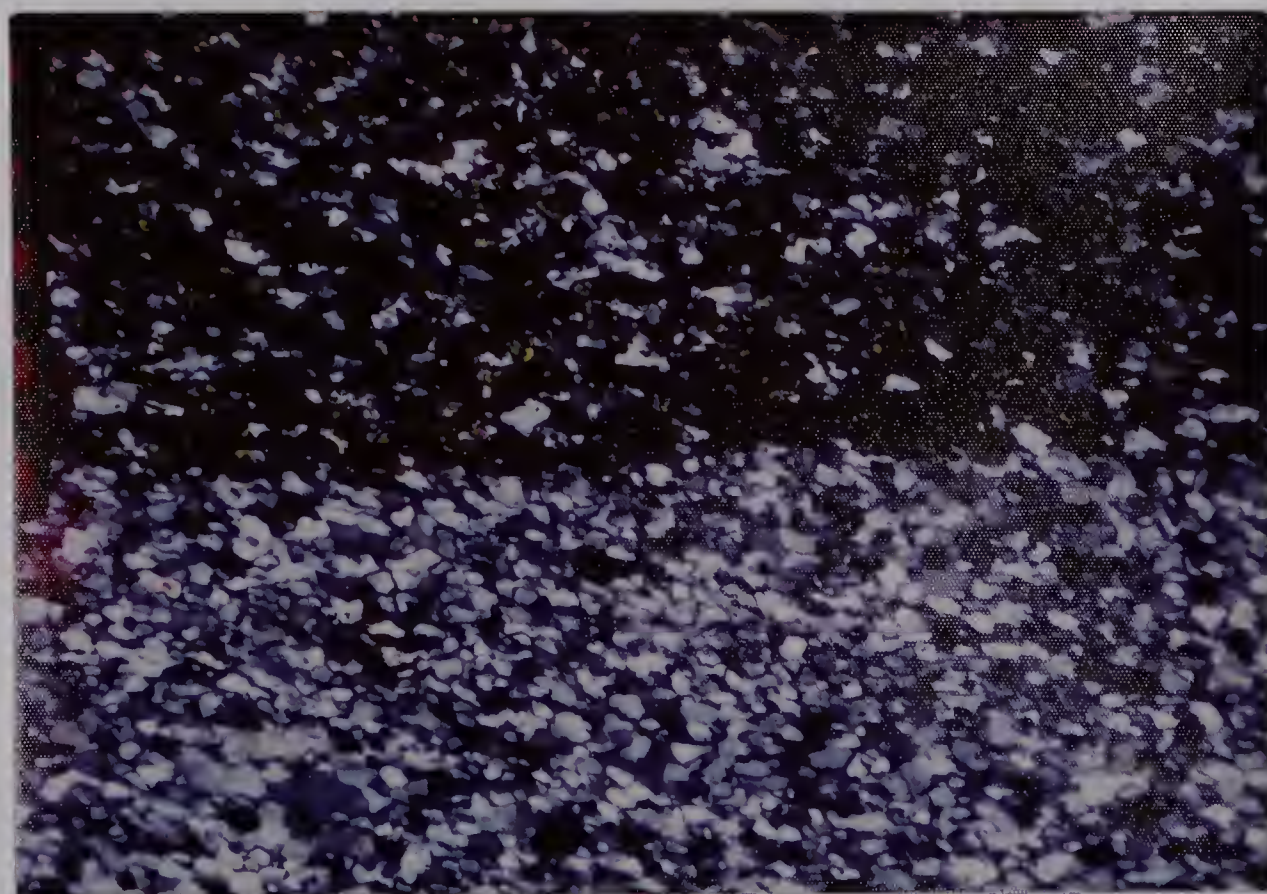






Plate 23 - Magnesioriebeckite displaying typical bluish-green color and  $120^{\circ}$  cleavage pattern. Green mineral is aegirine-augite and white background is composed of quartz and feldspar (plane polarized light, X16).

Plate 24 - Aegirine-augite displaying an olive green color and typical glomeroporphyritic habit. Black mineral is pitchblende and white background is composed of quartz and feldspar. Note the pleochroic haloes in the pyroxenes containing uranium mineralization (plane polarized light, X2.5).



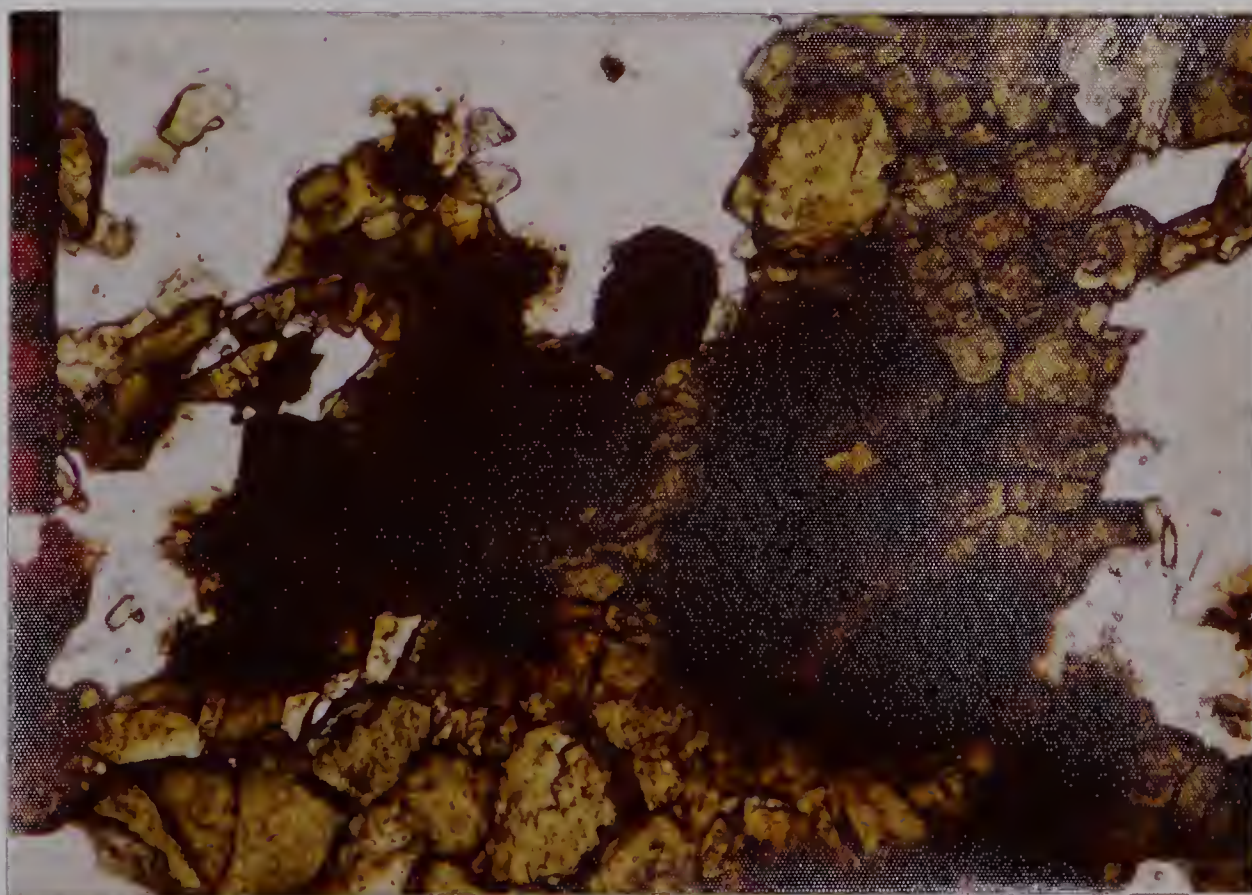
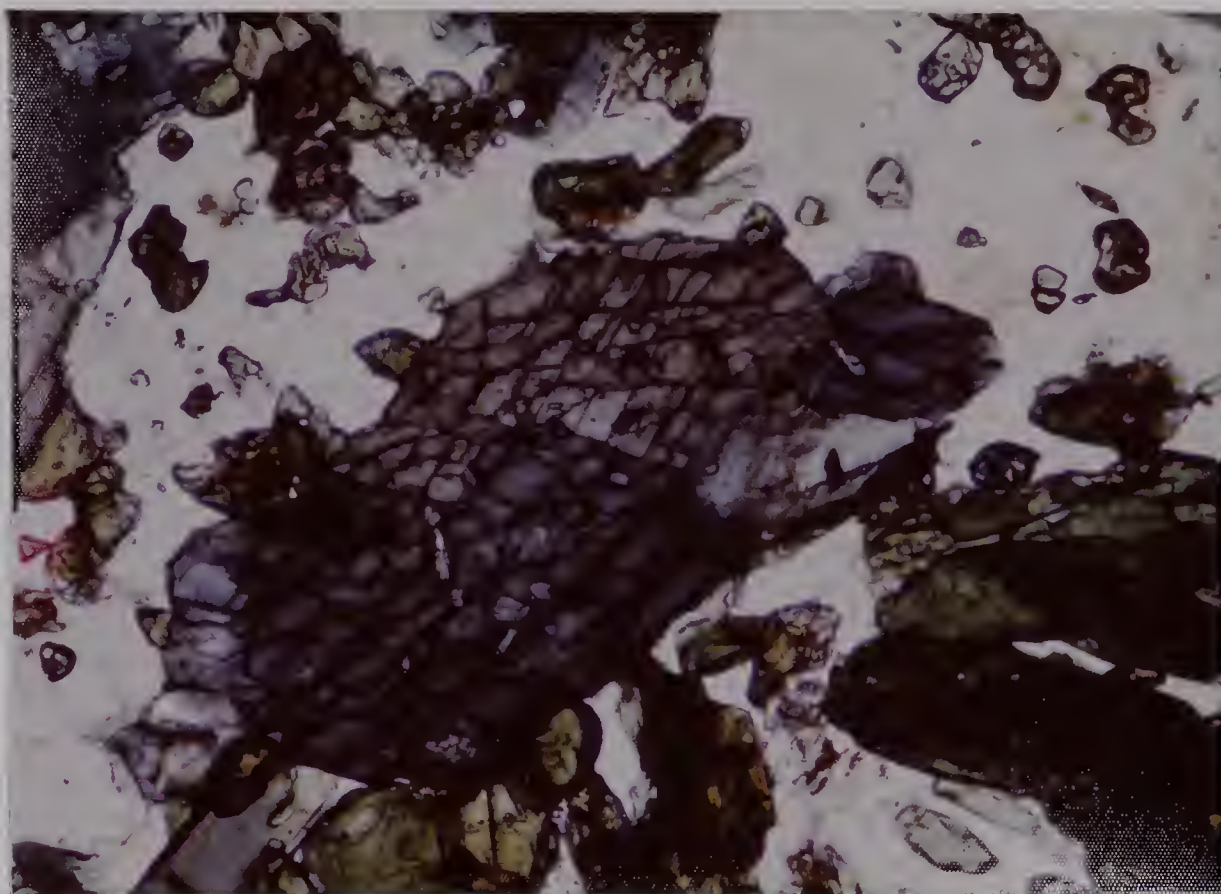








Plate 25 - Mineralized hand specimen and radioluxograph (exposure time 3 hours and 40 minutes) showing strong correlation between the mafic rich portion of the rock and uranium mineralization (true scale).

Plate 26 - Mineralized hand specimen and radioluxograph (exposure time 8 hours), again showing the strong association between melanocratic portions of the rock and uranium mineralization. Pitchblende from this specimen gave a  $^{207}\text{Pb}/^{206}\text{Pb}$  age of 1770 Ma.

Plate 28 - Pitchblende (grey) mineralization showing subhedral habit of individual grains. Galena (white) believed to be composed of radiogenic lead, is interstitial to the pitchblende with cumulate-like texture. Piece of chalcopyrite (bright) on lower left corner of grain (reflected light, X40).

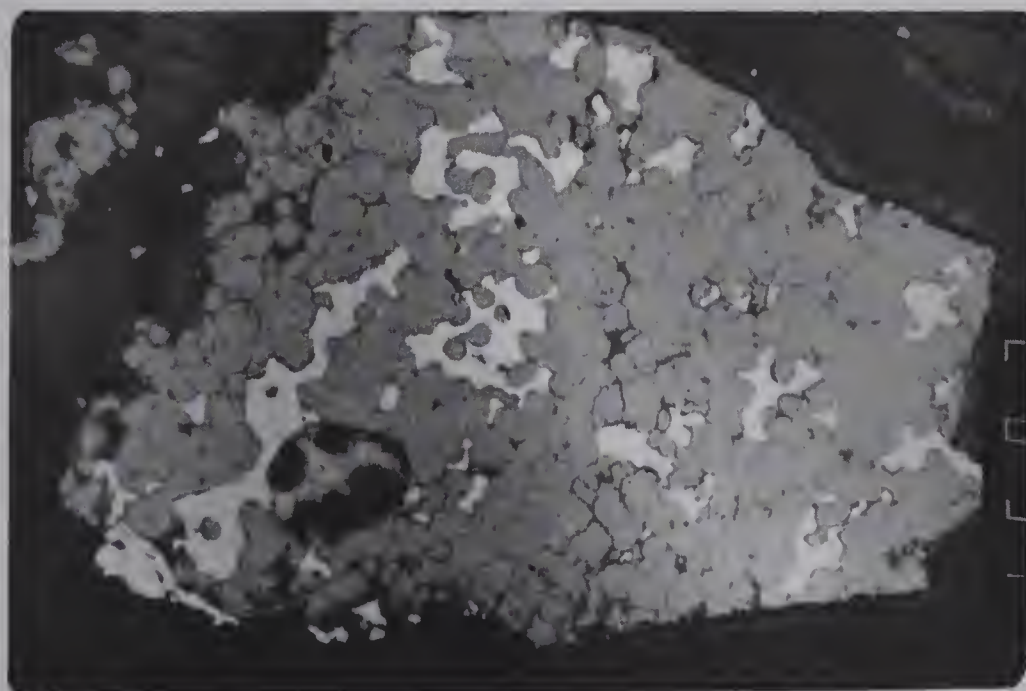
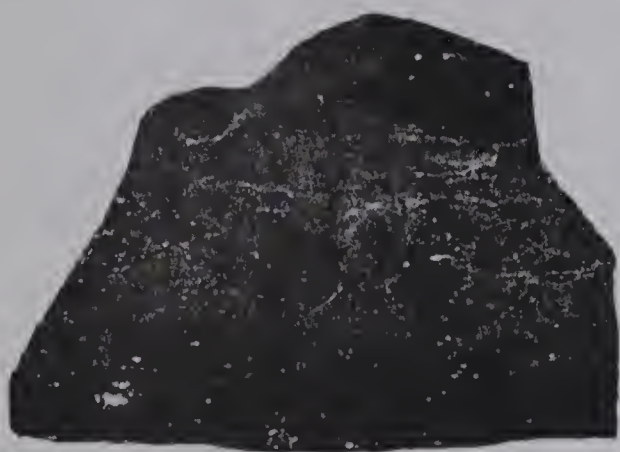






Plate 27 - Mineralized tuff with irregular-shaped mafic portions and intense red (hematite) alteration. The highest radioactivity corresponds to the red colored portions of the outcrop.

Plate 29 - Polymictic boulder conglomerate of the Heggart Lake Formation. Note the variety of clasts which make up the rock.











Plate 30 - Author sitting on the contact between dark green anorthositic dyke containing uranium mineralization and red metasediments. Note the thick cover of (damp) moss overlying the bedrock which inhibits the successful use of a gamma ray scintillometer in this area (see discussion in the text).

Plate 32 - Medium-grained anorthositic dyke displaying accicular habit of the plagioclase crystals (XNicols, X16).









Plate 33 - Green, feldspar porphyry dyke(unmineralized)  
cutting red siltstones which have been  
altered close to the dyke contact.

Plate 34 - Thin section of the feldspar porphyry dyke in  
plate 33. Note that the large feldspar grain  
is composed of several euhedral crystals  
intergrown together and that the carbonate  
alteration is most prominent after the  
feldspar phenocrysts rather than the matrix  
(X Nichols, X2.5).

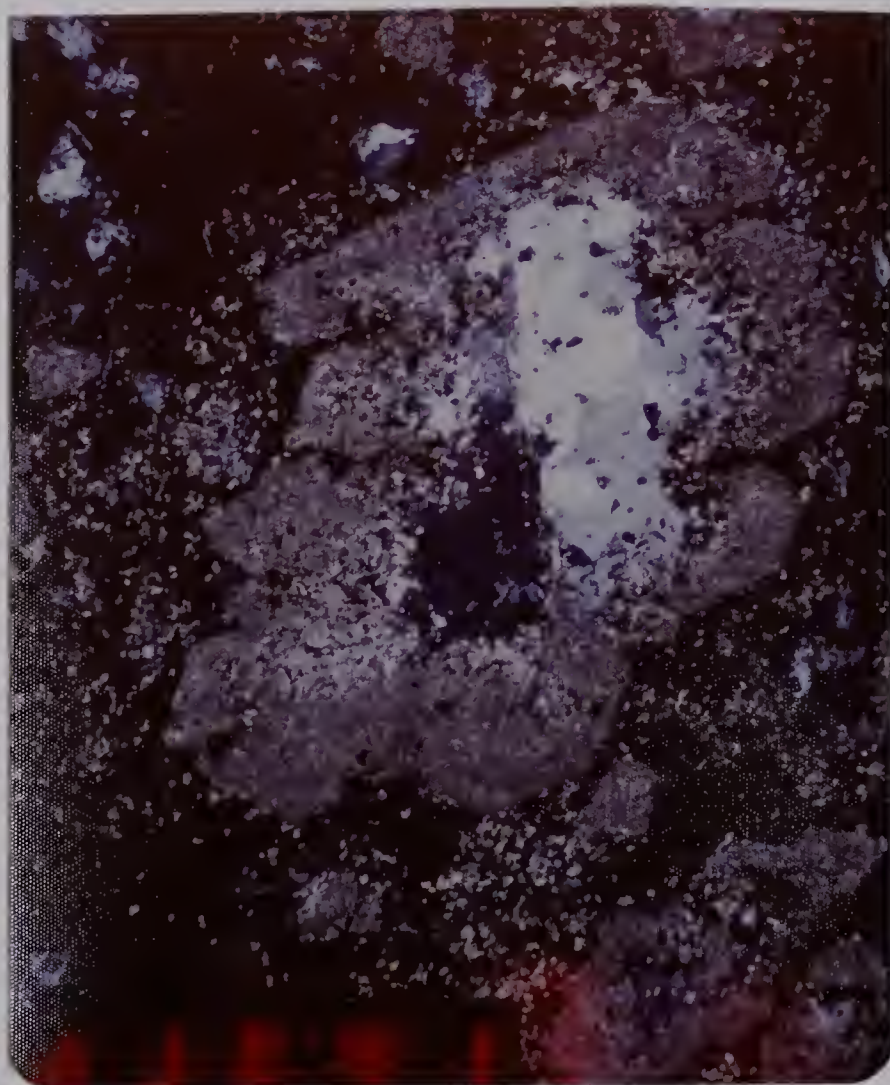








Plate 31 - Coarse-grained anorthositic dyke displaying typical equigranular texture. Black portions are composed of irregular-shaped patches of magnetite  $\pm$  penninite (X Nicols, X2.5).

Plate 36 - Hand specimen of mineralized anorthosite and radioluxograph (exposure time 9 hours) showing strong correlation between altered (hematite) part of the rock and uranium mineralization (true scale).

Plate 37 - Hand specimen of mineralized anorthosite and radioluxograph (exposure time 3 hours), again note the strong correlation between the altered portions of the rock and uranium mineralization(true scale).

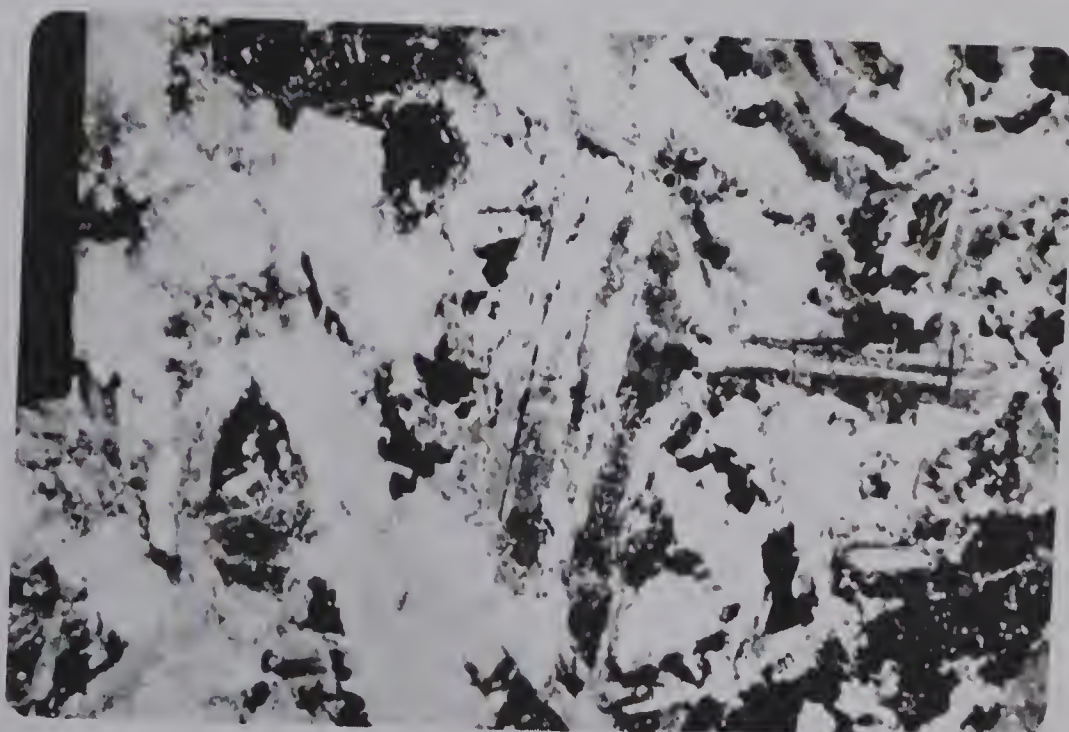
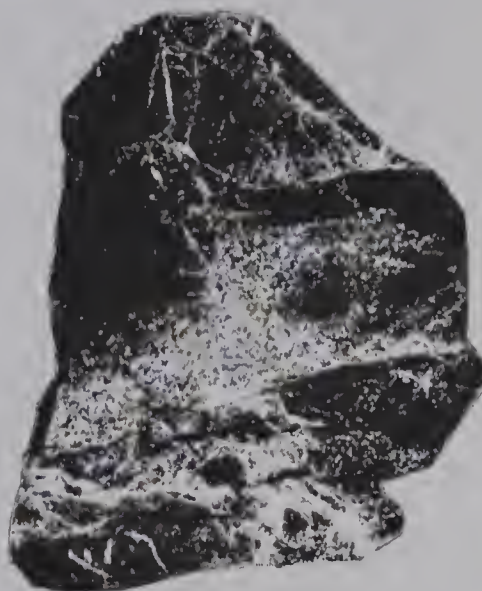


Plate 35 - Feldspar-pyroxene porphyry dyke. Euhedral phenocrysts of feldspar (upper left) and pyroxene (center; altered to actinolite and chlorite) in a fine grained, trachytic matrix. (X Nicols, X2.5)

Plate 38 - Euhedral sphene crystal being replaced by brannerite in coarse-grained anorthositic dyke. The green mineral is penninite and the white background is composed of pure albite. Note the reddish brown color of sphene adjacent to the uranium mineralization (plane polarized light, X16).



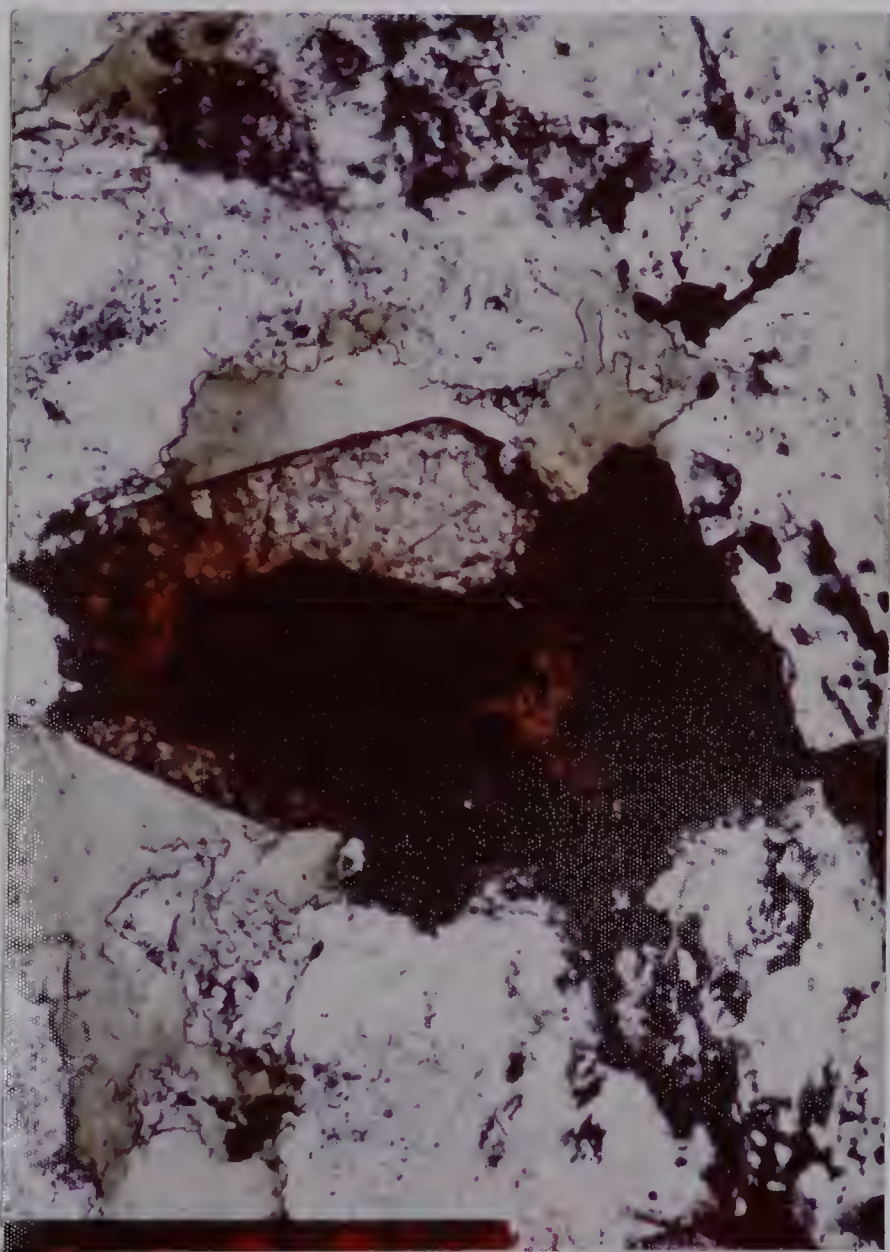
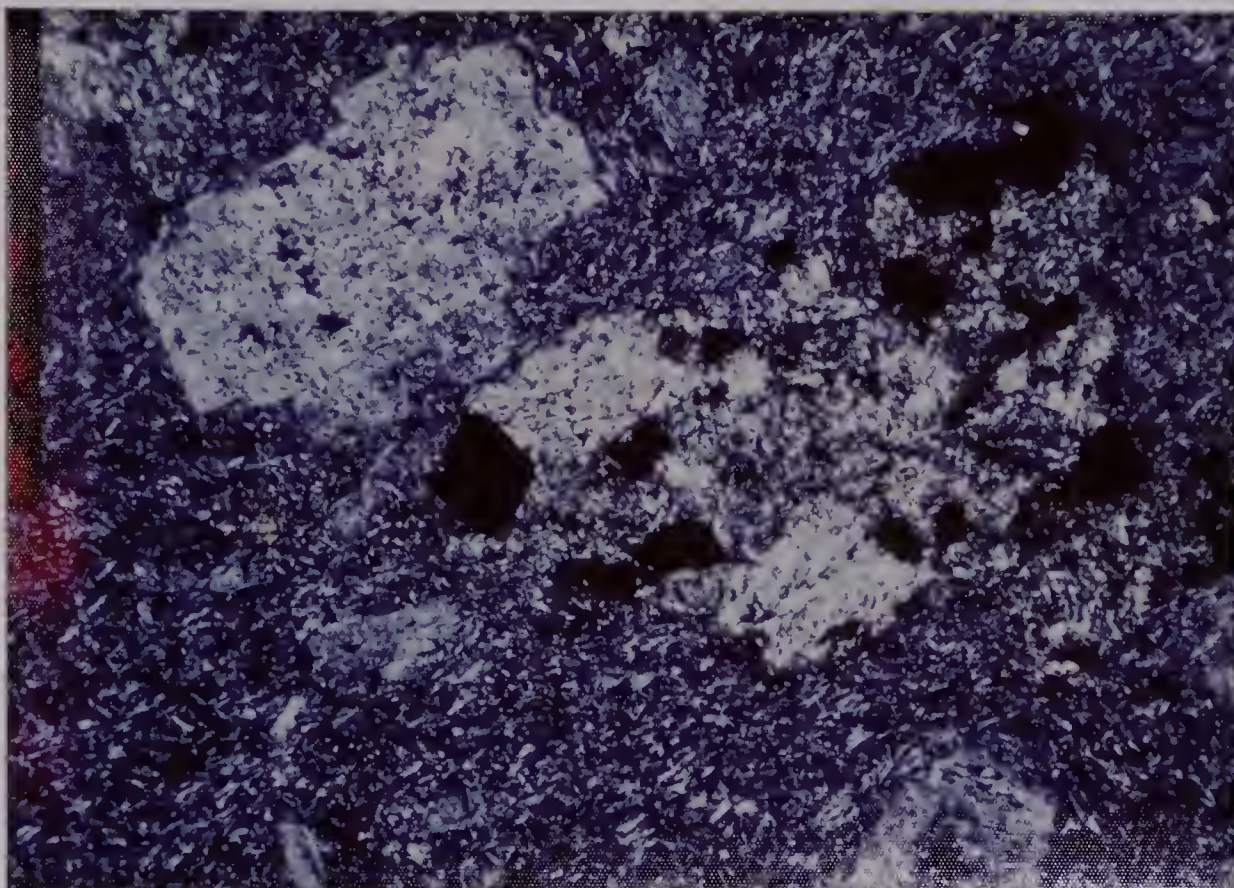








Plate 39 - Brannerite mineralization (grey) (reflected light, X40).

Plate 43 - Volcanic breccia or lithic tuff, exhibiting bedding. Note the alignment of the fragments and length of some as if they had been flattened post deposition due to compaction.

Plate 46 - Relatively unaltered part of the volcanic rocks showing the original andesitic textures (X Nicols, X10).

Plate 47 - Late stage veinlet composed of plagioclase laths cutting volcanic breccia unit (X Nicols , X2.5).

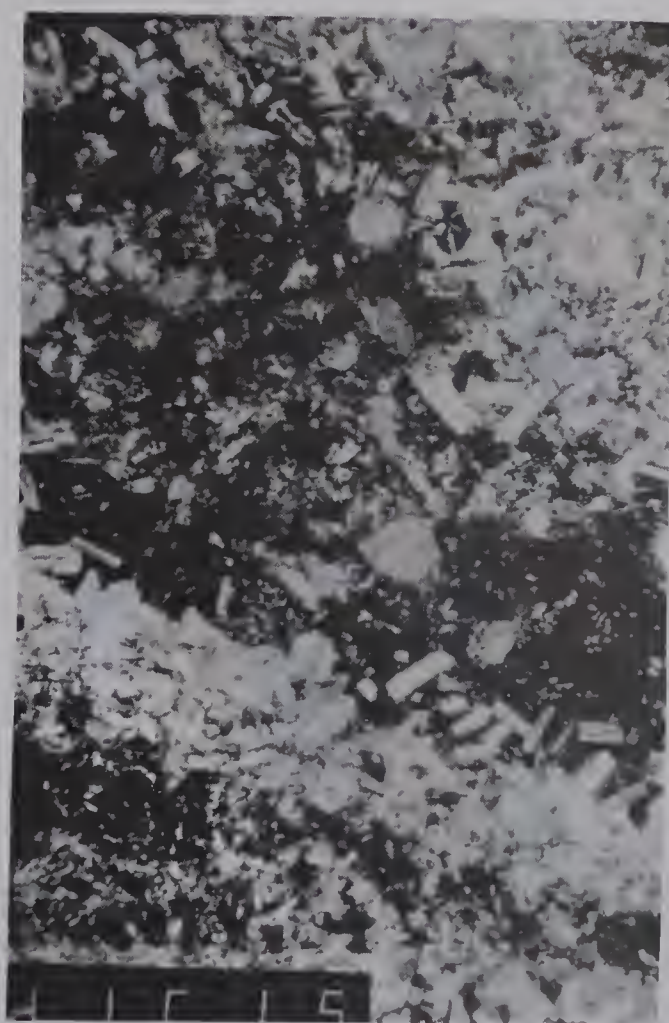
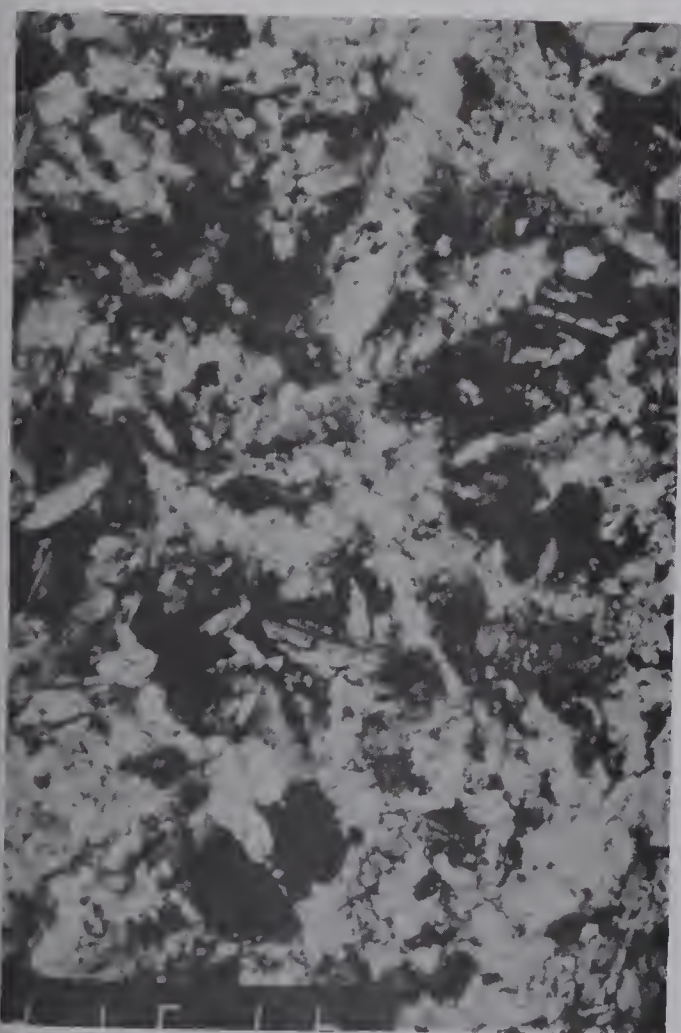
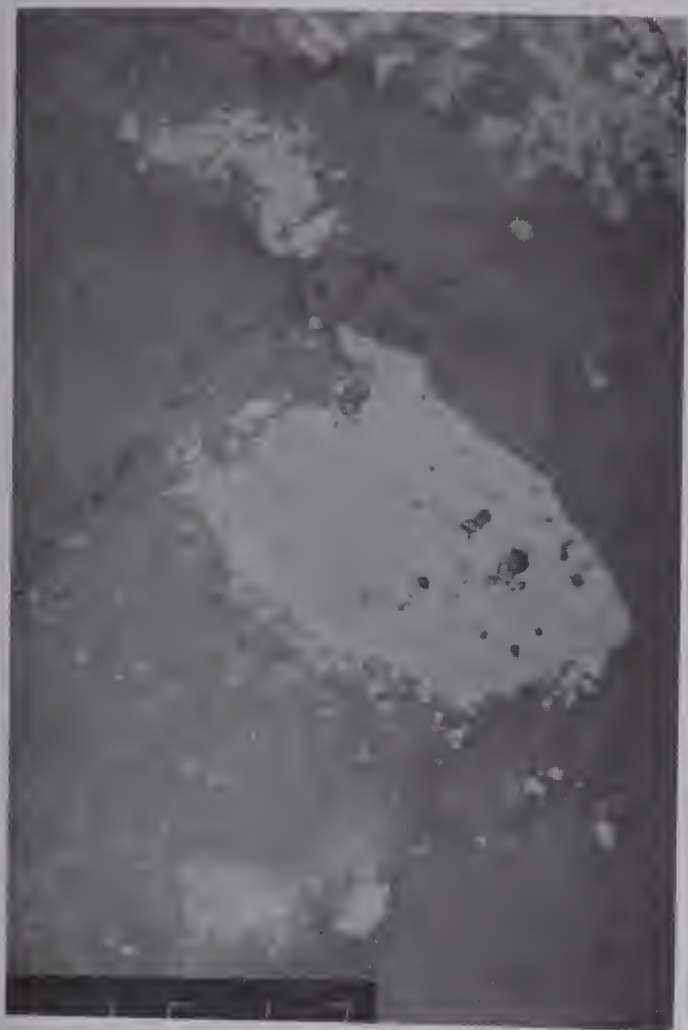








Plate 40 - Pillowed basalts of the Moran Group.

Plate 41 - Oligomictic, intraformational conglomerate  
of the Heggart Lake Formation. This immediately overlies a red silty mudstone, identical to the clasts in the conglomerate.







Plate 42 - Typical outcrop of the volcanic breccia.

Note the alignment of the clasts and their shapes (i.e. angular, flattened, etc.).

Plate 44 - Thin section of lithic tuff. Note the flowage of the matrix around the fragments (X Nicols, X2.5).



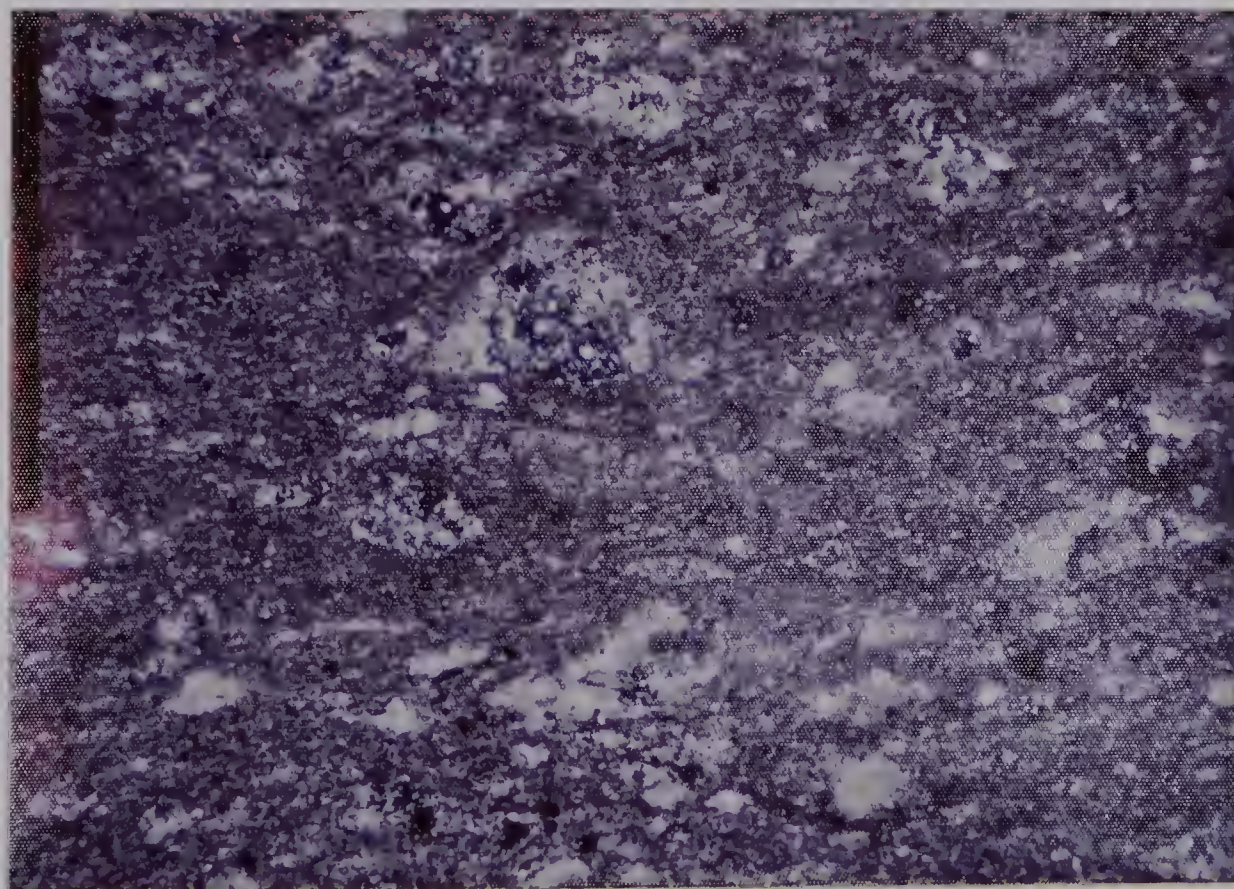








Plate 45 - Fragments of Moran Group basalts in volcanic matrix exhibiting quench textures such as rosettes and swallow tails (X Nicols, X2.5).

Plate 48 - Polymictic conglomerate overlying volcanic breccia. Notice the shallow dip of the contact, this argues against a diatrema or explosive breccia origin for the volcanic breccia.

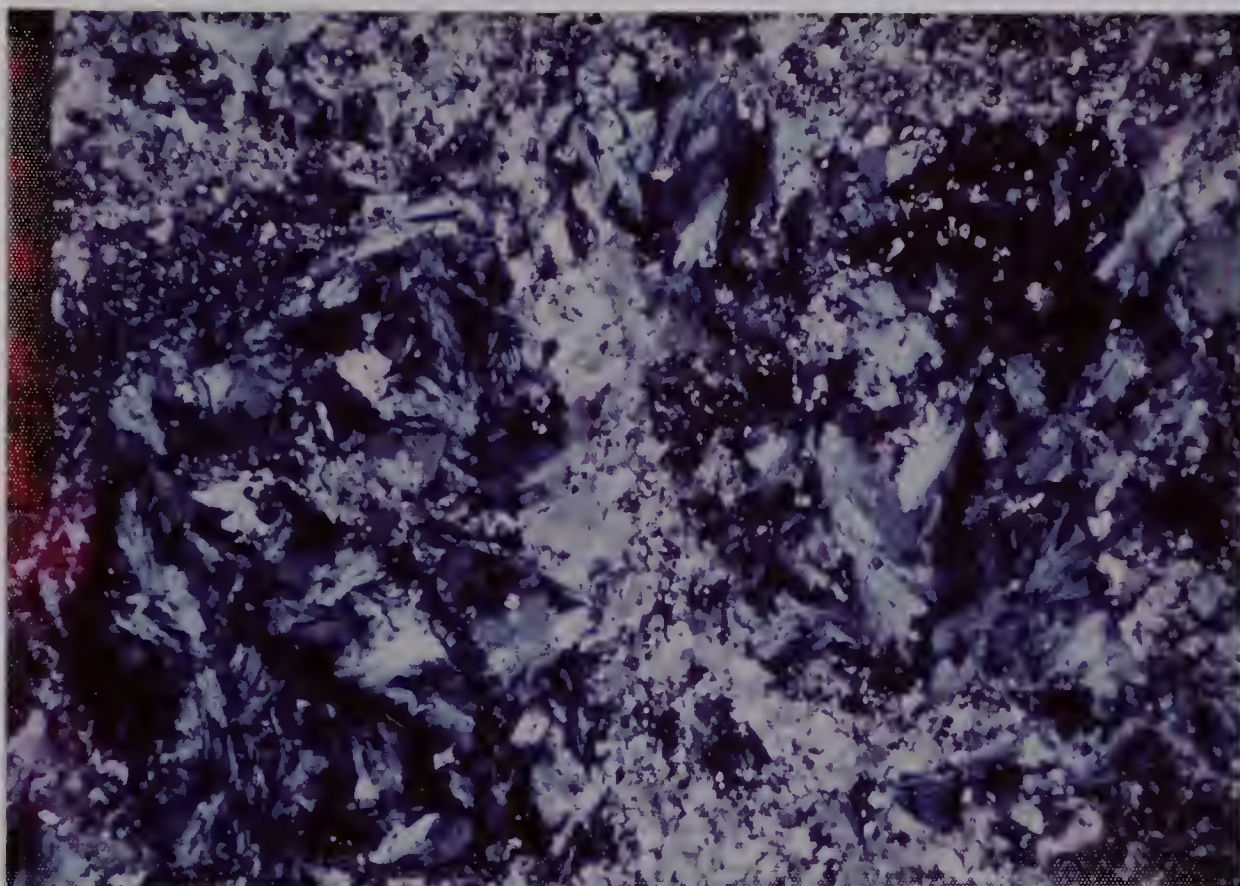








Plate 49 - Contact (vertical) between a dark green, aphanitic dyke and bleached grey sandstones of the Heggart Lake Formation. This dyke can be followed upwards before it disappears into conglomerates. It is thought possibly to be a feeder dyke for the overlying volcanic breccia (photo taken in the eastern part of the map area).







Plate 50 - Hand specimen of mineralized volcanic breccia  
and radioluxograph (exposure time 6 hours).

Note the correlation between mineralization and  
dark colored (hematite alteration) portions  
of the rock (true scale).

Plate 51 - Hand specimen of mineralized volcanic breccia  
and radioluxograph (exposure time 12 hours).

Again, note the strong correlation between the  
mineralization and the altered parts of the  
specimen (true scale).







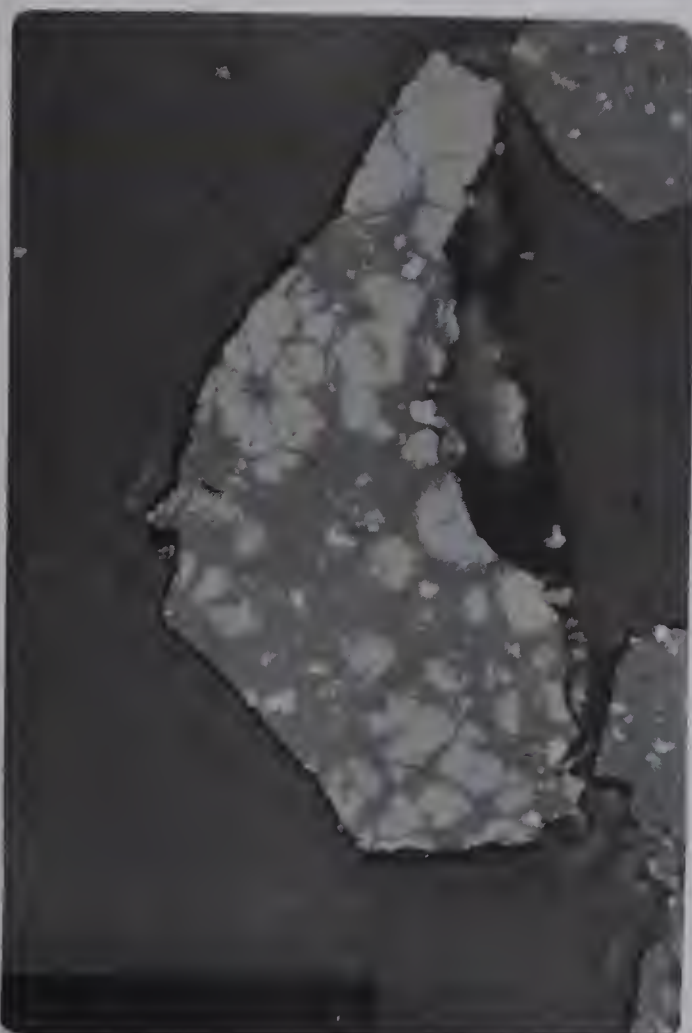
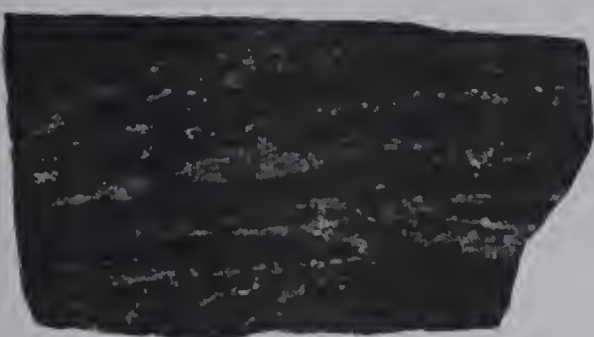
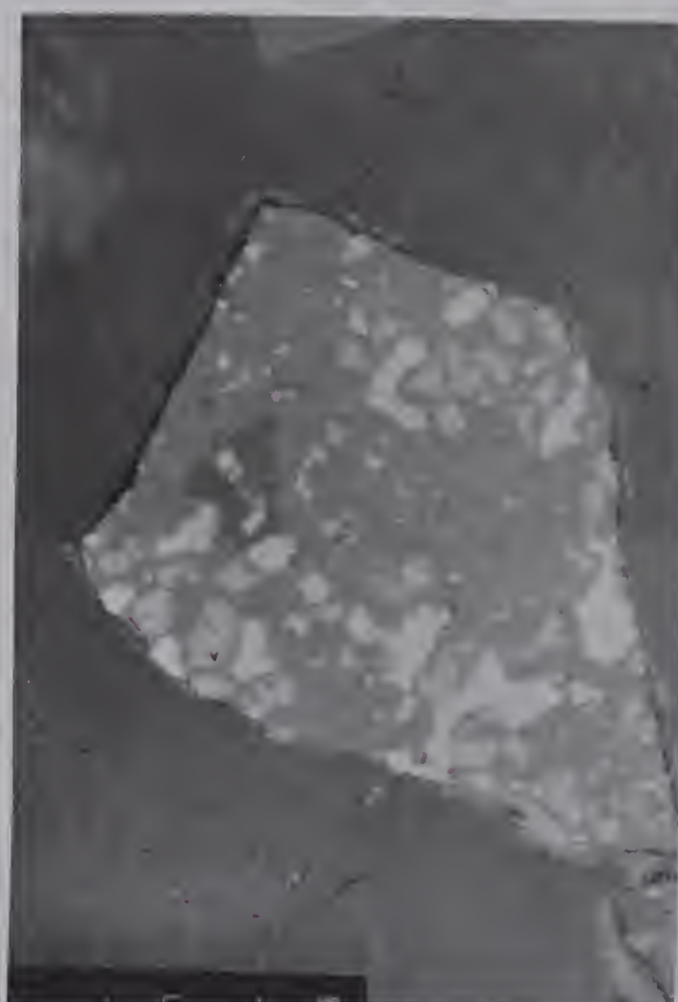
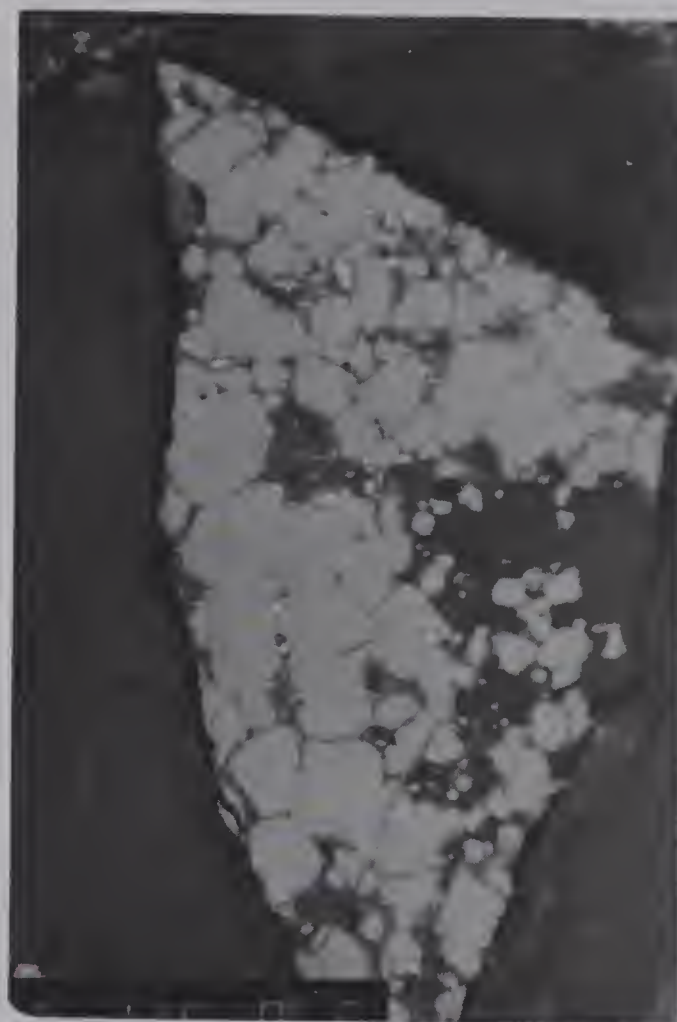


Plate 52 - Radioluxograph (exposure time 43 minutes)  
of meta-argillite showing the distribution  
of uranium mineralization which parallels the  
metamorphic fabric developed in the hand-  
specimen (true scale).

Plate 53 - Pitchblende mineralization (grey). Note the  
subcubic shape of the grains (reflected  
light, X40).

Plate 54 - Pitchblende mineralization (light grey)  
altered to coffinite (dark grey). Note the  
corroded edges of the pitchblende grains and  
development of shrinkage cracks (reflected  
light, X40).

Plate 55 - Pitchblende mineralization (light grey) nearly  
entirely altered to coffinite (dark grey) with  
remnant patches of galena (white) which  
originally formed as interstitial, cumulate-like  
grains to pitchblende (reflected light, X40).





## B I B L I O G R A P H Y

- Adamek, P. M. (1976): Geology and Mineralogy of the Koppar-  
asen Uraninite-Sulphide Mineralization, Norrbotten  
County, Sweden; Geological Survey of Sweden.
- Alsopp, H. A., Ulrych, T. J. and Nicolaysen, L. O. (1968):  
Dating some Significant Events in the History of  
the Swaziland System by the Rb-Sr Isochron Method;  
Canadian Journal Earth Science, Vol. 5, pp. 605-  
619.
- Appleman, D., Boyd, F. R., Brown, G. M., Ernst, W. G.,  
Gibbs, G. V. and Smith, J. V. (1966): Short Course  
lecture notes - Chain silicates.
- Armstrong, F. C. (1974): Uranium Resources of the Future -  
"Porphyry" Uranium Deposits; in Uranium Exploration  
Geology, IAEA Publication, pp. 625-635.
- Baadsgaard, H. (1973): U-Th-Pb dates on zircons from the  
early Precambrian Amitsoq gneisses, Godthaab  
district, West Greenland; Earth Planet. Sci.  
Lett., Vol. 19, pp. 22-28.
- Baadsgaard, H., Lambert, R. St. J., and Krupicka, J. (1976):  
Mineral isotopic age relationships in the poly-  
metamorphic Aritsoq gneisses, Godthaab district,  
West Greenland: Geochimica et Cosmochimica Acta.  
Vol. 40, pp. 513-527.
- Badham, J. P. N. (1974): Orogenesis and Metallogenesis  
with Reference to the Silver-Nickel-Cobalt Arsenide  
Ore Association; in Metallogeny and Plate Tectonics,  
D. F. Strong (ed.); Geological Association of  
Canada, Special Paper - 14, pp. 559-572.
- Bailey, D. G. (1978): The Geology of the Walker Lake-  
MacLean Lake Area (13K/9, 13J/12), Central Mineral  
Belt, Labrador; in Report of Activities for 1977,  
Newfoundland Department of Mines and Energy,  
Mineral Development Division, Report 78-1, pp. 1-8.
- \_\_\_\_ (1979): Geology of Eastern Central Mineral Belt  
(13J/10-15; 13O/2.3), Labrador; in Report of  
Activities for 1978, Newfoundland Department of  
Mines and Energy, Mineral Development Division,  
Report 79-1, pp. 103-108.





- Bain, J. H. C. (1977): Uranium Mineralization Associated with late Palaeozoic Acid Magmatism in Northeast Queensland; BMR Jour. of Australian Geology and Geophysics, Vol. 2, 137-147.
- Baragar, W. R. A. (1969): Volcanic Studies in the Seal Lake area (13K, L), Labrador; Geological Survey of Canada, Paper 69-14, pp. 142-146.
- \_\_\_\_\_ (1974): The Seal Lake and Croteau Volcanic Rocks of Labrador; (Abstract) Geological Association of Canada, Annual Mtg., Program and Abstracts, p. 5.
- Barsukov, V. L., Sushdrokaya, T. M. and Malyshev, P. I. (1971): Composition of Solutions Forming Pitchblende in a Uranium-Molybdenum Deposit (Abstract); Proceedings of COFFI, Vol. 4, p. 10.
- Barton, J. M., Jr. (1975): The Mugford Group Volcanics of Labrador: Age, Geochemistry and Tectonic Setting; Canadian Journal Earth Science, Vol. 12, pp. 1196-1208.
- Barua, M. C. (1969): Geology of Uranium-molybdenum bearing rocks of the Aillik-Makkovik Bay area, Labrador; Unpublished M.Sc. thesis, Queen's University, Kingston, Ontario.
- Bastin, S. (1939): The Ni-Co-Native Ag Ore type; Economic Geology, Vol. 34, pp. 1-40.
- Beaven, A. P. (1958): The Labrador Uranium area: Proceedings Geol. Assoc. Canada, Vol. 10, pp. 137-145.
- Beck, L. S. (1970): Genesis of Uranium in the Athabasca region and its significance in exploration; CIMM, Vol. 23, pp. 59-69.
- \_\_\_\_\_ (1977): Changing ideas on metallogenesis of Saskatchewan's uranium deposits; Canadian Mining Journal, pp. 49-51.
- Bell, R. T. (1978): Breccias and Uranium Mineralization in the Wernecke Mountains, Yukon Territory - A progress report; Current Research, Part A, Geological Survey Canada, Paper 78-1A, pp. 317-322.



- Bell, K. and Blenkinsop, J. (1978): Reset Rb/Sr whole-rock systems and chemical control; *Nature*, Vol. 273, pp. 532-534.
- Bell, R. T. and Delaney, G. D. (1977): Geology of some uranium occurrences in Yukon Territory; in Report of activities, Part A, Geological Survey of Canada, Paper 77-1A, pp. 33-37.
- Bernazeaud, J. (1965): Labrador uranium project, progress report for 1965; Unpublished private report, Mokta (Canada) Ltd.
- Bigeleisen, J. and Mayer, M. (1947): Isotopic exchange reactions; *Journal Chemistry and Physics*, Vol. 15, pp. 261-267.
- Boshe, H., Rose-Hansen, J., Sørensen, H., Steenfelt, A., Løvborg, L., Kunzendorf, H. (1974): On the behavior of uranium during crystallization of magmas - with special emphasis on alkaline magmas; in Uranium Exploration Geology, IAEA Publication, pp. 49-58.
- Bossi, J. (1974): Use of fluid inclusions in the genetic study of vein deposits; in Uranium Exploration Geology, IAEA Publication, pp. 583-592.
- Bostrom, K. and Fisher, D. E. (1971): Volcanogenic U, V, and Fe in Indian Ocean sediments; *Earth and Planetary Science Letters*, Vol. 11, pp. 95-98.
- Bowen, N. L. and Schairer (1929): The fusion relations of acmite; *American Journal of Science*, Vol. 18, pp. 365-375.
- Bridgewater, D. (1970): Observations on the Precambrian rocks of Scandinavia and Labrador and their implications for the interpretation of the Precambrian of Greenland; *Grøn. Geol. Under.*, Rapport No. 28, pp. 43-47.
- Brooks, C., Hart, S. P., Hofmann, A., James D. E. (1976): Rb-Sr mantle isochrons from oceanic regions; *Earth Planet. Science Letters*, Vol. 32, pp. 51-61.



- Brunner, J. J. and Mann, E. L. (1961): Geology of the Seal Lake area, Labrador; Geological Society of America Bulletin, Vol. 72, pp. 1361-1382.
- Bryner, L. (1961): Breccia and pebble columns associated with epigenetic ore deposits; Economic Geology, Vol. 56, pp. 488-508.
- Carmichael, I. S. E., Turner, F. J., and Verhoogen, J. (1974): Igneous Petrology; McGraw Hill Book Company, New York: p. 739.
- Chappel, B. W. and White, A. J. P. (1974): Two contrasting granite types; Pacific Geology, Vol. 8, pp. 173-174.
- Christie, A. M. (1953): Goldfields - Martin Lake map-area, Saskatchewan; Geological Survey of Canada, Memoir 269, p. 126.
- Christie, A. M., Roscoe, S. M. and Fahrig, W. F. (1953): Preliminary map, Central Labrador Coast; Geological Survey of Canada, Paper 53-1.
- Clark, A. M. S. (1970): A structural reinterpretation of the Aillik Series, Labrador; Unpublished M. Sc. thesis, Memorial University of Newfoundland, St. John's, Newfoundland.
- \_\_\_\_\_ (1971): Structure and Lithology of a part of the Aillik Series, Labrador; Proceedings of the Geological Association of Canada, Vol. 24, pp. 107-117.
- \_\_\_\_\_ (1974): A reinterpretation of the Stratigraphy and deformation of the Aillik Group, Makkovik, Labrador; Unpublished Ph.D. thesis, Memorial University of Newfoundland, St. John's, Newfoundland.
- Clayton, R. N. (1961): The use of oxygen isotopes in high temperature geological thermometry; Journal Geology, Vol. 69, pp. 447-452.
- Clayton, R. N. and Epstein, S. (1958): The relationship between  $^{18}\text{O}/^{16}\text{O}$  ratios in coexisting quartz, carbonate and iron oxides from various geological deposits; Journal Geology, Vol. 66, pp. 352-373.





- Clayton, R. N., O'Neil, R., and Mayeda, T. K. (1972): Oxygen isotope exchange between quartz and water; *Journal of Geophysical Research*, Vol. 77, pp. 3057-3067.
- Collerson, K. D., Jesseau, C. W. and Bridgewater, D. (1976): Crustal development of the Archean gneiss complex, Eastern Labrador; in B. F. Windley (ed.), The Early History of the Earth, Wiley, London: pp. 237-253.
- Collins, C. B., Farquhar, R. M. and Russell, R. C. (1954): Isotopic constitution of radiogenic leads and the measurement of geological time; *Bulletin Geological Survey of America*, Vol. 65, pp. 1-22.
- Collins, J. E. (1958): Geological report on Ferguson-Brown Lakes; Unpublished private report, Brinex.
- Cormier, R. F. (1969): Radiometric dating of the Coldbrook Group of Southern New Brunswick, Canada; *Canadian Journal of Earth Sciences*, Vol. 6, pp. 393-398.
- Corriveau, C. R. (1958): Report on the Montague No. 2 uranium prospect, Silas Lake area-Kaipokok concession; Unpublished private report, Brinex.
- Coté, J. J. G. (1970): Geology of the Indian Lake area, Seal Lake concession, Labrador; Unpublished private report, Brinex.
- Currie, K. L., Curtis, L. W. and Grittins, J. (1976): Petrology of the Red Wine Alkaline Complexes, Central Labrador and a comparison with the Illimaussag Complex, Southwest Greenland; *Geological Survey of Canada, Paper FS-1, Part A*, pp. 271-280.
- Curtis, L. W., Currie, K. L. and Grittins, J. (1974): The Red Wine Alkaline Province, Labrador; in *Report of Activities, Geological Survey of Canada, Paper 74-1, Part A*, pp. 145-146.
- Dalkamp, F. J. (1976): Uranium deposits, northern Saskatchewan, Canada; *Institute of Mining and Metallurgy, an International Symposium (London)*, pp.



- Daley, R. A. (1902): The geology of northeast coast of Labrador; Bulletin of Comparative Zoology Harvard, Vol. 38, Geology Series 5.
- Davis, D. W., Gray, J., Cumming, G. L. and Baadsgaard, H. (1977): Determination of the Rb decay constant; Geological Association Canada/Mineralogical Association Canada Programme Abstracts, Vol. 2, No. 15.
- Deer, W. A., Howie, R. A., Zussman, J. (1963): Rock-forming minerals, Vol. 2, Chain Silicates; J. Wiley and Sons, Inc., New York: p. 379.
- Deer, W. A., Howie, R. A., Zussman, J. (1971): An introduction to the rock-forming minerals; Longman, London: 528 p.
- DeGrace, J. R. (1969): Geology, Pocketknife Lake area; Unpublished private report, Brinex.
- Derry, D. R. (1970): "Geochemistry - the link between ore genesis and exploration;" Opening address at Third International Geochemical Symposium, Toronto, April 16.
- \_\_\_\_\_ (1977): New Types of deposit will provide future supplies of uranium; Canadian Mining Journal, 98, pp. 56-60.
- Dickinson, W. R. and Hatherton, T. (1967): Andesite volcanism and seismicity around the Pacific: Science, Vol. 157, pp. 801-803.
- Dodson, R. S., Needham, R. S., Wikes, D. G., Page, R. W., Smart, D. G., and Watchman, A. L. (1974); Uranium mineralization in the Rum Jungle, Alligator Rivers province, Northern Territory, Australia; Formation of Uranium Ore Deposits: IAEA Proceedings Symposium in Athens, 6-10 May, pp. 551-568.
- Dostal, J., Capedri, S. and Dupuy, C. (1976): Uranium and potassium in calc-alkaline volcanic rocks from Sardinia; Lithos, pp. 179-183.
- Douglas, G. V. (1953): Notes on localities visited on the Labrador coast in 1946 and 1947; Geological Survey Canada, Paper 53-1.





- Ellingwood, S. G. (1958): Geology of the Moran Lake area, Kaipokok concession; Unpublished private report, Brinex.
- Emslie, R. F. (1965): The Michikamau Anorthositic Intrusion, Labrador; Canadian Journal Earth Science, Vol. 2, pp. 385-399.
- \_\_\_\_\_ (1970): The Geology of the Michikamau Intrusion, Labrador (13L, 231); Geological Survey Canada, Paper 68-57, 85 p.
- Ernst, W. G. (1962): Synthesis, stability relations and occurrence of riebeckite and riebeckite-arfvedsonite solid solutions; Journal Geology, Vol. 70, pp. 689-735.
- Evamy, J. (1963); Stain for carbonates; Sedimentology, Vol. 2, pp. 164-170.
- Evans, E. L. (1952): Native copper discoveries in the Seal Lake area, Labrador; Proceedings Geological Association Canada, Vol. 5, pp. 111-116.
- Evans, E. L. and Desjardin, R. A. (1962): A unique beryllium deposit in the vicinity of Ten Mile Lake area, Labrador; Proceedings Geological Association Canada; Vol. 13, pp. 45-51.
- Everhart, D. L. and Wright, R. (1953): The geological characteristics of typical pitchblende veins; Economic Geology, Vol. 48, pp. 77-96.
- Fahrig, W. F. (1957): Geology of certain proterozoic rocks in Quebec and Labrador; in The Proterozoic in Canada. Royal Society of Canada, Special publication 2, pp. 112-123.
- \_\_\_\_\_ (1959): Snegamook Lake; Geological Survey Canada, Map 10794.
- Faure, G. (1977): Principles of Isotope Geology; J. Wiley and Sons, Inc., New York: 464 p.
- Faure, G. and Powell, J. L. (1972): Strontium Isotope Geology; Springer-verlag, New York, 188 p.
- Finch, W. I. (1967): Geology of epigenetic uranium deposits in Sandstone in the United States; U. S. Geological Survey Professional paper 538, 121 p.





- Fischer, R. W. (1961): Proposed classification of volcaniclastic sediment and rocks; Bulletin Geological Society America, Vol. 72, pp. 1409-1414.
- Floyd, P. A. and Winchester, J. A. (1975): Magma type and tectonic setting discrimination using immobile elements; Earth Planetary Science Letters, Vol. 27, pp. 211-218.
- 
- (1978) Identification and discrimination of altered and metamorphosed volcanic rocks using immobile elements; Chemical Geology, Vol. 21, pp. 291-306.
- Franklin, J. M., Kasarda, J. and Poulsen, K. H. (1975): Petrology and Chemistry of Mattabi deposit; Economic Geology, Vol. 70, pp. 63-79.
- Grabbleman, J. W. (1976): Expectations from uranium exploration; American Association of Petroleum Geologists, v. 60, pp. 1993-2004.
- 
- (1977): Migration of Uranium and Thorium - Exploration Significance; American Association of Petroleum Geologists Special Publication, Tulsa. Oklahoma, 98p.
- Gandhi, S. S. (1974): Exploration in the Kaipokok Bay - Big River Area, Labrador; Unpublished private report, Brinex.
- 
- (1976): Geology, isotopic ages and origin of uranium occurrences of Kaipokok Bay - Big River area, Labrador; Unpublished private report, Brinex.
- Gandhi, S.S., Grasty, R. L. and Grieve, R. A. F. (1969): The geology and geochronology of the Makkovik Bay area, Labrador; Canadian Journal Earth Science, Vol. 6, pp. 1019-1035.
- Gandhi, S. S. and Guiton, R. (1975): Geology and uranium occurrences of Active Pond-Elbow Pond Grid, Labrador; Unpublished private report, Brinex.
- Gandhi, S. S. Krajewski, J. K. and Turner, D. (1976): Surface Exploration of the Burnt Lake Prospect, Michelin-Emben Belt, Labrador; Unpublished private report, Brinex.



- Garaschi, A. T. and Kerr, P. F. (1968): Uranium emplacement at Garnet Ridge, Arizona; *Economic Geology*, Vol. 63, pp. 859-875.
- Gelinas, L. and Brooks, C. (1974): Archean Quench-texture tholeiites: *Canadian Journal of Earth Science*, Vol. 11, pp. 324-340.
- Gill, F. D. (1966): Petrology of molybdenite-bearing gneisses, Makkovik area, Labrador; (Abstract). *Canadian Mining Journal*, Vol. 89, pp. 100-101.
- Goodwin, A. M., Ambrose, J. W., Ayers, L. D., Clifford, D. M., Currie, K. L., Ermanovics, E. M., Fahrig, W. F., Gibb, R. A., Hall, D. H., Innes, M. J. S., Irvine, T. N., MacLaren, A. S., Norris, A. W. and Pettijohn, F. J. (1972): The Superior Province, in Variations in Tectonic Styles in Canada; edited by R. A. Price and R. W. Douglas, Geological Association Canada, Special Paper 11, pp. 527-624.
- Grasty, R. L., Rucklidge, J. C. and Elders, W. A. (1969): New K-Ar age determinations on rocks from the east coast of Labrador; *Canadian Journal Earth Science*, Vol. 6, pp. 340-344.
- Green, T. H. and Ringwood, A. E. (1968): Genesis of the calc-alkaline igneous rock suite; *Contrib. Mineralogy and Petrology*, Vol. 18, pp. 105-162.
- Greene, B. A. (1972): Geological map of Labrador.
- \_\_\_\_\_. (1974): An Outline of the Geology of Labrador; Department of Mines and Energy Mineral Development Division Information Circular No. 15, 64 p.
- Haas, J. L. Jr. (1971): The effect of salinity on the maximum thermal gradient of a hydrothermal system at hydrostatic pressure; *Economic Geology*, Vol. 66, pp. 940-946.
- Hack, J. T. (1942): Sedimentation and volcanism in the Hopi Buttes, Arizona; *Bulletin Geological Society America*, Vol. 53, pp. 335-372.
- Halet, D. (1946): Geological reconnaissance of the Nascaupi Mountains and adjoining coastal region; Unpublished private report, Dome Exploration Ltd.



- Harker, A. (1968): Igneous Petrology; Cambridge University Press, London.
- Hart, S. R. and Brooks, C. (1970): Rb-Sr mantle evolution models; Carnegie Institute, Washington: Department Terrestrial Magnetism Annual Report of Director, pp. 426-429.
- Hegge, M. R. (1972): Geologic setting and relevant exploration features of the Jabiluka uranium deposits; Canadian Institute Mining Metallurgy, Vol. 70, pp. 50-61.
- Heinrich, (1965):
- Hofmann, A. W. (1975): Diffusion of Ca and Sr in a basalt melt; Carnegie Institute Washington Yearbook, Vol. 74, p. 183.
- Hofmann, A. and Grauert, B. (1975): Effect of regional metamorphism on whole-rock Rb-Sr systematics in sediments; Carnegie Institute Washington Year Book, Vol. 74, p. 299.
- Hosteler, P. B. and Garrels, R. M. (1962): Transportation and precipitation of uranium and vanadium at low temperatures, with special reference to sandstone type uranium deposits; Economic Geology, Vol. 57, pp. 137-166.
- Hounsflow, A. W. (1976): Mineralogy of Uranium and Thorium, a tabular summary; Colorado School Mines Research Institute.
- Hughson, M. R. (1958): Mineralogical report on a uranium ore sample ("K-2") from British Newfoundland Exploration Limited, Kitts Prospect, Makkovik area, Labrador, Newfoundland, ref. No. 2/58-14; Canada Department of Mines and Technical Surveys. Mines Branch Investigation report IR 58-54.
- Irvine, T. N. and Barager, W. R. A. (1971): A guide to the chemical classification of the common volcanic rocks; Canadian Journal Earth Science, Vol. 8, pp. 523-548.





- Jakes, P. J. and White, A. J. (1972): Major and trace element abundance in volcanic rocks of orogenic areas; Bulletin Geological Society America, Vol. 83, pp. 29-39.
- Kimberley, M. M. (1978): High-temperature uranium geochemistry; in Short Course in Uranium Deposits: Their Mineralogy and Origin (edited, M. M. Kimberley), Mineralogical Association Canada, Vol. 3, pp.
- King, A. F. (1963): Geology of Cape Makkovik Peninsula, Aillik, Labrador; Unpublished M.Sc. thesis, Memorial University of Newfoundland, St. John's, Newfoundland.
- Kistler, R. W. and Peterman, Z. E. (1975): Variations in Sr, Rb, K, Na, and initial  $^{87}\text{Sr}/^{86}\text{Sr}$  in Mesozoic granitic rocks and intruded wall rocks in Central California; Bulletin Geological Society America, Vol. 84, pp. 3489-3512.
- Knight, I. (1973): The Ramah Group between Nachvak Fiord and Bears Gut, Labrador; in Report of Activities, Part A, Geological Survey of Canada, Paper 73-1A, pp. 156-161.
- Knight, I. and Morgan, W. C. (1976): Stratigraphic subdivision of the Aphebian Ramah Group, Northern Labrador; Geological Survey of Canada, Paper 77-15.
- Knipping, H. D. (1974): The concepts of supergene versus hypogene emplacement of uranium at Rabbit Lake, Saskatchewan, Canada; International Atomic Energy Agency, Vienna, Paper SM-183/38.
- Koeppel, V. (1968): Age and history of uranium mineralization of the Beaverlodge area, Saskatchewan; Geological Survey Canada, Paper 631-31.
- Konstantinov, V. M. and Yakunin, D. I. (1973): Some characteristics of the relationship between uranium-molybdenum mineralization and volcanogenic formations; Atomnaya Energiya (translated), Vol. 34, pp. 3-5.
- Kontak, D. J. (1978): Investigation of four uranium showings in the Central Mineral Belt, Labrador; in Report of activities for 1977, R. V. Gibbons (editor); Newfoundland Department of Mines and Energy, Mineral Development Division, Report 78-1, pp. 27-43.



- Kostov, E. I. et al. (1970): Formation temperatures of some hydrothermal uranium deposits (Abstract): in Proceedings of COFFI, Vol. 4, p. 38.
- Krajewski, J. (1975): Geology and uranium mineralization of the Walker Lake East showings, Labrador; Unpublished private report, Brinex.
- Kranck, E. H. (1939): Bedrock geology of the seaboard region of Newfoundland and Labrador: Geological Survey of Newfoundland, Bulletin 19.
- \_\_\_\_\_ (1953): Bedrock geology of the seaboard of Labrador between Domino Run and Hopedale, Newfoundland; Geological Survey of Canada, Bulletin 26.
- Krogh, T. (1973): A low-contamination method for hydrothermal decomposition of zircon and extraction of U and Pb for isotopic age determinations; Geochim. Cosmochim. Acta, Vol. 37, pp. 485-494.
- Krogh, T. E., David, G. L., Hart, S. R. and Aldrich, L. T. (1976): Geochronology of the Grenville Province; Carnegie Institute Washington Year Book, Vol. 75, pp. 224-229.
- Lambert, R. St. J. and Holland, J. G. and Owen, P. O. (1974): Chemical petrology of a suite of calc-alkaline lavas from Mount Ararat, Turkey; Journal Geology, Vol. 82, pp. 419-438.
- Langford, F. F. (1974): A supergene origin for vein-type; uranium ores in the light of the Western Australian calcrete-carnotite deposits; Economic Geology, Vol. 69, pp. 516-526.
- Larsen, E. S., Phair, G., Gottfried, D., and Smith, W. L. (1955): Uranium in magmatic differentiation; in Geology of Uranium and Thorium, International Conference.
- Laznicka, P. (1976a): Dolores Creek area provides one example of copper, cobalt, and radioactivity in Yukon's Ogilvie and Wernecke Mountains; Northern Miner, November 25, pp. 88-89.
- \_\_\_\_\_ (1976b): Geology and mineralization in the Dolores Creek area, Bonnet Plume Range, Yukon (N.T.S. 106-6).





- Leech, G. B., Lowdon, J. A., Stockwell, C. H. and Wanless, R. K. (1963): Age determinations and Geological Studies; Geological Survey Canada, Paper 63-17.
- Leroy, J. and Poty, B. (1969): Recherches préliminaires sur les fluides associés à la genèse des minéralization en uranium du Limousin (France); *Mineralium Deposita*, Vol. 4, pp. 395-400.
- Lieber, O. M. (1860): Notes on the geology of the coast of Labrador; Report of the U.S. Coast Survey.
- Lipman, P. W. (1965): Chemical comparison of glassy and crystalline volcanic rocks; U.S. Geological Survey Bulletin, 1201-D, pp. D1-D24.
- MacKenzie, D. E. and Clappell, B. W. (1972): Shoshonitic and calc-alkaline lavas from the Highlands of Papua New Guinea; *Contributions to Mineralogy and Petrology*, Vol. 35, pp. 50-62.
- Mann, E. L. and Collins, J. E. (1957): Moran Lake-Kaipokok concessions; Unpublished private report, Brinex.
- Marten, B. E. (1971): Preliminary report on the geology of the Marks Bight-Post Hill belt, Kaipokok Bay area, Labrador; Unpublished private report, Brinex.
- \_\_\_\_\_ (1972): Structural geology of the Marks Bight-Post Hill area, Kaipokok Bay Area, Labrador; Unpublished private report, Brinex.
- \_\_\_\_\_ (1975): Geology of the Letitia Lake Area, Labrador; in Report of Activities for 1974, Newfoundland Department of Mines and Energy, Mineral Development Division, Report 75-1, pp. 75-85.
- Mawer, M. (1977): Fluid inclusions, Highland Valley Porphyries; Unpublished M.Sc. thesis, University of Alberta, Edmonton, Alberta.
- McIntyre, G. A., Brooks, C., Compston, W. and Turek, A. (1966): The statistical assessment of Rb-Sr isochrons; *Journal Geophysical Research*, Vol. 71, pp. 5459-5468.
- McMillain, R. H. (1977): Metallogenesis of Canadian uranium deposits: a review; Institute Mining and Metallurgy, International Symposium, London: pp. 43-55.





- Miller, A. R. and LeCheminant, A. N. (1978): Uranium mineralization in the Baker Lake Basin, District of Keewatin (Abstract); *Economic Geology*, Vol. 73, p. 1394.
- Miller, L. J. (1958): The chemical environment of pitchblende; *Economic Geology*, Vol. 53, pp. 521-545.
- Milton, C. and Eugster, H. P. (1959): Mineral assemblages of the Green River formation; in Researches in Geochemistry, Wiley, New York.
- Minatidis, D. G. (1976): A comparative study of trace element geochemistry and mineralogy of some uranium deposits of Labrador, and evaluation of some uranium exploration techniques in a glacial terrain; unpublished M.Sc. thesis, Memorial University, Newfoundland, St. John's, Newfoundland.
- Mittempergher, M. (1970): Exhalative-supergenic uranium mineralization in the Quaternary alkaline volcanic rocks of central Italy; International Atomic Energy Agency, Athens, Paper IAEA-PL 39117, pp. 177-184.
- Moore, J. C. G. (1954): Report on the Kaipokok River concession area, Labrador; Unpublished private report, American Metal Company.
- Morgan, W. C. (1975): Geology of the Precambrian Ramah Group and basement rocks in the Nachvak Fiord-Saglek Fiord area, North Labrador; Geological Survey Canada, Paper 74-54.
- Morrison, G. (1976): The tectonic setting of the Shoshonite Association in Island arc environments; in *Essays in Volcanology, Geology 521 Seminar*, University of Western Ontario.
- Morton, R. D. (1976): The western and northern Australian U deposits - exploration guides or exploration deterrents for Saskatchewan; in Uranium in Saskatchewan; Saskatchewan Geol. Survey Special Publication 3.
- \_\_\_\_\_. (1977): The origin of the uranium deposits of the Athabasca region, Saskatchewan, Canada (Abstract); in Abstracts with Programs, Geological Society of America, Vol. 9, No. 7, p. 1104.



- Morton, R. D., Gandhi, S. S. and Aubit, A. (1978): Fluid inclusion studies and genesis of the Rexspar uranium-fluorite deposit, Birch Island, British Columbia; Geological Survey Canada, Paper 78-1, Part B.
- Mukhopadhyay, B., Brookline, D. G. and Bolivar, S. L. (1975); Rb-Sr whole rock study of the precambrian rocks of the Pedernal Hills, New Mexico; Earth Planetary Science Letters, Vol. 27, pp. 283-286.
- Neuman, W. and Hustler, E. (1976): Discussion of the  $^{87}\text{Rb}$  Half-life determined by absolute counting; Earth Planetary Science Letters, Vol. 33, pp. 277-288.
- O'Neil, J. R. and Clayton, R. N. (1964): Oxygen isotope geothermometry; in Isotopic and Cosmic Chemistry, edited by H. Craig et al., North Holland Publishing Co., Amsterdam: pp. 157-168.
- Orville, P. M. (1963): Alkali-ion exchange between vapor and feldspar phases; American Journal Science, Vol. 71, pp. 201-237.
- Packard, A. S. Jr. (1891): The Labrador Coast, N.D.C.; Hodges, New York.
- Page, L. R. (1960): The source of uranium in ore deposits; International Geological Congress 21st Session, Part 5, pp. 149-164.
- Pankhurst, R. J. and Pidgeon, R. T. (1976): Inherited isotope systems and the source region pre-history of early Caledonian Granites in the Dalradian series of Scotland, Earth Planetary Science Letters, Vol. 31, pp. 55-68.
- Peacock, M. A. (1931): Classification of Igneous rock series; Journal Geology, Vol. 39, pp. 54-67.
- Pearse, T. H. and Donaldson, J. A. (1974): Proterozoic quench-texture basalts from the Labrador Geosyncline; Canadian Journal Earth Science, Vol. 11, pp. 1611-1615.
- Piche, W. T. (1955): Madsen Lake Uranium Prospect; Unpublished private report, Brinex.





- Piloski, M. J. (1968): Report on operations, Kaipokok-Big River joint venture area 1968; Unpublished private report, Brinex.
- Poldervaart, A. and Hess, H. H. (1951): Pyroxenes in the crystallization of Basaltic magma; *Journal Geology*, Vol. 59, p. 472.
- Potter, R. W. (1973): Pressure corrections for fluid-inclusion homogenization temperatures based on the volumetric properties of the system  $\text{NaCl-H}_2\text{O}$ ; *Journal Research U.S. Geological Survey*, Vol. 5, No. 5, Sept-Oct 1977, pp. 603-607.
- Poty, B. P. (1977): Intragranitic uranium ore deposits at Limousin and Forez, France (Abstract): in Abstracts with Programs, Geological Society of America 1977 Annual Meeting, Vol. 9, No. 8, p. 1133.
- Poty, B. P., Leroy, J. and Cuney, M. (1974): Les inclusions fluides dans les minerals des gisements d'uranium intragranitiques du Limousin et du Forez (Massif Central, France); in Formation of Uranium Ore Deposits, International Atomic Energy Agency, Vienna, pp. 569-582.
- Preto, V. A. (1978): Setting and genesis of uranium mineralization at Rexport; *Canadian Institute Mining Metallurgy*, Vol. 71, pp. 82-88.
- Priem, H. N. A. Boelrijk, N. A. I. M., Hebeda, E. H., Shermerhorn, L. J. G., Verdurmen, E. A. Th., and Verschure, R. H. (1978): Sr. isotopic homogenization through whole-rock systems under low-green-schist facies metamorphism in carbon ferrous pyroclastics at Aljustrel (Southern Portugal); *Chemical Geology*, Vol. 21, pp. 307-314.
- Rafalsky, R. P. (1958): The experimental investigation of the conditions of uranium transport and deposition by hydrothermal solutions; in Proceedings of the Second U.N. International Conference on the Peaceful uses of Atomic Energy, Vol. 2, pp. 432-444.
- Rich, R. A., Holland, H. D. and Petersen, U. (1977): Hydrothermal Uranium Deposits; Elsevier Publishing Co., Amsterdam.





- Robinson, W. G. (1956): Exploration of Block "D" concession, Labrador during 1955; Unpublished private report, Frobisher Limited.
- Robertson, D. S. and Lattanzi, C. R. (1914): Uranium deposits of Canada, Geoscience Canada, Vol. 1, No. 2, pp. 8-19.
- Roddick, J. C. and Compston, W. (1977): Strontium isotopic equilibration: A solution to paradox; Earth and Planetary Science Letters, Vol. 34, pp. 238-246.
- Roedder, E. (1962): Studies of fluid inclusions. I: low temperature and application of a dual purpose freezing and heating stage; Economic Geology, Vol. 57, pp. 1045-1061.
- \_\_\_\_\_ (1963): Ancient fluids in crystals; Scientific American, October, pp. 2-11.
- \_\_\_\_\_ (1967): Fluid inclusions as samples of ore fluids; in Geochemistry of hydrothermal ore deposits, edited by H. L. Barnes, Pennsylvania State University, pp. 515-566.
- \_\_\_\_\_ 1977: Fluid inclusions as tools in mineral exploration; Economic Geology, Vol. 72, pp. 503-525.
- Rogora, V. P., Nikitin, A. A. and Naumov, G. B. (1971): Mineralogic-geochemical conditions of localization of U-Mo deposits in volcanogenic sedimentary formations (Abstract); Fluid Inclusion Research - Proceedings of COFFI, Vol. 4, pp. 68-69.
- Romberger, S. B. (1978): Hydrothermal transport and deposition of uranium and the origin of vein uranium deposits; Economic Geology, Vol. 73, p. 1397.
- Rosholt, J. N. and Noble, D. C. (1969): Loss of uranium from crystallized silicic volcanic rocks; Earth Planetary Science Letters, Vol. 6, pp. 268-270.
- Rosholt, J. N., Prijana and Noble, D. C. (1971): Mobility of uranium and thorium in glassy and crystallized silicic volcanic rocks; Economic Geology, Vol. 66, pp. 1061-1069.



- Ross, C. S. and Smyth, R. L. (1961): Ash-flow tuffs, their origin, geologic relationships and identification; United States Geological Survey, Paper, 266.
- Roy, J. L. and Fahrig, W. F. (1973): The paleomagnetism of Seal and Croteau rocks from the Grenville Front, Labrador; Polar wandering and tectonic implications; Canadian Journal Earth Science, Vol. 10, pp. 1270-1301.
- Ruzicka, V. (1975): New sources of uranium - types of uranium deposits presently unknown in Canada; Canadian Mining Journal, pp. 41-44.
- Ryan, A. B. (1977): Archean-Proterozoic geology of the Kanairiktok-Kaipokok River Valleys (NTS 13K/10), Labrador; in Report of Activities 1976, Newfoundland Department Mines and Energy, Mineral Development Division, Report 77-1, pp. 63-70.
- \_\_\_\_ (1979): Regional geologic mapping in the Central Mineral Belt (13K/East), Labrador; in Report of Activities for 1978, Newfoundland Department of Mines and Energy, Report 79-1, pp. 90-94.
- Ryan, A. B. and Harris, A. (1978): Geology of the Otter-Nipisish-Stipec Lakes area, Labrador, (13K/2, 3, 6, 7) in Report of Activities 1977, Newfoundland Department Mines and Energy, Mineral Development Division, Report 78-1, pp. 51-58.
- Ryan, G. R. (1977): Uranium in Australia; Institute Mining Metallurgy, International Symposium, London, pp. 24-42.
- Rydell, H. S. and Bonatti, E. (1973): Uranium in submarine metalliferous deposits; Geochim Cosmochim Acta, Vol. 37, pp. 2557-2565.
- Schimann, K. and Smith, D. G. W. (1979): A new method for the optical fusion of whole-rock powders and for their analysis by an energy dispersive electron microprobe technique; (submitted for publication), Canadian Mineralogist.
- Schrider, E. L. and Furbish, W. J. (1977): Correlations of uranium and trace metal concentrations in mineralized rhyolites from Nevada (Abstract); Economic Geology, Vol. 72, p. 739.





- Scott, R. B. (1966): Origin of chemical variations within ignimbritic cooling units; *American Journal Science*, Vol. 264, pp. 273-288.
- \_\_\_\_\_ (1971): Alkali Exchange during devitrification and hydration of glasses in ignimbritic cooling units; *Journal Geology*, Vol. 79, pp. 100-110.
- Shoemaker, E. M. (1955): Occurrence of uranium in diatremes on the Navajo and Hopi reservations, Arizona, New Mexico, and Utah; in Geology of Uranium and Thorium, International Conference.
- Smirnov, V. I. (Editor) (1977): Ore deposits of the USSR; Vol. II, Pitman Publishing, London: 424 p.
- Smith, R. L. (1960): Ash flows; *Bulletin - Geological Society America*, Vol. 71, pp. 795-842.
- Smyth, W. R. (1976): Geology of the Mugford Group, Northern Labrador; in Report of Activities for 1976; Newfoundland Department of Mines and Energy, Mineral Development Division, Report 77-1, pp. 72-79.
- \_\_\_\_\_ (1977): The geology of the Stipeck Lake-Walker Lake area, Central Mineral Belt, Labrador; in Report of Activities for 1976, Newfoundland Department of Mines and Energy, Mineral Development Division, Report 77-1, pp. 50-56.
- Smyth, W. R. and Knight, I. (1978): Correlation of the Aphebian supracrustal sequences, Nain Province, Northern Labrador; in Report of Activities for 1977, R. V. Gibbons (editor), Newfoundland Department of Mines and Energy, Mineral Development Division, Report 78-1, pp. 59-64.
- Smyth, W. R. and Marten, B. E. (1975): Uranium potential of the basal unconformity of the Seal Lake Group, Labrador; in Report of Activities for 1974, Newfoundland Department of Mines and Energy, Mineral Development Division, Report 75-1, pp. 106-115.
- Smyth, W. R., Marten, B. E. and Ryan, A. B. (1975): Geological mapping in the Central Mineral Belt, Labrador: Redefinition of the Croteau Group; in Report of Activities for 1974, Newfoundland Department of Mines and Energy, Mineral Development Division, Report 75-1, pp. 51-74.





- 
- (1978): A major Aphebian-Helikian unconformity within the Central Mineral Belt of Labrador: definition of new groups and metallogenic implications; Canadian Journal Earth Sciences, Vol. 15, pp. 1954-1966.
- Smyth, W. R. and Ryan, A. B. (1977): Geological setting of the Moran Lake uranium showings, Central Mineral Belt, Labrador, in Report of Activities for 1976, Newfoundland Department of Mines and Energy, Mineral Development Division, Report 77-1, pp. 57-62.
- Sørensen, H. (1970): Occurrence of uranium in alkaline igneous rocks; in Uranium Exploration Geology, Proceedings of a Panel, Vienna, pp. 161-168.
- Steacy, H. R. and Kaiman, S. (1978): Uranium minerals in Canada. Their description, identification and field guides, in Short Course in Uranium Deposits: Their Mineralogy and Origin, (edited M. M. Kimberley), pp. 107-140.
- Steiger, R. H. and Jager, E. (1977): Subcommittee on geochronology: convention on the use of decay constants in geo- and cosmochemistry; Earth and Planet Science Letters, Vol. 36, pp. 359-362.
- Steinhauer, H. (1814): Notes on the geology of the Labrador coast; Transactions Geological Society, Vol. 2, pp. 488-491.
- Stevenson, I. M. (1970); Rigolet and Groswater Bay map areas, Newfoundland (Labrador); Geological Survey Canada, Paper, 69-48.
- Stockwell, C. H. (1963): Third report on structural provinces; orogenies and time classification of rocks of the Canadian Shield; Geological Survey Canada, Paper 63-17, Part 2, pp. 125-131.
- 
- (1964): Fourth report on structural provinces, orogenies, and time classification of rocks of the Canadian Precambrian Shield; Geological Survey Canada, Paper 64-17, Part a, pp. 1-21.



- Stockwell, C. H., McGlynn, J. C., Emslie, R. F., Sanford, B. V., Norris, A. W., Donaldson, J. A., Fahrig, W. F. and Currie, K. L. (1970): Geology of the Canadian Shield; in Geology and Economic Minerals of Canada; Geological Survey Canada, Economic Geology Report 1, pp. 43-150.
- Sutton, J. S. (1972): The Precambrian gneisses and supra-crustal rocks of the western shore of Kaipokok Bay, Labrador, Newfoundland; Canadian Journal Earth Science, Vol. 9, pp. 1677-1692.
- Sutton, J. S., Marten, B. E. and Clark, A. M. S. (1971): Structural history of the Kaipokok Bay area, Labrador, Newfoundland; Geological Association Canada Proceedings, Vol. 24, pp. 103-106.
- Suzuki, J. (1931): On some soda-pyroxene and amphibole-bearing quartz schists from Hokkaido, Journal Faculty Science Kokkaido University, Series 4, Vol. 2, p. 339.
- Taylor, F. C. (1969): Reconnaissance geology of a part of the Precambrian Shield, northeastern Quebec and northern Labrador; Geological Survey Canada, Paper 68-43.
- \_\_\_\_\_ (1970): Reconnaissance geology of a part of the Precambrian Shield, northeastern Quebec and northern Labrador; Part 2, Geological Survey Canada, Paper 70-24.
- \_\_\_\_\_ (1971): A revision of Precambrian structural provinces in northeastern Quebec and northern Labrador; Canadian Journal Earth Science, Vol. 8, pp. 579-584.
- Taylor, H. P. Jr. and Epstein, S. (1962): Relationship between  $^{18}\text{O}/^{16}\text{O}$  ratios in coexisting minerals of igneous and metamorphic rocks; Bulletin Geological Society America, Vol. 73, pp. 461-480.
- Taylor, H. P. Jr. (1967): Oxygen isotope studies of hydrothermal mineral deposits; in Geochemistry of Hydrothermal ore deposits; edited by H. L. Barnes, Holt-Reinhart and Winston, Inc., New York.
- Urey, H. C. (1947): The thermodynamic properties of isotopic substances; Journal Chemical Society, pp. 562-581.





Walton, A. W. (1978): Fate of uranium during open system diagenesis of glass-rich volcanic sediment of the Tascotal Formation (Oligocene); Naus-Pecos Texas (Abstract), Economic Geology, Vol. 73, p. 1399.

Wanless, R. K. and Loveridge, W. D. (1972): Rubidium-Strontium isochron age studies; Report 1, Geological Survey Canada, Paper 72-23, pp. 5759.

---

(1978): Rubidium-strontium isotopic age studies; Report 2 (Canadian Shield); Geological Survey of Canada, Paper 77-14, pp. 47-49.

---

(1978): Rubidium-strontium isotopic age studies; Report 2 (Canadian Shield), Geological Survey Canada, Paper 77-14, pp. 44-46.

Wanless, R. K., Stevens, R. D., Lachance, G. R. and Delabio, R. N. D. (1974): Age determinations and geological studies, K-Ar isotopic ages; Report 12, Geological Survey Canada, Paper 74-2, pp. 54-55.

Wanless, R. K., Stevens, R. D., Lachance, G. R., and Edmonds, C. M. (1967): Age determinations and geological studies: K-Ar isotopic ages; Report 7, Geological Survey of Canada, Paper 66-17.

Wanless, R. R., Stevens, R. D., Lachance, G. R., and Rimsaite, R. Y. H. (1965): Age determinations and geological studies, Part 1 - Isotopic ages; Report 5, Geological Survey Canada, Paper 64-17, Part 1.

Watson-White, M. V. (1971): Geology of the Walker Lake-Mustang Lake area; Labrador; Unpublished private report, Brinex.

---

(1976): A petrological study of acid volcanic rocks in part of the Aillik Series, Labrador; unpublished M.Sc. thesis, McGill University, Montreal, Quebec.

Wetherill, G. W. (1956): Discordant uranium-lead ages; American Geophysical Union Transactions, Vol. 37, pp. 320-326.





- Wheeler, E. P. (1942): Anorthosite and associated rocks about Nain, Labrador; *Journal Geology*, Vol. 50, pp. 611-642.
- \_\_\_\_\_ (1960): Anorthosite-adamellite complex of Nain, Labrador; *Bulletin Geological Society America*, Vol. 71, pp. 1755-1762.
- White, A. J. R. (1962): Aegirine-Riebeckite schists from South Westland, New Zealand; *Journal Petrology*, Vol. 3, pp. 38-48.
- Williams, F. M. G. (1970): Snegamook Lake (east half), Newfoundland; Geological Survey Canada, open file 42.
- Windley, B. F. (1976): *The Evolving Continents*; John Wiley and Sons Ltd., New York: 385 pp.
- Winkler, H. G. F. (1967): *Petrogenesis of Metamorphic rocks*; Springer-Verlag, New York: 320 pp.
- Working Group 4 Report (1970): Uranium deposits of unusual occurrences; in *Uranium Exploration Geology, Proceedings of a Panel, Vienna*, pp. 367-374.
- Wynne-Edwards, H. R. (1972): *The Grenville Province*; in Variations in Tectonic Styles in Canada; edited by R. A. Price and R. W. Douglas, Geological Association Canada, Special paper No. 11, pp. 263-334.
- Yermolayev, N. P. (1973): Uranium and thorium in regional and contact metamorphism; translated from *Geokhimiga*, No. 4, pp. 551-558.
- York, D. (1966): Least square fitting of a straight line; *Canadian Journal Physics*, Vol. 44, pp. 1079-1086.
- Zielinski, R. A. (1978): Uranium abundance and distribution in associated glassy and crystalline rhyolites of the western United States; *Bulletin Geological Society America*, Vol. 89, pp. 409-414.
- Zielinski, R. A., Lipman, P. W. and Millard, H. R., Jr. (1977): Minor-element abundance in obsidian, perlite, and felsite of calc-alkalic rhyolites; *American Mineralogist*, Vol. 62, pp. 426-437.





University of Alberta Library



0 1620 1716 4995

**B30269**